GEOLOGICAL SURVEY BRANCH
DEPARTMENT OF MINES AND ENERGY
GOVERNMENT OF NEWFOUNDLAND AND LABRADOR

GEOLOGY OF THE WEIR'S POND AREA, NEWFOUNDLAND (NTS 2E/1)

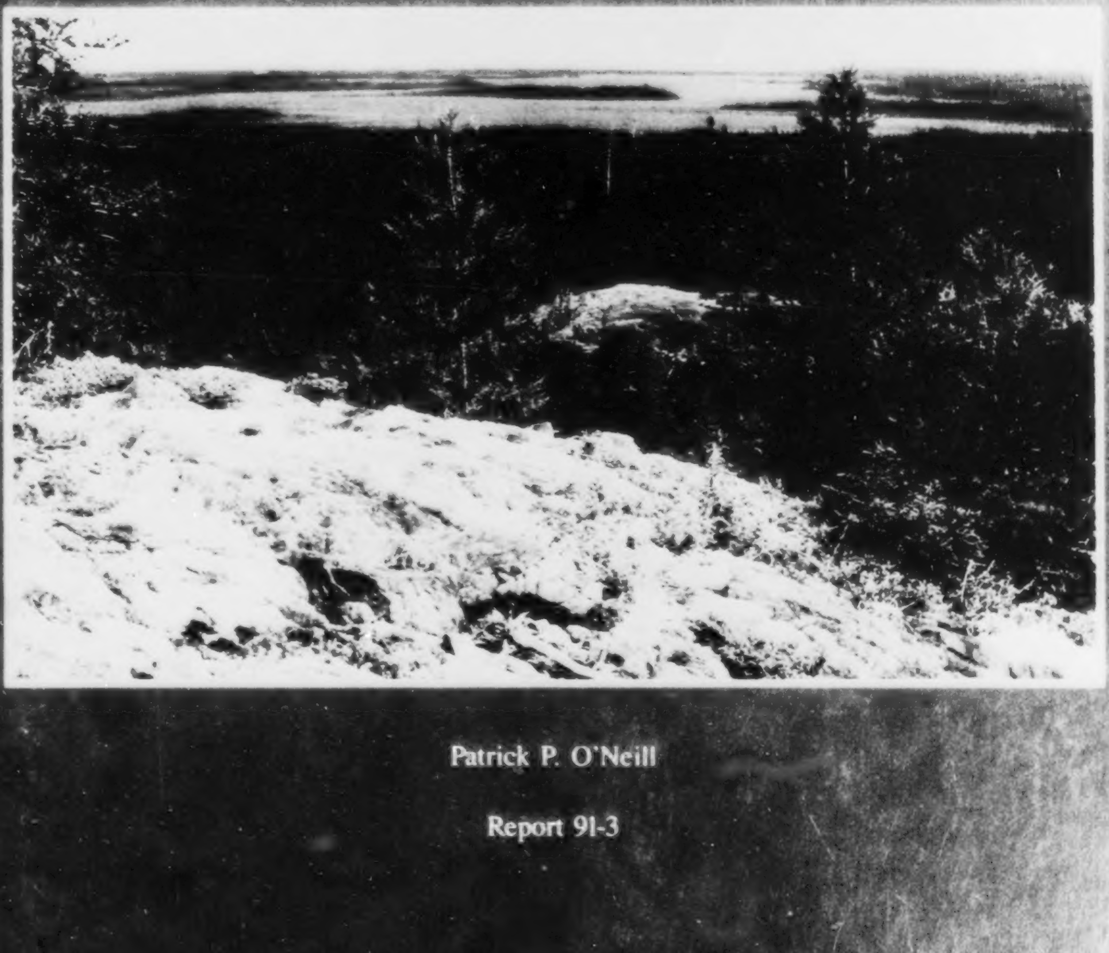

Patrick P. O'Neill

Report 91-3

St. John's, Newfoundland
1991

COVER

View looking east from ridge of ultramafic rock of the Gander River Complex toward the flat and gently rolling terrain underlain by the Gander Group. The ultramafic rocks of the complex are commonly altered to this distinctive, reddish-orange-weathering, magnesite-rich rock.

100-05690/

GEOLOGICAL SURVEY BRANCH
DEPARTMENT OF MINES AND ENERGY
GOVERNMENT OF NEWFOUNDLAND AND LABRADOR

GEOLOGY OF THE WEIR'S POND AREA, NEWFOUNDLAND (NTS 2E/1)

Patrick P. O'Neill

Report 91-3

St. John's, Newfoundland
1991

EDITING, LAYOUT AND DRAFTING

Senior Geologist R.F. Blackwood

Editor C.P.G. PEREIRA

Copy Editor D.G. WALSH

Typesetting B. STRICKLAND

Word Processing D. DOWNEY
J. MATTHEWS

Supervisor, Cartographic and Photomechanical Services K. BYRNE

Cartography D. LEONARD (Photomechanical)
G. DENIEF
T. PALTANAVAGE

Publications of the Geological Survey Branch are available through the Publications and Information Section, Geological Survey Branch, Department of Mines and Energy, P.O. Box 8700, St. John's, Newfoundland, A1B 4J6.
Telephone: (709) 729-3159
Telex: 016-4721
Fax: (709) 729-3493

This project is a contribution to the Canada–Newfoundland Mineral Development Agreement for the period 1984-1989. Project carried out by Newfoundland Department of Mines and Energy.

ISBN 0-920769-56-X

Author's Address *Patrick P. O'Neill*
Newfoundland Mapping Section
Geological Survey Branch
Department of Mines and Energy
P.O. Box 8700
St. John's, Newfoundland
Canada
A1B 4J6

CONTENTS

Page

ABSTRACT xvii

INTRODUCTION 1
  PREVIOUS WORK AND REGIONAL RELATIONSHIPS 1
    Mineral Exploration 6
  PRESENT INVESTIGATION 7
  PHYSIOGRAPHY 7
  GENERAL GEOLOGY 8
    General Statement 8

GANDER RIVER COMPLEX (Units 1 to 4) 9
  DEFINITION 9
  DISTRIBUTION AND TYPE SECTION 9
  CONTACT RELATIONSHIPS 9
  AGE 10
    Clinopyroxenite (Unit 1) 10
      Distribution and Contact Relationships 10
      Lithology 10
      Petrography 10
        Metamorphosed Ultramafic Rock (Subunit 1a) 10
          Distribution and Contact Relationships 10
          Lithology 10
          Petrography and Alteration Assemblages 11
    Gabbro and Diabase (Unit 2) 11
      Distribution and Contact Relationships 11
      Lithology 12
      Petrography 12
    Mafic Volcanic Rock (Unit 3) 13
      Distribution and Contact Relationships 13
      Lithology 13
      Petrography 13
    Plagiogranite (Unit 4) 13
      Distribution and Contact Relationships 13
      Lithology 13
      Petrography 14

DAVIDSVILLE GROUP (UNITS 5 to 9) 14
  THE WEIR'S POND FORMATION (UNITS 5 to 8) 14
    Definition and Distribution 14
    Sandstone (Unit 5) 15
      Distribution and Contact Relationships 15
      Lithology 15
      Petrography 15
      Paleontology and Age 15
    Conglomerate, Sandstone and Siltstone (Unit 6) 15
      Distribution 15
      Contact Relationships 15
      Lithology 15
      Petrography: i) Conglomerate (Subunit 6a) 17
        Granitoid Clasts 17
        Felsic Volcanic or Subvolcanic Detritus 17
        Sample # 86-16 17
        Intermediate Clasts 18
        Mafic and Ultramafic Clasts 18
        Sedimentary Clasts 18

Page

        - Sample # 86-381 18
        - Metamorphic Clasts 18
        - Individual Grains 18
      - Petrography: ii) Sandstone and Siltstone (Subunit 6b) 19
        - Lithic Clasts 19
      - Age 19
    - Limestone–Quartz Arenite (Unit 7) 19
      - Distribution and Reference Section 19
      - Contact Relationships 20
      - Lithology 20
      - Petrography 20
      - Paleontology and Age 20
    - Graphitic Black Shale (Unit 8) 21
      - Distribution and Reference Section 21
      - Lithology 21
      - Petrography 21
      - Paleontology and Age 21
  - THE HUNTS COVE FORMATION (UNIT 9) 21
    - Definition 21
    - Distribution and Contact Relationships 21
    - Lithology 22
    - Petrography 22
    - Age 22
  - THE OUTFLOW FORMATION 22
    - Definition, Regional Distribution and Contact Relationships 22

- **GANDER GROUP (UNITS 10 to 16)** 23
  - OVERVIEW 23
    - Jonathan's Pond Formation (Unit 10) 23
      - Definition and Distribution 23
      - Contact Relationships 23
      - Age 24
      - Lithology 24
        - Psammite and Semipelite 25
        - Pelite 26
        - Quartzite 26
        - Detailed Stratigraphic Log 26
        - Calc-Silicate-Rich Rocks 27
        - Coticules 27
        - Mafic Intrusive Bodies 27
      - Petrography 28
        - Chlorite Zone 28
          - Psammite and Semipelite 28
          - Pelite 29
          - Calc-Silicate-Rich Rocks 29
          - Mafic Intrusive Bodies 29
      - Ocean Pond Area 29
        - Biotite Zone 29
          - Psammite and Semipelite 29
          - Pelite 29
          - Calc-Silicate-Rich Rocks 30
          - Mafic Intrusive Bodies 30
        - Garnet Zone 30
          - Psammite and Semipelite 30
          - Pelite 30
          - Calc-Silicate-Rich Rocks 30
          - Mafic Intrusive Bodies 30

Page

Staurolite Zone 30
Psammite and Semipelite 30
Pelite 30
Calc-Silicate-Rich Rocks 30
Mafic Intrusive Bodies 31
Andalusite Zone 31
Psammite and Semipelite 31
Pelite 31
Calc-Silicate-Rich Rocks 31
Mafic Intrusive Bodies 31
Sillimanite Zone 31
Psammite and Semipelite 31
Pelite 31
Calc-Silicate-Rich Rocks 31
Mafic Intrusive Bodies 31
Moccasin Pond Area 31
Biotite Zone 32
Garnet Zone 32
Andalusite–Cordierite Zone 32
Sillimanite Zone 32
Wing Pond Area 32
Biotite Zone 32
Garnet Zone 32
Aluminosilicate–Staurolite Zone 32
Psammite, Grey and Black Pelite (Unit 11) 33
Distribution, Contact Relationships and Age 33
Lithology 33
Petrography 33
Indian Bay Big Pond Formation (Units 12 to 16) 33
Definition and Distribution 33
Grey to Dark Grey Psammite and Green and Black Pelite (Unit 12) 33
Distribution and Contact Relationships 33
Lithology 33
Petrography 34
Age 34
Black Pelite and Chert (Unit 13) 34
Distribution, Contact Relationships and Age 34
Lithology 34
Petrography 35
Intermediate Porphyry (Unit 14) 35
Distribution, Contact Relationships and Age 35
Lithology 35
Petrography 35
Pillow Basalt (Unit 15) 35
Distribution, Contact Relationships and Age 35
Lithology 35
Petrography 35
Psammite, Maroon and Black Metasiltstone and Calcareous Layers (Unit 16) 36
Distribution and Contact Relationships 36
Age 36
Lithology 36
Petrography 37

NON-STRATIFIED, PLUTONIC IGNEOUS ROCKS (Units 17 to 20) 37
ULTRAMAFIC ROCK AND GABBRO (UNIT 17) 37
Distribution 37
Contact Relationships 37

	Page
Age	38
Lithology	38
Petrography	38
UNIT 18	38
Distribution, Contact Relationships and Age	38
Lithology	38
Petrography	38
OCEAN POND GRANITE (UNIT 19)	38
Definition	38
Distribution, Contact Relationships and Age	38
Lithology	38
Petrography	39
Pegmatites and Other Veins Associated with the Ocean Pond Granite	39
DEADMAN'S BAY GRANITE (UNIT 20)	39
Distribution	39
Contact Relationships	40
Age	40
Lithology	40
Petrography	40
GEOCHEMISTRY	40
GANDER RIVER COMPLEX	40
Mafic and Ultramafic Rocks	41
Element Mobility and Effects of Alteration	41
Chemistry of the Ultramafic Rocks	41
Major- and Trace-Element Variation in Mafic Rocks	42
Tectonic Setting Based on Mafic Rock Chemistry	45
Major and Trace Elements	45
Rare Earth Elements	46
Plagiogranite Geochemistry	46
Low-Grade Metamorphism and Element Mobility	48
Classification	48
General Chemical Trends of the Felsic Rocks	48
REE Geochemistry	48
Comparison between Trondhjemites of the Gander River Complex and Trondhjemites of Other Settings	48
Genesis of the Trondhjemites	53
DAVIDSVILLE GROUP	53
JONATHAN'S POND FORMATION	55
INDIAN BAY BIG POND FORMATION	55
COMPARATIVE GEOCHEMISTRY OF THE GANDER AND DAVIDSVILLE GROUPS	55
GEOCHEMISTRY OF THE OCEAN POND AND DEADMAN'S BAY GRANITES	59
GEOCHRONOLOGY	61
^{40}Ar–^{39}Ar	61
Sample Description	61
Gander Group	61
Biotite Zone	61
Sillimanite Zone	61
Ocean Pond and Deadman's Bay Granites	61
Davidsville Group and Gander River Complex	62
Results	62
Gander Group	62
Muscovite	62
Biotite	63
Ocean Pond Granite	64
Deadman's Bay Granite	64
Davidsville Group	65

Page

- Gander River Complex 65
- Summary of Ar–Ar Results 66
- U–Pb DATING OF ZIRCON AND SPHENE 66
  - Results 66
  - Discussion 67

- **SEDIMENTOLOGY** 67
  - PROVENANCE OF THE DAVIDSVILLE GROUP 67
  - PROVENANCE OF THE GANDER GROUP 68

- **STRUCTURE** 69
  - GANDER RIVER COMPLEX 69
    - Microfabrics 70
  - DAVIDSVILLE GROUP 71
    - Microfabrics 72
  - GANDER GROUP 72
    - D_2 Deformation 72
    - D_3 Deformation 73
    - Post D_3 Deformation 75
    - High Strain Zones 75
    - Microfabrics 79
      - Ocean Pond Area 79
        - Chlorite, Biotite and Garnet Zones 79
        - Staurolite, Andalusite and Sillimanite Zones 80
        - Calc-Silicate-Rich Rocks and Amphibolites 81
      - Moccasin Pond Area 82
      - Wing Pond Area 82
      - Big Bear Cove Pond Area 84
  - STRUCTURAL SYNOPSIS 84

- **METAMORPHIC HISTORY** 86
  - METAMORPHISM OF THE GANDER RIVER COMPLEX 86
  - METAMORPHISM OF THE DAVIDSVILLE GROUP 87
  - METAMORPHISM OF THE JONATHAN'S POND FORMATION, GANDER GROUP 87
    - Chlorite Zone 88
    - Ocean Pond Area 88
      - Psammitic, Semipelitic and Pelitic Rocks 88
      - Calc-Silicate-Rich Rocks 88
      - Mafic Intrusive Bodies 89
    - Moccasin Pond Area 89
    - Wing Pond Area 89
  - METAMORPHISM OF THE INDIAN BAY BIG POND FORMATION, GANDER GROUP 90
    - Biotite Zone 90
    - Garnet Zone 90
    - Andalusite Zone 90
    - Cordierite Zone 90
  - METAMORPHIC ASSEMBLAGES AND REACTIONS IN THE GANDER GROUP 90
    - General Description 90
    - Ocean Pond Area 91
    - Moccasin Pond Area 93
    - Big Bear Cove Pond Area 94
    - Aureole of the Deadman's Bay Granite 94
    - Wing Pond Area 95
  - METAMORPHIC HISTORY 96
  - LOW PRESSURE–HIGH TEMPERATURE METAMORPHISM 97
  - REGIONAL CHRONOLOGICAL CORRELATIONS 99

Page

SYNOPSIS 99
  PALEOTECTONIC SETTING OF THE GANDER RIVER COMPLEX 99
  DEPOSITIONAL SETTING OF THE GANDER AND DAVIDSVILLE GROUPS 100

ECONOMIC POTENTIAL 102

MAJOR RESULTS 103

ACKNOWLEDGMENTS 104

REFERENCES 104

APPENDICES

Page

APPENDIX 1–ELECTRON MICROPROBE TECHNIQUES AND ANALYSES........ 114
Table 1 Replicate analyses of Standard Samples of FCPX........ 114
Table 2 Electron Microprobe Analyses of Selected Samples from Mafic Rocks of the Gander River Complex.... 114

APPENDIX 2–GEOCHEMISTRY METHODS AND ANALYSES........ 115
Table 1 Precision (P) of major element analyses........ 115
Table 2 Precision (P) of trace element analyses........ 115
Table 3 Precision (P) of rare-earth element and some trace-element analyses........ 116
Table 4 Accuracy of major-oxide analyses........ 116
Table 5 Accuracy of trace-element analyses by XRF........ 117
Table 6 Accuracy of rare-earth-element analyses........ 117
Table 7 Detection limits (D.L.) for trace elements analyzed by XRF........ 117
Table 8 Detection limits (D.L.) for trace elements analyzed by ICP-MS........ 117
Table 9 Detection limits (D.L.) for trace elements analyzed by ICP-MS........ 118
Table 10 Normalizing values used in extended REE plots........ 118
Table 11 Major- and trace-element analyses of clinopyroxenite from the Gander River Complex........ 118
Table 12 Anhydrous, major- and trace-elements analyses of altered ultramafic rocks of the Gander River Complex 119
Table 13a Major oxide and trace-element analyses of mafic rocks of the Gander River Complex........ 120
Table 13b Rare-earth element analyses of selected mafic rocks from the Gander River Complex........ 121
Table 14a Major oxide and trace-element analyses of trondhjemite from the Gander River Complex........ 122
Table 14b Rare-earth-element analyses of selected trondhjemite samples from the Gander River Complex........ 122
Table 15 CIPW norms for trondhjemite from the Gander River Complex........ 123
Table 16 Major- and trace-element analyses of sandstone and siltstone and one limestone (sample # 86-800) from the Weir's Pond Formation, Davidsville Group........ 124
Table 17a Major- and trace-element analyses of sandstone, pelites (sample #'s 86-293, 89-625 and 87-839), calc-silicate rock (sample # 86-296) and a coticule rock (sample # 86-288) from the Jonathan's Pond Formation..... 126
Table 17b Major- and trace-element analyses of intrusive mafic bodies in the Gander Group........ 128
Table 17c Major- and trace-element analyses of intrusive intermediate bodies in the Gander Group........ 129
Table 18 Major- and trace-element analyses of sandstone, pelite (sample #'s 87-653, 87-760, 87-677), mafic volcanic rock (sample # 87-698) and intermediate intrusive rock (sample # 87-678) from the Indian Bay Big Pond Formation........ 130
Table 19 Major- and trace-element analyses of the Deadman's Bay and Ocean Pond granites and Unit 18 (sample # 86-269)........ 132
Table 20 CIPW norms of the Deadman's Bay and Ocean Pond granites and Unit 18........ 134

APPENDIX 3–GEOCHRONOLOGY........ 135
Table 1 The $^{40}Ar/^{39}Ar$ analytical data on muscovites, biotites and amphibole from the Weir's Pond Area, northeastern Gander Zone........ 136

APPENDIX 4–RESULTS OF POINT COUNTING REPRESENTATIVE SAMPLES FROM THE GANDER AND DAVIDSVILLE GROUPS........ 140
Table 1 Point counts of sedimentary rocks of the Davidsville Group........ 141
Table 2 Point counts of sedimentary rocks of the Jonathan's Pond Formation........ 142
Table 3 Point counts of sedimentary rocks of the Indian Bay Big Pond Formation........ 143

APPENDIX 5–TABLE OF SAMPLES MENTIONED IN TEXT AND THEIR GRID REFERENCES........ 144
Table 1 Location numbers and military grid references (MGR) for all samples mentioned in the text and for which geochemical analyses are listed........ 144

Numbers in parenthesis (six digit numbers) found in the text refer to Military Grid References.

FIGURES

Page

Figure 1: Location map of the Weir's Pond area (NTS 2E/1), northeastern Newfoundland.......... 2

Figure 2: Simplified geological map of northeastern Newfoundland showing the principal rock units; enlarged part on left, is part of the Gander River Complex and Davidsville Group between Weir's Pond and Gander Lake. The circled numbers refer to location of stratigraphic sections described in the text (see Figure 39).......... 3

Figure 3: Location map showing the Ocean Pond, Moccasin Pond, Wing Pond and Big Bear Cove Pond areas as defined in the text. 'Condensed isograd' refers to 'isograd' bounding zone, in which the assemblage kyanite−sillimanite−andalusite−staurolite−garnet−biotite, is present.......... 24

Figure 4: Representative stratigraphic sections from the Jonathan's Pond Formation (Vf, F, M, C and VC = very fine, fine, medium, coarse, very coarse; SST = sandstone).......... 27

Figure 5: The igneous spectrum plot of Hughes (1973). Squares (open and closed) are gabbros, x are diabase and inverted triangles are basalt of the Gander River Complex.......... 41

Figure 6: An AFM diagram for representative analyses of mafic, ultramafic and felsic rocks of the Gander River Complex, Weir's Pond area. Fields for ultramafic and mafic cumulate rocks and the Skaergaard trend from Coleman (1977) and the Annieopsquotch trend from Dunning (1984). Field of Papua and Oman ultramafic rocks from Malpas and Stevens (1977).......... 41

Figure 7: A selection of Harker diagrams illustrating the prinicipal chemical trends in ultramafic rocks of the Gander River Complex. The diamonds are fresh clinopyroxenites and the number symbol represents altered ultramafic rocks.......... 42

Figure 8: The SiO_2 vs. $FeO_{(tot)}/FeO + MgO$ plot for ultramafic rocks from the Gander River Complex. Fields from Coleman (1977). Squares (open and closed) are gabbros, x are diabase, inverted triangles are basalt, diamonds are fresh clinopyroxenites and number symbol represents altered ultramafic rocks.......... 43

Figure 9: The classification of mafic rocks of the Gander River Complex according to the fields of Winchester and Floyd (1977). Squares (open and closed) are gabbros, x are diabase and inverted triangles are basalt.......... 43

Figure 10: Basalt and diabase display their tholeiitic nature whereas gabbros are split into two groups in this tholeiitic vs. calc-alkalic discriminant plot of Miyashiro (1975). Squares (open and closed) are gabbros, x are diabase and inverted triangles are basalt.......... 43

Figure 11: The TiO_2 vs. Y plot for mafic rocks of the Gander River Complex. Gabbros are already split into two groups, neither of which are apparently related to the diabase and basalt. Squares (open and closed) are gabbros, x are diabase and inverted triangles are basalt.......... 43

Figure 12: Variation of some oxides and trace elements with the Mg #. Squares (open and closed) are gabbros, x are diabase and inverted triangles are basalt.......... 44

Figure 13: Tectonic discrimination of mafic rocks of the Gander River Complex based on Zr/Y vs. Zr ratios. Fields from Pearce and Norry (1979). Squares (open and closed) are gabbros, x are diabase and inverted triangles are basalt.......... 45

Figure 14: Tectonic discrimination of mafic rocks of the Gander River Complex based on Ti vs. V ratios. Fields from Shervais (1982). Squares (open and closed) are gabbros, x are diabase and inverted triangles are basalt.......... 45

Page

Figure 15: Island-arc affinity of mafic rocks of the Gander River Complex based on Ni vs. Ti/Cr ratios. Fields from Beccaleuva *et al.* (1979). Squares (open and closed) are gabbros, x are diabase and inverted triangles are basalt 45

Figure 16: Partial extended REE plots for mafic rocks of the Gander River Complex. In lowest diagram, the + pattern represents Group 1 gabbro and the open circle and square represent Group 2 gabbros 47

Figure 17: Partial extended REE plots for mafic rocks of the Gander River Complex compared to island-arc tholeiite field of New Britain (B.V.S.P., 1981) 48

Figure 18: Selection of Harker diagrams displaying geochemical trends in plagiogranite of the Gander River Complex. Triangles are coarse grained, and squares are porphyritic plagiogranites 49

Figure 19: Selection of Harker diagrams displaying variation between major oxides and trace elements and SiO_2 in plagiogranite of the Gander River Complex. Triangles are coarse grained, and squares are porphyritic plagiogranites 50

Figure 20: Normative Ab–An–Or diagram (after O'Connor, 1965) for plagiogranite of the Gander River Complex 51

Figure 21: The AFM plot for trondhjemites of the Gander River Complex. Closed squares are oceanic plagiogranites (Coleman and Donato, 1979). Triangles are coarse grained, and squares are porphyritic plagiogranites 51

Figure 22: Partial extended REE plot for trondhjemites of the Gander River Complex 51

Figure 23: The CaO vs. Zr and Y for trondhjemite of the Gander River Complex. Fields for the Little Port Complex from Malpas (1979); field from Twillingate Complex from Payne and Strong (1979) 52

Figure 24: The Rb vs. Sr for trondhjemite of the Gander River Complex. Fields are–Little Port Complex (Malpas, 1979), Twillingate Complex (Payne and Strong, 1979), continental granophyre, continental trondhjemite and quartz diorite, oceanic plagiogranite (Coleman and Peterman, 1976); grey area denotes field of arc-related trondhjemite and high SiO_2, low-K rhyolite (Swinden, 1988) 53

Figure 25: Selection of Harker diagrams displaying geochemical variation within the Davidsville Group 54

Figure 26: Selection of Harker diagrams illustrating geochemical trends of major oxides and trace elements in rocks of the Jonathan's Pond Formation 56

Figure 27: Selection of Harker diagrams illustrating geochemical trends in sedimentary rocks of the Indian Bay Big Pond Formation 58

Figure 28: Comparative plot of sandstones from Gander and Davidsville groups. Solid triangles–Davidsville Group; X–Indian Bay Big Pond Formation; O–Jonathan's Pond Formation. Fields are 1) greywacke, 2) lithic arenite, 3) arkose, 4) subarkose, 5) sublithic arenite. Fields from Pettijohn *et al.* (1973) 59

Figure 29: Petrography-based discriminant plot of Zuffa (1979) showing results of point counted samples from Gander and Davidsville groups. Solid triangles–Davidsville Group; X–Indian Bay Big Pond Formation; O–Jonathan's Pond Formation. Fields are 1) greywacke, 2) lithic arenite, 3) arkose, 4) subarkose, 5) sublithic arenite. Fields from Pettijohn *et al.* (1973) 59

Figure 30: Normative Ab–An–Or diagram (after O'Connor, 1965) for Ocean Pond and Deadman's Bay granites and Unit 18 59

Page

Figure 31: Selected Harker diagrams illustrating geochemical trends in major and trace elements of Ocean Pond Granite (x) and Deadman's Bay Granite (open triangle) and Unit 18 (closed circle) 60

Figure 32: The $^{40}Ar-^{39}Ar$ age spectra on muscovite from the Jonathan's Pond Formation, Ocean Pond area 63

Figure 33: The $^{40}Ar-^{39}Ar$ age spectra on biotite from the Jonathan's Pond Formation, Ocean Pond area 63

Figure 34: The $^{40}Ar-^{39}Ar$ age spectra on granites within the Weir's Pond map area 64

Figure 35: The $^{40}Ar-^{39}Ar$ age spectra on detrital muscovite from a Davidsville Group sandstone and on hornblende from a gabbro of the Gander River Complex 64

Figure 36: The $^{40}Ar-^{39}Ar$ spectra and their locations in the Weir's Pond map area 65

Figure 37: Concordia plot for single zircon grains from a Jonathan's Pond Formation sandstone 66

Figure 38: Concordia plot for single sphene grains from a Jonathan's Pond Formation sandstone 67

Figure 39: Interpretive correlations between schematic sections from various parts of the Weir's Pond Formation (Davidsville Group). The locations of these sections are shown as circled numbers on Figure 2. (See Map 90-02 for key to unit numbers) 69

Figure 40: Contoured plot of poles to regional foliation in the Davidsville Group. Contour intervals are at 1, 3, 6, 9 and 12 percent per 1 percent area. The total number of measurements is 94 71

Figure 41: Simplified geological map of Weir's Pond map area, showing 4 sectors, defined for ease of representation of structural data 73

Figure 42: Contoured stereoplots of poles to S_2 as well as F_2 fold axes for the Gander Group. C.I. = Contour intervals (at x percent per 1 percent area). Two L_2 measurements, (filled squares) taken east of Harveys Pond, are also plotted with F_2 fold axes 74

Figure 43: Contoured stereoplots of poles to S_3 in the Gander Group 76

Figure 44: Contoured stereoplots of F_3 fold axes and L_3 lineations in the Gander Group 77

Figure 45: Relationship between porphyroblastesis and timing of deformational phases in the Ocean Pond area, Gander Group 79

Figure 46: Relationship between porphyroblastesis and timing of deformational phases in the Moccasin Pond area, Gander Group 82

Figure 47: Relationship between porphyroblastesis and timing of deformational phases in the Big Bear Cove Pond area, Gander Group 84

Figure 48: Isobaric equilibrium curves of reactions relevant to the metamorphic mineral assemblages in the Gander River Complex; (part reproduction of Figure 11-2, page 157 *in* Winkler, 1979) 87

Figure 49: Schematic AFM diagrams (from Winkler, 1979) depicting the mineral assemblages in the Ocean Pond area, Jonathan's Pond Formation. Prograde reactions that occurred in the study area may not necessarily have involved the exact assemblages shown here. BIO–Biotite, CHL–Chlorite, GT–Garnet, SILL–Sillimanite, STA–Staurolite, AND–Andalusite 91

Page

Figure 50: Pressure–temperature grid inferred from mineral assemblages in the Ocean Pond area. Curve (1) staurolite-in-reaction band from Winkler (1979); Curve (2) staurolite breakdown in presence of muscovite and quartz; unpublished curve from Carmichael (personal communication to T. Rivers (1990); Curve (3) from Hoschek (1969); Curve (4) from Winkler (1979). Stippled band represents a geothermal gradient of 100°C per km 92

Figure 51: Schematic AFM diagrams (Winkler, 1979) depicting the mineral assemblages west of Moccasin Pond, Gander Group 93

Figure 52: Pressure–temperature grid inferred from mineral assemblages in the Moccasin Pond area. Curves 1 to 4 from Winkler (1979). Stippled band represents a geothermal gradient of 100°C per km 94

Figure 53: Schematic AFM diagrams (Winkler, 1979) depicting mineral assemblages north of Big Bear Cove Pond, Gander Group 95

Figure 54: Schematic pressure–temperature grid inferred from partial metamorphic assemblages in the Wing Pond area, Gander Group. The stippled band represents a possible P-T path followed by the rocks as suggested by the mineral assemblages 96

Figure 55: Geophysically modelled plutons (J. Todd, personal communication, 1986) and simplified geology in the Weir's Pond map area. The 'x' pattern represents areas underlain by granite 98

Map 90-02: Geology of the Weir's Pond area .... back pocket

Map 90-03: Metamorphic geology and ^{40}Ar/^{39}Ar geochronology of the Weir's Pond area .... back pocket

Map 90-04: Geology of Davidsville Group and Gander River Complex, northwest Weir's Pond area .... back pocket

PLATES

Page

Plate 1: Layering in altered ultramafic rock due to compositional variations; Gander River Complex 11

Plate 2: Alternating plagioclase- (light coloured) and pyroxene-rich cumulate layers in gabbro of the Gander River Complex 12

Plate 3: Pillowed mafic volcanic rock from the Gander River Complex, Weir's Pond area 13

Plate 4: Foliated, coarse-grained plagiogranite having fine-grained mafic inclusions 13

Plate 5: Cataclastic brecciation in plagiogranite, collected from the largest exposure of plagiogranite (roadcut on Route 330), in the Weir's Pond area 14

Plate 6: Thickly bedded conglomerate of Unit 6 of the Weir's Pond Formation, Davidsville Group 16

Plate 7: Foliated gabbro cobble within conglomerate of subunit 6a of the Weir's Pond Formation, Davidsville Group 16

Plate 8: Coarse pebbly lenses in sandstone, interbedded with white-weathering quartz-rich, thinly bedded sandstone; Unit 6 of the Weir's Pond Formation, Davidsville Group 17

Plate 9: Volcanic detritus in Unit 6 of the Weir's Pond Formation, Davidsville Group, contains rounded quartz phenocrysts having distinctive authigenic overgrowths (scale bar is 1 mm long) 18

Plate 10: Thinly interbedded medium-grained quartzitic beds and black shale in gradational contact zone of Jonathan's Pond and Indian Bay Big Pond formations, Gander Group 25

Plate 11: Thinly bedded psammite and pelite of the Jonathan's Pond Formation 25

Plate 12: Thickly bedded (note metre stick) quartzite and semipelite of the Jonathan's Pond Formation: note lack of gradation between beds and sharp contacts 25

Plate 13: Plane-parallel laminations in siltstone–pelite of the Jonathan's Pond Formation, north shore of Indian Bay Pond 26

Plate 14: Regularly spaced parallel laminations in quartzitic beds of the Jonathan's Pond Formation; laminae are pelitic and are 1 to 3 mm thick. The main foliation (S_2) runs from top left to bottom right 26

Plate 15: Chert, on the left and black pelite on the right, marking the contact between Units 12 and 13 of the Indian Bay Big Pond Formation, north of Little Bear Cove Pond 34

Plate 16: Thinly bedded and laminated black pelite–siltstone containing minor sandy layers in Unit 13 of the Indian Bay Big Pond Formation 34

Plate 17: Morphologically well-preserved pillowed mafic volcanic rocks of Unit 15 of the Indian Bay Big Pond Formation 35

Plate 18: Foliated metasedimentary clasts in lithic arenite of Unit 16, Indian Bay Big Pond Formation (scale bar is one half millimetre) 37

Plate 19: Quartz vein, which intrudes the Gander Group, containing psammitic blocks of country rocks 39

Plate 20: The megacrystic, biotite-bearing Deadman's Bay Granite 40

Plate 21: Shear-band foliation in medium-grained gabbro of the Gander River Complex; pencil points southwestward 70

Page

Plate 22: Late brittle folding of an earlier foliation in ultramafic rock of the Gander River Complex.................. 70

Plate 23: High-strain foliation in altered ultramafic rocks of the Gander River Complex. (Scale bar is approximately 2.5 mm).. 70

Plate 24: Photomicrograph of high-strain foliation in conglomeratic or trondhjemitic rock from the western margin of the Gander River Complex (scale bar represents 1 mm).. 71

Plate 25: Intensely foliated conglomerate of subunit 6a, Weir's Pond Formation, Davidsville Group; the shear band implies a dextral sense of shear.. 71

Plate 26: Two phases of deformation affect rocks throughout much of the Gander Group................................. 72

Plate 27: Spaced, solution-seam cleavage (S_2) typically developed in psammite and quartzite of the Jonathan's Pond Formation.. 72

Plate 28: Isoclinal F_2 folds with associated axial-planar spaced solution-seam cleavage (S_2) in psammite and slaty cleavage in pelite; Jonathan's Pond Formation.. 75

Plate 29: Poor to incipient development of axial-planar cleavage (S_3) to slightly asymmetric F_3 folds in Jonathan's Pond Formation semipelite.. 75

Plate 30: Crenulation lineation (L_3) in pelite of the Jonathan's Pond Formation, Ocean Pond area. (Note blueberry for scale).. 78

Plate 31: High-strain zone near Wing Pond is developed in predominantly pelitic rock types which characteristically contain profuse quartz veins.. 78

Plate 32: Anastomosing high-strain foliation in chert of the Indian Bay Big Pond Formation............................ 78

Plate 33: Photomicrograph of high-strain foliation in quartzitic rock, characterized by intrafolial folds (of quartz lenticles); Jonathan's Pond Formation, west of Ocean Pond. (Scale bar = 1 mm)................. 78

Plate 34: Photomicrograph showing relationship between S_1, the earliest defined foliation (runs north-south in plate), S_2 the principal regional foliation (runs east-west) and F_3 microfolds; Jonathan's Pond Formation near Ocean Pond. (Scale bar is 0.5 mm approximately).. 80

Plate 35: Photomicrograph of biotite porphyroblast overprinting S_2 foliation defined mostly by fine-grained muscovite. (Scale bar is 1 mm approximately).. 81

Plate 36: Photomicrograph showing high-strain foliation developed in sillimanite-zone rock of the Ocean Pond area, Gander Group. (Scale bar is 1 mm approximately).. 81

Plate 37: Photomicrograph showing high-strain foliation, defined mostly by syntectonic muscovite, parallel to quartz lenticles in Wing Pond area, Gander Group. (Scale bar is 1 mm approximately)................... 83

Plate 38: Photomicrograph showing microfolds in andalusite defined by sillimanite, Wing Pond high strain zone, Gander Group. (Scale bar is 1 mm approximately).. 83

Plate 39: Random network of thin quartz veins that crisscross exposures of the sillimanite zone (Jonathan's Pond Formation) close to the Deadman's Bay Granite, west and north of Ten Mile Pond..................... 89

Plate 40: Disaggregated, sillimanite-rich pelitic layers within quartz-veined psammitic 'matrix', northwest of Ten Mile Pond, Jonathan's Pond Formation.. 89

Plate 41: Part of a calc-silicate lens in the Ocean Pond area, Jonathan's Pond Formation................................ 89

TABLES

Page

Table 1: Evolution of nomenclature of major geological units of northeastern Newfoundland 4

Table 2: Average element values of mafic rocks of the Gander River Complex, compared to average values of mafic rocks from various published sources 46

Table 3: Average element values of trondhjemite from the Gander River Complex, compared to published trondhjemite analyses from various sources 52

Table 4: List of mean analyses of sandstone and pelite from the Gander and Davidsville groups and published means for arkose, shale and greywacke 57

Table 5: List of samples dated by U–Pb and Ar–Ar methods and their location 62

Table 6: The U–Pb and Pb–Pb ages from single zircon grains, separated from a quartz granule sandstone of the Jonathan's Pond Formation 66

Table 7: The U–Pb and Pb–Pb ages from single sphene grains, from a quartz granule sandstone of the Jonathan's Pond Formation 66

ABSTRACT

The Weir's Pond map area in northeastern Newfoundland straddles the contact between the Dunnage Zone, represented by the Gander River Complex and Davidsville Group, and the Gander Zone, represented by the Gander Group.

Much of the map area is underlain by metasedimentary and granitoid rocks of the Gander Zone. The metasedimentary rocks form the Gander Group, which is subdivided into the Jonathan's Pond and Indian Bay Big Pond formations. The Jonathan's Pond Formation comprises psammite, semipelite, pelite and minor conformable, intrusive mafic bodies. The quartz-rich nature of the Jonathan's Pond Formation suggests that deposition occurred near a continental source. The U–Pb ages, from single zircon grains separated from a sandstone bed, imply a wide spread of source-rock ages from Late Archean to the Cambrian; however, the age of deposition of the formation is uncertain.

The Indian Bay Big Pond Formation comprises grey and maroon sandstone, grey and black pelite and mafic and intermediate volcanic rocks. Fossiliferous sandstone boulders, which occur locally, are interpreted to be derived from the Indian Bay Big Pond Formation and have been assigned a late Arenig to early Llanvirn age. The northwestern contact of the Indian Bay Big Pond Formation is apparently gradational with Jonathan's Pond Formation, whereas the southeastern contact with the southern belt of the Jonathan's Pond Formation, is marked by a high-strain zone. Arenaceous rocks of the Indian Bay Big Pond Formation contain higher than average chromium levels (between 2 and 3 times the levels found in the Jonathan's Pond Formation) and some volcanic detritus, suggesting the presence of a volcanic source that was not available during deposition of Jonathan's Pond Formation.

In the northwest map area, the Gander Group is structurally juxtaposed with the Gander River Complex and Davidsville Group. The Gander River Complex is composed of variably metamorphosed ultramafic, gabbroic, mafic volcanic and trondhjemitic rocks. Immobile-element chemistry of the mafic and felsic rocks suggests that they have an island-arc affinity. The ultramafic rocks may form imbricated parts of a substrate to the island arc.

The Davidsville Group is divided into three formations, two of which, the Weir's Pond and Hunts Cove formations, occur in the map area. The basal division, the Weir's Pond Formation, comprises fossiliferous late Arenig to early Llanvirn sandstone, conglomerate and sandstone of uncertain age, Middle Ordovician bioclastic limestone and quartz arenite and Caradoc graphitic black shale. This formation is structurally imbricated with the Gander River Complex. In one locality, unconformable relationships are preserved between Middle Ordovician limestone and ultramafic rock. Abundant ultramafic, mafic and felsic detritus characterizes sedimentary rocks of the Weir's Pond Formation, which suggests that the formation was deposited close to an igneous complex, most likely the Gander River Complex; therefore, the complex was probably exhumed and eroded during late Arenig times. The Hunts Cove Formation lies mainly to the northwest of the complex and consists of a monotonous sequence of shale, siltstone and fine-grained sandstone. This formation is not seen in contact with rocks of the Weir's Pond Formation. However, because of sedimentologic similarities between the two, they are assumed to be stratigraphically conformable.

In the northeast map area, the Gander Group is intruded by two granites; the garnetiferous, leucocratic Ocean Pond Granite and the megacrystic, biotite-rich Deadman's Bay Granite. The Ocean Pond Granite is associated with a regional high-temperature–low-pressure metamorphism, characterized by a prograde andalusite–sillimanite facies series. The Deadman's Bay Granite has a relatively narrow (relative to the Ocean Pond Granite), high-temperature–low-pressure contact metamorphic aureole, characterized by andalusite, cordierite and locally K-feldspar-bearing assemblages. In the southeast map area, near Wing Pond, a rapid increase in metamorphic grade occurs within a high-strain zone. Toward the centre of the zone, relict assemblages of kyanite–sillimanite–staurolite, overprinted by andalusite, are preserved within low-strain augen, enveloped by synkinematic muscovite. Outside of these specific higher grade areas, the Gander Group is regionally metamorphosed to chlorite grade.

Two main phases of deformation are defined in the Gander Group; the earlier phase is characterized by isoclinal folds, which are overprinted by a later phase of upright to asymmetric

folds. Porphyroblastesis within the regional metamorphic area, around the Ocean Pond Granite, overlaps this later phase of folding. In the Weir's Pond area, the Davidsville Group is affected by one main deformation, which has produced a steep foliation axial-planar to tight folds. Similarly, the rocks of the Gander River Complex record one main deformation, which, however, is much more heterogeneously preserved due to the contrasting rheologies of the rocks.

The regional northeast strike of the main foliation in the Davidsville Group and Gander River Complex is oblique to the regional north to north-northeast strike of the Gander Group. The complex, imbricated nature of the relationship between the Davidsville Group and the Gander River Complex and the absence of any apparent imbrication between either of these units and the Gander Group, suggest that the Davidsville Group and Gander River Complex were juxtaposed as one entity, with the Gander Group. Thus, the Gander Group may have acquired its predominant north-northeast structural grain before juxtaposition with rocks of the Dunnage Zone. A steep, northeast-striking high-strain foliation is heterogeneously developed in the Gander River Complex and Davidsville Group. Sparse kinematic indicators such as a moderately southwest-plunging pebble lineation and shear bands suggest some strike-parallel movement along this zone boundary. Whether this transcurrent motion was responsible for the juxtaposition of the zones or, was merely concentrated along this zone boundary, requires more detailed work. The timing of these events also remains unresolved.

The $^{40}Ar-^{39}Ar$ *ages on muscovite from the Ocean Pond Granite, and muscovite and biotite from the surrounding regional metamorphic rocks, suggest cooling through lower greenschist-facies conditions at approximately 400 to 390 Ma. The Deadman's Bay Granite is dated by U–Pb (zircon) at 385 Ma.*

INTRODUCTION

The Weir's Pond map area is centred 30 km northeast of the town of Gander in northeastern Newfoundland (Figure 1). It is bounded by latitudes 49°00' and 49°15'W and longitudes 54°00' and 54°30'N. Access to the northwest part of the area is provided by the Gander Bay Highway (Route 330) and old logging roads. The central part of the eastern half of the area is accessible by logging roads, which connect with Route 320, near Indian Bay. Helicopter-supported fly camps were used to map the northern and central parts of the area. Numerous lakes in the eastern half of the map area allowed easy access by boat.

PREVIOUS WORK AND REGIONAL RELATIONSHIPS

Previous geological studies in the Weir's Pond map area have been largely of a reconnaisance nature. However, the three principal geological subdivisions, the Gander and Davidsville groups and the Gander River Complex (formerly the Gander River Ultrabasic Belt) (Figure 2), are well established. In this section, rock descriptions and regional correlations of the three units are summarized, based on reports by researchers in the Weir's Pond and adjoining areas. Table 1 outlines the evolution of geological nomenclature and ages of the major units in the Gander Lake–Gander Bay region.

Murray and Howley (1881) carried out the earliest geological reconnaisance work in northeastern Newfoundland. They suggested that rocks exposed at First Pond (Figure 1) on Gander River were part of the Lower Silurian Quebec Group and that slates near Gander Lake were similar to Upper Silurian slates in Hamilton Sound and the Bay of Exploits. Rocks of the Quebec Group were considered to be in tectonic or nonconformable contact with schistose rocks to the east. They also mapped ultramafic rocks exposed along Gander River and assigned sedimentary rocks in the Gander Lake area to the Silurian period; granitic bodies south and east of Gander Lake were classified as Precambrian Laurentian gneiss.

Chromite occurrences near Gander River were examined by Snelgrove (1933, 1934), who assigned the host ultramafic rocks to the Eastern Serpentine Belt. In the early 1940's and again in 1951-1952, personnel from the Geological Survey of Newfoundland re-examined the Eastern Serpentine Belt and documented most of the ultramafic bodies north and south of Gander Lake (Jenness, 1954).

Phyllite, slate and quartzite exposed on the shores of Gander Lake and along Gander River were assigned to the 'Gander Lake Series' by Twenhofel (1947), who interpreted these rocks as unconformably overlying the mica schists to the east. He correlated, on the basis of lithological similarities, the Gander Lake Series with dated Silurian rocks in the eastern part of Gander Bay. However, Twenhofel (1947) considered that all strata on the Gander River below Glenwood were Ordovician (although the rocks are unfossiliferous); the nature of the contact between the Silurian and Ordovician units was unknown. Granitic bodies south and east of Gander Lake were considered to be post-Silurian intrusions.

One of the earliest regional mapping programs in northeastern Newfoundland was carried out by Baird *et al.* (1951). This survey covered the area from Hamilton Sound southward to Fortune Bay, and from Ocean Pond in the east to Grand Falls, in the west. They documented a muscovite granite at Ocean Pond that intruded garnetiferous, mica schists, which they interpreted to be metamorphosed equivalents of quartzite, greywacke and phyllite farther west. These strata were considered to be Silurian in age. Baird *et al.* (1951) disagreed with Twenhofel's (1947) interpretation of the Gander Lake sedimentary rocks as a single series of Silurian age and suggested that the west half of Gander Lake is underlain by Ordovician rocks. They described ultramafic rocks of the Gander River Complex as being interbedded with sedimentary and minor volcanic rocks and noted that the association of gabbro, pyroxenite, volcanic rocks and talc carbonate schists are generally typical of the complex. The volcanic rocks in the Gander region were first recognized by Baird *et al.* (1951).

Jenness (1958) proposed the term Gander Lake Group, to replace the term Gander Lake Series (Twenhofel, 1947), for the great thickness of interbedded sedimentary and volcanic rocks, exposed on Gander Lake. He assigned the group to the Middle Ordovician, based on graptolite and brachiopod fauna, and he mapped northeast-trending linear belts of volcanic, volcaniclastic and plutonic rocks within slate, sandstone, limestone, phyllite and conglomerate. He regarded the volcanic rocks, which comprise tuff, agglomerate and lava, as being conformably interbedded with the sedimentary rocks. Jenness (1954, 1958) provided the first detailed descriptions of the ultramafic rocks north of Gander Lake and included them in the Gander River ultrabasic belt (partly equivalent to the Gander River Complex of this report). He proposed that the ultramafic rocks were small lenticular bodies intrusive into the sedimentary rocks of the Gander Lake Group and described the gabbro and ultramafic bodies as being almost entirely restricted to the volcanic belt.

Jenness (1963) subdivided the Gander Lake Group into conformable lower, middle and upper units. The lower unit was composed mainly of arenaceous rocks, the middle unit of mixed sedimentary and volcanic rocks and the upper unit of mainly argillaceous rocks. Gabbro and ultramafic rocks were located within the middle unit. Paragneiss and migmatite that were exposed in the east were included in the lower unit. He noted that the Gander Lake Group may also continue southwestward to the south coast to merge with the Baie d'Espoir Group of Jewell (1939).

Williams (1964) extended Jenness's three-fold subdivision of the Gander Lake Group northward. He interpreted

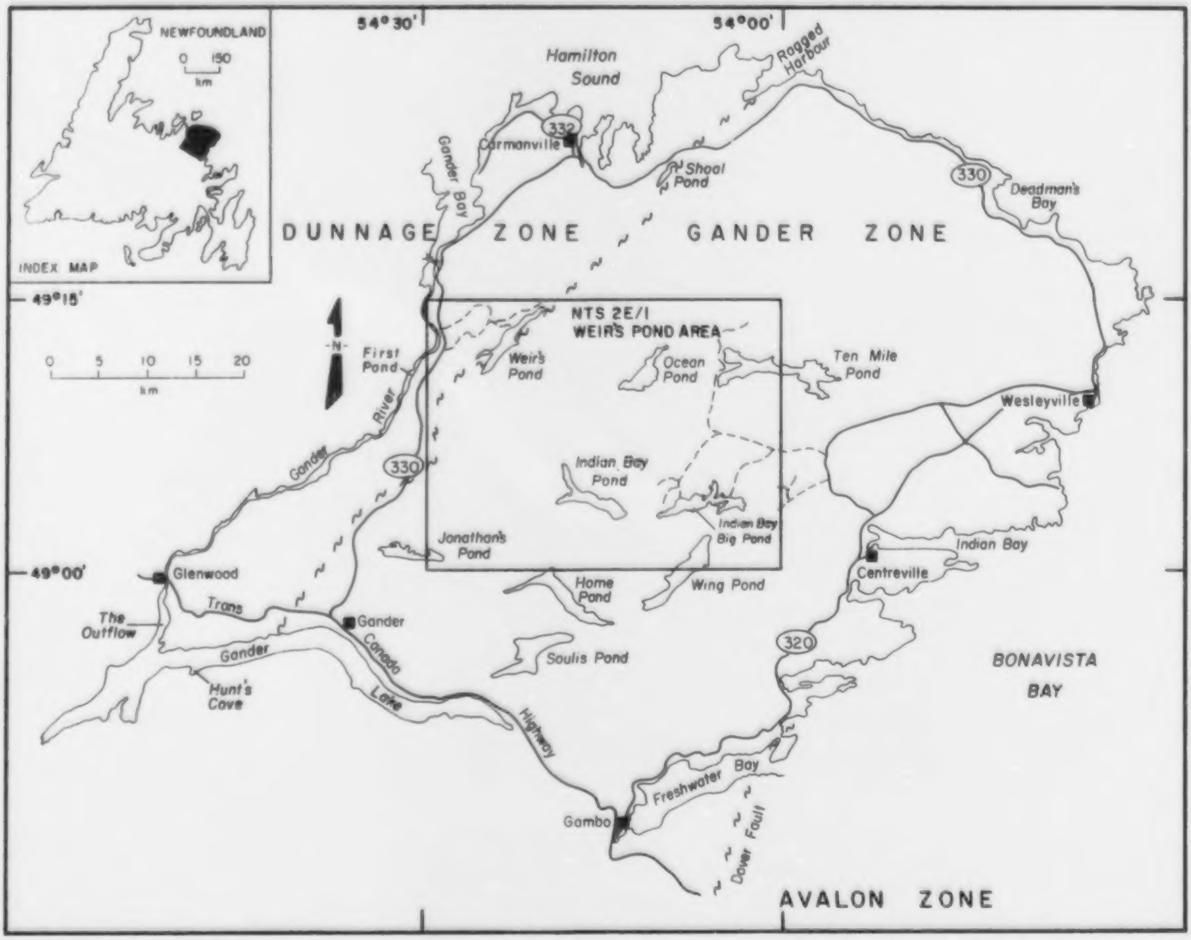
NEWFOUNDLAND
0 150
km
INDEX MAP
54°30'
54°00'
49°15'
49°00'
0 5 10 15 20
km
-N-
Hamilton Sound
Ragged Harbour
332
Carmanville
Gander Bay
Shoal Pond
330
Deadman's Bay
DUNNAGE ZONE
GANDER ZONE
NTS 2E/1
WEIR'S POND AREA
First Pond
Weir's Pond
Ocean Pond
Ten Mile Pond
Wesleyville
Gander River
330
Indian Bay Pond
Indian Bay Big Pond
Indian Bay
Jonathan's Pond
Centreville
Glenwood
Home Pond
Wing Pond
The Outflow
Trans
Gander
Canada
Highway
Gander Lake
Hunt's Cove
Soulis Pond
320
BONAVISTA BAY
Freshwater Bay
Gambo
Dover Fault
AVALON ZONE

Figure 1. *Location map of the Weir's Pond area (NTS 2E/1), northeastern Newfoundland.*

ultramafic bodies of the belt as being related to the gabbro and volcanic rocks. Stevens *et al.* (1974) and Malpas and Strong (1975) interpreted the ultramafic rocks as mantle diapirs intrusive into the sedimentary rocks of a Paleozoic marginal ocean basin. Kennedy (1975) suggested that the complex may represent remnants of an ophiolite suite. The term Gander River ultrabasic belt (Jenness, 1958) was retained by Blackwood (1978, 1979) and given the acronym GRUB (line) by Blackwood (1980). However, Blackwood (1982) redefined the term GRUB to include not only the pyroxenites and altered ultramafic rocks, but also volcanic and felsic plutonic rocks intimately associated with them. These rock types are retained in this report under the name Gander River Complex.

The Gander Lake Group was redefined by Kennedy and McGonigal (1972) so that it consisted only of the lower (arenaceous) unit, and the new term, Davidsville Group, was proposed for the fossiliferous middle and upper units. They included mafic volcanic rocks within the Davidsville Group and concluded that the ultramafic and mafic plutonic rocks are Middle Ordovician and older. A well-exposed contact, on the north shore of Gander Lake, between conglomerate of the Davidsville Group and serpentinized ultramafic rock was described by Kennedy (1975) as an unconformity.

The Gander (Lake) Group was interpreted by Kennedy and McGonigal (1972) as the western part of a continental rise prism, of possible Cambrian to Eocambrian age, which thinned eastward to the Avalon 'platform'. Blackwood (1982) supported these conclusions and suggested that the group formed in pre-Middle Ordovician times. The term Gander Lake Group was informally amended to Gander Group by McGonigal (1973) and formally proposed by Blackwood (1982). The redefinition of the Gander Lake Group, generated much criticism (Brückner, 1972; Jenness, 1972) mainly because the change contravened the Code of Stratigraphic Nomenclature (see Blackwood, 1982, for discussion). However, the term Gander Group is now well-established.

Rocks of the Weir's Pond area were briefly examined by Blackwood (1978), who carried out a regional reconnaisance

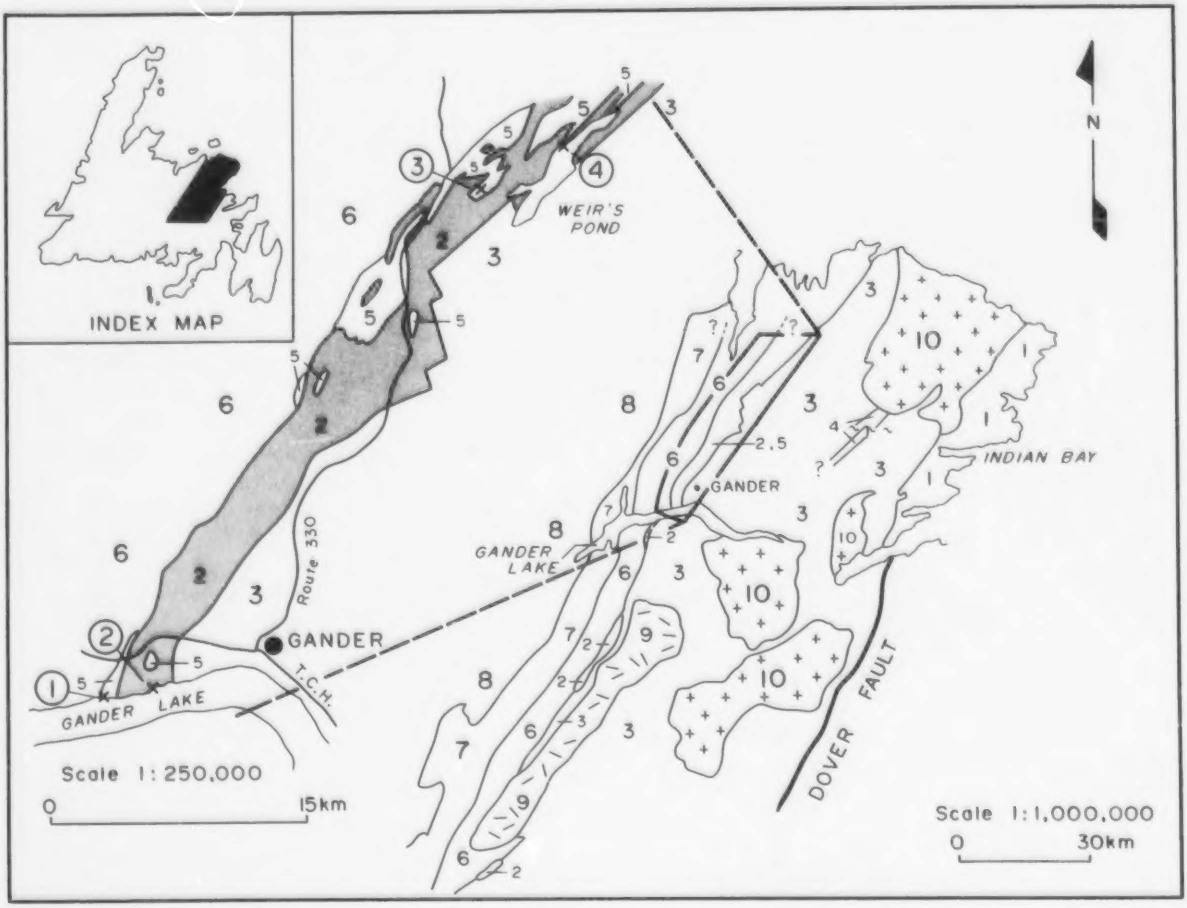
INDEX MAP
1.
N
WEIR'S POND
GANDER
GANDER LAKE
Route 330
T.C.H.
Scale 1: 250,000
0
15km
INDIAN BAY
DOVER FAULT
GANDER LAKE
GANDER
Scale 1: 1,000,000
0
30km
①
②
③
④
2.5
?

LEGEND

10 DEVONIAN GRANITE

9 SILURO—DEVONIAN GRANITE

SILURIAN

8 BOTWOOD GROUP

ORDOVICIAN

DAVIDSVILLE GROUP (Units 5 to 7)

7 THE OUTFLOW FORMATION

6 HUNTS COVE FORMATION

5 WEIR'S POND FORMATION

EARLY ORDOVICIAN OR EARLIER

GANDER GROUP (Units 3 and 4)

4 INDIAN BAY BIG POND FORMATION

3 JONATHAN'S POND FORMATION

2 **GANDER RIVER COMPLEX**

SILURO—DEVONIAN AND OLDER

1 UNSEPARATED HARE BAY GNEISS AND GRANITOID ROCKS

Figure 2. *Simplified geological map of northeastern Newfoundland showing the principal rock units; enlarged part on left, is part of the Gander River Complex and Davidsville Group between Weir's Pond and Gander Lake. The circled numbers refer to location of stratigraphic sections described in the text (see Figure 39).*

Table 1. Evolution of nomenclature of major geological units of northeastern Newfoundland

AUTHOR / AGE		Murray and Howley (1881)	Snelgrove (1933, 1934)	Twenhofel (1947)	Jenness (1954, 1958, 1963)	Kennedy and McGonigal (1972)	Uzuakpunva (1973)
NO AGE ASSIGNED		ULTRABASIC ROCKS	EASTERN SERPENTINE BELT	POST-SILURIAN GRANITES MICA SCHISTS IN EAST			
DEVONIAN					DEVONIAN GRANITE		
SILURIAN		UNNAMED SLATES NEAR GANDER LAKE AND BY GANDER BAY QUEBEC GROUP OR UNSEPARATED SCHISTS		GANDER LAKE MEMBER			
ORDOVICIAN	UPPER				GANDER RIVER ULTRABASIC BELT		
	MIDDLE				GANDER LAKE GROUP	DAVIDSVILLE GROUP	DAVIDSVILLE GROUP PYROXENITES + SERPENTINITES + GARNET – MUSCOVITE – BIOTITE GRANITES GANDER GROUP
	LOWER					ULTRAMAFIC AND MAFIC PLUTONIC BODIES GANDER LAKE GROUP	
CAMBRIAN							
PRECAMBRIAN		LAURENTIAN GNEISS					

KEY
Conformable contact ——
Unconformable contact ∿∿∿
Fault ⟶
Age range unknown ┆┈┆

mapping program, focussing on the Gander River Complex and the Davidsville and Gander groups. He collected fossils from a limestone (first mapped by Jenness, 1958), which unconformably overlies serpentinized ultramafic rock on the west shore of Weir's Pond. Dr. R.J. Neuman (in a written communication to Blackwood, 1978) identified the fauna as Early to early Middle Ordovician. This age was refined by Stouge (1979, 1980) to late Llanvirn to early Llandeilo, based on conodont identification.

The Gander and the Davidsville groups appear to come in contact locally, due to the discontinuous nature of the Gander River Complex, and the nature of this boundary has been the subject of much debate. Kennedy and McGonigal (1972) proposed that deformation and metamorphism of the Gander (Lake) Group occurred prior to deposition of the Davidsville Group, and cited as evidence the presence of detrital biotite and garnet, and mafic schist and psammite fragments in basal conglomerate and greywacke of the Davidsville Group. Therefore, the Davidsville Group was interpreted to overlie the Gander Lake Group with an inferred major angular unconformity. Blackwood (1978) noted that the nature of the contact between the Davidsville and Gander groups is enigmatic where the Gander River Complex is present. In areas where the complex is absent, near Island Pond in the Carmanville area and south of Gander Lake, the contact relationships between the Davidsville and Gander groups have been interpreted as conformable (Currie and Pajari, 1977; Blackwood, 1982, respectively). However, Currie and Pajari (1977) also describe rocks exposed along Ragged Harbour River that contain a mylonitic foliation. They also note that complex relict fold structures in rocks of the Gander Group do not occur in the Davidsville Group, 'possibly indicating a structural discontinuity between Gander and Davidsville sequences'.

Uzuakpunwa (1973) carried out detailed studies of the Gander and Davidsville groups and associated igneous rocks in the Ladle Cove–Ragged Harbour–Island Pond area (northeast of Weir's Pond). Based on detailed structural studies, he concluded that there were four main phases of deformation in the Gander Group and two in the Davidsville Group and that the Gander Group had acquired a composite fabric before emplacement of the Davidsville Group. He also noted that the metamorphic fragments in the melange of the Davidsville Group have F_3 folds that predate incorporation of the fragments. The melange also contains blocks of serpentinized dunite breccia, mafic pillow lava and hornblende gabbro, which he asserted were not genetically related to pyroxenite and serpentinite nearby. He considered the melange to be tectonic and to have formed during upthrusting of the Davidsville Group onto the Gander Group as a folded nappe. Further, he interpreted the two groups to be separated by either a melange, an ultramafic belt or a fault and he mapped a narrow band of intensely foliated phyllite in the Ragged Harbour River area.

Table 1. Continued

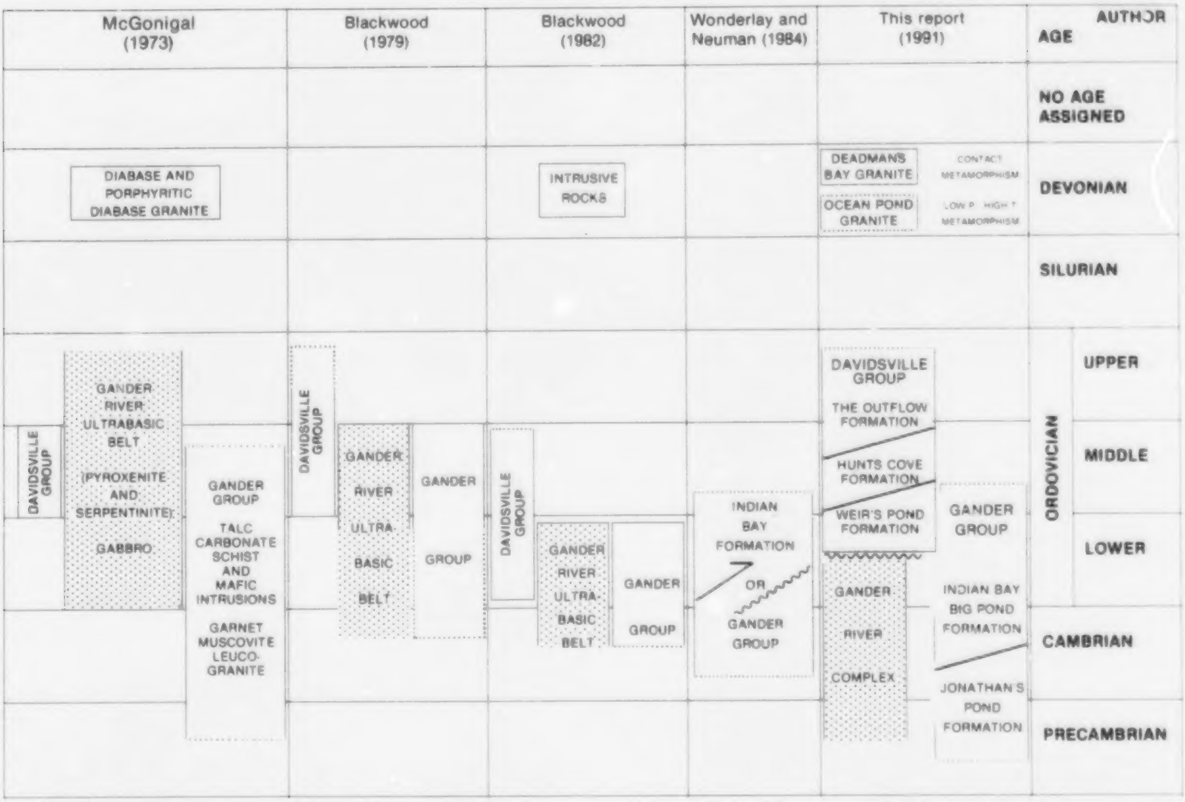
McGonigal (1973)
Blackwood (1979)
Blackwood (1982)
Wonderlay and Neuman (1984)
This report (1991)
AUTHOR
AGE
NO AGE ASSIGNED
DEVONIAN
SILURIAN
ORDOVICIAN
UPPER
MIDDLE
LOWER
CAMBRIAN
PRECAMBRIAN
DIABASE AND PORPHYRITIC DIABASE GRANITE
DAVIDSVILLE GROUP
GANDER RIVER ULTRABASIC BELT (PYROXENITE AND SERPENTINITE) GABBRO
GANDER GROUP
TALC CARBONATE SCHIST AND MAFIC INTRUSIONS
GARNET MUSCOVITE LEUCOGRANITE
DAVIDSVILLE GROUP
GANDER RIVER ULTRABASIC BELT
GANDER GROUP
INTRUSIVE ROCKS
DAVIDSVILLE GROUP
GANDER RIVER ULTRA-BASIC BELT
GANDER GROUP
INDIAN BAY FORMATION
OR
GANDER GROUP
DEADMANS BAY GRANITE
CONTACT METAMORPHISM
OCEAN POND GRANITE
LOW P, HIGH T METAMORPHISM
DAVIDSVILLE GROUP
THE OUTFLOW FORMATION
HUNTS COVE FORMATION
WEIR'S POND FORMATION
GANDER GROUP
GANDER RIVER COMPLEX
INDIAN BAY BIG POND FORMATION
JONATHAN'S POND FORMATION

The Carmanville map area, located immediately north of the Weir's Pond map area, was also the focus of a number of studies, carried out under the auspices of the Geological Survey of Canada in the 1970's (Pickerill *et al.*, 1978, 1979, 1981; Pajari and Currie, 1978; Pajari *et al.*, 1979; Currie and Pajari, 1977; and Currie *et al.*, 1979, 1980). Currie and Pajari (1977) described the upper part of the Davidsville Group as consisting of a monotonous repetition of greywacke, black pelite and minor pebble conglomerate, which comprised an 'extensively bioturbated, shallow water unit'. They concluded that hyaloclastite and debris flows in the basal part of the Davidsville Group, near Carmanville, form part of an allochthonous sheet, spatially associated with olistostromal melange at its base. Pajari *et al.* (1979) have interpreted this melange, which contains granule- to kilometre-size fragments in a shale matrix, to be ophiolitic. They suggested that olistostrome formation may have commenced as early as Arenig times and they used tentative correlations between the Dunnage and Carmanville melanges to infer that the melanges represent the northern margin of a sheet of ocean-floor and island-arc rocks. They suggested that the fragments were derived mainly from early Paleozoic oceanic crust and volcanic rocks (now represented by the Gander River Complex), which they interpreted to have been obducted eastward over the eastern continental margin. Pickerill *et al.* (1981) quoting unpublished chemical data, suggested that the chemical characteristics and relationships between volcanic facies in the Carmanville melange, indicate that these igneous rocks formed on oceanic islands or guyots on oceanic crust.

Blackwood (1982) indicated that the Gander River ultrabasic belt formed the hanging wall of a faulted contact with the Gander Group, west of Jonathans Third Pond, and that it is nonconformably overlain and bounded to the west by the Davidsville Group. He interpreted the Davidsville Group as representing a submarine fan having distal deposits in the east and proximal deposits in the west; spatially restricted proximal conglomerates, which occur in the basal Davidsville Group, were a product of erosion of ophiolitic basement that was uplifted along wrench–transform faults. He proposed (in contrast to Currie *et al.*, 1979) that this initial uplift was due to 'oceanic disturbances' (rather than obduction) and interpreted the faulted contact between the Gander River Complex and the Gander Group as a major west-dipping thrust along which the complex was emplaced above the Gander Group during later, regional deformation. Blackwood (1982) also noted that the Davidsville Group formed part of the hanging wall of this thrust sheet. Pajari *et al.* (1979) also described the contact between the complex and the Gander Group, southeast of Shoal Pond, as a fault.

Piasecki (1988) suggested that the contact between the Gander and Davidsville groups is tectonic, based on preliminary work northeast of Weir's Pond, and defined by a kilometre-wide mylonite zone, in which kinematic indicators imply south- to southwest-directed shear movements of Davidsville Group over the Gander Group.

In contrast to the western part of the map area, little detailed work has been carried out in the eastern half. The Wesleyville area, immediately to the east of the study area, was mapped by Williams (1968) who defined greywacke and quartzite (Gander Group) in the southwest as being conformable with muscovite–biotite schists in the east that locally contain garnet, andalusite and sillimanite.

Kennedy and McGonigal (1972), Blackwood and Kennedy (1975), Kennedy (1975) and Blackwood (1976, 1977) interpreted the metasedimentary rocks of the Gander Group as a cover sequence to schists and gneisses in the east. Blackwood and Kennedy (1975) termed these eastern gneissic rocks the Bonavista Bay Gneiss Complex, which they considered to be basement. Blackwood (1976, 1977) subdivided this complex into a paragneiss unit, the Square Pond Gneiss, and a migmatitic unit, the Hare Bay Gneiss. The Square Pond Gneiss included rocks immediately west and south of the Deadman's Bay Granite in the Weir's Pond map area. The contact zone between the gneissic units was described by Blackwood (1976, 1977) as a migmatite front. Blackwood (1978) re-evaluated the nature of the contact between the gneissic units and the Gander Group on the basis of further mapping and suggested that the Gander Group, Square Pond and Hare Bay gneisses were a conformable sequence, showing an eastward increase in metamorphic grade.

Strong *et al.* (1974) as part of a regional geochemical study of granitoid rocks in eastern Newfoundland, described the Deadman's Bay Granite as very homogeneous quartz-, plagioclase-, biotite-bearing and containing abundant microcline megacrysts. Their chemical analyses showed that the pluton (Deadman's Bay Granite), although petrographically a granite, locally containing over 40 percent alkali feldspar, also contains a large proportion of phases classified as quartz monzonite and granodiorite, based on molecular proportions of the CIPW norms. The Deadman's Bay Granite was mapped in the Wesleyville area by Jayasinghe (1976, 1978) who described it as a homogeneous, coarse-grained biotite granite, characterized by K-feldspar megacrysts.

Hanmer (1981) briefly examined rocks in the southeast part of the map area as part of a regional structural study, and proposed that much of the northeastern Gander Zone was an Acadian ductile shear zone exhibiting a dominant sinistral component of shear. He concluded that the intensity of the shearing and metamorphism increased toward the Dover Fault and that the ductile deformation occurred simultaneously with diapiric granite intrusions.

Detailed geological work was undertaken by P.R. Wonderley (see Wonderley and Neuman, 1984) around Indian Bay Big Pond, which resulted in the definition of the 'Indian Bay formation' (the Indian Bay Big Pond Formation of this study). Fossiliferous boulders found on the shores of Indian Bay Big Pond, were interpreted as *in situ* and derived from the Indian Bay Big Pond Formation. The included brachiopod fauna was assigned a late Arenig to early Llandeilian age. The Indian Bay Big Pond Formation was described by P.R. Wonderley (*op. cit.*) as having the same deformational and metamorphic history as the surrounding rocks. On the other hand, R.B. Newman (*op. cit.*) favoured interpreting the formation as an autochthonous sequence representing an isolated island in Iapetus, which was accreted to North America. P.R. Wonderley (*op. cit.*), however, preferred an allochthonous origin, in which the formation represents a transported slice of Dunnage Zone rocks.

Gravity and aeromagnetic data have been combined with geochemical patterns by Miller (1988) to model two belts of ultramafic and mafic rocks, of Dunnage Zone affinity, at depth, in the northeastern Gander Zone. The western belt, termed the Ocean Pond belt, was postulated as consisting of a series of granitic plutons underlain by mafic and ultramafic rocks. The eastern belt was modelled as underlying and being represented on the surface by, the Indian Bay Big Pond Formation. Miller (1988) used these models to conclude that the northeastern Gander Zone was allochthonous and that the Gander River Complex does not represent the easternmost extent of the Dunnage Zone.

Mineral Exploration

Prior to the 1970's, much of the exploration work in the area focussed on chromite and asbestos occurrences in ultramafic rocks. In his study of the serpentine areas of Newfoundland, Snelgrove (1934) defined two major serpentine belts, the Eastern and Western belts. He examined a significant chromite prospect, termed Chrome Hill, in the northeastern part of the Eastern Belt near Shoal Pond, 16 km north of Weir's Pond. Further, he described the chromite as occurring in serpentinite and serpentinized dunite. The largest body described was 2 m thick and 12 m long; approximately 50 other bodies of chromite, the largest being 25 cm by approximately 2 m long, were also present. A representative analysis of massive chromite yielded 47.77 percent Cr_2O_3, 18.67 percent FeO, 4.18 percent Al_2O_3, 4.1 percent SiO_2, 1.46 percent CaO and 19.69 percent MgO. Up to 2 percent chalcopyrite was also present in many samples. Baird *et al.* (1951) noted small and rare asbestos and chromite occurrences between Gander Lake and Shoal Pond. Geological Survey geologists working in the area in the 1940's and early 1950's, noted small asbestos veins locally (reported in Jenness, 1954). In 1951 and 1952, geologists with the Geological Survey of Canada conducted a magnetometer survey of Chrome and Cole hills. Small asbestos veinlets found on Cole Hill, approximately 1 km north of Weir's Brook, led to renewed interest in the Gander River Complex as a source of asbestos. However, these early studies revealed only small quantities of potentially economic minerals.

Newfoundland and Labrador Corporation (NALCO) carried out exploration work in this area in the 1950's, concentrating on rocks covering the area of the Gander River

Complex and investigating the potential for asbestos, chromite and base metals (Coleman, 1954a, b; Wall, 1954; Dunlop, 1955). Most of the asbestos found consisted of (platy to fibrous) antigorite or (columnar) picrolite. Chromite occurs commonly in the ultramafic rocks of the complex as disseminations and in 1- to 2-cm-wide bands, up to 2 m long and in lenses from several centimetres to 2 m across (Blackwood, 1982). Magnesite is also common throughout the complex, particularly north of Jonathan's Pond (Blackwood, 1982).

International Mogul Mines Limited, while exploring for base metals in the 1970's, carried out extensive magnetometer surveys of the area. Ground follow-up (which included two diamond-drill holes near Weir's Pond) of anomalies, defined minor pyrrhotite, pyrite and chalcopyrite mineralization associated with mafic volcanic or gabbroic rocks, and numerous graphitic conductors (Zurowski, 1974, 1977). Minor work was carried out by Minorex Limited (Durocher, 1979) but they then discontinued their base-metal exploration.

During the 1980's, gold exploration became the predominant theme. In 1981, following the discovery of arsenopyrite–pyrite in gabbro of the Gander River Complex (Blackwood, 1981), Westfield Minerals Limited staked a property near Jonathan's Pond (immediately west of the map area) based on an anomalous Au value (12.8 g/t) from a grab sample (Gagnon, 1981). At this prospect, quartz veins in a deformed gabbro, yielded assays of 1.2 g/t over 2.06 m and 1.5 g/t over 1.89 m. Noranda Exploration Limited also staked a property between Route 330 and Gander River in 1981 and were involved there in precious-metal exploration (MacKenzie, 1985). Several kilometres south of Weir's Pond, Noranda Exploration Limited also held property near Island Pond within the Gander Group. No information is available yet for this property. In 1988, Noranda Exploration Limited entered into a joint venture with NORONT, to spend 30 million dollars on exploration work in the Gander River Complex and eastern parts of the Davidsville Group (Tallman, 1989).

Duval International Limited acquired ground in 1984, several kilometres northeast of Westfield's Jonathan's Pond claims, based on anomalous values of gold in stream sediments. Follow-up work involved geological mapping, geophysics, soil and till sampling and analyses of panned concentrates. 'Wires and flakes of gold' were reported from silt samples, but no bedrock source was defined (Stephenson, 1985). Duval conducted no further work and their ground was dropped in the fall of 1986.

Esso Minerals Canada Limited carried out work in the Gander River Complex near Weir's Pond, to investigate an arsenopyrite–pyrite showing (Lenters, 1986, 1988). Anomalous gold values occur in late quartz–pyrite–arsenopyrite veins and associated silicified zones in mafic rock. This prospect is similar to the Jonathan's Pond showing in mineralization type and occurrence.

James Wade Engineering Limited carried out geological and geochemical surveys in 1988 in the Shoal Pond area for Exmar Resources Limited; these reports became available in March 1991.

Kidd Creek Mines Limited also carried out geological and geochemical surveys in the Shoal Pond and Jonathan's Pond areas; these reports are confidential until December 31, 1991.

Exploratory work in the Gander River Complex has been conducted by Newfoundland Resources and Mining Company Limited (Strickland, 1989; report confidential until July, 1992) and Newfoundland Minerals Incorported (Strickland and Sheppard, 1989; report confidential until September, 1992). Falconbridge Limited conducted geological and geochemical surveys in the Third Pond area of Gander River (Butler, 1988; report confidential until March, 1992).

Little mineral exploration work has been carried out in the eastern half of the map area. Butler *et al.* (1984) reported hand-size mineralized float containing chalcopyrite in argillite and pyrite in a graphitic pelite, south of Big Bear Cove Pond; these fragments may have been derived from the Indian Bay Big Pond Formation, which contains such rock types. In 1987, Noranda Exploration staked a property south of Indian Bay Big Pond based on a spot high gold value, 2200 ppb Au, from quartz veins and silicified psammite of the Indian Bay Big Pond Formation. Corona Corporation have also acquired property adjacent to Indian Bay Big Pond and are carrying out exploratory work there (Dimmell and Jacobs, 1989).

An Open File release on the distribution of gold and associated elements in the NTS 2/E map area was recently made available by the Newfoundland Department of Mines and Energy (Davenport and Nolan, 1988). The occurrence of anomalous gold concentrations within the Davidsville Group and particularly near the Indian Bay Big Pond Formation is of interest to this study.

PRESENT INVESTIGATION

This report presents the results of mapping of the Weir's Pond map area (NTS 2E/1) in 1986 and 1987, and subsequent research on the petrology, mineralogy, geochemistry and geochronology of the samples collected. Four reports (O'Neill 1987; O'Neill and Knight 1988; O'Neill and Blackwood, 1989; O'Neill and Lux, 1989) and preliminary Maps 86-62 (O'Neill, 1986) and 87-84 (O'Neill, 1987) have already been published. The project represents the continuation of mapping in the Gander River and Gander Lake area started by Blackwood (1977, 1978, 1979, 1980, 1981, 1982), the purpose of which was to map, at 1:50,000 scale, the Gander Zone and its boundaries. Maps 90-2, 90-3 and 90-4 accompany this report (in back pocket).

PHYSIOGRAPHY

Much of the map area is characterized by an undulating topography having an average elevation of approximately 80 m a.s.l. The highest elevations, approximately 150 m, occur west of Ten Mile Pond, whereas the floodplain of the Gander River marks the lowest elevations at approximately 15 m. West of Weir's Pond, ultramafic and gabbroic rocks of the Gander River Complex underlie some of the most rugged terrain in the map area. East of Weir's Pond, the topography is subdued and peat bog and forest cover equal proportions of the area. The sharpest contrast in elevation is found adjacent to Wing Pond, particularly along the east side, where the land rises, in places precipitously, from less than 45 to 150 m.

Drainage patterns in the area are varied, reflecting the combined effects of bedrock geology and Quaternary glaciation. Most of the larger lakes lie in the eastern half of the area and show no strong alignment. However, west and southwest from Ocean Pond in the north central part of the map area, lakes, including Weir's Pond, and brooks are strongly aligned north-northeast–south-southwest, reflecting the underlying geological grain. Locally, chains of small lakes outline lineaments. Weir's Brook flows southwest and then westward from Weir's Pond to Gander River, the major waterway in the map area. In the southwest, small brooks such as Traverse Brook flow south-southeastward. In the east and southeast, Ten Mile Pond, Moccasin Pond, Big Bear Cove Pond, Indian Bay and Indian Bay Big ponds drain eastward into Indian Bay.

A regional study of glaciation in eastern Newfoundland included the area in the 'outer drift zone' (Jenness, 1960). More detailed Quaternary studies, including till sampling, were conducted by Butler *et al.* (1984) and Vanderveer (1985). Results of these studies indicate that two ice flows affected the area. An earlier flow displayed a dominant west to east direction, whereas a later flow was partly topographically controlled, exhibiting a radial pattern, possibly related to a remnant ice cap in central Newfoundland as suggested by Grant (1974).

Numerous ultramafic boulders noted throughout the area during the present investigation suggest a westerly derivation from the Gander River Complex. One north-trending esker was noted in the map area, east of Wing Pond. Numerous rôches moutonnées have scarp slopes on the west side and gentle slopes on the east side, suggesting some east to west flow. Along the north central edge of the map area, the terrane is covered by an extensive boulder field. The boulders are mainly angular, up to several metres across and are predominantly locally derived. However, many of the boulders are of banded granitic material, a rock type not exposed in the map area, but may have been derived from the South Pond Complex in the Carmanville area (Currie *et al.*, 1979).

In 1961, much of the area north and northeastward from Indian Bay Pond was ravaged by a fire. Although completely destroying the logging operations in this part of Newfoundland, the fire has resulted in excellent rock exposures and blueberry 'fields'. Elsewhere in the south and west, the area is heavily forested or covered with small peat bogs and exposure is patchy.

GENERAL GEOLOGY

General Statement

The Weir's Pond map area straddles the boundary between the Dunnage and Gander tectonostratigraphic zones in northeastern Newfoundland (Williams *et al.*, 1974). The Gander River Complex and Davidsville Group represent the eastern part of the Exploits Subzone of the Dunnage Zone and the Gander Group represents the Gander Lake Subzone of the Gander Zone (subzone terminology after Williams *et al.*, 1988).

Here, the Davidsville Group is divided into the Weir's Pond (basal division), Hunts Cove and The Outflow formations, which range in age from late Arenig to Caradoc (note that The Outflow formation is not exposed in the map area (Map 90-04); however, it is briefly described herein). The Weir's Pond Formation, which is structurally imbricated with the Gander River Complex, comprises quartzose sandstone, conglomerate, quartz arenite and bioclastic limestone and interbedded grey and graphitic black shale. The conglomerate contains detritus representative of most rock types mapped in the Gander River Complex. To the northwest, the Hunts Cove Formation consists of a monotonous sequence of grey to green, and rarely purple shale. The Outflow Formation consists predominantly of fine- to coarse-grained sandstone, locally containing shale intraclasts, interbedded with grey to black siltstone and slate; conglomeratic beds form a minor component.

The Gander Group comprises interbedded psammite, semipelite and pelite having minor mafic and intermediate intrusions, and mafic flows; in the map area, the Gander Group is divided into the Jonathan's Pond and Indian Bay Big Pond formations. In the southeast of the map area, sedimentary rocks of the Indian Bay Big Pond Formation are bounded on both sides by rocks of the Jonathan's Pond Formation. The northwestern contact, previously interpreted as a thrust (Wonderley and Neuman, 1984) is here reinterpreted as stratigraphic. The southeastern contact, also previously interpreted as a thrust is coincident with a shear zone.

A critical contact relationship between ultramafic rocks of the Gander River Complex and Middle Ordovician limestone of the Davidsville Group is exposed on the western shore of Weir's Pond. This was described previously as a nonconformity by Blackwood (1978), an interpretation which is also adopted here, with the reservation that the contact zone contains a very strong foliation and, therefore, has been modified by deformation. The contact between the Gander River Complex and the Gander Group is not exposed in the mapped area.

Rocks of the Davidsville Group and the Gander River Complex have been heterogeneously affected by low-grade regional metamorphism. The effects of the regional deformation are seen as a penetratively developed, northeast-striking cleavage although strain intensity is heterogenous, particularly in the Gander River Complex.

In the north central part of the map area, the foliated, peraluminous Ocean Pond Granite is emplaced into the Gander Group and is associated with a regional low-P-high-T metamorphic facies series in the adjacent rocks. Biotite, garnet, andalusite, staurolite and sillimanite isograds are spatially related to the granite. The posttectonic, megacrystic, biotite-rich Deadman's Bay Granite intrudes the Gander Group in the east and cuts across the regional sillimanite isograd locally. The latter granite has a well-defined, hornfelsed contact aureole, which locally contains andalusite-, K-feldspar- and cordierite-bearing assemblages.

In the southeast of the map area near Wing Pond, local higher grade metamorphism is spatially associated with a high-strain zone in the Gander Group. The spatial proximity between low and higher grade zones suggests that isograds are locally compressed. Relict kyanite–staurolite–sillimanite assemblages, preserved within andalusite porphyroblasts indicate somewhat higher pressure than extant in the northwest.

The $^{40}Ar-^{39}Ar$ ages on muscovite and biotite from the Ocean Pond Granite and adjacent rocks, range from 385 to 400 Ma approximately (Map 90-03), and indicate cooling through greenschist-facies conditions in Middle Devonian (time scale of Haq and van Eysinga, 1987). The metamorphism occurred after the main, isoclinal phase of folding, but prior to or partly synchronously with a late, upright phase of open folding.

GANDER RIVER COMPLEX (Units 1 to 4)

DEFINITION

The term Gander River Complex is formally proposed here for ultramafic, mafic plutonic and extrusive rocks and plagiogranite that outcrop in the vicinity of Weir's Pond. The Gander River Complex replaces the term 'Gander River Ultrabasic Belt'. This redefinition is proposed for the following reasons:

1) 'Ultrabasic Belt' is an inadequate description of the complex as ultrabasic rocks only make up approximately 30 percent of the exposed outcrop in the area; gabbro, mafic volcanic rocks and plagiogranite are also critical rock types in the complex.

2) Unmetamorphosed pyroxenites previously included under the term 'ultrabasic' are relatively rich in silica, containing approximately 50 percent SiO_2. These rocks are better described as ultramafic in composition (Streckeisen, 1975).

3) Recently, the Pipestone Pond, Coy Pond and Great Bend complexes in central Newfoundland have been described and named in accordance with the North American Stratigraphic Code (1983). They contain a variety of rock types similar to those mapped in the Gander River Complex, i.e., ultramafic to felsic. Redefining the ultrabasic belt as a complex is in accordance with the Code and lends continuity to tectonostratigraphic nomenclature of northeastern and central Newfoundland.

Metamorphism does not pervasively affect rocks of the Gander River Complex and therefore, the individual units are referred to as e.g., gabbro rather than metagabbro.

DISTRIBUTION AND TYPE SECTION

The Gander River Complex is a northeast-striking, discontinuous unit of ultramafic, mafic and plagiogranitic rocks, best exposed in a 0- to 7-km-wide zone, extending northeastward from Gander Lake to the northeast coast of Newfoundland. The complex reaches its maximum width between Gander Lake and Weir's Pond. The most readily accessible and best exposed outcrops of the complex occur in this area. Several kilometres north of Weir's Pond, the complex pinches out and farther northeast toward Ragged Harbour, ultramafic rocks are again exposed. South of Gander Lake, the complex is apparently displaced westward by the Gander Lake Fault (McGonigal, 1973), and is represented by thin slivers of ultramafic rocks or altered equivalents. Plagiogranitic rocks are either very rare or nonexistent both in the Ragged Harbour area and south of Gander Lake. Adjacent to and west of Weir's Pond, the complex is distributed on a gross scale, into two discontinuous linear belts as defined by aeromagnetic anomalies (GSC Map # 4474G). These linear belts correspond roughly to mapped surface units of the Complex, which are structurally interleaved with sedimentary rocks of the Weir's Pond Formation (Map 90-04).

CONTACT RELATIONSHIPS

The complex is in presumed tectonic juxtaposition with the Gander Group (contact is not exposed in the Weir's Pond area) as Blackwood (1982) and Pajari *et al.* (1979) have described the contact, west of Jonathans Third Pond and southeast of Shoal Pond respectively, as a fault. On the west shore of Weir's Pond, serpentinized ultramafic rocks are in exposed contact with fossiliferous limestone of the Davidsville Group. This is the only exposed contact in this area between the ultramafic belt and sedimentary rocks of the Davidsville Group and it has been previously interpreted as an unconformity by Blackwood (1978). A contact of similar nature is exposed on the north shore of Gander Lake between conglomerate and serpentinized ultramafic rock and was interpreted by Kennedy (1975) as an unconformity.

Due to the complex structural interleaving of the Gander River Complex and Davidsville Group, there is no well-defined northwestern contact to the complex. However, in the southwest of the map area, approximately 1 km east of First Pond on Gander River, steeply dipping mafic, plagiogranitic and conglomeratic rocks exhibit a northeast-trending high-strain foliation. This high-strain zone appears to mark, at least locally, the contact between the complex and the monotonous shale sequence of the Hunts Cove Formation of the Davidsville Group.

AGE

The complex has not been directly dated and a minimum age can only be inferred from the age of overlying sedimentary rocks. Approximately 2 km west of the south end of Weir's Pond, an exposure of arenaceous rocks contains late Arenig fossils and abundant chromite detritus. The chromite is assumed to have been derived from the Gander River Complex and indicates a minimum late Arenig age for exhumation and erosion of the ultramafic rocks. Several plagiogranite samples from the complex were crushed at the Royal Ontario Museum for zircon extraction and U–Pb dating, however, no zircons were found.

Clinopyroxenite (Unit 1)

Distribution and Contact Relationships

Fresh clinopyroxenite has very limited distribution, occurring in single exposures that are generally less than 10 m across. Contacts between clinopyroxenite and adjacent rocks are not exposed: however, the approximate location of contacts is commonly marked by lineaments, which in most cases, are interpreted as faults.

Lithology

Unaltered clinopyroxenite is typically massive, coarse to very coarse grained and contains interlocking, approximately equidimensional clinopyroxene crystals up to 3 cm across. It is a very dark-green rock, which displays a smooth-weathering, brown surface. Pale-green patches and thin veinlets of serpentine, less than 1 cm thick, occur in places. Magnetite seams, 1 to 2 mm thick, also occur locally, and in the southwestern exposures, small pods of magnetite several centimetres across are present.

Petrography

Clinopyroxenite consists predominantly of clinopyroxene and minor alteration products such as amphibole and magnetite. The clinopyroxene generally is colourless, but in places it is slightly brownish. It has the composition of diopside and/or augite (See Appendix 1, Table 2, Sample # 86-117; Appendix 1, Table 1 contains replicate analyses of standard samples of FCPX). Orthopyroxene has not been positively identified; however, discrete patches of serpentine, up to 2 mm across, occurring within an interlocking aggregate of clinopyroxene, may be pseudomorphous after orthopyroxene.

Alteration in relatively fresh pyroxenites is confined to patches of serpentine less than 1 to 2 mm across and/or veinlets 1 mm or less wide. Magnetite is a commonly associated minor alteration product of serpentinization. A cataclastic deformation resulting in grain-size diminution is typically confined to narrow zones, less than 2 mm wide, locally forming intersecting networks. Individual pyroxene crystals may exhibit brittle deformation effects, such as displaced twin lamellae and a marginal alteration of clinopyroxene grains to tremolite–actinolite occurs in places.

Metamorphosed Ultramafic Rocks (Subunit 1a)[1]

Distribution and Contact Relationships. Metamorphosed ultramafic rocks occur throughout the area, but are in greatest abundance at the north end of Weir's Pond and in the southwest near Muddy Gullies and north of Weir's Brook. The largest exposures, which occur in the southwest, are several hundred metres across and form prominent ridges having steep flanks. These ridges are commonly bound by lineaments, easily seen on airphotos, which are interpreted to be faulted contacts. Exposed contacts between these rocks and adjacent units are rare; the best observed occurs on the northwest shore of Weir's Pond (Grid reference, (G.R.) 905554), where serpentinized ultramafic rock is in contact with bioclastic limestone of the Weir's Pond Formation. A tectonic foliation is developed in the rocks at the contact, the original nature of which has therefore, been modified by deformation. However, a discrete zone of shearing is absent and the previous interpretation of an unconformity (Blackwood, 1978) seems reasonable. Carbonatized and serpentinized ultramafic rock is also seen in sheared contact with gabbro in a roadside quarry on Route 330 (G.R. 842531). Elsewhere, bogs or lineaments define the locations of contacts between altered ultramafic rocks and adjacent units.

Lithology. Metamorphosed ultramafic rocks are, typically, easily recognized due to the characteristic colours in weathered outcrops, from bright green to variable hues of red to orange in serpentinites and carbonatized rocks, respectively. Magnesite alteration particularly, results in a very characteristic bright reddish-orange-weathering colour. Talc-rich rocks are typically foliated and weather grey to rusty brown.

Intense deformation has apparently affected many of the metamorphosed rocks and has resulted in further colour variation. In a roadside exposure on Route 330 (G.R. 833503), in the southwest of the area, a metamorphosed ultramafic rock displays wispy rose-coloured streaks (of hematite?) in a fine-grained cream-coloured matrix; this texture was produced by intense deformation of a carbonate–quartz–hematite assemblage. In one exposure southwest of Weir's Pond (G.R. 830500), intensely deformed talc-serpentine rocks weather to a very distinctive, streaky blue-grey colour. Deformational features of these metamorphosed rocks will be discussed in detail in the section on Structure (page 69).

---

[1] Included under this heading are all those ultramafic rocks exhibiting 60 percent or greater conversion to assemblages consisting of serpentine, carbonate, talc and chlorite mostly. The majority of the rocks described below display 100 percent hydration and/or carbonatization.

Generally, the metamorphosed rocks contain carbonate, talc and serpentine in variable amounts. One exposure, in the southwest, west of Route 330 (G.R. 822508) contains interlayered magnesite and foliated talc. The magnesite layers consist of 80 percent magnesite, as indicated by the reddish-weathering colour, minor quartz, talc and disseminated chromite. Fresh surfaces are white and the rock has a saccharoidal texture. Compositional layering in ultramafic rock (Plate 1), occurs locally (G.R. 830560) in the southwest corner of the area shown on Map 90-04; the origin of the layering is unknown. Disseminated magnetite and chromite are common and locally the magnetite forms small pods. Quartz veins up to 5 cm thick and, less commonly, serpentine veins 1 cm thick or less, occur locally.

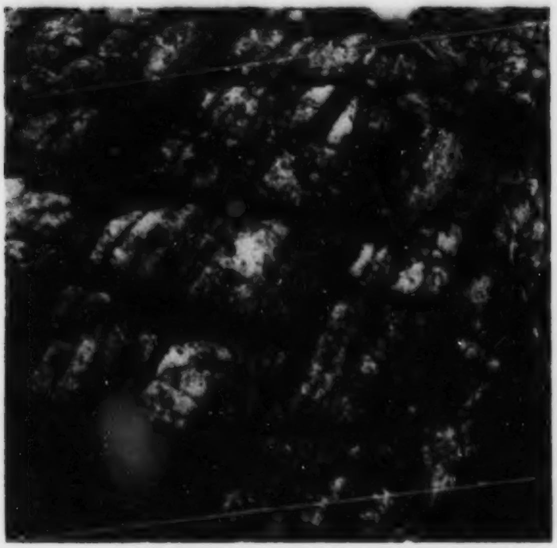

Plate 1. *Layering in altered ultramafic rock due to compositional variations; Gander River Complex.*

Petrography and Alteration Assemblages. The ultramafic rocks exhibit extremely heterogeneous effects of low-grade metamorphism. In this section, a general description of the metamorphic mineralogy is given; the metamorphic mineral assemblages and their equilibrium relationships are described later in the section on Metamorphic History (page 86).

The assemblages consist of variable proportions of the following minerals–serpentine, carbonate, talc, quartz and magnetite. Serpentine, the most abundant mineral, is colourless to pale green, typically, and consists predominantly of anhedral patches of fibrous antigorite. In some samples, it is associated with another unidentified fibro-lamellar mineral that exhibits a red-brown to green pleochroism and locally occurs in veinlets, up to 0.1 mm thick. Xenomorphs of magnetite, less than 0.5 mm across, commonly occur along with the serpentine.

Carbonate is the second most common alteration product, typically occurring as patches of fine- to coarse-grained xenomorphic grains or more rarely as rhombs, and as veins and patches in some samples. Crystals range up to 0.5 mm across. Although calcite occurs in minor veinlets, most of the carbonate is magnesite and/or dolomite. The presence of dolomite was confirmed in one sample by electron microprobe analysis.

Talc generally occurs as a minor constituent but forms up to approximately 30 modal percent of some assemblages. It occurs as a fine grained, felted mass.

Quartz is a minor component, forming less than 5 modal percent of assemblages. It is typically associated with carbonate and minor talc and occurs as small granular patches and in veins. Grains are up to 0.2 mm across, are locally polygonal and, rarely, exhibit triple-grain junctions of 120°.

Disseminated relict chromite grains are anhedral to subhedral and are generally less than 1 mm across. They occur in variable but minor amounts in most of the metamorphosed ultramafic rocks.

Gabbro and Diabase (Unit 2)

Distribution and Contact Relationships

The largest gabbroic unit occurs west and southwest of the south end of Weir's Pond on and near Weir's Hill (G.R. 862515). It generally coincides with an area characterized by an aeromagnetic low that forms an embayment in the positive aeromagnetic anomaly that outlines the Gander River Complex. However, the largest exposure of gabbro within this unit underlies a northeast-trending ridge immediately west of Weir's Brook coincident with a localized, elliptical aeromagnetic high within this low. This latter feature may be partly due to small pods of ultramafic rock, which are included in the gabbro in this area. Other bodies of gabbro are small and dispersed throughout the complex.

Diabase dykes occur in a quarry adjacent to Route 330 (G.R. 838525) where they intrude gabbro. They also can be seen cutting mafic volcanic rock on a logging road west of Weir's Pond.

Gabbro and plagiogranite exhibit intrusive relations in many exposures. Plagiogranite typically intrudes the gabbro and commonly contains fine grained chloritic xenoliths; chilled margins are absent. Although pods of ultramafic rock up to several metres across occur in gabbro, no clear intrusive relations were noted between these two rock units. In a quarry adjacent to Route 330 (G.R. 838525), gabbro and serpentinite are juxtaposed along a sheared contact. Contacts between sedimentary rocks of the Davidsville and Gander groups and gabbro are not exposed in the map area.

Lithology

The grain size of gabbro varies from coarse to medium grained both between and within exposures, and locally, very coarse-grained pegmatitic patches were observed. The gabbro is typically massive, but contains a foliation defined by elongate feldspar and hornblende in places. In some outcrops, the gabbro is brecciated into angular blocks 10 to 20 cm across. The heterogeneous nature of this deformation is indicated by the apparent variable development of the fabric in different blocks. The blocks also may show relative rotation with respect to each other. In several localities southwest of Weir's Pond (e.g., G.R. 885535), a centimetre- to decimetre-scale cumulate banding is defined by alternating ferromagnesian- and plagioclase-rich layers (Plate 2). Locally, a coarser metre-scale layering of similar nature, occurs within the same unit. Dark green hornblende is the common ferromagnesian phase. Pyroxene and olivine were not identified in exposure. The diabase dykes are fine grained, green weathering and approximately 1 m thick. They locally intrude gabbro and exhibit chilled margins up to 1 cm thick. The dykes are massive and show little variation in grain size.

Plate 2. *Alternating plagioclase- (light coloured) and pyroxene-rich cumulate layers in gabbro of the Gander River Complex.*

Petrography

Gabbro contains variable amounts of plagioclase, hornblende, clinopyroxene and opaque minerals. In unaltered or slightly altered gabbro, plagioclase and hornblende or clinopyroxene exhibit a hypidiomorphic texture in which grains are up to 3 mm across. Primary hornblende is pleochroic from brown to green and forms approximately 50 modal percent of most samples. Plagioclase may form up to 40 percent of the rock and locally encloses hornblende poikilitically. Primary anorthite-rich feldspar is preserved locally and was confirmed by microprobe analysis; the feldspar is extremely turbid. Clinopyroxene is typically augitic (e.g., see Appendix 1, Table 2; Sample # 86-347), colourless and forms less than 20 modal percent of the rock.

Members of the epidote group of minerals are common in the metamorphosed gabbros. Epidote itself is colourless or exhibits pale-yellow pleochroism and characteristic patchwork-quilt birefringence colours. In some samples, columnar aggregates of colourless crystals and xenomorphs display deep-blue anomalous birefringence colours characteristic of zoisite or clinozoisite. Some of the aggregates contain crystals that only have this deep-blue colour whereas in other aggregates, some of the crystals have low first-order yellows and greens. These minerals are referred to as zoisite–clinozoisite.

In many samples, the primary mineralogy is partly to almost completely metamorphosed to actinolite + albite ± zoisite–clinozoisite ± epidote ± chlorite ± calcite ± sphene ± prehnite. Plagioclase feldspar is commonly sericitized and hemitized and in places, partially metamorphosed to an assemblage consisting of albite ± epidote ± sphene ± prehnite ± calcite ± zoisite–clinozoisite.

In rocks that display slight hydration, primary hornblende and clinopyroxene are commonly retrogressed along their margins to blue-green hornblende. In more highly metamorphosed rocks, the assemblage consists of granular aggregates of actinolite ± tremolite, and zoisite–clinozoisite. Prehnite occurs less commonly and is associated with actinolite and/or zoisite–clinozoisite. Locally, the prehnite is rimmed by zoisite–clinozoisite.

Gabbroic rocks are locally cut by narrow veins of prehnite ± zoisite–clinozoisite ± calcite ± sphene ± epidote up to a few centimetres wide. Some of these veins are loci of cataclastic grain-size reduction (imposed on the metamorphic mineralogy). Prehnite is more common in these veins than in the rock matrix. In places, secondary, undeformed, granular calcite occurs in the matrix, but is strongly foliated within the narrow cataclastically deformed zones. Pyroxene and plagioclase also exhibit the effects of brittle deformation, e.g., bent twin lamellae.

Diabase dykes have a well-preserved ophitic texture, in which colour-zoned clinopyroxene crystals are intersertal to plagioclase laths. Minor green hornblende may represent a replacement of clinopyroxene. Plagioclase is typically sericitized and/or hematized and partially replaced by albite. Zoned clinopyroxene was probed in one section and has a ferroaugite composition in the rim and augite in the core (Appendix 1, Table 2; Sample # 86-339). The secondary mineral assemblage consisted of sphene ± calcite ± quartz ± hornblende. Prehnite occurs only in veins and in association with calcite; its presence in a diabase dyke sample was confirmed by microprobe analysis (Appendix 1, Table 2; Sample # 86-339). Pyrite and pyrrhotite occur as accessory phases.

Mafic Volcanic Rock (Unit 3)

Distribution and Contact Relationships

Mafic volcanic rocks are poorly exposed along two narrow belts within the Gander River Complex. They exhibit complex and equivocal intrusive relations with plagiogranite and gabbros in scattered exposures.

Lithology

Mafic volcanic rocks are basaltic and dark-green. They are typically unfoliated but brecciated and are often cut by a network of narrow veins. One small exposure northeast of Mill Pond contains pillows and pillow breccias (Plate 3); the interpillow material is very fine grained. Other exposures in which the rock is brecciated may consist of either pillow breccia or intrusion breccias; poor outcrop precludes any positive identification. Volcaniclastic rocks have not been found in this unit.

Plate 3. *Pillowed mafic volcanic rock from the Gander River Complex, Weir's Pond area.*

Petrography

Basalt contains phenocrysts of both clinopyroxene and plagioclase, up to 0.1 mm across, which together form 20 percent or less of the rock in a mesostasis of similar composition. The matrix is locally flow-aligned. The igneous mineralogy in basalts is, generally, partially replaced by chlorite ± albite ± actinolite ± epidote ± sphene ± prehnite. Prehnite mainly occurs in veins.

Plagiogranite (Unit 4)

Distribution and Contact Relationships

Plagiogranite bodies are defined by small exposures and occur in the central part of the Complex. In more than 80 percent of exposures, plagiogranite is associated with and commonly intrudes gabbro and/or mafic volcanic rock. Plagiogranite is not seen in contact with ultramafic rocks of the Complex. A contact between the largest plagiogranitic body and black shale of the Davidsville Group is well-exposed on the north side of a roadcut on Route 330. This contact is interpreted to be tectonic because the foliation in black shale immediately adjacent to the trondhjemite truncates the foliation in the adjacent shale.

Lithology

Plagiogranite here includes coarse and porphyritic varieties, which are unseparated on the map (90-04). The plagiogranite consists of 85 to 95 percent plagioclase and quartz (Plate 4) and minor mafic material. Pyrite, in disseminated form, is a common but minor, accessory phase and malachite stain has occasionally been observed. The plagiogranite is commonly greenish due to metamorphism of feldspar and locally contains inclusions, up to approximately 20 cm across, of fine-grained, chloritized mafic material (Plate 4). Quartz and feldspar grains up to 0.5 cm across occur in coarse-grained types. The porphyritic plagiogranite contains phenocrysts of quartz and feldspar, up to 0.4 cm across. The various plagiogranite types occur in contact with each other but chilled contacts are absent and the relative ages of intrusion are not known.

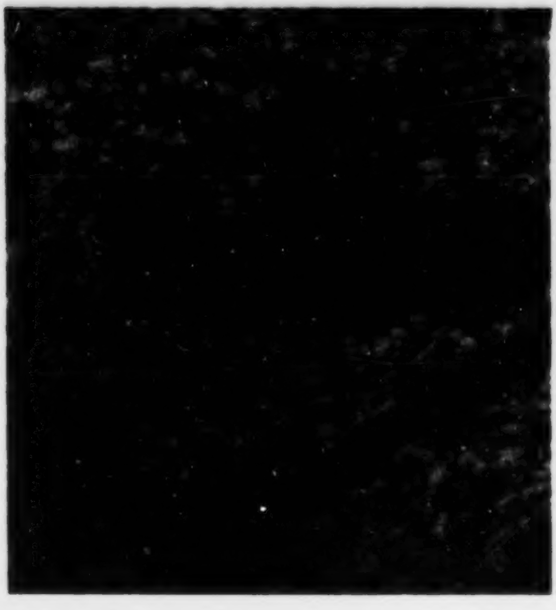

Plate 4. *Foliated, coarse-grained plagiogranite having fine-grained mafic inclusions.*

Many of the coarse-grained plagiogranitic bodies are cataclastically brecciated (Plate 5), a feature particularly well-developed in the roadside (Route 330) exposure of the largest plagiogranite body in the area, on the eastern edge of map area NTS 2E/2. In this rock, much opaque material has been concentrated along grain boundaries and the rock has a more melanocratic aspect than normal. A brittle, black mineral having conchoidal fractures, occurs in 0.5-cm-thick quartz-rich veins in this plagiogranite and has been identified as anthraxolite (John Welhan, personal communication, 1988). Numerous quartz veins and less commonly chlorite–epidote veins also cut the plagiogranite. A foliation is heterogeneously developed (Plate 4).

Petrography

Quartz and plagioclase occur in approximately equal amounts (between 40 and 60 percent each) in coarse-grained plagiogranite. The plagioclase is commonly dusty due to sericitization and more rarely hematization. Primary brown-green hornblende is rare. In porphyritic types, phenocrysts of quartz and feldspar, forming no more than 30 percent of the rock, are commonly euhedral and are set in a fine-grained, granophyric mesostasis of quartz and feldspar. Graphic texture is rarely developed. Radial intergrowth of fine-grained quartz and feldspar, possibly due to devitrification, is a common feature in some aphanitic and porphyritic types. In some samples, equant, sericitized feldspar phenocrysts have rims of granophyric-textured quartz–feldspar intergrowths. In some medium-grained to porphyritic types, plagioclase is predominant and quartz occurs as a minor component.

Plate 5. *Cataclastic brecciation in plagiogranite, collected from the largest exposure of plagiogranite (roadcut on Route 330), in the Weir's Pond area.*

The plagiogranite typically exhibits the effects of brittle deformation. Quartz is invariably strained and locally polygonized and deformation subgrains are widespread in some samples. Plagioclase crystals are broken and twin lamellae offset. Narrow, millimetre-scale zones of cataclasis locally affect these rocks and contain epidote ± chlorite ± sphene. These metamorphic minerals are present in variable but generally small amounts. Chlorite is common and replaces primary hornblende.

DAVIDSVILLE GROUP (UNITS 5 to 9)

It is formally proposed here to divide the Davidsville Group into three formations (Figure 2) based on data collected by the author and on that of Blackwood (1979, 1980) (see also O'Neill and Blackwood, 1989). The part of the Davidsville Group, which is west of the Gander River Complex, has been divided into two units by Blackwood (1979, 1980). These two units are used to define the central and western formations; they are now termed the Hunts Cove and The Outflow formations, respectively. The eastern formation is defined and extrapolated to the southwest and is termed the Weir's Pond Formation; its extension to the northeast (Carmanville map area) is uncertain.

THE WEIR'S POND FORMATION (UNITS 5 TO 8)

Definition and Distribution

The name Weir's Pond Formation is proposed here for the eastern, basal unit of the Davidsville Group. The formation consists of chromite-bearing late Arenig sandstone and conglomerate, Middle Ordovician limestone that is unconformable on serpentinite, and Caradoc graphitic black shale. These sedimentary rocks are exposed on the northwestern shores of Weir's Pond and for several kilometres west of the pond (see Map 90-04). Based on their exposure pattern in the area, rocks of the Weir's Pond Formation form imbricated structural slices that are associated with the Gander River Complex. Within at least one of these slices, nonconformable relationships between ultramafic rocks of the complex and the Weir's Pond Formation are preserved. The map pattern is complicated by later cross faulting. These rocks have formerly been included in the basal parts of the Davidsville Group (Blackwood, 1979). Similar rock types have also been mapped to the southwest in the Gander River (map area NTS 2E/2) and Gander Lake (map area NTS 2D/15) by Blackwood (1979, 1980) and to the northwest in the Carmanville area (map area NTS 2E/8) by Currie *et al.* (1978), and are included in the Weir's Pond Formation.

There is no defined reference section for the formation as a whole; however, exposures in which individual units are best exposed are described in the text, where applicable.

The Weir's Pond Formation is subdivided into four rock units (Units 5 to 8), all of which are exposed in the Weir's Pond area.

Sandstone (Unit 5)

Distribution and Contact Relationships

Only one exposure of this rock type occurs in the map area, several hundred metres west of Bulb Pond (informal name, Map 90-04). It occurs in thick bush and is not seen in contact with any other unit.

Lithology

The sandstone is whitish-grey on weathered surfaces and grey on fresh faces. The rock is thinly bedded and otherwise appears structureless. Bedding planes are locally characterized by abundant fossil fragments (see below). The sandstone is generally fine to medium grained, poorly sorted and contains scattered red volcanic pebbles, up to 2 cm across, and shale flakes. Bedding and cleavage both dip steeply to the northwest.

Petrography

Although the sandstone is deformed, the clastic nature of the detrital components is preserved. Clear, monocrystalline, locally embayed quartz is the dominant detrital component and most grains show strain extinction. (See Appendix 4, Table 1, Sample # 87-860, for results of point counting). Some quartz grains are extremely well-rounded and some are spherical. Minor syntaxial quartz overgrowth is marked by internal rims of opaque dust, near the edge of some grains. Polycrystalline quartz is a minor component.

Feldspar is mostly plagioclase, which generally appears unaltered. K-feldspar, occasionally micro-perthitic and granophyric, typically appears cloudy due to sericitization and/or hematization. Several pristine, subrounded microcline grains, up to 0.15 mm across, are present. Detrital biotite, chlorite and muscovite are subordinate constituents.

Lithic fragments are predominantly aggregates of quartz and mica; some of these contain a foliation that may predate incorporation. Quartz and feldspar aggregates and pelitic fragments containing cryptocrystalline material and fine-grained white mica form most of the remainder of the lithic clasts. Red pebbles, up to 2 cm across, are composed of spherical to ellipsoidal aggregates (0.2 to 0.3 mm across) of cryptocrystalline to polycrystalline quartz and opaque material (hematite, magnetite or pyrite). These pebbles may represent felsic spherulites of volcanic derivation. Volcanic fragments containing radial microlites (possibly intergrown feldspar and quartz), and coarser-grained quartz and feldspar occur rarely.

Accessory mineral grains include magnetite, epidote, zircon, apatite, sphene, tourmaline, ilmenite and chromite. The zircons tend to be round to euhedral and are rarely zoned. Chromite is typically rounded and magnetite commonly occurs in rounded, partly oxidized grains. Tourmaline grains are rare and commonly broken. It is not clear whether the sphene and epidote are of detrital or metamorphic origin.

The matrix, which forms a significant proportion of the rock (up to 70 percent), chiefly comprises fine- to very fine-grained white mica, chlorite and recrystallized quartz commonly stained with iron oxide. Sparry calcite locally replaces detrital material.

A geochemical analysis of this sandstone is given in Appendix 2, Table 16 (Sample # 87-851).

Paleontology and Age

The general state of preservation of the fossils is good although some extension along the cleavage planes has occurred. The locality has yielded an abundant brachiopod fauna, including *Orthambonites* and the trilobite *Annamitella* sp. cf. *A. Insulana* Dean (Boyce *et al.*, 1988). The trilobite fauna are of mixed North American and Baltoscandian (European) aspect and the brachiopod fauna are indicative of the Celtic Faunal Province (Boyce *et al.*, 1988). The fauna appear to be comparable to the late Arenig—early Llanvirn fauna of the Summerford Group on New World Island (Dean, 1978; Boyce, 1987) and to those of the Indian Bay Big Pond Formation (Wonderley and Neuman, 1984).

Conglomerate, Sandstone and Siltstone (Unit 6)

Distribution

Much of this unit is exposed in the northern and central parts of the area near Fifth Pond and Mill Pond (Map 90-04). Exposures of the cobble conglomerate are generally several tens of metres across in the north, but in the southwest, near Route 330, this unit is discontinuously exposed over several hundred metres. Sandstone—siltstone exposures are scarce, rarely more than several metres across and occur in the north and west central part of the area.

Contact Relationships

Contacts between rocks of Unit 6 and Units 5 and 7 of the Weir's Pond Formation and igneous rocks of the Gander River Complex were not observed in this area.

Lithology

Conglomerate of **subunit 6a** weathers brown and is green or mottled green and red on fresh surfaces; monomictic plagiogranite-rich varieties are light-weathering. Black shale forms the matrix locally (thin unit of subunit 6a northwest of Skull Pond, Map 90-04). Conglomerate exposures are typically massive; however, on the northeast shore of Skull Pond, bedding is present (Plate 6) and is defined by variation

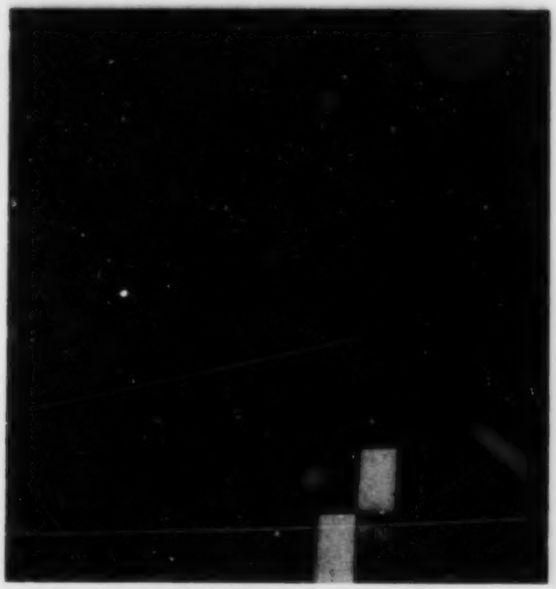

Plate 6. *Thickly bedded conglomerate of Unit 6 of the Weir's Pond Formation, Davidsville Group.*

in clast size. The beds at this exposure are tens of centimetres thick. Apart from this one instance, conglomeratic rocks are characterized by an absence of sedimentary structures.

In this area, it is not known if the disparate conglomerate occurrences form part of one structurally dismembered horizon or several horizons because of the lack of rock exposure. However, the proportion of clast types in different exposures is quite variable, thus, some outcrops are monomictic (invariably plagiogranite) or contain abundant gabbro clasts or abundant fine-grained mafic volcanic rock fragments. Several conglomerate outcrops in the north, immediately southwest of Fifth Pond, contain abundant sedimentary clasts. In one locality (a roadcut on Route 330, west of Muddy Gullies), the cobble conglomerate contains small, extremely fine-grained, siliceous interbeds.

The conglomerate is generally matrix-supported, particularly the plagiogranite-rich variety, and contains clasts ranging in size from granule to boulder, dispersed in a finer grained psammitic or more rarely pelitic matrix. The proportion of matrix can only be approximated but appears to range from 10 to 20 percent. In places, the conglomerate may vary from matrix- to clast-supported across an exposure. The degree of sphericity of the clasts is generally low, and the majority of them are poorly to moderately rounded.

The clasts are composed of gabbro, granitoid, fine-grained mafic volcanic rock, jasper, sandstone, siltstone, black shale and quartz. Granitoid clasts, varying from coarse grained to quartz and/or feldspar porphyritic, are most common, ranging from approximately 80 percent in monomictic varieties to about 10 to 20 percent; they also form the largest clasts, e.g., a granitoid boulder, approximately 2 m across, occurs in a conglomerate in Weir's Brook adjacent to Route 330. Coarse-grained gabbro clasts, commonly foliated (Plate 7), up to 20 cm across, may form up to 50 percent of the rock. Fine-grained, dark-green mafic fragments up to approximately 15 cm across, form up to 30 percent of the rock but are more difficult to distinguish from the matrix on the hand specimen or exposure scale. Aphanitic, felsic fragments form a minor component. Bright-red, angular jasper clasts up to 20 cm across were noted in several exposures.

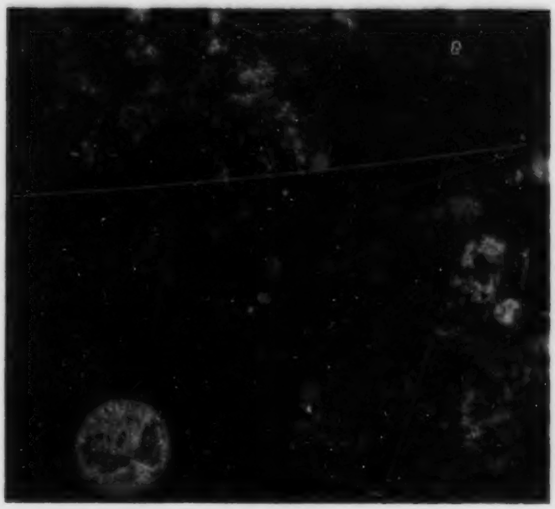

Plate 7. *Foliated gabbro cobble within conglomerate of subunit 6a of the Weir's Pond Formation, Davidsville Group.*

Immediately southwest of Fifth Pond, several exposures of conglomerate contain clasts, up to 6 cm across, of fine- to medium-grained psammite, siltstone and quartz in a green chloritic matrix.

In a roadcut (Route 330) exposing conglomerate west of Muddy Gullies, approximately 1 m of greyish white-weathered, very fine-grained siliceous sedimentary rock occurs in the centre of the exposure (See Appendix 2, Table 16 for geochemical analysis, sample # 86-185). This grey rock is colour-banded and the bands vary from 1 to 10 cm thick. Some of the layers are white and cherty, fracture conchoidally and display an internal, plane-parallel, compositional lamination, which produces a subtle colour banding. On the southern side of the exposure, this fine-grained sedimentary rock contains distinctive chalky-weathering ellipsoidal areas, up to 5 cm long and 1 to 2 cm across. The material within these ellipsoids is extremely friable.

Sandstone and siltstone of **subunit 6b** are greyish white to green on weathered and typically light green or grey on fresh surfaces. Coarse-grained layers range from approximately 10 to 50 cm thick, whereas the finer grained beds are 10 cm or less and are laminated in places. Sandstone beds are mostly massive but in roadside exposures immediately north of Lower Fifth Pond, they are crossbedded. Erosional bases are rarely seen. Grading is either absent, poorly displayed or ambiguous, particularly where coarse lenses are developed in the beds. In the southwest, west of Route 330, a small exposure of interbedded sandstone and siltstone (Plate 8) is characterized by pebbly lenses, 20 to 30 cm thick and 1 to 2 m long. The lenses occur throughout the beds and the concentration of pebbles (which are up to 1 cm across) is variable within the lenses. This same exposure also contains thinly bedded (Plate 8) white-weathering, siliceous layers, which display plane-parallel lamination (see Appendix 2, Table 16 for geochemical analysis of one of these layers, Sample # 86-151). The identifiable pebbles are typically of granitoid composition. Rip-up shale flakes are locally abundant in sandstone beds. Bright-green shaly flakes, probably derived from an altered ultramafic rock, occur locally. A small sandstone exposure north of Lower Fifth Pond contains possible A and B members of a Bouma sequence. Graded or ungraded parts from 1 cm to 20 cm thick, are overlain by laminated layers 2 to 15 cm thick. Angular rip-up clasts are composed of black graphitic shale.

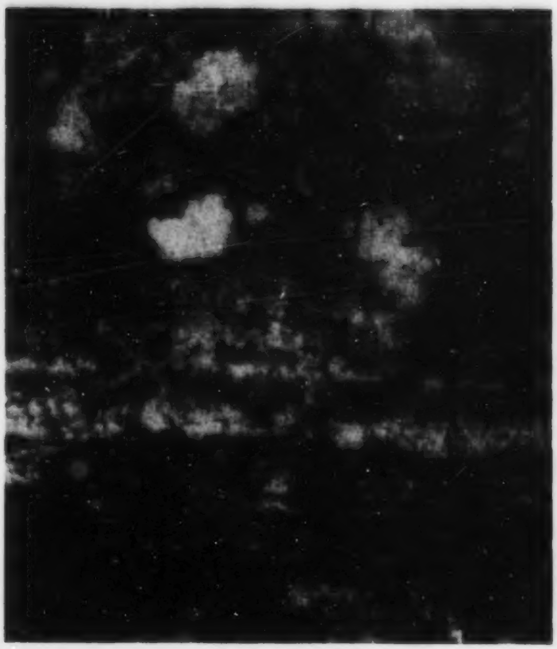

Plate 8. *Coarse pebbly lenses in sandstone, interbedded with white-weathering quartz-rich, thinly bedded sandstone; Unit 6 of the Weir's Pond Formation, Davidsville Group.*

In most exposures, dark-green-weathering siltstone is interlayered with the sandstone and most commonly displays a plane-parallel lamination.

Petrography: i) Conglomerate (Subunit 6a)

The diversity of lithic type and proportion in conglomerate exposures is remarkable and adjacent conglomerate beds may contain quite different assemblages of clasts. Therefore, the conglomeratic rocks are best described under general rock headings; the following lithic components are approximately in order of abundance.

Granitoid Clasts

Fragments of approximately equally abundant, coarse-grained quartz and feldspar dominate; they normally contain a minor chlorite component (less than 10 percent). The quartz and feldspar (both up to 4 mm across) are equigranular and generally show curved and locally lobate grain boundaries. The feldspar is plagioclase, which is variably altered to sericite and/or hematite or epidote ± sphene. In some grains, the plagioclase exhibits excellent micrographic or granophyric texture. Individual grains commonly exhibit the effects of cataclastic deformation; quartz displays strain extinction or deformation lamellae, and plagioclase twin lamellae are offset. A mortar texture, in which quartz and feldspar crystals are surrounded by fine recrystallized material, is present in places.

Some clasts contain masses of spherulitic quartz and feldspar, which locally show micrographic texture. Plagioclase laths approximately 0.2 mm long, predominate in some grains and are, in places, roughly aligned. Coarse-grained aggregates of muscovite, plagioclase and quartz occur rarely.

In monomictic conglomerate, a spectrum of felsic clast-types is present. These range from clasts having radial dendritic patterns only, to those having radial dendrites and feldspar laths, to those having fine- to medium-grained intergrowths of quartz and feldspar laths with or without granophyric texture. Porphyritic types also occur and these gradationally pass to the coarse-grained granitoid types.

Felsic Volcanic or Subvolcanic Detritus

Fragments of plagioclase and quartz porphyry are common. The phenocrysts, up to 1.3 mm across, occur in highly variable proportions. Quartz is normally present as individual crystals having no corrosion embayments, whereas the plagioclase phenocrysts commonly form glomeroporphyritic texture. The quartz–plagioclase groundmass is characterized by common spherulitic and variolitic aggregates. The groundmass crystals range in size from approximately 63 microns to 0.02 mm. There is a subordinate component of clasts composed exclusively of plagioclase laths, often showing trachytic and variolitic textures, and fragments of plagioclase–quartz porphyry within a cryptocrystalline groundmass.

Sample # 86-16

Sample # 86-16 contains distinctive clasts of quartz and biotite porphyry. The quartz phenocrysts are 0.2 to 0.9 mm across, rounded, have a high sphericity and are always surrounded by authigenic overgrowths (Plate 9). The biotite

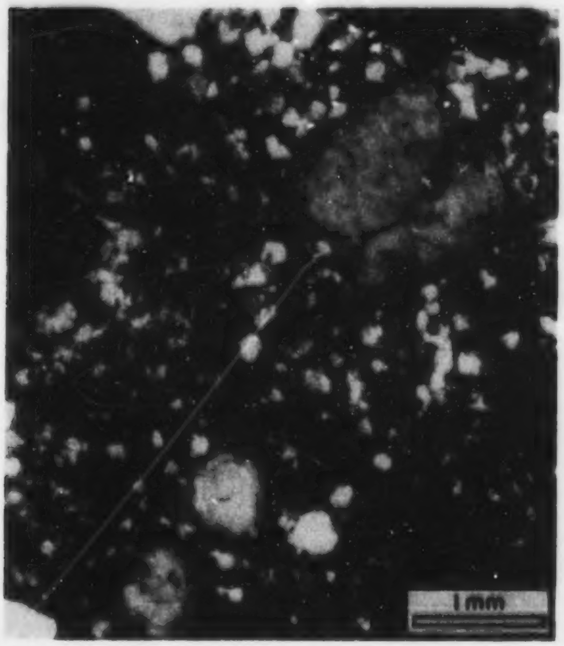

Plate 9. *Volcanic detritus in Unit 6 of the Weir's Pond Formation, Davidsville Group, contains rounded quartz phenocrysts having distinctive authigenic overgrowths (scale bar is 1 mm long).*

phenocrysts, commonly altered to chlorite, are up to 0.4 mm across, and occur locally in foliated aggregates containing quartz and garnet. Single garnet crystals have also been identified in some of the clasts. Groundmass ranges from polycrystalline to cryptocrystalline quartz.

Intermediate Clasts

Clasts that are approximately intermediate in composition contain quartz and plagioclase grains, no bigger than 0.3 mm across and abundant chlorite, the latter forming up to 40 percent. These clasts also commonly include fine-grained epidote and sphene.

Mafic and Ultramafic Clasts

Mafic and ultramafic detritus is normally not as abundant as felsic debris in the conglomerate. The larger gabbro clasts, either foliated or non-foliated, occasionally preserve some of their (?)original mineralogy of plagioclase and brown hornblende ± clinopyroxene, however, most mafic debris comprises chlorite, epidote, sphene, calcite and (?)prehnite. Ultramafic clasts are usually identified by their chromite, which commonly resides in a strongly foliated chloritic or serpentinized groundmass. Individual clinopyroxene and hornblende grains are rare. Ultramafic clasts containing primary mineralogy were not observed.

Sedimentary Clasts

The proportion of sedimentary clasts in the conglomerate varies between exposures from less than 10 to about 60 percent. Such clasts include shale, locally graphitic, having a single foliation, invariably parallel to the matrix fabric; cherty fragments, which may contain trace detrital muscovite (very rarely biotite); poorly sorted, matrix-rich, fine-grained quartz wacke associated with minor detrital muscovite and fine-grained quartzite and trace detrital biotite. Fragments of jasper contain hematite, pyrite and fine-grained quartz. Medium-grained quartz arenite contains minor plagioclase, tourmaline, sphene, zircon and opaque material. The shale clasts occur commonly throughout the area, however, conglomerate, rich in sedimentary detritus only occurs near Fifth Pond. This conglomerate contains numerous arenaceous clasts as well as granitoid and felsic volcanic detritus as described above and mafic and ultramafic debris including abundant chromite detritus. The sedimentary clasts range up to 6 cm in their long axis.

Sample # 86-381

The following detailed description of one of the larger cobbles from the Fifth Pond area, allows comparison with sandstone from the Davidsville Group and Jonathan's Pond Formation. The cobble is a moderately sorted, fine-grained sandstone comprising generally angular grains, a small proportion of which are very well-rounded. Contacts between grains are not always well-defined due to minor recrystallization, and grain boundaries are commonly sutured. A foliation defined by fine-grained, metamorphic white mica and chlorite is present. Fine-grained quartz and chlorite fill pressure fringes on some grains. Quartz grains show undulose extinction and are mostly monocrystalline having occasional syntaxial overgrowths; rutile needles abound in some of the grains. Polycrystalline quartz is minor, may show slight foliation, and is difficult to distinguish from recrystallized matrix material. Feldspars were not identified in the thin section. Trace detrital muscovite and chlorite are present. Lithic fragments include shale composed of very fine-grained quartz and mica or mica only; intergrown muscovite and chlorite; chert-like clasts with foliated very fine-grained chlorite and muscovite and monocrystalline quartz aggregates. The matrix forms a minor component and is composed of fine-grained quartz, some calcite and minor iron oxide. Accessory mineral grains identified are zircon, clinozoisite, magnetite, ilmenite (with leucoxene coatings), epidote, sphene and tourmaline.

Metamorphic Clasts

These clasts are most difficult to identify and form a very minor component of the total lithic component. They are generally foliated polycrystalline quartz and muscovite containing some chlorite and locally trace zircon.

Individual Grains

Single grains in the conglomeratic rocks are mostly monocrystalline, clear to cloudy quartz commonly containing lines of inclusions and locally exhibiting corrosion embayments. Abundant, randomly oriented (?)rutile needles characterize some quartz grains. Polycrystalline quartz occurs in massive and foliated, i.e., ribboned or high-strain, forms. Plagioclase is typically cloudy and some grains are cataclastically deformed; minor calcite and white mica locally replace the feldspar. Detrital muscovite, occasionally up to 1 mm long and biotite grains occur sporadically. Chromite is typically an accessory mineral, but forms up to 5 percent in some samples. It occurs as rounded to subrounded grains varying from black (with reddish margins) to deep red to brownish red. Epidote varies from trace amounts in monomictic granitoid-rich conglomerate, to approximately 25 percent in mafic types as both single and compound grains.

Accessory minerals include zircon, apatite, sphene, magnetite, ilmenite, hematite and tourmaline. Microcline grains, up to 0.5 mm across, occur very rarely in quartz-rich sandstone.

In matrix-supported conglomerate, it is difficult to discriminate very fine-grained lithic material from the matrix and, therefore, a proportional figure for the latter is meaningless. The matrix typically comprises very fine-grained sericite, chlorite and framework silicates and its composition generally reflects the principal components.

Petrography: ii) Sandstone and Siltstone (Subunit 6b)

Sandstone of subunit 6b displays poor to moderate sorting and contains rounded to angular grains in a pelitic matrix. Single quartz grains are present in both monocrystalline and massive to foliated, locally ribboned, polycrystalline forms. Quartz overgrowths are developed locally. Zircon may form inclusions in quartz and (?)rutile needles are abundant in some grains. In the finer grained sandstones, some quartz grains are well-rounded and more rarely, spherical.

Feldspar is predominantly plagioclase, which occasionally has micrographic texture; perthitic and microcline grains occur rarely. Detrital muscovite is common in some fine-grained sandstone but biotite is very rare.

Lithic Clasts

The nature and the proportion of lithic fragments vary between samples and include the following:

1) aggregates of epidote containing mono- and polycrystalline quartz;
2) plagioclase and quartz porphyry having a quartzose groundmass, the phenocrysts are commonly corroded;
3) coarse-grained quartz and plagioclase granitoid clasts;
4) quartz, plagioclase and chlorite–the feldspar may appear as a phenocrystic phase, and
5) quartz and feldspar showing micrographic and spherulitic texture.

Sedimentary clasts include fine-grained quartzite containing minor detrital biotite; poorly sorted, matrix-rich, fine-grained quartz wacke comprising mostly quartz and fine-grained detrital white mica and chert fragments; and arenaceous clasts, comprising mostly quartz, fine-grained white mica and accessory tourmaline. Elongated brown to black fragments of phyllite or shale are common and some are graphitic. Accessory mineral grains include zircon (mostly rounded), apatite, chromite, magnetite, epidote and tourmaline (the latter is quite common in finer grained sandstone).

The proportion of matrix varies from approximately 60 percent to less than 20 percent. Fine-grained sandstone commonly has a cryptocrystalline dark matrix whereas coarse-grained sandstone contains a small amount of matrix, much of it indistinguishable from fine-grained sedimentary or volcanic clasts. Siltstone is typically composed of very fine-grained, predominantly monocrystalline quartz, chorite and detrital muscovite. Plagioclase is generally a minor component. Lithic fragments comprise intergrown chlorite and muscovite, and muscovite and quartz. Opaque grains, zircon and tourmaline occur sporadically; calcite rarely forms an important cementing component. The matrix normally forms a significant proportion of the rock and is cryptocrystalline or very fine grained, locally recrystallized, quartz, mica and calcite.

A bedding-parallel primary lamination is preserved in some sandstone beds and is defined by alternating pelitic and quartz-rich, in some places cherty, layers that are 1 mm or less thick. The results of point counting of representative samples of sandstones and siltstones are shown in Appendix 4, Table 1.

Age

In the Weir's Pond area, the rocks of Unit 6 are nonfossiliferous and do not occur in continuous exposure with rocks that have been assigned an age using fossil material. Here, their age is unknown. However, on the north shore of Gander Lake, rocks containing a late Arenig fauna and somewhat similar to those described in Unit 5, pass conformably to the northwest into massive conglomeratic rocks, compositionally similar to the conglomerate described above. Thus, the rocks of Unit 6 in the Weir's Pond area may also be of late Arenig or younger age.

Limestone–Quartz Arenite (Unit 7)

Distribution and Reference Section

Unit 7 principally occurs as a discontinuous, fault-offset band on the northwestern shore of Weir's Pond. Sporadic exposures suggest a minimum strike length of approximately 3 km in this area. Farther southwest, 1 km south of Skull

Pond, several limestone boulders rest on what appears to be outcrop. One other exposure of limestone occurs 100 m west of Route 330, in the brook that runs from Muddy Gullies.

The reference section for Unit 7 is exposed on the western shore of Weir's Pond (marked as a fossil locality on Map 90-04). The exposed section is approximately 15 to 20 m thick.

Contact Relationships

The best exposed contact of Unit 7 lies at the eastern margin of the reference section, on Weir's Pond, between serpentinized ultramafic rock and fossiliferous limestone. The contact has previously been interpreted as a nonconformity (Blackwood, 1982). This interpretation is followed here, although a steep high-strain foliation is developed in the area of the contact and, therefore, the contact has probably been modified to some extent. It is also difficult to place the contact precisely because the ultramafic rock is extensively metamorphosed to carbonate, minor serpentine and talc and relict chromite. The western margin of the reference section for Unit 7 is marked by a 2-m-exposure gap between Unit 7 and black shale of Unit 8.

Several hundred metres east of Lower Fifth Pond (Map 90-04), the exposed contact (small exposure, 1 m wide) between limestone and black shale is deformed and may be a fault. Thus, the limestone is usually in closest proximity to black shale, whereas limestone–conglomerate contact relationships were not observed. Contacts are not exposed at either of the other two outcrops at Skull Pond and Route 330.

Lithology

Much of the reference section on Weir's Pond contains 0.5 to 1.5 m-thick, blue-grey-weathering, quartz arenite beds. Many of the beds are massive, however, locally a vague crossbedding is present. Finer grained beds are laminated on a millimetre to centimetre scale. Quartz grains are distinguishable in some of the coarser beds and range up to 2 mm across. Pyrite crystals up to 5 mm across and pyrite nodules up to 2 cm across are locally abundant.

Within several metres of the nonconformity, the quartz-arenites pass downward into very coarse-grained, massive limestone beds. Some of these beds are characterized by spectacular concentrations of fossil debris, which weather-out positively on some exposed bedding planes. Many of the fossils are preserved whole. Although generally thick-bedded, the coarse beds are interlayered in places with muddy limestone; the fine-grained beds range from 0.5 to 4 cm thick and the coarse beds from 1 to 5 cm thick. The finer grained layers are typically laminated on a millimetre scale; laminae are defined by alternating dark-grey to grey layers.

One kilometre from the north end of Weir's Pond, a distinctive limestone breccia is exposed on the western shore of the pond. Blue-grey-weathering, angular to irregular clasts are randomly dispersed in a white- to buff-weathering ?dolomitic 'matrix'. Fossil fragments are locally abundant and bedding or other sedimentary structures are absent.

South of Skull Pond, a small exposure of Unit 7, several metres across, is composed of a very distinctive, off-white-weathering calc-arenite and bright-green-weathering micaceous layers. The green mica may be fuchsite. The calc-arenite beds are tens of centimetres thick, whereas the pelitic seams are generally less than 2 cm thick. The calc-arenite beds are speckled throughout with the same green material that forms the pelitic layers. Some of the arenaceous beds exhibit plane-parallel lamination whereas some others are crossbedded; the lamination is defined invariably by the green layering.

Quartz grains up to 4 mm across occur locally and pyrite nodules up to 5 cm across are prominent and weather-out, leaving numerous rounded holes in the surface. Fossil fragments are abundant.

Calc-arenite of Unit 7, which outcrops immediately west of Route 330, is brecciated and poorly exposed.

Petrography

The sandstone is a fine-grained, moderately to well-sorted quartz arenite and subarkose, which is characterized by extensive quartz overgrowths. Some of the quartz grains contain abundant, randomly oriented ?rutile needles. Zircon, apatite, chromite and sphene are accessory components. Some beds also contain trace amounts of detrital, massive aggregates of muscovite and sericite. The depositional and diagenetic features of the sandstone have been obscured by deformation, which produced abundant crypto- to polycrystalline quartz material intergrown with fine-grained, commonly foliated mica and pyrite. A localized cement of sparry calcite appears to have postdated the deformation.

Paleontology and Age

Jenness (1958, 1963) was the first to report fossils, chiefly brachiopods and cephalopods, from the two Weir's Pond localities. He sent specimens to Professor W.C. Bell (University of Minnesota) who was unable to find any diagnostic features but suggested that the assemblage might be of Ordovician age. Jenness (1958) assigned a Middle Ordovician age to the rocks, on the basis of fossils he identified from localities on the north shore of Gander Lake. Bolton (*in* Williams, 1972) identified fossils collected by Williams as–

dolerorthid brachiopod impression
endoceroid? cephalopod structure
Maclurites sp. aff. *M. speciosa* (Billings).

Blackwood (1978) collected brachiopods, gastropods and samples for conodont identification from the same exposures.

Dr. R.B. Neuman (in Blackwood, 1978) identified the brachiopod *Orthambonites* and assigned it an Early Ordovician to early Middle Ordovician age. Dr. Yochelson (in Blackwood, 1978) identified the gastropods as *Maclurea speciosa* Billings and *Pararaphistoma* and assigned them a late Early Ordovician to early Middle Ordovician age. Stouge (1979, 1980) examined the conodont assemblage and assigned a definitive age of late Llanvirn to early Llandeilo to the sample collected by Blackwood (1978). Stouge (op. cit.) suggested that the conodonts were of North Atlantic affinity.

Dr. R.B. Neuman (written communication to S.P. Colman-Sadd and W.D. Boyce, 1987) identified the following brachiopod genera from the southern locality– *Orthambonites, Chaulistomella, Platystrophia, Eremotoechia, Atelesma, Leptaena.*

Boyce *et al.* (1988) identified the following trilobites (discovered by Ian Knight in 1987) also in the southern locality–

Annamiteila sp. undet.
Geragnostus/Trinodus sp. undet.
Hyboastis sp. cf. *H. depressa* Raymond
Illaenus sp. undet.

The boulders south of Skull Pond yielded trilobites and a gastropod. Boyce (in Boyce *et al.*, 1988) reported the trilobite *Annamitella* and noted that the gastropod is identical to one of the species (Yochelson, in Blackwood, 1978) that occurs at the northern Weir's Pond locality. The probable age of this limestone is, therefore, late Llanvirn to early Llandeilo.

Boyce *et al.* (1988) notes that the late Llanvirn–early Llandeilo trilobite fauna typically occur in limestone and display strong North American affinities along with minor Baltoscandian affinities. Elsewhere, these fauna have been recognized in the Cobbs Arm Limestone of the Summerford Group (New World Island) and in limestone exposed within the area of outcrop of the Spruce Brook Formation of the Through Hill area (Boyce, 1987).

Graphitic Black Shale (Unit 8)

Distribution and Reference Section

Graphitic black shale is exposed on the northwest shore of Weir's Pond, between Weir's Pond and Lower Fifth Pond, and between Gander River and Route 330 in the southwest. The best reference section is exposed on Weir's Pond several metres south of the reference section for the limestone–calcarenite of Unit 7. The section is approximately 30 m thick.

The two sections are separated by an exposure gap of several metres. Contacts between the shale unit and all other units are either not exposed or where they are exposed, the contact is tectonic.

Lithology

The rock is typically thinly bedded and contains 1- to 5-cm-thick layers, which exhibit plane-parallel, millimetre- to centimetre-thick laminations. Black graphitic shale is common and is interbedded with dark-green and dark-grey shale on decimetre to metre scale. The rock commonly weathers black to dark green. Centimetre-thin siltstone–sandstone layers occur rarely and sedimentary structures are absent.

Petrography

Much of the rock is composed of very fine-grained carbonaceous material, quartz and mica. Detrital muscovite and chlorite occur sporadically. Plane-parallel laminae are locally defined by variation in mica and quartz content of adjacent layers.

Paleontology and Age

The shales contain abundant graptolites, first reported by Williams (1972) and later by Dean (1978). The following species were identified by Erdtmann (in Williams, 1972):

Climacograptus sp. cf. *C. scharenbergi* Lapworth
Climacograptus sp.
Orthograptus sp. cf. *O. calcaratus grandis* Ross and Berry
Orthograptus sp. cf. *O. Quadrimucronatus* (Hall)

Dean (1978), stated that the graptolites 'are middle Caradocian in age probably belonging to the *Diplograptus multidens Zone*'.

THE HUNTS COVE FORMATION (UNIT 9)

Definition

The name Hunts Cove Formation (Unit 9) is formally proposed here for a shale unit, some of which is exposed in the northwest of the Weir's Pond area and the main part outcrops in the Gander River (Unit 12 of Map 80-31, and Blackwood, 1981) and Gander Lake areas (Unit 12, Map 80-189; Blackwood, 1980). The formal name is taken from a cove on the southern shore of Gander Lake where sections of this formation are well-exposed (R.F. Blackwood, personal communication, 1988).

Distribution and Contact Relationships

The Hunts Cove Formation is exposed in the northwestern corner of the Weir's Pond area, near Gander River. A small exposure also occurs east of Fifth Pond along a logging road. To the southwest, the formation is interpreted to extend through map areas NTS 2E/2, 2D/15, 2D/10, 2D/11, 2D/6 to 2D/3 where it passes into the St. Joseph's Cove

Formation (Dickson, 1987) of the Baie d'Espoir Group. The St. Joseph's Cove Formation was defined by Colman-Sadd (1976) for associated siltstone, sandstone and volcanic rocks in the St. Alban's map area (NTS 1M/13). A stratigraphically continuous section from the graphitic shale of Unit 8 to the Hunts Cove Formation is not exposed in the map area. Therefore, the precise relationship between the two formations is unknown.

Lithology

Monotonous, grey, greyish-green, greyish-black siltstone and shale characterize this unit. Minor purple siltstones are locally interbedded with green siltstones near Gander River (on Muddy Gullies Brook) and in the isolated exposure of this formation, east of Fifth Pond. Millimetre-scale shale partings occur in places and sandy layers (less than 5 cm) typically form less than 10 percent of exposures and generally weather a characteristic rusty colour. Fine-grained to pebbly sandstone beds, ranging from 1 to 10 cm thick, are common but are a minor component of the unit. Some of these beds are graded and younging directions are consistently to the northwest. Shale flake conglomerate, locally containing flakes up to 20 cm long, was noted in a few places. Near the northern edge of the map area, adjacent to Route 330, a poorly exposed conglomerate contains brecciated limestone clasts up to 0.5 m long and decimetres across and graphitic black shale. The latter either forms matrix and/or represents fragments molded by the more competent clasts. Cherty bands, 1 to 3 cm thick, occur locally.

Generally, the only sedimentary structure in the rock is a plane-parallel lamination, which is rarely convoluted. However, in one roadcut on Route 330, near the northern edge of the area, some beds contain a fining-upward sequence defined by sandy layers (up to 1 cm thick) that have sharp bases and undulating tops, followed upward by sand-dominated and finally mud-dominated lenticular layering. Most of the beds in the outcrop are massive or exhibit a variably developed plane-parallel lamination. Lack of grain-size variation commonly precludes clear bed definition, but individual layers are generally less than 10 to 15 cm thick.

Petrography

Siltstones are typically massive or bedded on a millimetre scale and laminae are defined by compositional alternations of quartz-rich and pelitic layers. Plagioclase feldspars generally form a minor component of the rock and very fine-grained chlorite and white mica and rare detrital muscovite, form the pelitic parts.

The coarse-grained sandstone beds are petrographically similar to those of Unit 6 (Weir's Pond Formation). Granitoid clasts, comprising coarse-grained quartz and plagioclase having minor chlorite, are abundant; some show micrographic texture. Felsic volcanic fragments, including porphyritic types, are common and some contain spherulites in various stages of devitrification. Plagioclase laths in some volcanic clasts are flow-aligned. Clasts comprising fine-grained chlorite and opaque material may be derived from mafic and/or ultramafic rocks. Moderate to well-sorted, granular quartz or sub-quartz arenite, containing accessory detrital muscovite and tourmaline, are also common. Other sedimentary clasts include greyish-green and graphitic black shale. Individual quartz grains, most of which show undulose extinction, occur in both mono- and polycrystalline forms and some contain abundant ?rutile needles. Grain boundaries in the polycrystalline forms are commonly sutured. Feldspar is plagioclase only and offset twin lamellae indicate that the rock has undergone cataclastic deformation. Detrital muscovite in narrow flakes, up to 1 mm long, occurs locally.

Age

No new fossil localities were found in the mapped area. However, Bergstrom *et al.* (1974) reported poorly preserved Caradocian graptolites in strongly cleaved Davidsville Group black slates, at Main Point, on the eastern side of Gander Bay, several kilometres to the north of the present map area. Pickerill *et al.* (1978) reported Cambro-Ordovician trace fossils from olistostromal shales in the Carmanville area. The fossils include *Tomaculum, Planolites, Sinusites, Lockeia?, Phycodes, Chondrites* and *Bergauria.*

THE OUTFLOW FORMATION

Definition, Regional Distribution and Contact Relationships

Although this formation is not exposed in the map area, it is formally defined here (see O'Neill and Blackwood, 1989) so that all major subdivisions of the Davidsville Group are named and defined in this report. The formation is named 'The Outflow' after the geographic locality on the north side of Gander Lake.

The formation comprises fine- to coarse-grained sandstone, locally containing shale intraclasts, interbedded with grey to black siltstone and slate; conglomeratic beds form a minor component.

The formation includes Unit 13 on Map 80-31 (Blackwood, 1981) and Unit 13 on Map 80-189 (Blackwood, 1980). The formation can be mapped southwestward through map areas NTS 2E/2, 2D/15, 2D/14, 2D/11, 2D/6 to 2D/5 where it passes into the North Steady Pond Formation (Colman-Sadd, 1980a). The North Steady Pond Formation grades laterally into the St. Joseph's Cove Formation and comprises greenish-grey pelite, siltstone and sandstone as well as minor conglomerate and mafic to felsic volcanic rocks (Colman-Sadd, 1979). Dickson (1987) however, in the Mount Sylvester map area (NTS 2D/3), interpreted the contact between the St. Joseph's Cove and the North Steady Pond formations to be a fault, locally marked by ultramafic lenses.

GANDER GROUP (UNITS 10 to 16)

OVERVIEW

The Gander Group, in the Weir's Pond map area, is subdivided into two formations, 1) the Jonathan's Pond Formation, which is separated into two belts by 2) the Indian Bay Big Pond Formation (Figure 3). The Jonathan's Pond Formation is composed predominantly of psammite and semipelite containing lesser proportions of greyish-green pelite and minor mafic and calc-silicate-rich layers. The Indian Bay Big Pond Formation consists of grey and maroon sandstone, black pelite, red and green siltstone, mafic pillows and intermediate volcanic rock.

Approximately two thirds of the northwest belt of the Jonathan's Pond Formation and most of the southeast belt, are affected by chlorite grade, greenschist-facies metamorphism. In these areas particularly, bedding is well-preserved. Locally, in the sillimanite zone, immediately west of the Deadman's Bay Granite, bedding is disrupted by profuse quartz-vein networks. In general, the combined effects of several phases of deformation and the development of penetrative foliations and porphyroblastesis obscure or have obliterated sedimentary structures.

The part of the map area underlain by biotite and higher grade rocks of the Gander Group is divided into four areas for the purpose of describing metamorphic assemblages and textures (Figure 3). These are the Ocean Pond, Moccasin Pond and Wing Pond areas in the Jonathan's Pond Formation and the Big Bear Cove Pond area, mostly in the Indian Bay Big Pond Formation.

The Ocean Pond area displays a roughly northeast-trending pattern of biotite, garnet, staurolite, andalusite and sillimanite isograds, reflecting one episode of progressive, regional metamorphism. The metamorphism reaches local culminations (fibrolite) at Ocean and Little Ocean ponds, which are approximately coincident with the synmetamorphic Ocean Pond Granite. Locally, adjacent to the margin of the Deadman's Bay Granite, the metasedimentary rocks are hornfelses. In the Moccasin and Big Bear Cove ponds area, the rocks become coarse grained within several hundred metres of the Deadman's Bay Granite.

In the southern belt of the Jonathan's Pond Formation, in the vicinity and east of First Pond, biotite, garnet, andalusite and sillimanite isograds can be mapped and the Gander Group passes, conformably, up metamorphic grade into the western belt of Hare Bay Gneiss (Blackwood, 1976). Although outside the map area, several traverses were conducted across strike to check the relationship of the Gander Group to the westernmost exposures of the Hare Bay Gneiss. Near Wing Pond, a localized metamorphism is characterized by the presence of relict kyanite, sillimanite and staurolite assemblages overprinted by andalusite.

The Gander Group displays evidence of three phases of deformation of which the first, D_1, is cryptic, being defined only on the basis of a relict microscopic and rarely mesoscopic, crenulated foliation. Deformation D_2 is a phase of isoclinal folding and associated, variably dipping and north- to northeast-striking axial-planar foliations. D_2 is overprinted by D_3, a phase of upright, open folding with variably developed, axial-planar foliations, striking northeast. Locally, high-strain foliations are developed, of which the Wing Pond high-strain zone is the best example.

The regional metamorphism in the Ocean Pond area developed after the D_2 event, but overlapped with the D_3 event. In the contact aureole associated with the Deadman's Bay Granite, near Moccasin Pond, there appears to be synchronous porphyroblastesis and deformation.

Jonathan's Pond Formation (Unit 10)

Definition and Distribution

The name Jonathan's Pond Formation is formally proposed for two belts of metasedimentary rocks, which underlie approximately 60 percent of the map area. The northern belt is exposed between Weir's Pond and the west side of Indian Bay Big Pond and the southern belt outcrops in the southeast corner of the map area. The two belts of rocks thus defined, are separated by the Indian Bay Big Pond Formation. (The Jonathan's Pond Formation can be mapped northward to the Carmanville area (Currie *et al.*, 1978) and southwestward to the Gander River and Gambo areas (Blackwood, 1977, 1982)). The formation is named after Jonathan's Pond, in the southwest corner of the Weir's Pond map area. Included with the Jonathan's Pond Formation, are metasedimentary rocks previously classified as the Square Pond Gneiss (Blackwood, 1977). It is proposed that the term Square Pond Gneiss be abandoned as the rocks are not gneissic, at least in the Weir's Pond map area. The base of the Jonathan's Pond Formation is not defined in the map area. The top of the formation is interpreted, with reservations stated below, to coincide with its contact on the southeast margin of the northern belt, with the Indian Bay Big Pond Formation. The structural complexity of the rocks precludes any meaningful estimation of thickness.

Contact Relationships

In the northwest of the map area, the contact between the Gander River Complex and the Jonathan's Pond Formation is not exposed, but is inferred to be a steep fault. In the central and northeast parts, the Ocean Pond and Deadman's Bay granites intrude the formation.

Southeast of Alleys Pond, the Jonathan's Pond Formation is apparently stratigraphically continuous with Unit 14 of the Indian Bay Big Pond Formation (Plate 10). Elsewhere, a definitive statement on the nature of the contact between the two formations cannot be made because of poor exposure. The nature of the northern contact of the southern belt of the

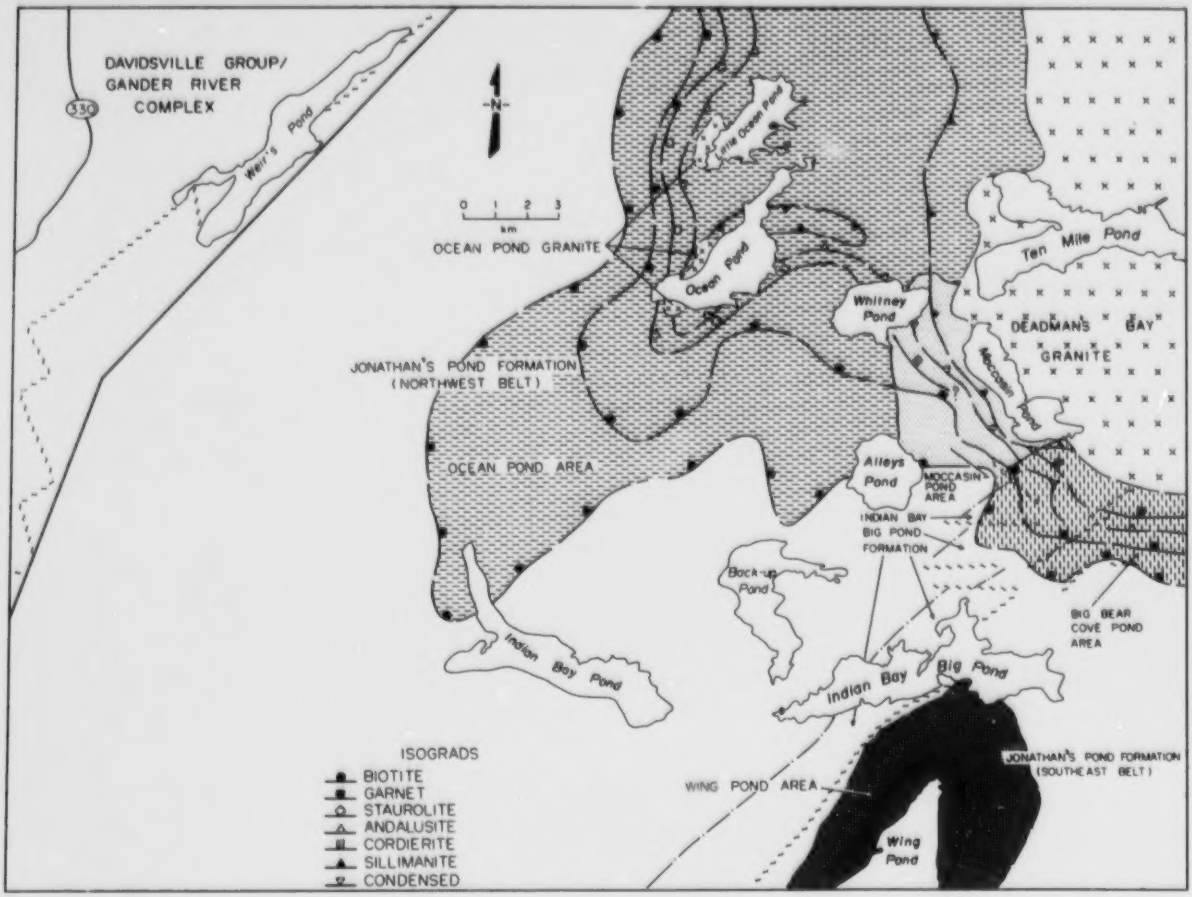
DAVIDSVILLE GROUP/
GANDER RIVER
COMPLEX
330
Weir's Pond
N
0 1 2 3
km
OCEAN POND GRANITE
Little Ocean Pond
Ocean Pond
Whitney Pond
Ten Mile Pond
DEADMAN'S BAY
GRANITE
Moccasin Pond
JONATHAN'S POND FORMATION
(NORTHWEST BELT)
OCEAN POND AREA
Alleys Pond
MOCCASIN POND AREA
INDIAN BAY BIG POND FORMATION
Bock-up Pond
BIG BEAR COVE POND AREA
Indian Bay Pond
Indian Bay Big Pond
ISOGRADS
BIOTITE
GARNET
STAUROLITE
ANDALUSITE
CORDIERITE
SILLIMANITE
CONDENSED
JONATHAN'S POND FORMATION
(SOUTHEAST BELT)
WING POND AREA
Wing Pond

Figure 3. *Location map showing the Ocean Pond, Moccasin Pond, Wing Pond and Big Bear Cove Pond areas as defined in the text. 'Condensed isograd' refers to 'isograd' bounding zone, in which the assemblage kyanite–sillimanite–andalusite–staurolite–garnet–biotite, is present.*

Jonathan's Pond Formation (with the Indian Bay Big Pond Formation) is less clear. South of Indian Bay Big Pond, the contact coincides with the western margin of a steep high-strain zone. North of Indian Bay Big Pond, the contact is located within a poorly exposed area in which highly strained rocks occur locally. The contact is interpreted to be largely structurally controlled.

Farther southeast, toward Centreville, the Jonathan's Pond Formation is progressively metamorphosed to sillimanite grade and where anatexis occurs, the Gander Group passes conformably into the western belt of the Hare Bay Gneiss.

Age

There are no radiometric dates or fossil ages for the Jonathan's Pond Formation. The tentative minimum age for that part of the formation, in exposed stratigraphic contact with the Indian Bay Big Pond Formation, is late Arenig to early Llanvirn based on the fossil age of this latter formation. Six, single titanite crystals, separated from a quartzose sandstone and individually dated by the U–Pb method, give ages that cluster around 540 Ma (T. Krogh, personal communication, 1988, interpreted the titanites to be detrital). A single detrital zircon U–Pb age of approximately 550 Ma substantiated the detrital titanite ages. Therefore, this allows a lower age limit of 540 Ma (Middle Cambrian), to be placed on the Jonathan's Pond Formation.

Lithology

The observations presented in this section pertain to the lower grade (chlorite zone) parts of the map area in particular, because it is in these areas that sedimentary structures are best preserved.

The Jonathan's Pond Formation comprises interbedded psammite, semipelite and pelite with localized calc-silicate layers and rare mafic to intermediate intrusive bodies. The

Plate 10. *Thinly interbedded medium-grained quartzitic beds and black shale in gradational contact zone of Jonathan's Pond and Indian Bay Big Pond formations, Gander Group.*

approximate proportions of the main rock types are 60 to 70 percent psammite—semipelite and 30 to 40 percent pelite. Calc-silicate and mafic layers form 5 percent or less. Many exposures are typified by pelitic, semipelitic and psammitic beds of variable thickness and proportion.

Individual beds in the Jonathan's Pond Formation are generally less than 1 m thick (Plates 11 and 12). Primary sedimentary layering is well-defined in most exposures because the boundaries between the beds are typically sharp; gradational contacts between semipelitic, pelitic or psammitic beds are rare. Grading within individual beds is also rarely observed and occurs only in coarser grained psammite.

Psammite and Semipelite

They are typically grey- to white-weathering rocks although some are rusty to pinkish weathering due to minor pyrite. Near Boot Pond in the southwest, some psammitic beds weather a distinctive pale red due to the presence of hematite. Fresh surfaces of psammitic rocks are generally grey. The rocks are mostly medium to thick bedded and fine to medium grained. The coarsest beds contain granules, are clast-supported, typically 10 to 30 cm thick and rarely reach 1 m in thickness. Grading from granule to medium-grain size is developed locally but is not common. One small exposure of psammite on the shore of Back-Up Pond contains small load casts, 3 to 4 cm across, preserved on the base of one overturned bed.

Coarse-grained, granule-rich psammite is characterized by subangular quartz displaying a distinctive blue or blue-grey colour. Bleached white feldspar grains occur locally and form 15 percent or less of the rock. Pyrite crystals up to 4 mm across, also occur infrequently.

Plate 11. *Thinly bedded psammite and pelite of the Jonathan's Pond Formation.*

Plate 12. *Thickly bedded (note metre stick) quartzite and semipelite of the Jonathan's Pond Formation: note lack of gradation between beds and sharp contacts.*

In the north-central parts of the map area, patchy exposures of semipelite occur over several hundred metres of cross-strike width. It is not known whether these exposures form units hundreds of metres thick, or, whether individual exposures represent units metres or tens of metres thick separated by some other rock type. Bedding is rarely observed in these semipelitic rocks and its absence partly reflects the intense penetrative fabric but also the lack of grain size and compositional variation.

Pelite

Pelitic rocks are light-green weathering and grey to green on fresh surfaces. They form very thin, thin or medium thick interbeds in thicker semipelitic or psammitic layers. Locally, pelite forms units, metres to tens of metres thick, at least, (apparent thickness only due to deformation), in which individual beds are impossible to define because of the penetrative foliation. A very thin, plane-parallel lamination, defined by colour and compositionally banded layers is present in places in these thicker units (Plate 13); the compositional variation is due to alternating mica-rich and mica-poor laminae.

Plate 13. *Plane-parallel laminations in siltstone–pelite of the Jonathan's Pond Formation, north shore of Indian Bay Pond.*

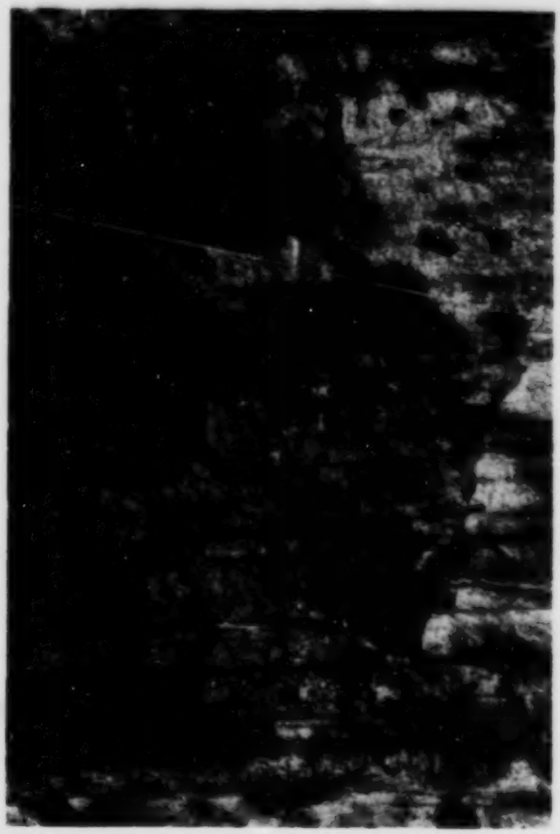

Plate 14. *Regularly spaced parallel laminations in quartzitic beds of the Jonathan's Pond Formation; laminae are pelitic and are 1 to 3 mm thick. The main foliation (S_2) runs from top left to bottom right.*

Quartzite

These rocks consist of approximately 90 percent quartz, are typically white-weathering, thin to medium bedded but thick-bedded locally (Plate 12) and form only a minor component of Unit 10. The quartzitic beds may be massive or laminated on centimetre to decimetre scale. The plane-parallel lamination (Plate 14) is defined by 1- to 2-mm-thick, melanocratic seams, which commonly are rich in calc-silicate minerals, mica, tourmaline and in places magnetite. The seams separate massive layers approximately 3 to 6 cm thick. Quartzite beds generally have sharply defined boundaries.

Detailed Stratigraphic Log

(The following section is synthesized from O'Neill and Knight, 1988). Short sections (less than 25 m), in which the bedding is normal to foliation and which contain original sedimentary features, occur locally. Several such sections are described here and provide some limited indications of the sedimentological character of the Jonathan's Pond Formation (Figure 4).

An exposure of interbedded psammite, quartzite and pelite, 1 km north of the east end of Indian Bay Pond (G.R. 032378), contains a 20 m section (Section A, Figure 4) exhibiting the best preserved sedimentary structures in the area. Pelite-dominated units, up to 500 cm thick, vary from structureless pelite to thin (< 3 cm) and thick (20 to 60 cm) interbedded pelite and psammite. The pelite is typically fine to very fine grained and exhibits sharp, planar to locally erosive or scoured bases and sharp planar tops. Above the base, the sedimentary character of psammite beds is variable. Some crosslamination occurs in the psammite and is undulose in places. Thicker psammite interbeds are 0.9 to 30 cm thick and subtly graded from medium to fine grained. Some psammite beds are apparently structureless, but locally contain scour surfaces between beds and minor lamination. These massive beds either grade up into pelite or are overlain by beds of laminated and crossbedded psammite. The most common structure is thin (< 1 cm) planar lamination. Other

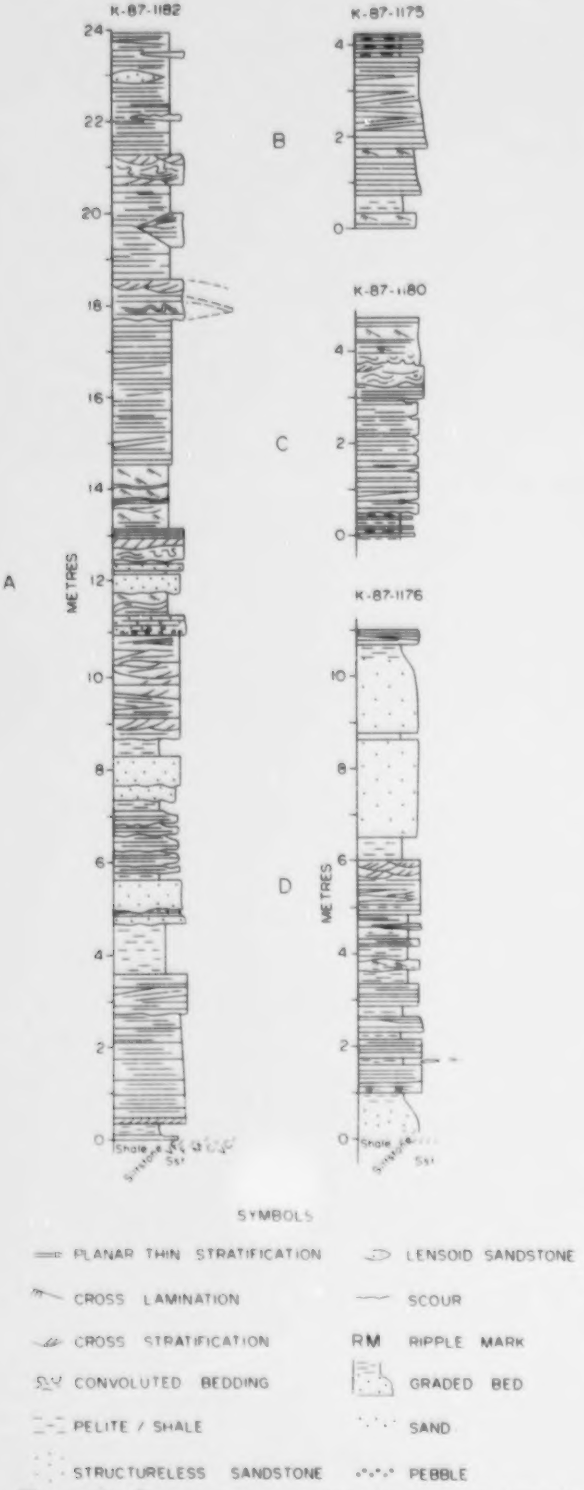

Figure 4. *Representative stratigraphic sections from the Jonathan's Pond Formation (VF, F, M, C and VC = very fine, fine, medium, coarse, very coarse; SST = sandstone).*

psammite beds are composed of planar-laminated layers separated every 20 to 80 cm by either shallowly inclined surfaces or by pelitic partings. A single 10-cm-thick set of possibly planar cross-stratification overlies the basal contact of one unit. Crossbeds are, however, more commonly developed at the top of the thick-bedded psammite. The trough cross-sets rework the top of the laminated psammite and are commonly convoluted. A prominent erosional surface locally underlies either the cross-sets or a bed of stratified psammite consisting of clean, medium- to coarse-grained psammite containing well-rounded quartz grains. This suggests that in some sections, there are coarsening- and maturing-upward sequences (Section C, Figure 4).

Psammite also forms lenticular bodies, 15 to 80 cm thick and several metres long, enclosed by metasiltstone facies. The latter is current-bedded and greenish white-weathering. Sharp bases and convex-upward tops characterize the psammite bodies. The core of the thicker lenses contain undulose to planar lamination. Offlapping, narrowing psammite wedges of gently inclined to curved foresets occur near the margins of the psammite bodies. Trough crossbeds, produced by the unidirectional paleoflow, rework the top of the psammite bodies. Crossbeds dominate the entire thickness of other psammite beds. Ripple marks form the top of some of the thinner psammite lenses, which have internal wavy lamination. The enclosing metasiltstone is up to 10 m thick and displays wavy lamination to ripple crosslamination, including climbing-ripple drift.

Some conclusions as to the depositional setting of the Jonathan's Pond Formation, based on the above, are given later.

Calc-Silicate-Rich Rocks

Calc-silicate minerals are locally concentrated in lenses and thin layers, usually less than 20 cm thick, which commonly are colour-zoned (concentrically in the lenses) in various shades of green and white in low-grade rocks. The colours reflect a mineralogical layering into epidote-rich and quartz-rich bands. The layers, which may display a plane-parallel lamination, occur in more psammitic rocks and grade into the adjacent sandstone over several millimetres.

Coticules

Southwest of Ocean Pond (G.R. 005475), abundant, ptygmatically folded pink layers, 0.2 to 2 cm thick are interlayered with semipelite and pelite in several exposures. These are fine-grained garnet–quartz rocks that are characterized by high Mn content (See Appendix 2, Table 17a, sample # 86-288) and are coticules (Renard, 1878).

Mafic Intrusive Bodies

Dark-weathering, mafic sill-like bodies occur commonly throughout the Jonathan's Pond Formation, but form 1 percent or less of total exposures. They are typically 0.2 to 2 m thick, although one exposure near First Pond has an apparent thickness of 15 m. They are commonly concordant but locally crosscut the sedimentary rocks. They invariably have sharp contacts with the surrounding rocks and some contain angular blocks of sedimentary rock near their margins. Most are internally massive but several have a grain-size variation in feldspars particularly, from coarse in the centre to fine or medium grained on the margins. In the chlorite zone, the mafic bodies are olive green and are rich in chlorite and epidote.

Thin, concordant bodies of approximately intermediate composition occur in a few places. They are medium to coarse grained, feldspar-rich, pink to buff weathering and leucocratic on fresh surfaces.

Petrography

As outlined in the lithology section, the biotite and higher grade zones are described with reference to the Ocean Pond, Moccasin Pond and Wing Pond areas (Figure 3). The chlorite zone lies outside these areas and is described first. The effects of metamorphism are at a minimum in this zone and some microscopic sedimentary textures have survived. The relationships between porphyroblasts and foliation are described in the section entitled Structure.

Chlorite Zone

Psammite and Semipelite. Psammitic and semipelitic rocks contain the same principal and accessory detrital minerals. Most psammitic rocks have less than 10 percent mica, whereas semipelitic rocks contain 30 to 50 percent mica. The mica in the semipelitic rocks maybe either evenly dispersed or concentrated in thin laminae, the latter being derived either from primary sedimentary layers or from metamorphic segregation during transposition.

Clastic textures of the sedimentary protolith are not well-preserved on the microscopic scale. The matrix is invariably recrystallized to very fine-grained mica and quartz and grain boundaries of the clastic grains are commonly affected by recrystallization and syntaxial overgrowth. The extent of this recrystallization varies because the amount of strain is heterogeneous on the outcrop scale.

Quartz, in mono- and polycrystalline forms, is the principal detrital component in all samples and ranges from approximately 50 percent to 90 percent of the rock. All forms of quartz generally show some strain extinction. Many grains are free of inclusions, however, some grains contain abundant, randomly arranged (?rutile) needles. In psammite, the quartz is typically granoblastic and grain boundaries are curved or sutured. Secondary overgrowths are developed locally on monocrystalline quartz. Extensive recrystallization of matrix and fine-grained quartz and recrystallization of medium-grain quartz, has resulted locally in an apparent bimodality of grain size, defined by the coarser, relict clastic grains and the recrystallized 'matrix'. Grains of polycrystalline quartz vary from those in which the individual crystals are elongated or ribboned, producing a foliation to those in which the grains are equant. In the foliated varieties, the grain boundaries vary from polygonal to sutured and the foliation may be accentuated by fine-grained mica aligned along the quartz-grain boundaries.

Detrital feldspar is common and forms 20 percent or less of the psammite. Grains are typically angular to subangular but are elongate in more highly strained samples. Plagioclase is the predominant feldspar and is rarely zoned. Grains vary from dusty, sericitized and/or hematized to clear. Some grains contain numerous small inclusions of white mica, chlorite, epidote and other unidentified material. The mica locally defines a foliation. More rarely, feldspars are turbid with opaque inclusions. Some complexly twinned plagioclase may be albite. Untwinned grains, invariably sericitized, may be either plagioclase or K-feldspar. Microcline and untwinned perthitic feldspar occur in a few specimens.

Lithic fragments are a subordinate component and are mostly schist, phyllite and slate containing quartz, feldspar and mica. The fragments of schist and phyllite consist of mono- and polycrystalline quartz and white mica. Biotite, chlorite, apatite and garnet are also present in some of the schist clasts. The subordinate slate fragments consist either of very fine-grained white mica (with or without chlorite) or of a mixture of very fine-grained mica and cryptocrystalline silica. Chert and quartzite are present in minor amounts.

In the lowest grade psammite, detrital muscovite occurs locally as flakes up to 0.5 mm long, and commonly bend around clastic grains.

Epidote, sphene and allanite form a minor component of the rock and tourmaline, apatite, magnetite, zircon, pyrite and ilmenite are accessory minerals. The opaque minerals are secondary and overprint the fine-grained foliation.

Tourmaline is ubiquitous in psammite as subidiomorphic, prismatic crystals up to 0.3 mm long having rounded edges. Its colours vary through shades of blue, green, yellow brown and crystals are normally colour-zoned. Some of these grains have secondary syntaxial rims overgrowing a detrital core and matrix chlorite and muscovite laths.

Identification of the nature of the sphene in the psammite is critical because six individual sphenes in sample # 86-387 (G.R. 957489) were dated by the U–Pb method (see Geochronology Section). Sphene is moderately common as an accessory mineral and occurs in several morphologies and settings. A very fine-grained 'fuzzy' type of sphene, up to 0.01 mm across, appears to be composed of clusters of tiny grains and is clearly secondary because it occurs in solution seams and in pressure shadow regions. There is a complete gradation between this very fine-grained type and the coarsest grains, which reach 0.15 mm. The coarse-grained type varies in morphology from anhedral to subhedral and partly diamond-shaped. These sphene grains are larger than the matrix chlorite and muscovite, which define the foliation and superficially appear detrital. Detailed examination of the relationships between the coarse sphene and metamorphic micas has revealed that fine-grained chlorite and muscovite abut directly against some sphene grains. The margin of the sphene appears to overprint the micas, thus implying that it is secondary. In contrast, the micas wrap around clastic quartz grains. In some samples, greenschist-facies quartz veins contain chlorite and euhedral, diamond-shaped sphene, which is clearly secondary. Both matrix and vein sphene occur together and have similar colour and birefringence.

The quartz-rich nature and rarity of lithic fragments in the medium- to coarse-grained rocks of the Jonathan's Pond Formation, suggest that the rocks are relatively mature and therefore, unlikely to contain detrital sphene, a mineral that degrades easily. Therefore, the relative abundance of sphene appears difficult to reconcile with a detrital origin. Despite these reservations, the detrital nature of the sphene is apparently confirmed by an identically aged single zircon grain from the same concentrate. The rocks from which the sample was collected are at too low a metamorphic grade to allow zircon to grow and the zircon must, therefore, be detrital.

Detrital epidote grains, up to 0.4 mm across are dark, particularly around the rims and are rounded to subrounded or even spherical. Epidote grains of uncertain origin, vary from colourless through pale yellow to greenish-yellow and commonly display pleochroism. Grains with anomalous blue birefringence and inequant to prismatic shape, may be zoisite—clinozoisite. Detrital allanite, a deep-brown epidote, forms subrounded grains up to 0.2 mm across in some psammitic rocks and is rarely intergrown with epidote. Detrital apatite is a common but very minor component in many psammitic rocks and forms subrounded crystals up to 0.25 mm across. Tourmaline and zircon are also commonly present and magnetite less so.

In some psammite samples, sphene, apatite, and epidote-group minerals are concentrated in seams or layers, generally less than 0.3 mm wide, and may represent recrystallized marly or calcareous layers. Whereas, clearly some of the sphene, and epidote-group minerals, are of secondary origin, e.g., those that occur in late veins, it is difficult if not impossible to establish whether others are detrital or secondary.

Metamorphic chlorite occurs throughout the chlorite zone, predominantly as fine laths, up to 0.1 mm long, which are commonly intergrown with fine-grained white mica, and also as disseminated porphyroblasts, up to 0.5 mm across, which overprint the fine-grained laths. Amorphous masses of chlorite are associated with vein quartz, minor sphene and in one sample, prehnite.

In order to determine the approximate modal composition of the original sedimentary rock, point counting of 300 detrital grains (following the approach of Zuffa, 1979) has been done in three suitable samples (Table 2, Appendix 4). Utilizing the classification of Pettijohn *et al.* (1972) the three samples plot in the area of quartz-rich sublitharenite (see Depositional Setting Section for discussion).

Pelite. Little if any discernible variation in degree of recrystallization or of grain size has been observed in pelitic rocks from the Gander River Complex eastward to the biotite isograd. Pelitic rocks contain 60 percent or more, of fine-grained chlorite and muscovite. The mica laths are typically less than 0.1 mm long, and are commonly intergrown. Chlorite porphyroblasts, up to 0.5 mm across, occur locally and overprint the earlier fine-grained chlorite and muscovite. Close to the biotite isograd, the chlorite is a yellowish-brown and contains inclusions of opaque minerals, sphene and zircon. Amorphous masses of chlorite are widespread in veins or concentrated in the hinge regions of late folds where they are usually associated with quartz. Granoblastic quartz forms much of the remainder of the rock and feldspar is generally a minor constituent (less than 5 percent). Accessory minerals are similar to those described in psammite above. Extensive recrystallization has destroyed all clastic textures in pelitic rocks.

Calc-Silicate-Rich Rocks. Calc-silicate-rich layers were not observed in the chlorite grade rocks. This may be partly due to the lack of colour differences, at low grade, between them and psammitic rocks in which they are commonly found.

Mafic Intrusive Bodies. A few conformable mafic layers were noted in the chlorite zone. They are completely recrystallized and consist of chlorite, epidote, calcite, plagioclase and quartz.

Ocean Pond Area

The Ocean Pond area encompasses much of the northern central portion of the map area and for the purposes of petrographic description, it is subdivided into zones on the basis of metamorphic index minerals, viz., biotite, garnet, staurolite, andalusite and sillimanite.

Biotite Zone

Psammite and Semipelite. Although the outlines of the coarser grained detrital mineral grains and lithic fragments are preserved, the primary grain boundaries are recrystallized and are generally sutured, curved or rarely polygonal. In semipelitic rocks, fine-grained, metamorphic biotite forms a minor component of the rock and coarse-grained chlorite is ubiquitous.

Pelite. In the lower grade part of the biotite zone, biotite occurs throughout the rock as small porphyroblasts 2 mm across or less, but at higher grades, as it progressively replaces the finer grained micas, it reaches 5 mm across and forms up to 25 percent of the pelite. In places, two generations of biotite occur; an earlier fine-grained type, up to 0.1 mm, overprinted by a poikiloblastic, coarse-grained type. Biotite is locally intergrown with prograde chlorite but is also commonly retrogressed to chlorite, opaque minerals and sphene. The biotite is typically olive-green to brownish-green and is associated with fine-grained muscovite and chlorite. Some coarser grained muscovite laths, up to 0.3 mm across, are locally associated with the coarser grained biotite. Very small garnet grains, 0.1 mm across or less, were noted in several samples. In the northern part of the area, near Ocean Pond, the biotite–chlorite zone is 2 to 4 km wide but widens to the south near Indian Bay Pond, to as much as 8 km. The zone narrows again south of Moccasin Pond.

Calc-Silicate-Rich Rocks. These are typically fine- to medium-grained granoblastic rocks containing 30 to 60 percent modal quartz and the remainder consists of the epidote-group minerals, apatite, sphene, albite, mica and garnet. Epidote and sphene, up to 0.4 mm and 0.2 mm across, respectively, occur in all calc-silicate samples from the biotite zone. Biotite and chlorite, which are 0.4 mm across or less, occur in most samples and garnet, 1 mm across, is found locally. Albite is poikiloblastic, occurs rarely and contains numerous inclusions of biotite, chlorite, epidote and locally forms graphic intergrowths with quartz. A fine banding is present in some samples, defined by alternating quartz-rich and calc-silicate ± mica layers, which have gradational boundaries. Detrital minerals were not identified in these rocks. Tourmaline and opaque minerals are accessory.

Mafic Intrusive Bodies. Mafic rocks are medium- to coarse-grained recrystallized aggregates, composed of epidote, chlorite, biotite, ± actinolite, bluish-green hornblende, sphene, plagioclase and quartz. Epidote is granular, pale-yellow to colourless and may form up to 20 percent of the rock. The amphibole occurs as rosettes and fasciculate bundles in many of the samples. Actinolite is present in some samples mostly in the lower grade part of the biotite zone. Bluish-green hornblende forms rims on some actinolite grains.

Garnet Zone

Psammite and Semipelite. Psammitic and semipelitic rocks are fully recrystallized in the garnet zone and, thus, primary microscopic features are absent. Quartz displays a granoblastic texture, which is locally polygonal.

Pelite. The disposition of the garnet zone mimics that of the biotite–chlorite zone, being narrow to the north and wider to the south of Ocean Pond. Garnet is abundant in the rocks southwest, west and north of Ocean Pond but is rare southeast of the pond; it is also abundant south of Big Bear Cove Pond.

Garnet grains are generally idiomorphic to subidiomorphic and range up to 6 mm across. They normally do not form more than 15 to 20 percent of the rock. Some garnet grains have a vague colour- and inclusion-zoning caused by turbid brownish cores and clear margins. Small (0.1 mm or less) garnet grains (spessartine?) locally form inclusions in biotite, but garnet growth typically postdates biotite. Primary chlorite is stable and the common assemblage is garnet–biotite–chlorite; muscovite and quartz are ubiquitous. Rocks in the garnet zone are schistose and muscovite laths range up to 1 mm long.

Calc-Silicate-Rich Rocks. Garnet is present in all calc-silicate rocks in this zone as poikiloblastic, dendroidal grains several millimetres across. Inclusions of quartz, epidote and sphene are common and locally sprays of actinolite or blue-green hornblende are present. Garnet is locally colour-zoned from a colourless core to a pale pinkish or rose rim; other garnets are very pale-yellow. Epidote forms irregular, anhedral crystals up to 0.3 mm across and is ubiquitous. Blue-green hornblende is present in most samples as fasciculate bundles. Plagioclase feldspar is commonly sericitized and typically occurs in the quartz-rich layers. The colour-zoning, which is typical of these calc-silicate layers in hand specimen, is produced by an abundance of garnets, giving a pinkish hue and usually associated with hornblende. These layers alternate with quartz and plagioclase layers, which commonly contain hornblende crystals. Locally, epidote forms up to 30 percent of the rock and gives an overall greenish hue to the layers.

In the garnet zone, garnet, epidote and blue-green hornblende form the most typical calc-silicate assemblage; chlorite, biotite and sphene occur locally.

Mafic Intrusive Bodies. Two occurrences were noted in this zone and both are amphibolites, containing more than 50 percent bluish-green hornblende. The rocks also contain quartz, plagioclase, biotite, epidote and minor chlorite.

Staurolite Zone

Psammite and Semipelite. These rocks are recrystallized in the staurolite zone. In the more aluminous samples, coarse-grained biotite and muscovite are common.

Pelite. Although the relative time relationship between the growth of staurolite and andalusite is unclear in outcrop, in thin section staurolite invariably forms inclusions in andalusite, never the reverse, and therefore, staurolite clearly developed before andalusite. In all thin sections but one that contain staurolite, it is associated with andalusite and the samples are from the andalusite zone. The one exception, in which andalusite is absent, contains the assemblage staurolite, biotite and chlorite and occurs west of Ocean Pond. The staurolite zone is defined on the basis of this sample. The zone is extrapolated north and east and parallels the andalusite isograd but, in the absence of staurolite-bearing samples to the southeast, is terminated near Whitney Pond.

Staurolite occurs as small xenomorphic crystals, 0.3 mm across or less, but prismatic crystals several centimetres long also occur. It usually contains abundant quartz and opaque inclusions; biotite and muscovite inclusions are rare. Retrograde alteration to sericite is common.

Calc-Silicate-Rich Rocks. A layered calc-silicate–psammite rock occurs in the staurolite zone, south of Ocean Pond. Calc-silicate-rich layers contain epidote, garnet, bluish-green hornblende, plagioclase and quartz, whereas quartz-rich layers contain plagioclase, sericite and bluish-green hornblende.

Mafic Intrusive Bodies. No mafic intrusive rocks were sampled in the staurolite zone.

Andalusite Zone

Psammite and Semipelite. In psammitic and semipelitic rocks in the andalusite zone, quartz is granoblastic and grain boundaries are predominantly curved to polygonal. The quartz (and minor feldspar) is equigranular and ranges from 0.1 to 0.4 mm across. Feldspars are variably sericitized and/or hematized. Semipelitic rocks contain assemblages similar to those in pelitic rocks but modal proportions of micas and aluminosilicate minerals are considerably lower or andalusite may be absent.

Pelite. Andalusite occurs profusely in coarse-grained schists and semischists, in an elliptical zone extending northeast from Ocean Pond and southward through Whitney Pond. The zone is extensive in the north, approximately 10 km wide but narrows to less than 1 km south of Whitney Pond. In the western part of the zone, andalusite is associated with staurolite in many samples; staurolite always forms inclusions in andalusite. These armoured relicts are xenomorphic to subhedral and up to 0.2 mm across. Staurolite is absent from the matrix or occurs as resorbed, partly to completely sericitized xenomorphic crystals. Andalusite also contains numerous inclusions of biotite, muscovite and garnet, which are of similar or smaller grain size to those in the matrix. Locally, garnet crystals, less than 0.1 mm across, form trains through andalusite grains. The andalusite is generally colourless but the central parts of some crystals are pink. Partial or complete alteration to sericite occurs locally. Coarse-grained brown biotite, up to 1 mm across and garnet up to 2 mm across, are common associates of andalusite. Most of the chlorite in this zone is retrograde but some appear to be primary.

Calc-Silicate-Rich Rocks. The assemblage in calc-silicate-rich rocks is essentially the same as in the staurolite zone, i.e., epidote, garnet and blue-green hornblende. Biotite occurs in one sample also and close to the sillimanite isograd, green hornblende is present in one sample. Chlorite is absent from the assemblages.

Mafic Intrusive Bodies. Although mafic bodies may occur in the andalusite zone, none were sampled.

Sillimanite Zone

Psammite and Semipelite. Quartz and feldspar in semipelitic and psammitic rocks in the sillimanite zone are coarser grained than in low-grade rocks, reaching 1 mm in grain size, and display a granoblastic polygonal texture. Where profusely developed, the fibrolite forms discontinuous, anastomosing seams in more psammitic rocks, which locally, appear as 1- to 2-mm-wide, greyish-white layers in hand specimen.

Pelite. Three occurrences of fibrolite define a localized zone around Ocean Pond, and fibrolite also occurs in one locality southwest of Little Ocean Pond. These four occurrences were observed in thin section only. All contain andalusite (containing staurolite inclusions), garnet and biotite (quartz and primary muscovite are ubiquitous). However, fibrolite−sillimanite occurs predominantly in a zone immediately west of the Deadman's Bay Granite. In west to east traverses within this main zone, the high-temperature aluminosilicate polymorph first appears as fibrolite. The fibrolite occurs as wispy aggregates and localized, light-brownish felted knots nucleating on pre-existing grain boundaries of quartz, biotite or andalusite. In many samples that contain andalusite, the fibrolite does not preferentially nucleate on the low-temperature polymorph. Northwest of Ten Mile Pond, fibrolitic sillimanite coexists with andalusite in a 2-km-wide transitional zone. Toward the eastern part of this zone, the andalusite becomes progressively replaced by coarse-grained prismatic sillimanite. Fibrolitic sillimanite also replaces biotite, which is characteristically a deep red-brown.

Coarse-grained prismatic sillimanite, up to 3 mm long, locally forms radial aggregates 3 to 4 mm across. Basal sections of sillimanite range up to 0.2 mm across. In places, sillimanite is retrogressed to fine-grained white mica. In one sample, relict coarse-grained sillimanite grains are surrounded by coronas of fine-grained muscovite and lie randomly in a fine-grained matrix of biotite and granoblastic polygonal quartz.

Near Ten Mile Pond, adjacent to the Deadman's Bay Granite, a retrograde assemblage of chlorite, sericite ± biotite ± garnet is developed; relict sillimanite occurs locally.

Within the sillimanite zone, from the north end of Moccasin Pond northward, coarse- to very coarse-grained muscovite overprints all other phases in the rock. The muscovite is up to 3 mm across and contains inclusions of biotite, sillimanite and andalusite.

Calc-Silicate-Rich Rocks. There is no discernible mineralogical variation in these rocks from staurolite grade up. The assemblages include hornblende, garnet, epidote, sphene, plagioclase and quartz and are essentially the same as those defined in the garnet zone, although chlorite is absent. Textural characteristics are also similar to those described for calc-silicate rocks in the garnet−biotite zone.

Mafic Intrusive Bodies. Several mafic intrusive bodies are exposed in the staurolite and higher grade zones. They are amphibolites, containing 60 percent or more hornblende, which is either bluish-green or green, together with epidote, plagioclase ± garnet ± biotite. Chlorite is absent from the assemblages.

Moccasin Pond Area

This small area lies between Whitney Pond and the southern side of Moccasin Pond. Biotite, garnet, andalusite and locally cordierite and sillimanite isograds are defined here. The principal reason for separating this area from the Ocean Pond area, is the presence of cordierite. The area is also characterized, however, by the association of cordierite, sillimanite, andalusite and K-feldspar in several samples.

Biotite Zone

Fine-grained biotite, 0.3 mm across or less, occurs in pelitic and semipelitic rocks along with finer grained chlorite and muscovite. Inequant pseudomorphs (after ?) of sericite up to a millimetre across, occur in a few places and contain inclusions of biotite of similar size as that in the matrix. The pseudomorphs are rarely zoned with quartz-rich cores and sericite-rich rims.

Garnet Zone

Garnet occurs in one sample in this zone, near Whitney Pond, together with biotite, fine-grained muscovite and quartz. The garnet is subidiomorphic and up to 0.4 mm across. Some grains are retrogressed to chlorite.

Andalusite–Cordierite Zone

Andalusite occurs with cordierite in two localities near Whitney Pond. The northwestern locality lies very close to the sillimanite isograd and contains the assemblage andalusite–cordierite–biotite–muscovite–quartz–magnetite. The second sample, from the southern shore of Whitney Pond, contains the assemblage andalusite–cordierite–biotite–muscovite–quartz as well as rosettes of chlorite, which appears to be retrograde. Andalusite and cordierite, which are not in contact in these samples, occur as inequant crystals up to several millimetres across. They are commonly partly or completely sericitized. Numerous yellow pleochroic haloes around tiny radioactive inclusions, together with the presence of sector twinning, characterize the xenoblastic to idioblastic cordierite. It is partly altered to sericite. Andalusite contains only very minor biotite inclusions but locally is surrounded by a biotite-rich halo. Garnet is notably absent from all the assemblages.

Sillimanite Zone

Fibrolitic sillimanite occurs commonly in pelitic exposures as far south as the northern portion of Moccasin Pond. Elsewhere in the Mocasin Pond area, only one other outcrop 2 km west of the south end of Moccasin Pond contain sillimanite. All sillimanite-bearing samples in this area contain andalusite and biotite; muscovite and quartz are ubiquitous. Fibrolite occurs in minor amounts commonly rimming and partially replacing andalusite.

Northwest of Moccasin Pond, two samples within the sillimanite zone contain fibrolite, cordierite, andalusite and K-feldspar. The samples contain up to 20 modal percent, granoblastic K-feldspar containing inclusions of biotite and sillimanite. Plagioclase was not observed in the rock. Cordierite and K-feldspar are commonly in contact and are stable; neither form inclusions in the other. Numerous small biotite, quartz and some muscovite inclusions are present in the cordierite. Although in one sample, fibrolite rimming andalusite and biotite is included in cordierite, the equilibrium relationships between sillimanite and cordierite are not clear as the two minerals are so rarely in contact. Biotite is typically reddish-brown in these assemblages.

Near the northern end of Moccasin Pond and close to the Deadman's Bay Granite, the rocks are hornfelses. Coarse random muscovite crystals up to 2 mm across contain inclusions of biotite and locally andalusite. In one sample, relics of andalusite, 0.1 mm across and almost completely sericitized, occur locally enclosed in muscovite.

At the south end of Moccasin Pond, the Deadman's Bay Granite appears to intrude across the sillimanite isograd.

Wing Pond Area

The metamorphic descriptions in this section are based on textures in phyllitic rocks as they preserve the best record of the rock's history in this area.

Biotite Zone

The biotite zone is defined on the occurrence of this mineral in one sample, east of Wing Pond. The light brownish-green biotite, up to 1 mm across, occurs with muscovite and quartz.

Garnet Zone

Garnet, up to 2 mm across, occurs as the sole ferromagnesian phase in several samples to the west of Wing Pond and coexists with biotite in several samples on the northwest side of the pond. The morphology of the garnets varies from idiomorphic to xenoblastic and the grains are commonly partly chloritized. In some samples, the garnet contains dusty cores having a higher proportion of opaque inclusions than the rims; some of these cores outline perfect idioblastic crystal shapes.

Aluminosilicate–Staurolite Zone

North of Wing Pond, andalusite was identified in outcrop with garnet, but was not noted in thin section. On the shores of and close to Wing Pond, five schist samples were collected that contain the metastable assemblage sillimanite–kyanite–staurolite–biotite, enclosed in porphyroblastic andalusite. Garnet is present in the matrix of one sample and muscovite is ubiquitous. In all cases, the kyanite and staurolite are present as inclusions in andalusite crystals, several centimetres across. Quartz, opaque minerals, coarse biotite and muscovite also occur as inclusions in the andalusite. Coarse-grained biotite locally overprints kyanite in the andalusite. Staurolite inclusions in andalusite are generally less than 0.5 mm across and are either clear, or contain a distinctive myrmekite-like texture, which, locally, has a radial pattern. The cores of these staurolite grains are commonly brownish. Sillimanite is ubiquitous and occurs in anastomosing narrow seams that cut across and replace kyanite locally. Sillimanite is present as inclusions in andalusite in places and in one thin section, the andalusite clearly contains a microfolded fabric, which is outlined by sillimanite.

A retrograde assemblage of chlorite and sericite is commonly developed in most samples.

The significance of these assemblages is discussed later in the section titled, Metamorphism.

Psammite, Grey and Black Pelite (Unit 11)

Distribution, Contact Relationships and Age

Unit 11 is restricted to three exposures south-southwest of Weir's Pond and has no formal name. All exposures of the unit are less than 10 m across and their contacts with the rocks of Unit 10 are not defined. Fossils have not been found and, thus, the age of this unit is unknown.

Lithology

Psammite and black shale are the predominant rock types of Unit 11. The psammite is greyish-black or greyish-green, fine grained and contains minor shale flakes at one location. The black shale is locally graphitic and contains minor amounts of thinly interbedded greyish-black siltstone. In the northernmost outcrop, green pelite is interbedded with graphitic black shale and greenish, fine-grained psammite. Calcareous layers or lenses are present in the southernmost exposure.

Petrography

The psammite contains 75 to 80 percent quartz and less than 5 percent plagioclase, which is locally dusted with fine-grained hematite. The matrix is entirely recrystallized and no clastic grain boundaries are preserved. Fine-grained chlorite and white mica form about 2 to 3 percent of the rock and define the fabric, which is locally parallel to rusty solution seams. Late secondary calcite forms 2 percent or less of the rock. Tourmaline and opaque minerals are accessory components.

The shale is extremely fine grained and contains mostly sericite, chlorite, opaque minerals, minor quartz and locally graphite.

Indian Bay Big Pond Formation (Units 12 to 16)

Definition and Distribution

The Indian Bay Big Pond Formation was first defined, described and informally named the Indian Bay formation by Wonderley and Neuman (1984). It referred to a unit of sedimentary and volcanic rocks in the vicinity of Indian Bay Big Pond. The term Indian Bay Big Pond Formation is formally proposed here for these rocks. The formation outcrops between Little Wing Pond in the south and Big Bear Cove Pond in the north. Some of the best exposures occur on the shores of Indian Bay Big Pond and other good exposures are present west of Big Bear Cove Pond. Thickness estimates are not given for any of the units because the structural complexity precludes any meaningful measurements.

Several kilometres to the south, Blackwood (1977) described a conglomerate lens, exposed west of Wing Pond that may represent a southward extension of this formation.

Units within the Indian Bay Big Pond Formation are sequentially numbered from west to east, but stratigraphic indicators are lacking and the relative ages of the units are unknown. Contacts between adjacent units within the formation were not observed; therefore, stratigraphic continuity of units is only inferred.

Grey to Dark-Grey Psammite and Green and Black Pelite (Unit 12)

Distribution and Contact Relationships. Unit 12 comprises rocks that are gradational between the Jonathan's Pond and Indian Bay Big Pond formations and is best exposed north of Little Bear Cove Pond. Exposure is semicontinuous west of Big Bear Cove Pond and the nature of the gradational contact can be examined there. South of Little Bear Cove Pond, however, outcrop is limited and the unit appears to pinch out at Indian Bay Big Pond. The southeastern contact of the unit with Unit 13 is gradational and is defined north of Little Bear Cove Pond.

Lithology. Grey psammite and greyish-green pelite (typical of Unit 11 of the Jonathan's Pond Formation) is interbedded with dark-grey psammite and black laminated pelite (Plate 10). The rocks are generally medium to thinly bedded.

Pelites generally form 30 to 50 percent of the outcrops but in places are predominant. Grey-weathering, black pelite, which distinguishes the unit from the Jonathan's Pond Formation, increases eastward through Unit 13 and locally forms 50 percent of exposures near the eastern boundary of the unit. The laminae in the black pelite are alternating grey and black layers, interspersed with 1- to 2-cm-thick, light-grey psammite layers. Sedimentary structures, other than the plane-parallel lamination, are absent. Grey- to brownish-weathering semipelite is fine grained and thin bedded.

These rocks have been metamorphosed, and biotite, garnet and andalusite isograds were defined in pelitic rocks during mapping. Despite the metamorphism, the rocks are generally non-schistose. Within several hundred metres of the contact with the Deadman's Bay Granite, however, the pelite is coarse grained. In the biotite zone, biotite up to 2 to 3 mm across is abundant. Garnet, in the garnet zone, occurs locally and typically forms a very minor component of the rock. Profuse growth of white-weathering andalusite up to 4 mm across, characterizes black pelite particularly, and results in spotted rocks. Within 100 m of the Deadman's Bay Granite, andalusite growth is profuse and the crystals are several centimetres long. Minor metamorphic segregation is evident, defined by biotite—andalusite pods, up to 20 cm long, separated by quartz-rich layers. Localized quartz–feldspar pods with biotite selvedges suggest some minor partial melting occurred within this contact zone. Megacrysts of K-feldspar, several centimetres across, also occur in pelitic rocks within metres of the granite.

Psammitic beds are grey to greyish-white weathering and are generally massive. They are mostly fine to medium grained but some coarser grained, thin, white-weathering quartz granule beds occur. The dark-grey quartzitic beds are medium grained and range from 0.2 to 1 m in thickness.

Petrography. Metamorphic aspects of all rocks in the Indian Bay Big Pond Formation are collectively described later. The clastic textures are described here.

Psammitic rocks are poorly to moderately sorted and clastic grains, where preserved, are angular to subangular. Quartz forms 60 to 90 modal percent of the rocks, which have the composition, therefore, of quartz or sub-quartz arenites. Monocrystalline quartz grains locally contain abundant rutile? needles. Plagioclase grains are an ubiquitous but minor component although in one sample the feldspar forms approximately 20 modal percent. Minor, dusty, sericitized and/or hematized, untwinned grains may be K-feldspar. Lithic fragments are predominantly polycrystalline quartz and quartz–mica grains. Tourmaline, epidote, sphene, zircon and opaque minerals are present in accessory amounts. Results of point counting representative thin sections from the Indian Bay Big Pond Formation are listed in Appendix 4, Table 3.

Age. No fossils have been found in this unit.

Black Pelite and Chert (Unit 13)

Distribution, Contact Relationships and Age. Unit 13 occurs immediately southeast of Unit 12 and is exposed between Big Bear Cove Pond in the north and Four Mile Pond in the south. The unit appears to pinch out at Indian Bay Big Pond. The best exposures occur in the northern part of the unit. On the northwestern side, its contact with Unit 12 is locally marked by a cherty horizon (Plate 15). Contact with units to the southeast, however, are poorly exposed and the location of the contact is approximate and its nature is unknown. The age of this unit is unknown.

Lithology. Unit 13 consists predominantly of black pelite, ubiquitously intercalated with 3- to 5-cm-thick psammite layers; both pelite and psammite bands contain millimetre-thin, plane-parallel laminations defined by compositional alternations of sandy, light-coloured and pelitic, grey to black layers (Plate 16). Locally, thin- to medium-bedded, dark-grey quartzite is interbedded with the pelite. Green pelite forms a minor component of this unit.

At several localities on the northwestern contact of Unit 13, a 6-m-thick siliceous layer is exposed. Weathered surfaces of this layer are greyish-white and fresh surfaces are dark-grey. At most exposures, the layer lies immediately west of a thick unit of black pelite. However, on the northwestern corner of Four Mile Pond, the siliceous layer lies east of a thick black pelite. Black metasiltstone or very fine-grained psammite is in contact with the siliceous layer on its western margin and appears to become more siliceous as the layer is appoached. At the contact, fine-grained disseminated pyrite and molybdenite occur.

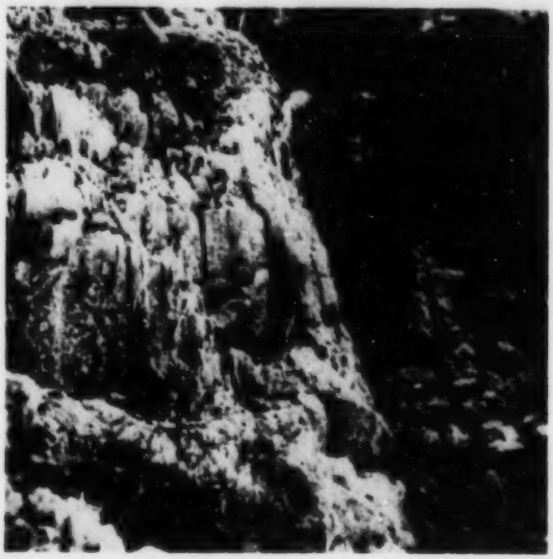

Plate 15. *Chert, on the left and black pelite on the right, marking the contact between Units 12 and 13 of the Indian Bay Big Pond Formation, north of Little Bear Cove Pond.*

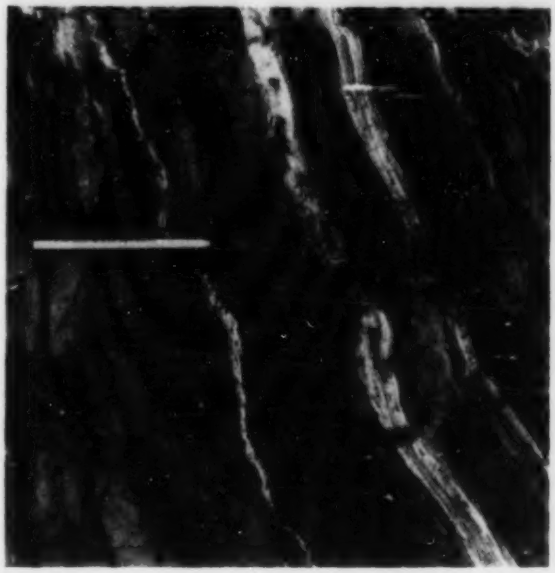

Plate 16. *Thinly bedded and laminated black pelite–siltstone containing minor sandy layers in Unit 13 of the Indian Bay Big Pond Formation.*

The stratiform and stratabound nature of the rock suggests that it represents a bedded chert (although no sedimentary structures were observed), a volcanic exhalative layer possibly associated with volcanic rocks elsewhere in the formation, or a stratigraphic layer that has been selectively silicified. The latter seems least likely as there are no relict features suggestive of replacement.

Petrography. In the chlorite-grade pelitic rocks, fine-grained white mica and chlorite are abundant, along with very fine-grained wispy graphite. Laminae are defined by alternating semipelitic to pelitic layers. The metamorphic mineralogy and textures described above for black pelite in Unit 12 also pertain to this unit and are not repeated.

The chert consists of approximately 90 percent granular quartz and 10 percent very fine-grained, wispy carbonaceous material and/or Fe–Ti oxides or Fe sulphides. The opaque material is locally concentrated into stylolitic seams, across which quartz veins are apparently displaced.

Intermediate Porphyry (Unit 14)

Distribution, Contact Relationships and Age. Unit 14 is exposed in several localities on the northern side of Indian Bay Big Pond; exposures in two localities south of Southern Pond, which were originally assigned to this unit (O'Neill and Knight, 1988), appear to be brecciated and possibly partly silicified psammite of the Jonathan's Pond Formation (to which they are now assigned). Contacts between Unit 14 and surrounding rocks are not exposed and, therefore, the nature of its relationship with adjacent units is inferred. The unit has not been directly dated.

Lithology. Unit 14 is a sub-intrusive or extrusive, massive porphyry of intermediate to felsic composition. The matrix is aphanitic and typically purplish to greenish. Dark laths, from 1 to 6 mm long, form approximately 15 to 20 percent of the rock. Feldspar phenocrysts, up to 4 mm across, form 10 to 20 percent of the rock, whereas quartz phenocrysts, up to 3 mm across, form less than 10 percent.

The exposures are locally brecciated and the angular fragments are typically cemented by calcite. Disseminated pyrite occurs in places and quartz-vein networks are common.

Petrography. These rocks are composed predominantly of phenocrysts of plagioclase, quartz and pseudomorphs of chlorite and opaque material, which may have formed after hornblende, set in a mesostasis of fine-grained plagioclase, 0.15 mm across or less and quartz. Biotite crystals, up to 0.2 mm across are a minor component. Sericite occurs locally but is usually restricted to foliation seams. Calcite and sphene are also accessory minerals.

The modal composition of the rock approximates that of a quartz monzodiorite.

Pillow Basalt (Unit 15)

Distribution, Contact Relationships and Age. Unit 15 is represented by two exposures of pillowed mafic volcanic rock that occur on two small islands in the north central part of Indian Bay Big Pond. Contact relations with adjacent units are not exposed and the nature of the contacts are, therefore, unknown. The age of this unit is also unknown.

Lithology. The pillows are morphologically well-preserved and range up to approximately 1 m in diameter (Plate 17). The rocks are weathered to a greenish-grey and are light-green on fresh surfaces. Alteration to a calcite-rich assemblage is pervasive. Consistent indicators of stratigraphic younging were not observed in the outcrops.

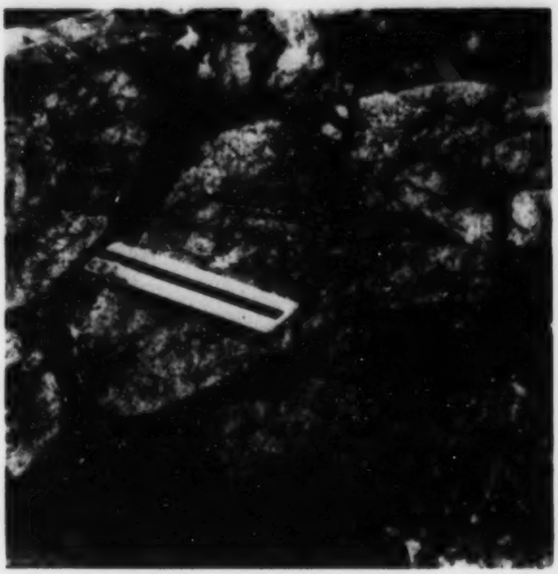

Plate 17. *Morphologically well-preserved pillowed mafic volcanic rocks of Unit 15 of the Indian Bay Big Pond Formation.*

A hyaloclastite, containing blocks of vesicular mafic material, is exposed near one of the pillow lava localities and occurs as numerous boulders on the shoreline. Some malachite stain is present locally on the hyaloclastite.

Although Unit 15 is not exposed north or south of Indian Bay Big Pond, boulders of similar material were observed on the shore of Little Bear Cove Pond to the north.

Petrography. Vesicles, up to 2 mm across, form approximately 20 percent of the rock. They consist almost invariably of a core of coarsely crystalline calcite, surrounded by a mixture of chlorite and opaque material and minor quartz; prehnite occurs rarely. In many of the vesicles, calcite contains vague relics of pseudomorphed radial aggregates, possibly of feldspar microlites. The groundmass consists predominantly of feldspar microlites replaced by calcite, up to 0.3 mm long and minor euhedral pseudomorphed feldspar phenocrysts. These microlites define a trachytic texture, which locally swirls arounds the vesicles and phenocrysts. Intersertal to the pseudomorphed feldspar laths, is an unidentified mass of diffuse brown material.

Psammite, Maroon and Black Metasiltstone and Calcareous Layers (Unit 16)

Distribution and Contact Relationships. Unit 16 can be mapped from Indian Bay Big Pond southward to Little Wing Pond. To the south, in the Gambo, NTS 2D/16 map area, Blackwood (1982) has mapped a lens of conglomerate that may form part of this unit. The best exposures occur on the north and south side of Indian Bay Big Pond. Contact relationships with adjacent units are not clearly exposed.

Age. Wonderley and Neuman (1984), who were the first to report and describe the fossils from the Indian Bay Big Pond area, stated that fossiliferous rocks outcrop on the south shore of the pond. Numerous fossiliferous boulders were observed by the present author on the shore of Indian Bay Big Pond, but no exposures were found. These boulders have not been noted elsewhere in the map area and were interpreted by Wonderley and Neuman (1984) to be derived from the Indian Bay Big Pond Formation. They assigned a late Arenig to early Llanvirn age to the brachiopod and trilobite fauna and compared them to similar fauna from tuff interbedded with volcanic flows of the Summerford Group on New World Island. Boyce *et al.* (1988) also noted that the trilobite fauna from the Indian Bay Big Pond Formation closely resembles the late Arenig–early Llanvirn Annamitella insulana Dean from the Summerford Group. The brachiopod fauna are indicative of the Celtic Faunal Province (Neuman, 1976, 1984) and are characteristically associated with the trilobite Annamitella (Bruton and Harper, 1985).

Lithology. Unit 16 consists mainly of medium- to thick-bedded, buff and maroon psammite, thinly bedded maroon and green metasiltstone and black pelite. These rocks are well-exposed on a small peninsula on the south side of Indian Bay Big Pond (G.R. 115377). Here, they are typically interbedded with grey, fine- to medium-grained psammite and thinly bedded, brown-weathering pelite. Maroon psammite beds, 30 cm to several metres thick, occur locally. The buff psammite weathers light-brown and beds are several metres thick in places. The rocks are medium to coarse grained, typically massive and do not exhibit well-developed grading. A characteristic feature of these beds is the ubiquitous presence of detrital muscovite flakes. Toward the eastern end of the exposure, maroon metasiltstone is interbedded with white-weathering, fine-grained psammite. Psammite also occurs on the north shore of the pond, and has a somewhat tuffaceous, scaly appearance. Also, at this locality, numerous fossiliferous boulders occur on the beach. They are typically angular and up to several metres across, have a distinctly mottled grey to brown appearance and are generally greyish-white on fresh surfaces.

Brown pelite forms less than 20 percent of the exposure. Laminated black pelite similar to that described in Unit 11, is also interbedded with the rocks at this locality, but in subordinate amounts.

A similar sequence is exposed 1 km away, on the other side of the lake (G.R. 124385). Locally, thinly interbedded brown psammite and brown-weathering pelite pass into mottled reddish-brown, shaly, calcareous, fine-grained psammite, which appears lithologically similar to the fossiliferous boulders. Some boulders contain calcareous layers, which have shelly debris, interlayered with mottled pelite–semipelite. The calcareous shales are typically white to greyish-white on fresh surfaces. In one part of the sequence, a 1- to 3-m-thick, very coarse-grained psammite layer cuts across bedding locally and appears to form a channel deposit. Fossiliferous boulders, up to 6 m by 3 m, also occur abundantly in this area. The fossils occur in both shaly rocks and in fine-grained psammite. The fauna in all of these boulders is typically brachiopod-rich.

Approximately 1.5 km west of the above locality, an exposure of Unit 15 contains 6 m of plane-parallel, laminated grey-black metasiltstone and pelite with localized occurrences of some plane-parallel crossbeds, indicating younging to the northwest. This unit is overlain by massive, ungraded and poorly sorted quartz granule beds.

Southwestward, Unit 16 is poorly defined but thinly interbedded maroon sandstone, maroon, green and dark-grey shale and grey psammite are exposed on the shores of Southern Pond.

Conglomerate boulders, containing rounded to subangular clasts, occur abundantly on the shores of the north-central and south-central parts of Indian Bay Big Pond. These may represent a subunit within Unit 16, unexposed within this area but equivalent to a conglomerate unit mapped farther south by Blackwood (1977). A poorly developed bedding is present in some of these boulders. The matrix varies from red and silty to grey and more quartz-rich. The boulders are either clast-supported or matrix-supported. The clasts in some boulders are composed predominantly of quartz ± feldspar ± amphibole porphyry having a purplish or green matrix, which closely resemble rocks from Unit 14. Other boulders contain the following clasts in various proportions:

1) chert and/or rhyolite

2) jasper

3) intermediate volcanic rocks

4) porphyritic clasts with white-weathering, 4-mm-thick rind

5) partly altered gabbro

6) vein quartz

7) laminated, maroon and green siltstone, and

8) conglomerate cobbles with maroon matrix and quartz-rich fragments.

Many of the clasts are similar to in situ rocks of the surrounding Indian Bay Big Pond Formation.

The conglomerate lens described by Blackwood (1977), 10 km along strike to the southwest in the Gambo map area, is 1200 m long and 300 m wide. It consists of predominantly well-rounded sedimentary clasts, is reddish-brown in the coarsest parts and is greenish-grey in finer parts.

Petrography. Unit 16 lies in the chlorite zone and although some of the rocks have been considerably modified by deformation, the gross clastic textures and the primary nature of the clasts are generally well-preserved. The rocks are poorly sorted and most grains are angular although a small proportion are rounded. The matrix forms a significant proportion of the rock and many of the samples examined are matrix-supported.

Quartz is the predominant clastic component and occurs mainly as mono-crystalline grains, which are typically clear but may be cloudy due to fine inclusions. Rutile(?) needles, muscovite, biotite, vermicular chlorite also form inclusions in quartz. Syntaxial quartz overgrowths are locally present. Some corroded grains exhibit rounded embayments and may be of volcanic origin. Polycrystalline quartz varies from massive to foliated and some grains contain white mica.

Plagioclase feldspar occurs in all samples and is commonly dusty due to sericitic and/or hematitic alteration. An irregularly twinned variety may be albite. K-feldspar is uncommon, untwinned and mostly appears dusty. Fresh, clear microcline was identified in several samples. Small amounts of perthite are widespread.

Detrital muscovite is a ubiquitous component of the psammitic rocks of Unit 16. Grains range up to 0.5 mm long and are commonly bent.

Lithic fragments are represented by foliated aggregates of poly- and mono-crystalline quartz, muscovite and chlorite. Biotite has also been found in some of the lithic fragments in sample #'s 87-641, 87-684, 87-734 and 87-771 (See Appendix 4, Table 3 for a complete listing of components in these samples). Fragments of phyllite, slate and chert have been recorded in subordinate amounts. Accessory components are represented by zircon, apatite, epidote, sphene, tourmaline, garnet, magnetite and ilmenite.

Sample #'s 87-696a and b are lithic-rich psammites, which are texturally and compositionally distinct from the other psammites of Unit 16. Their conspicuous lithic component (see Appendix 4, Table 3) is represented by fragments of clastic sedimentary and metasedimentary rocks. The former group comprises clasts of quartzite (some of them with tourmaline) and fine- to very fine-grained arenite and greywacke. The fragments of clastic rocks contain quartz, muscovite, biotite (occasionally altered to chlorite) all set in recrystallized quartz and a very fine-grained micaceous matrix. Siltstone, shale and mudstone clasts are also present and consist of well- to poorly-sorted grains of quartz, white mica, chlorite and biotite. The metamorphic fragments are represented by a range of foliated rocks from slate to schist (Plate 18) consisting of white mica, chlorite, mono- and polycrystalline quartz and plagioclase. Garnet porphyroblasts have been found in some of the schist fragments. Fragments of groundmass from felsic volcanic rocks have also been identified in trace amounts. Quartz appears as mono- and polycrystalline forms. Some of the former grains have round corrosion embayments. The polycrystalline quartz occurs as massive and foliated grains. Authigenic quartz overgrowths are rare. Plagioclase is the main detrital feldspar and subordinate amounts of albite occur. Accessory mineral grains are zircon, apatite, garnet, tourmaline, epidote and sphene.

Plate 18. *Foliated metasedimentary clasts in lithic arenite of Unit 16, Indian Bay Big Pond Formation (scale bar is one half millimetre).*

NON-STRATIFIED, PLUTONIC IGNEOUS ROCKS (Units 17 to 20)

ULTRAMAFIC ROCKS AND GABBRO (UNIT 17)

Distribution

This unit is exposed in only one locality, approximately 3.5 to 5.5 km north of Indian Bay Pond. The unit is 100 to 200 m wide and extends for approximately 2 km along strike. The ultramafic rock is exposed on the western side and appears to form approximately 60 percent of the unit. Gabbro is exposed on the east side of the unit.

Contact Relationships

Contacts between the ultramafic rock and gabbro with the surrounding metasedimentary rocks are not exposed. The western margin of the ultramafic rock is intensely foliated and suggests that the body is fault bounded. The contact between gabbro and ultramafic rock is not exposed.

Age

The age of the unit is unknown.

Lithology

The ultramafic rock is very coarse grained, dark-green on fresh surfaces and weathers to a dark brown. It appears superficially monomineralic, the principal mineral being pyroxene-like in habit and up to 1 cm across. The surface of the exposure is rusty and locally gossanous. No internal structure or stratigraphy is present, other than a heterogeneous tectonic foliation. This foliation dips steeply northwest on the western margin and dips steeply southeast on the eastern margin of the ultramafic body; the foliation strikes northeast and is most intensely developed on the margins.

The gabbro is coarse grained and appears relatively fresh. It consists of dark-green pyroxene, up to 1 cm across and plagioclase feldspar up to 0.7 cm across in approximately equal proportions. The only structure is a poorly developed foliation, dipping steeply to the southeast, which is not as well-developed as in the ultramafic rock. The gabbro is pegmatitic in places and near the eastern margin of the body there are small (less than 10 cm) patches of granitic pegmatite containing coarse-grained tourmaline. Quartz is also present as veinlets and discrete blobs several centimetres across.

Petrography

In the ultramafic rock, the pyroxene has been replaced by fine-grained masses of colourless amphibole, probably tremolite, and subordinate chlorite. A very fine-grained opaque mineral is disseminated throughout. The alteration assemblage is locally deformed and crenulated.

In the gabbro, most of the plagioclase feldspar has been extensively sericitized and the mafic minerals are altered to colourless to pale-green or very pale bluish-green actinolite or actinolitic hornblende. Basal sections of amphibole are turbid and brownish. Fine-grained biotite inclusions are present in some hornblende crystals. Most of the very fine-grained opaque material is restricted to the alteration assemblage of actinolite. The grade implied by the alteration assemblage is compatible with that in the surrounding pelitic sedimentary rocks. The rock contains no obvious foliation in thin section.

UNIT 18

Distribution, Contact Relationships and Age

Unit 18 is a small body of a muscovite-bearing granitoid rock that appears to intrude the Hunts Cove Formation of the Davidsville Group, approximately 0.5 km west of Route 330, near the northern edge of the map area. Aeromagnetic and gravity maps show no obvious geophysical signature for this body. Contacts are not exposed and contact effects appear to be negligible. An ^{40}Ar$-^{39}$Ar age (muscovite) of 426 Ma has been obtained for this rock and is discussed in the section titled Geochronology.

Lithology

The granitoid is exposed, in patches, within an area several hundred metres across. The rock is massive, contains equigranular quartz, feldspar and muscovite, and is locally rusty due to disseminated pyrite.

Petrography

Quartz and plagioclase feldspar are the principal minerals. Grain boundaries are straight, curved or irregular and there is little evidence for recrystallization. Numerous, rounded inclusions of quartz, less than 0.1 mm across, occur in plagioclase and untwinned feldspar, some of which is probably orthoclase. Some feldspar grains are partially altered to white mica. Muscovite occurs as sprays and rosettes, commonly along grain boundaries and forms 5 percent or less of the rock. Opaque material forms 3 percent of the rock. Trace amounts of calcite occur locally. Many crystals show undulose extinction but there is no evidence of penetrative deformation.

OCEAN POND GRANITE (UNIT 19)

Definition

Baird *et al.* (1951) first documented the occurrence of a muscovite granite near Ocean Pond. Since then, the term Ocean Pond Granite has remained in informal use and is formally proposed here for this granite.

Distribution, Contact Relationships and Age

The Ocean Pond Granite is exposed on the southern and western sides of Ocean Pond and southwest of Little Ocean Pond. North and northwest of Little Ocean Pond, the area is strewn with boulders predominantly of a leucocratic granite similar to the Ocean Pond Granite; however, no definite exposures were identified. Contacts between the granite and the host metasedimentary rocks are generally sharp. The intrusive age of the granite is not known; a ^{40}Ar$-^{39}$Ar age on muscovite of 398 ± 5 Ma (plateau age) has been determined and is discussed in the section Geochronology.

Lithology

The Ocean Pond Granite is a leucocratic, equigranular, fine- to coarse-grained foliated granite. Feldspar forms irregular anhedra up to 1 cm across. Quartz anhedra range up to 5 mm across and muscovite forms flakes up to 8 mms across. Biotite is generally absent but is widespread in the exposure southwest of Little Ocean Pond. Deep red garnet crystals up to 3 mm across, are dispersed throughout the granite. Tourmaline also occurs locally.

The fine-grained variety forms a minor component of the Ocean Pond Granite. It contains no biotite and less muscovite than the coarse phase. Tourmaline, however, is more abundant and defines a subhorizontal lineation in one exposure, plunging 21° toward 014 degrees.

The Ocean Pond Granite contains an ubiquitous shallowly dipping tectonic foliation mainly defined by muscovite, and also by quartz. The foliation maintains a consistent attitude and does not appear to be folded.

Petrography

The Ocean Pond Granite consists of quartz, plagioclase, K-feldspar ± biotite ± tourmaline ± garnet. In the coarse-grained variety, the essential minerals are feldspar (approximately 60 percent), quartz (20 percent or less) and muscovite (5 to 20 percent). Biotite (0 to 5 percent), garnet (1 percent or less), apatite and tourmaline (1 percent or less) are accessory phases. The muscovite occurs along quartz–feldspar grain boundaries and as inclusions in other phases. Some of the K-feldspar displays characteristic microcline twinning and appears to be modally subordinate to plagioclase. Patches of K-feldspar form inclusions in coarse-grained plagioclase. Microcline grains are 4 mm across or less and contain inclusions of plagioclase in places. String perthite, up to 5 mm across, contains inclusions of zoned plagioclase, quartz and biotite. A granophyric texture is locally developed. Feldspars are variably sericitized.

The following observations indicate that the granite was affected by deformation, some of which was cataclastic in nature, after crystallization. Twin planes in plagioclase are bent or displaced and individual crystals are cracked. Quartz is commonly polygonized and subgrains have lobate or scalloped boundaries. Quartz ribbons are oriented parallel to the foliation. Flakes of muscovite are bent and show strained extinction. Thus, neither muscovite nor quartz recrystallized after the deformation.

Pegmatites and Other Veins Associated with the Ocean Pond Granite

Pegmatitic phases of the Ocean Pond Granite are common and are considered to be associated with the granite because of their close spatial association and mineralogical similarities. They are very common in the area between Whitney and Ocean ponds for which a separate subunit is defined, comprising metasedimentary rocks and pegmatitic–granitic sheets. The pegmatites are characterized by abundant pale green muscovite, which locally forms layers 15 cm thick or less, and bright red garnets up to 1 cm across, which generally form isolated crystals but also are concentrated into clusters or bands several centimetres long. Tourmaline crystals, 5 cm long or less, are ubiquitous. Beryl occurs in one exposure near Ocean Pond and specks of molybdenite were also noted in one locality. Ilmenite, chlorite and biotite are other accessory minerals.

The central parts of many of the pegmatites are very coarse grained and become finer grained toward the margin. Some pegmatites contain a foliation that is better developed in their finer grained margins.

Veins of very fine-grained tourmaline ± quartz occur within several kilometres of the Ocean Pond Granite. They range from 1 to 10 mm thick, have pyritic haloes in places and are steeply dipping. Some of the the veins are offshoots of tourmaline-bearing pegmatites. Commonly, the fine-grained tourmaline has infiltrated the host rocks along the foliation or bedding planes, up to 10 cm from the vein. Pink, feldspathic veins, 1 to 3 mm thick, which invariably have a 1- to 2-mm-thick hematite-rich halo, also occur in the same area. Throughout the central part of the map area, distinctive, fine-grained, white, quartz veins 1 to 6 m wide and several kilometres long, form very linear features subparallel to the regional strike. Included angular blocks of psammite, in a fine-grained quartz matrix (Plate 19), are common and together with the linear nature, suggest a dilation origin. Vuggy cavities are locally present in the veins.

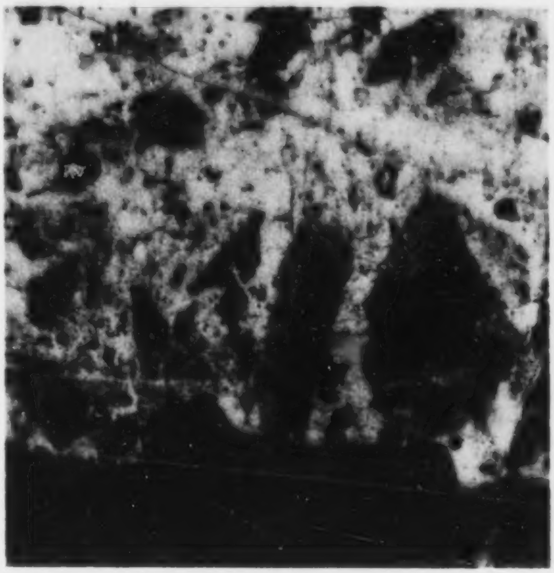

Plate 19. *Quartz vein, which intrudes the Gander Group, containing psammitic blocks of country rocks.*

DEADMAN'S BAY GRANITE (UNIT 20)

Distribution

The Deadman's Bay Granite (Strong *et al.*, 1974; formerly called the Deadman's Cove pluton, Fairbairn and Berger, 1969) underlies approximately 80 sq km of the northeastern corner of the map area. Much of the land area of map area NTS 2F/5 (Jayasinghe, 1978), the northwestern portion of NTS 2F/4 and the southeastern corner of NTS 2E/8 are also underlain by the granite. Geophysical evidence indicates that the granite is continuous offshore. The Deadman's Bay Granite forms the largest granitoid body in northeastern Newfoundland.

Contact Relationships

The contact between the Deadman's Bay Granite and the country rocks is defined by a gradational intrusive zone up to 5 m wide. Within this zone, screens of metasedimentary rock occur parallel to the granite contact. The metasedimentary rocks in the intrusive zone are characterized by the profuse growth of feldspar megacrysts, which appear identical to those in the granite.

Age

The age of crystallization of the Deadman's Bay Granite has been determined as 385 ± 2 Ma (U–Pb on monazite and zircon; Greg Dunning, personal communication, 1989). This U–Pb age is probably closer to the actual crystallization age of the granite than earlier K–Ar ages and is more precise than previous U–Pb ages. The previous ages include igneous crystallization ages of 342 ± 14 Ma (K–Ar, biotite; Wanless *et al.*, 1965), 352 ± 15 Ma (K–Ar, biotite; Wanless *et al.*, 1972), 510 ± 10 Ma (U–Pb, zircon; Berger and Naylor, 1974), 353 $^{+12}_{-17}$ Ma (U–Pb, zircon; Currie *et al.*, 1982), 430 ± 2 Ma (Pb–Pb, zircon; Currie *et al.*, 1982), 400 ± 13 Ma (K–Ar, biotite; Stevens *et al.*, 1982). It agrees with a U–Pb zircon age of 385 ± 10 determined by Berger and Naylor (1974) who, however, interpreted the age to represent possible evidence of post Late Cambrian regional deformation.

Lithology

The Deadman's Bay Granite is a homogeneous, K-feldspar megacrystic biotite granite (Plate 20). The K-feldspar megacrysts are characteristic and form 40 to 70 percent of the rock. In the map area, the megacrysts range up to 10 cm across; elsewhere, near Lumsden (personal observation) they reach 20 cm in diameter. Quartz forms 30 percent or less of the rock and in places, is a distinctive blue. There are a few occurrences of a leucocratic, equigranular granite, which contains accessory garnet and trace amounts of biotite. The Deadman's Bay Granite is typically unfoliated; however, in a few places, there is a moderate flow foliation that is defined by aligned megacrysts and trends 120 degrees. The only evidence of deformation within the granite is a steep, cataclastic foliation that strikes 090° and is restricted to narrow zones, several tens of centimetres across. Feldspars are disaggregated and biotite is retrogressed to chlorite within these zones. Millimetre-thin epidote veinlets occur locally. Close to the margin of the granite, blocks of the metasedimentary host rock occur in the granite and are hornfelsed. No pegmatites, which might be associated with the granite, have been observed.

Plate 20. *The megacrystic, biotite-bearing Deadman's Bay Granite.*

Petrography

The Deadman's Bay Granite consists of large subhedral feldspar megacrysts in a matrix of K-feldspar, plagioclase, quartz, biotite and accessory sphene and apatite. The majority of the feldspar megacrysts are microcline and some show rapakivi texture. Plagioclase feldspar occurs mostly in the matrix as anhedral to subhedral crystals and rarely as megacrysts. The feldspar is variably sericitized and coarser grained white mica and epidote are also developed in the most intensely sericitized crystals. Locally, lobate myrmekite structures extend into microcline where adjacent to perthite. Some fine-grained biotite and trace muscovite occur as inclusions in feldspar. Biotite is locally altered to chlorite and magnetite.

GEOCHEMISTRY

GANDER RIVER COMPLEX

Representative samples of ultramafic, mafic and felsic rocks from the Weir's Pond area of the Gander River Complex were analyzed at the Newfoundland Department of Mines and Energy for major oxides and some trace elements. Rare-earth elements (REEs) and some trace elements were also determined on selected samples by ICP-MS at Memorial

University of Newfoundland. The analytical methods, precision and accuracy of the determinations and the analyses are given in Appendix 2.

The geochemical data presented here are from the Weir's Pond area only and conclusions drawn from this dataset strictly pertain to this area. Extrapolation of any conclusions to the complex as a whole, therefore, are made reservedly.

Mafic and Ultramafic Rocks

Element Mobility and Effects of Alteration

Prior to using the geochemical data, the effects of alteration and low-grade metamorphism on the chemistry of the rocks need to be assessed. Many authors (e.g., Cann, 1970; Floyd and Winchester, 1975, 1978; Pearce, 1980; review by Goff, 1984) have shown that the high-field-strength elements (HFSE) Zr, Nb, Y and Ti, the low-field-strength element (LFSE) Th and heavy rare-earth elements (HREE), are relatively immobile during low-grade metamorphism and various alteration processes. The review by Goff (1984) also points out that other elements such as Cr, Ni, V and the light rare-earth elements (LREE) are also relatively immobile and can be used as petrogenetic indicators. Elements such as Zr and Y are incompatible in early formed phases in mafic magmas and may provide useful differentiation indices (Pearce and Norry, 1979; Perfit *et al.*, 1980).

In order to assess alkali-element mobility, all mafic rocks are plotted on the igneous spectrum diagram of Hughes (1973; Figure 5). Most of the gabbros plot within the igneous spectrum, suggesting limited overall change in K_2O or Na_2O, whereas most of the diabase and basalt samples lie above the field, implying K_2O loss and Na_2O addition. Trace elements such as Rb and Ba, which vary sympathetically with the alkalies, are likely to have been similarly affected.

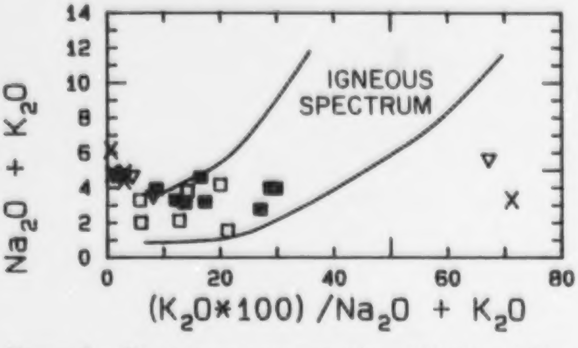

Figure 5. *The igneous spectrum plot of Hughes (1973). Squares (open and closed) are gabbros, x are diabase and inverted triangles are basalt of the Gander River Complex.*

In some of the diagrams in the following section, use is made of the Mg# (Mg number), which is derived from atomic proportions of Mg and Fe [Mg# = Mg / Mg + 0.9 (FeO as total iron)] and is, therefore, an index of differentiation. It has been shown (Cann, 1971; Seyfried *et al.*, 1978; Seyfried and Bischoff, 1981) that Mg can be mobile during hydrothermal alteration of basalts. However, much of this alteration takes place adjacent to the main fluid conduits in the rock, i.e., along pillow rims and fractures where the ratios of sea water to rock are high (Spooner *et al.*, 1977; Mottl, 1983). Swinden (1988) in a review of the advantages of the Mg#, concluded that under low water/rock ratios, in the solid rock, mass transfer of Mg is negligible; if fractured samples are avoided and pillow cores only are sampled, the Mg# can be a useful differentiation index.

Chemistry of the Ultramafic Rocks

Major- and trace-element analyses of altered and fresh ultramafic rocks from the Gander River Complex are presented in Appendix 2, Tables 11 and 12. The relationships between the ultramafic rocks and other units in the Gander River Complex are well illustrated by their AFM (K_2O + $Na_2O-FeO-MgO$) ratios (Figure 6). The general chemical characteristics of the ultramafic rocks are described below and a selection of variation diagrams illustrating chemical trends is shown in Figure 7.

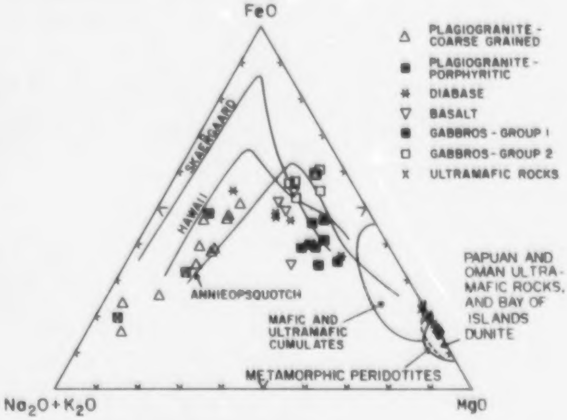

Figure 6. *An AFM diagram for representative analyses of mafic, ultramafic and felsic rocks of the Gander River Complex, Weir's Pond area. Fields for ultramafic and mafic cumulate rocks and the Skaergaard trend from Coleman (1977) and the Annieopsquotch trend from Dunning (1984). Field of Papua and Oman ultramafic rocks from Malpas and Stevens (1977).*

Silica averages 50 percent in fresh pyroxenite but exhibits a range of 17 to 55 percent in metamorphosed rocks. The values of MgO in clinopyroxenite average 20 percent; however, in the metamorphosed ultramafic rocks, MgO ranges from 18 to 60 percent (anhydrous values). The CaO averages 17 percent in clinopyroxenite; in metamorphosed rocks, however, it ranges from negligible amounts up to 42 percent, reflecting the extremely varied degree of carbonatization. The values of FeO (as total iron) shows a range from approximately 4.7 to 10.4 percent in metamorphosed rocks compared to about 5 percent in unaltered types; Cr values

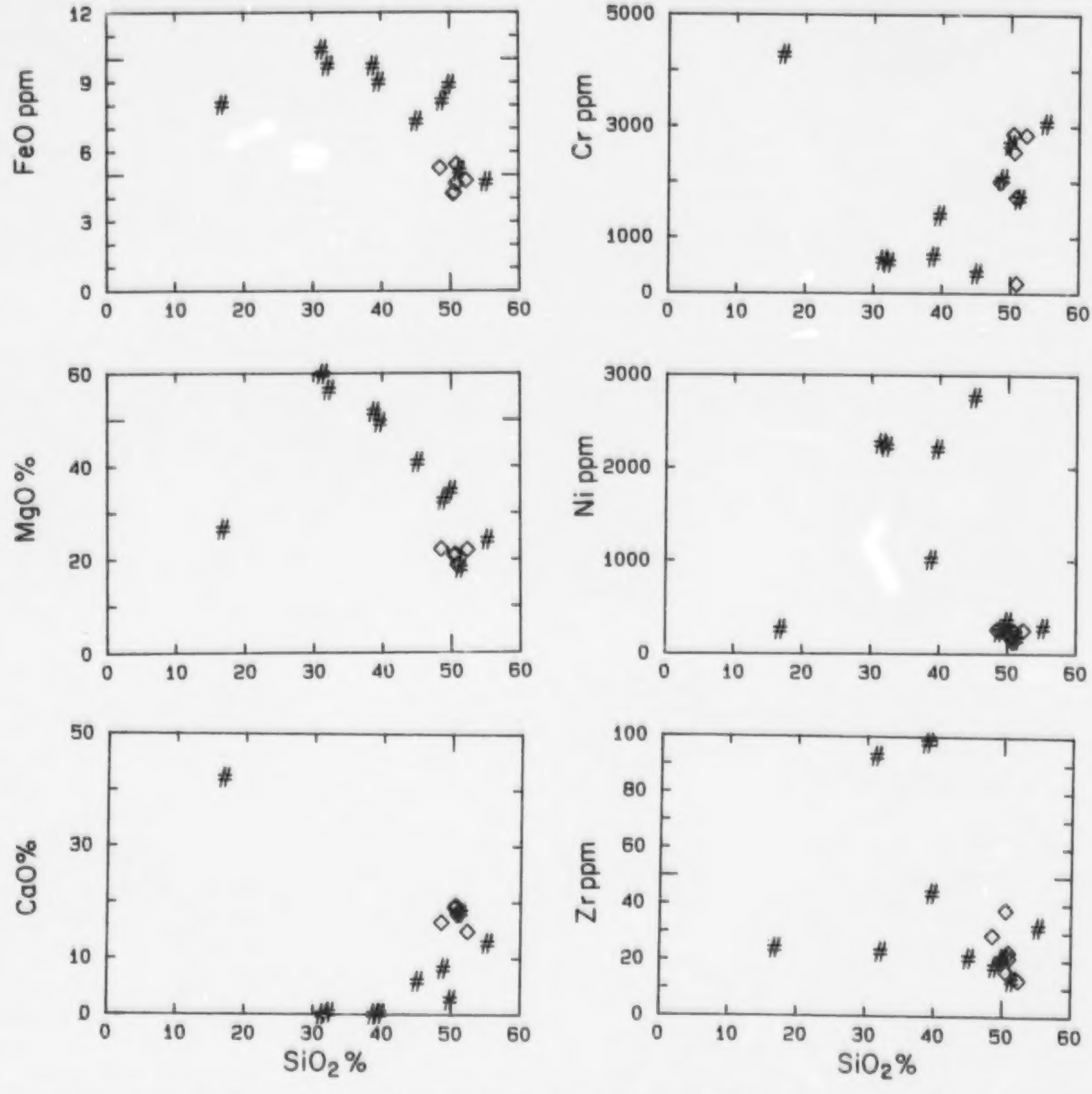

Figure 7. *A selection of Harker diagrams illustrating the principal chemical trends in ultramafic rocks of the Gander River Complex. The diamonds are fresh clinopyroxenites and number symbol represents altered ultramafic rocks.*

vary widely in all ultramafic rocks, whereas Ni values are scattered only in those that are altered. Abundances of Zr are essentially similar in all types, except for two metamorphosed rocks, which have relatively high values at 98 and 93 ppm.

In Figure 6, both fresh and metamorphosed ultramafic rocks from the Gander River Complex, are compared to Papuan and Oman ultramafic rocks; dunites from the Bay of Islands ophiolite also plot in the same field. On the SiO_2 versus FeO/FeO + MgO (FeO as total iron), the fresh clinopyroxenites plot above the field of mafic cumulates, reflecting their high SiO_2 content (Figure 8). The altered samples show a range of SiO_2 values; some plot within the field of ultramafic cumulates and close to average metamorphic dunitic and harzburgitic compositions. It is likely, therefore, that at least some of the metamorphosed ultramafic rocks were originally peridotites.

Major- and Trace-Element Variation in Mafic Rocks

Major-oxide-, trace- and rare-earth element analyses of mafic rocks from the Gander River Complex are presented in Appendix 2, Table 13. The majority of mafic rocks from

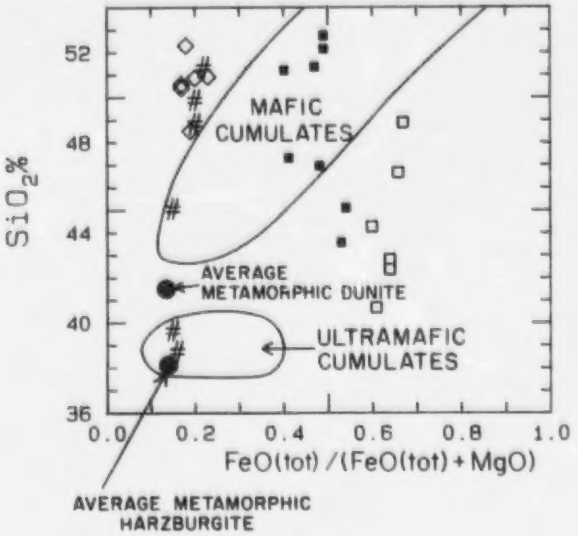

Figure 8. *The SiO_2 vs. $FeO_{(tot)}/FeO_{(tot)}$ + MgO plot for ultramafic rocks from the Gander River Complex. Fields from Coleman (1977). Squares (open and closed) are gabbros, x are diabase, inverted triangles are basalt, diamonds are fresh clinopyroxenites and number symbol represents altered ultramafic rocks.*

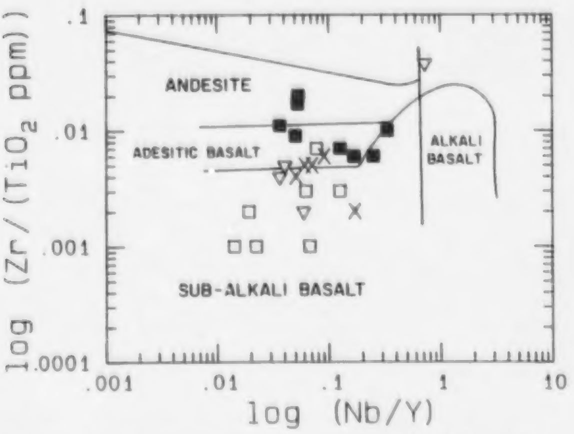

Figure 9. *The classification of mafic rocks of the Gander River Complex according to the fields of Winchester and Floyd (1977). Squares (open and closed) are gabbros, x are diabase and inverted triangles are basalt.*

the Weir's Pond area are basaltic, containing less than 53 percent SiO_2 (Basaltic Volcanism Study Project, 1981), and are sub-alkaline basalts or andesitic basalts (Figure 9), based on their Nb/Y and Zr/TiO_2 ratios (Winchester and Floyd, 1977). On a TiO_2 versus FeO/MgO plot (Miyashiro, 1975), diabase and basalt together show a strong tholeiitic trend (Figure 10). This plot together with that in which TiO_2 is plotted against Y (Figure 11) serve to illustrate several features of the geochemistry that will recur in most of the other variation diagrams:

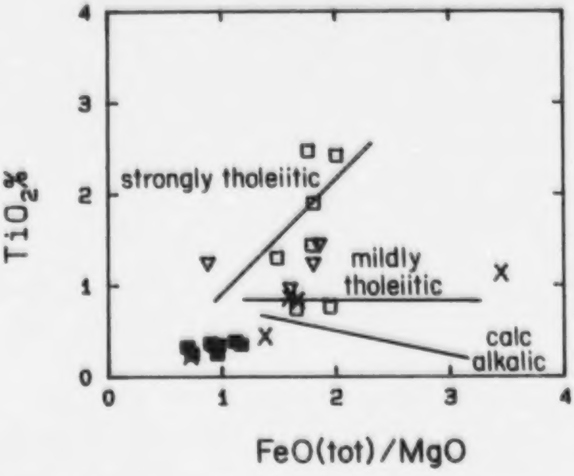

Figure 10. *Basalt and diabase display their tholeiitic nature whereas gabbros are split into two groups in this tholeiitic vs. calc-alkalic discriminant plot of Miyashiro (1975). Squares (open and closed) are gabbros, x are diabase and inverted triangles are basalt.*

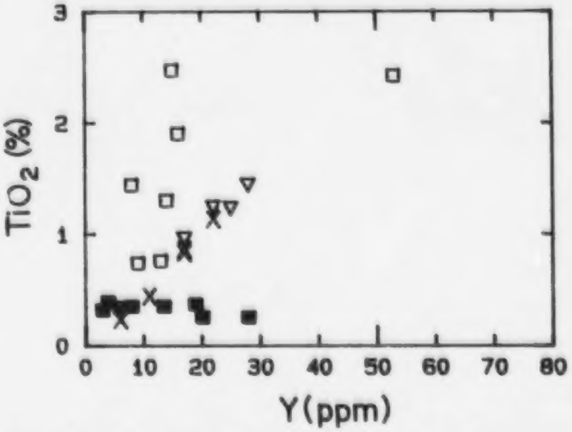

Figure 11. *The TiO_2 vs. Y plot for mafic rocks of the Gander River Complex. Gabbros are already split into two groups, neither of which are apparently related to the diabase and basalt. Squares (open and closed) are gabbros, x are diabase and inverted triangles are basalt.*

1) the gabbros define two groups, one, depleted (group 1), at low TiO_2 and low FeO/MgO, and a more evolved group (group 2), which typically overlaps with the basalt and diabase;

2) although based on limited numbers, the majority of the basalt and diabase define a trend, suggesting that they form part of one magma series; and

3) basalt and diabase show no consistent chemical links with either of the two gabbro groups.

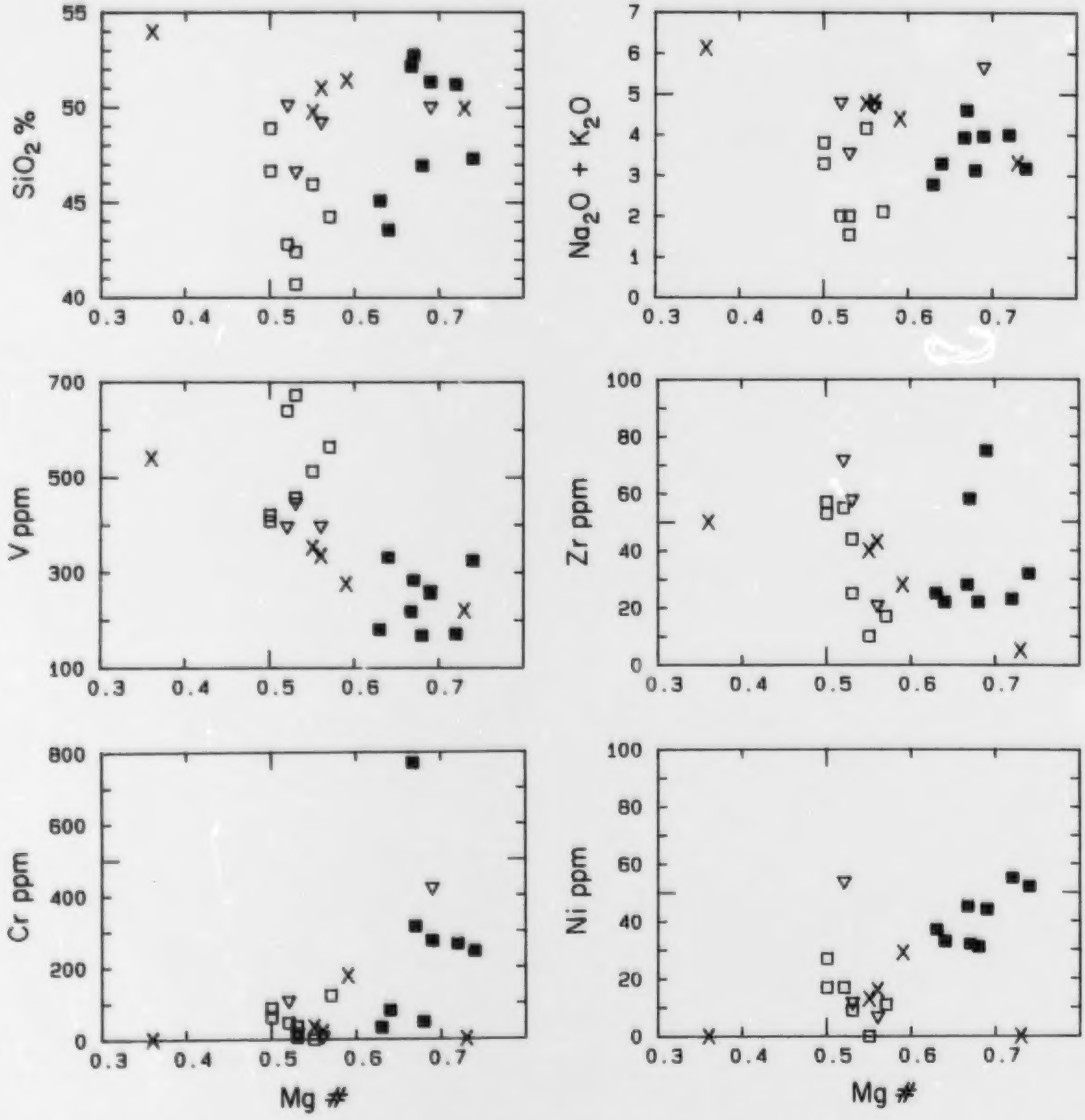

Figure 12. *Variation of some oxides and trace elements with the Mg #. Squares (open and closed) are gabbros,* x *are diabase and inverted triangles are basalt.*

Note that four of the group-2 gabbro samples come from the same location (a quarry on Route 330) and 3 of the diabase samples also were collected in this quarry.

In Figure 12, a sequence of plots illustrates the variation in major and trace elements with the Mg#. Group 1 is relatively primitive, plotting at high Mg numbers and no trends are apparent, whereas group 2 shows a perceptible increase in V and Zr with differentiation (decreasing Mg#). In both Zr versus Mg# and V versus Mg# plots, the lack of correlation between the gabbro groups is evident. Plots of Cr and Ni against Mg# also preserve the gabbro groupings; however, only the Ni plot suggests a magmatic link between group 1 and the basalt and diabase. The combined alkalies and SiO$_2$ show scatter and have been affected by alteration.

Diabase and basalt of the Complex exhibit tholeiitic fractionation trends on the TiO$_2$ versus FeO/MgO (Miyashiro, 1975) and on the TiO$_2$ versus Mg# and V versus Mg# plot (continuous iron enrichment and increasing TiO$_2$ and V with differentiation) (Miyashiro and Shiro, 1975; Shervais, 1982). Gabbros of Group 1 show no tholeiitic trends and are quite primitive, plotting in and near the field of mafic–ultramafic cumulates (Figures 6 and 8) and contain very low TiO_2 values. Group 1 gabbros typically show no differentiation trends, e.g., Figure 11, increasing Y is not accompanied by an increase in TiO_2. Group 2 gabbros indicate some fractionation in certain diagrams, e.g., Zr versus Mg#, however, generally, they show no consistent trends.

Tectonic Setting Based on Mafic Rock Chemistry

Major and Trace Elements

A number of plots, based on the immobile high-field-strength (HFS) elements, are used to place constraints on the tectonic setting of the Gander River Complex. The majority of the samples plot within or close to the volcanic arc basalt (VAB) field on a Zr/Y versus Zr diagram (Pearce and Norry, 1979) (Figure 13). All diabase and basalt samples with one exception in each case, fall in this field. Some diabase and basalt also plot within the area of overlap between the VAB and mid-ocean ridge basalt (MORB) fields. One basalt (sample # 86-64) has very high Zr (473 ppm), high K_2O (3.81 percent), high Ba (1940 ppm), high Cr (422 ppm) and Ni (101 ppm). This unusual chemical character may reflect some sialic crustal contamination of a basaltic magma. Diabase sample (86-370) also falls outside the field and has chemical traits that distinguish it from the other diabase samples, e.g., high Ba (2445 ppm), K_2O (2.35 percent), MgO (13.13 percent), and very low Zr and Y. These features may be result of crustal contamination and/or alteration. Most of the group 1 gabbros plot above the VAB field. On the Ti versus V plot (Shervais, 1982) most mafic rocks from the Complex fall within or very close to the field of island-arc tholeiites (IAT) (Figure 14). Group 1 gabbros and one diabase sample (# 86-370) are marginal to this field. One other diabase sample plots just inside the IAT field. Basalt and two of the diabase samples plot off the V/Ti ratio line of 10, which Group 1 gabbros fall on, suggesting these rocks do not form a magmatic series. Note that two of the basalts and one gabbro from Group 2 fall in the MORB field.

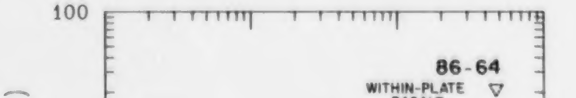

Figure 13. *Tectonic discrimination of mafic rocks of the Gander River Complex based on Zr/Y vs. Zr ratios. Fields from Pearce and Norry (1979). Squares (open and closed) are gabbros,* x *are diabase and inverted triangles are basalt.*

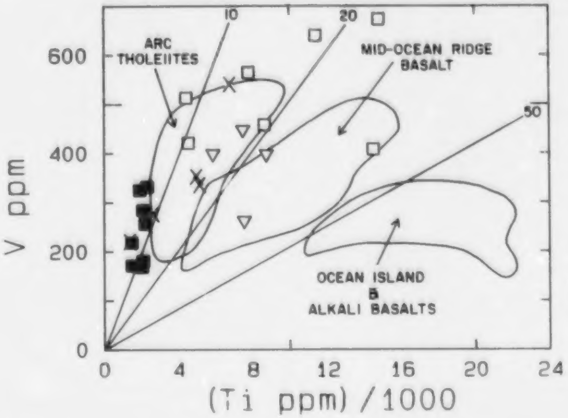

Figure 14. *Tectonic discrimination of mafic rocks of the Gander River Complex based on Ti vs. V ratios. Fields from Shervais (1982). Squares (open and closed) are gabbros,* x *are diabase and inverted triangles are basalt.*

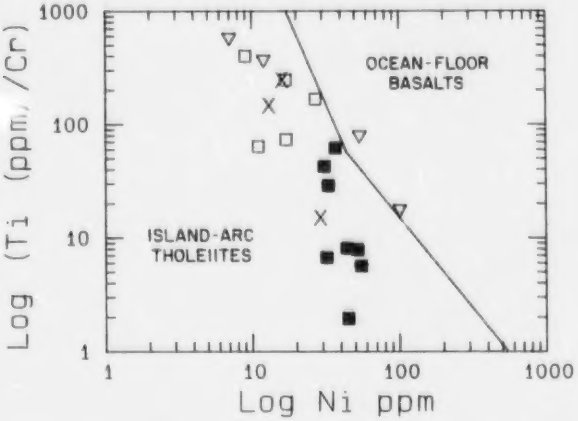

Figure 15. *Island-arc affinity of mafic rocks of the Gander River Complex based on Ni vs. Ti/Cr ratios. Fields from Beccaleuva* et al. *(1979). Squares (open and closed) are gabbros,* x *are diabase and inverted triangles are basalt.*

Figure 15 (Ni versus Ti/Cr), illustrates a plot devised by Beccaleuva *et al.* (1979) to discriminate island-arc and ocean-floor tholeiites, which shows the majority of mafic rocks from the Complex in the island-arc tholeiite field.

In Table 2, the average values of mafic rocks from the Gander River Complex are compared to those of mafic rocks from various tectonic settings in Newfoundland and elsewhere. The Cr and Ni values are lower and Rb abundances are slightly higher in the complex and in island arcs compared to ocean-floor basalt (OFB) and ophiolitic rocks. The Sr values are high and more typical of IATs. The Ba abundances are very high compared to both IATs and OFBs (note that Ba in Pipestone Pond basalt and diabase is also relatively high). The Zr and Y levels are very similar to those of IATs.

Table 2. Average element values of mafic rocks of the Gander River Complex, compared to average values of mafic rocks from various sources

	GANDER RIVER COMPLEX			OCEAN FLOOR BASALTS		ANNIEOPSQUOTCH OPHIOLITE		ISLAND ARC BASALT			PIPESTONE POND COMPLEX		
	BASALT (3)	DIABASE (4)	GABBRO (14)	OFB -1	OFB -2	DYKES	LAVAS	IAT -1	IAT -2	IAT -3	BASALT (5)	DIABASE (8)	GABBRO (11)
Cr	46.0	46.0	170.0	270.0	251.0	170.0	123.0	111.0	82.0	176.0	143.0	353.0	139.0
Ni	24.0	12.0	29.0	135.0	90.0	74.0	44.0	18.0	36.0	69.0	56.0	75.0	36.0
Sc	52.0	48.0	11.0	-	-	-	-		-	-	-	-	-
V	415.0	345.0	364.0	250.0	-	326.0	352.0	-	286.0	254.0	395.0	318.0	335.0
Cu	62.0	76.0	30.0	86.0	-	30.0	38.0	-	98.0	94.0	48.0	63.0	78.0
Pb	1.0	1.0	1.0	-	-	2.0	3.0	-	4.0	2.4	-	-	-
Zn	104.0	81.0	72.0	85.0	-	86.0	143.0	-	78.0	71.0	88.0	77.0	58.0
Rb	11.0	2.0	14.0	1.0	2.0	1.0	1.0	4.7	4.1	5.7	20.0	4.0	6.0
Ba	159.0	153.0	474.0	12.0	20.0	62.0	50.0	60.0	90.0	63.0	189.0	182.0	51.0
Sr	199.0	137.0	171.0	127.0	121.0	95.0	83.0	231.0	224.0	337.0	91.0	94.0	81.0
Ga	23.0	18.0	15.0	17.0	-	14.0	14.0	-	-	15.0	10.0	10.0	8.0
Nb	1.0	1.0	1.0	-	4.6	1.0	2.0	1.7	1.7	1.6	4.0	2.0	1.0
Hf	1.0	1.2	0.14	-	-	-	-	-	-	-	-	-	-
Zr	52.0	40.0	38.00	-	90.0	57.0	70.0	40.0	31.0	41.0	78.0	11.0	5.0
Y	23.0	17.0	16.00	-	33.0	36.0	42.0	17.0	16.0	17.0	40.0	9.0	4.0
Th	1.0	0.3	1.2	-	-	-	-	-	-	-	-	-	-
U	0.4	0.1	0.02	-	-	-	-	-	-	-	-	-	-

All values in ppm: OFB-1 = Basaltic Volcanism Study Project (1981)−Oceanic tholeiite; OFB-2 = Mid ocean ridge tholeiite (Pearce, 1982); IAT-1 = Tholeiitic volcanic arc basalt (Pearce, 1982); IAT-2 = Average basalt values of low K-orogenic volcanic rocks; IAT-3 = Average New Britain Island arc basalt (B.V.S.P., 1981); Pipestone Pond Complex (Swinden, 1988)

Rare Earth Elements

Partial extended REE plots on which Nb and Th are plotted as well as the usual REEs, are used to help discriminate the mafic rocks in terms of tectonic setting. The HFS element Nb, in island-arc volcanic rocks, is typically underabundant with respect to REE of similar ionic character (Wood *et al.*, 1979; Sun, 1980), and on primitive-mantle normalized plots, this feature is expressed as a negative Nb anomaly, relative to La and Ce. The low-field-strength (LFS) element Th is relatively overabundant in island-arc lavas and has normalized abundances generally greater than the light REEs. Extended REE plots for three gabbro, three diabase and one basalt sample are illustrated on Figure 16. All exhibit distinctive negative Nb anomalies and normalized Th at similar values to or greater than the light REEs.

In the case of the two gabbro samples with the lowest Nb values, the negative Nb anomalies are an artifact of the low analytical value at the level of detection. The basalt and diabase samples have very similar, smooth, slightly convex-up REE patterns and all except one diabase display well-defined to slight negative Eu anomalies. The light REEs are depleted in all four samples. The negative Eu anomalies are probably indicative of plagioclase fractionation in the source magma (Basaltic Volcanism Study Project (BVSP), 1981). The very similar patterns of basalt and diabase suggest that these rocks are genetically related.

The REE patterns of the gabbros are dissimilar from those of the basalt and diabase above. Two of the samples, from group 2 gabbros, show severe light REE depletion relative to the middle REE and negative Eu anomalies. Light rare-earth element depletion is a characteristic feature of MORB (Kay and Senechal, 1976; Suen *et al.*, 1979; Dunning, 1984). The third sample, from group 1, has a flat, light REE pattern and in contrast to all the other patterns, the light REEs show a slight enrichment. The REE patterns of samples from the Gander River Complex are similar, with the exception of the two group-2 gabbros, to those of arc tholeiites from New Britain (BVSP, 1981) having the slightly depleted light REEs, flat middle REEs and flat to slightly depleted heavy REEs (Figure 17). One gabbro from group 1 shows a light REE pattern of enrichment, which is similar to the upper part of the New Britain Arc field. Note that one of the diabase samples from this study shows a pronounced negative Eu anomaly, atypical of island-arc tholeiites.

In summary, the above discussion of geochemical characteristics of the mafic rocks of the Gander River Complex suggest that they formed in an island-arc setting.

Plagiogranite Geochemistry

Major-oxide-, trace-element and REE analyses of felsic rocks from the Gander River Complex are presented in Appendix 2, Table 14a and 14b. CIPW norms are listed in Appendix 2, Table 15. The samples were collected throughout

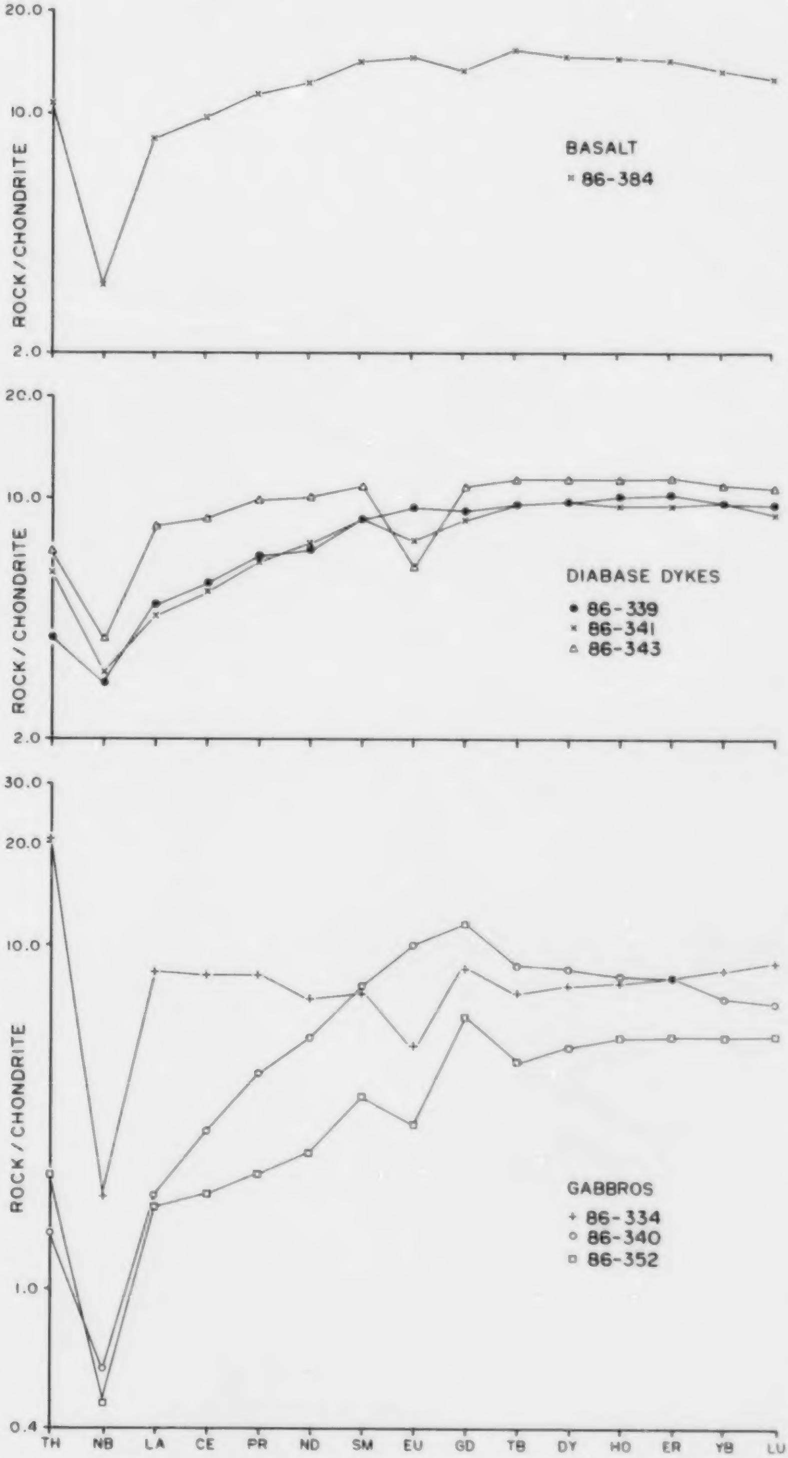

Figure 16. *Partial extended REE plots for mafic rocks of the Gander River Complex. In lowest diagram, the + pattern represents Group 1 gabbro and the open circle and square represent Group 2 gabbros.*

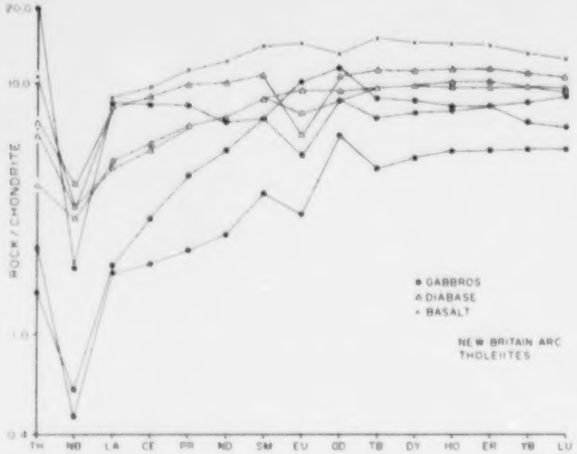

Figure 17. *Partial extended REE plots for mafic rocks of the Gander River Complex compared to island-arc tholeiite field of New Britain (B.V.S.P., 1981).*

the Weir's Pond area from exposures that range in size from small pods, metres across, to the Weir's Brook pluton, which is approximately 500 m across. In the majority of exposures, the plagiogranite is associated with gabbro and both coarse-grained and porphyritic types of plagiogranite were sampled.

Low-Grade Metamorphism and Element Mobility

Petrographic examination of these rocks, described in an earlier section, has shown little pervasive metamorphism, although a cataclastic deformation is ubiquitous. Feldspars are commonly dusty due to the presence of very fine-grained sericite, however, coarse-grained white mica, which would suggest K_2O mobility, is absent. Thin epidote and sphene veins occur locally and are commonly associated with narrow zones of cataclasis. Quartz veinlets also occur locally, but samples were chosen so as to avoid vein material where possible. Plots of K_2O and Sr against the immobile elements Zr and Y show little scatter and indicate the absence of large-scale mobility of the alkali and alkaline earth elements (Figure 18). Figures 18 and 19 illustrate the variation among the major oxides and trace elements in binary plots.

Classification

The felsic rocks from the Gander River Complex are mostly trondhjemites and three plot as tonalites in the normative An–Ab–Or feldspar diagram of O'Connor (1965) (Figure 20). Most of the felsic rocks, with three exceptions, are low in alumina (less than 15 percent Al_2O_3) based on the classification of Barker *et al.* (1976). The rocks are characteristically K_2O-poor (< 1 percent), Na_2O-rich (2 to 6 percent) and contain silica values in the range from 61 to 77 percent.

On the AFM plot (Figure 21), the felsic rocks fall mostly within the calc-alkaline field, but the trend approximately parallels that of oceanic plagiogranites; the latter follow a tholeiitic trend (Coleman and Donato, 1979).

General Chemical Trends of the Felsic Rocks

Variations in major- and trace-element contents of the felsic rocks are illustrated in Figures 18 and 19. Three samples are porphyritic but show no deviation from trends defined by the remaining, coarse-grained types. With increasing SiO_2, the oxides Al_2O_3, FeO, TiO_2 and MgO all show distinct negative correlation. CaO also has a negative correlation with SiO_2 but does show some scatter. Although Na_2O and K_2O values are somewhat scattered, the positive and negative trends respectively, are perceptible; these contrasting trends in alkalis, are probably due to ion exchange rather than alteration (since evidence for alteration of these rocks is absent). The consistently well-defined nature of these trends suggests a lack of pervasive mobilization of the major oxides.

The HFSEs Zr and Y have flat trends at low SiO_2 values but appear to exhibit steep positive slopes at higher SiO_2. The LFSEs Ba and in particular Sr, show a negative correlation with SiO_2; Rb shows no systematic variation with SiO_2.

REE Geochemistry

Partial extended, rare-earth element patterns for six felsic rocks from the Gander River Complex are illustrated on Figure 22. All samples are coarse grained except sample # 86-361, which is porphyritic. Four of the samples have very similar REE patterns and abundances between 2.5 to 9 times chondrite. Sample # 86-329 has strongly enriched light REE and heavy REEs, which are slightly enriched compared to the other samples. Sample # 86-361 has a flat pattern but is strongly enriched in all REEs and has a distinct negative Eu anomaly. This latter rock contains the highest SiO_2 value (77 percent) and the lowest FeO (total iron) and MgO contents; it appears to be the most evolved sample.

All patterns show distinct negative Nb anomalies and three have slight positive Th anomalies compared to the light REEs. Wood *et al.* (1979) suggested that negative Nb and positive Th anomalies in extended REE plots of felsic rocks are signatures of island-arc rocks. REE patterns of the trondhjemites are dissimilar to those patterns exhibited by the mafic rocks and this point, coupled with the lower abundance levels of REEs in trondhjemites, suggests that the trondhjemites were not derived by differentiation from the mafic rocks.

Comparison between Trondhjemites of the Gander River Complex and Trondhjemites of Other Settings

Average values of major and trace elements from the Gander River Complex trondhjemites are compared to those of other trondhjemites in Table 3. Malpas (1979) described contrasting chemical behaviour between trondhjemites of the ophiolitic Bay of Islands complex and those of the island-

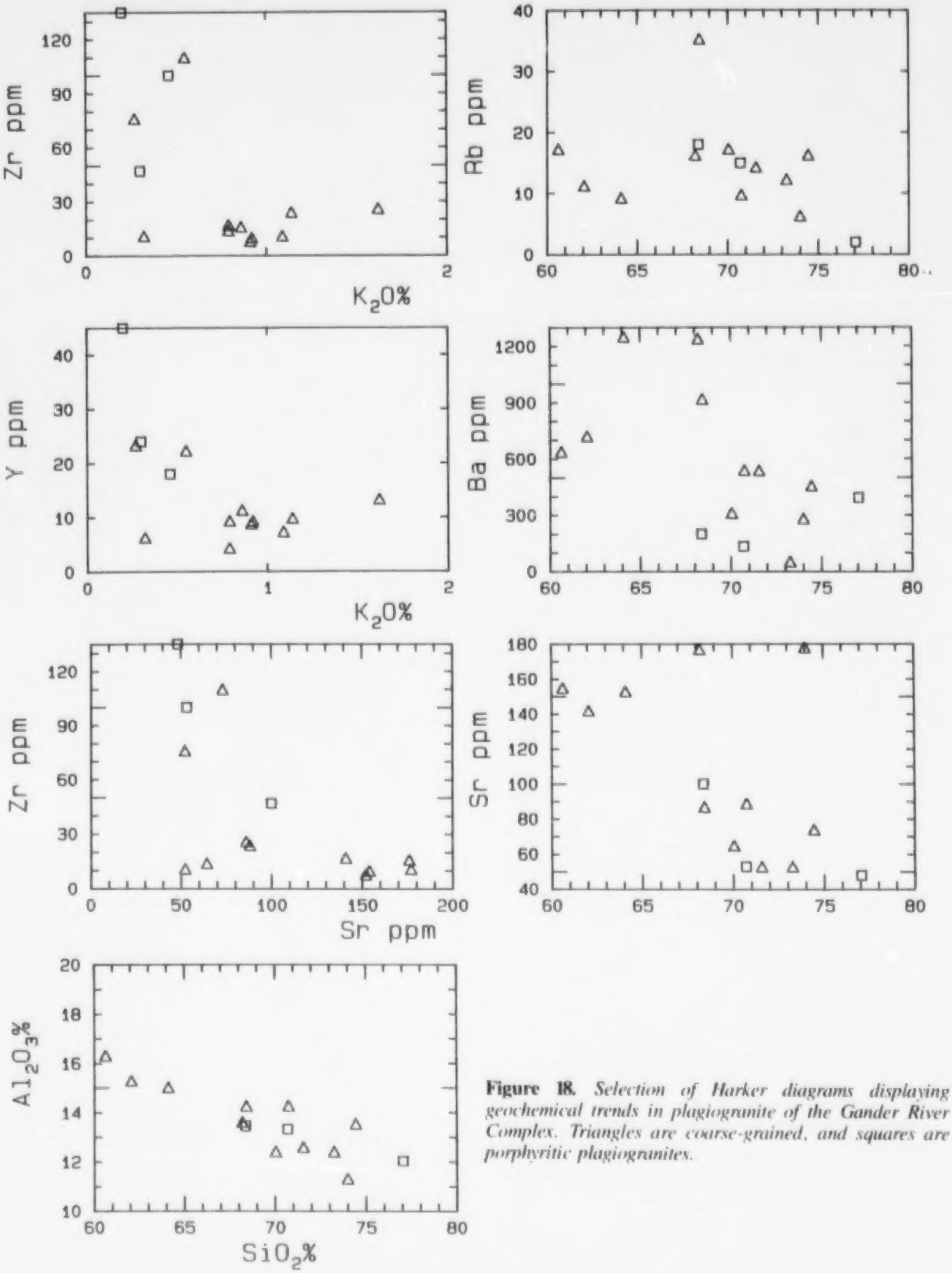

Figure 18. *Selection of Harker diagrams displaying geochemical trends in plagiogranite of the Gander River Complex. Triangles are coarse-grained, and squares are porphyritic plagiogranites.*

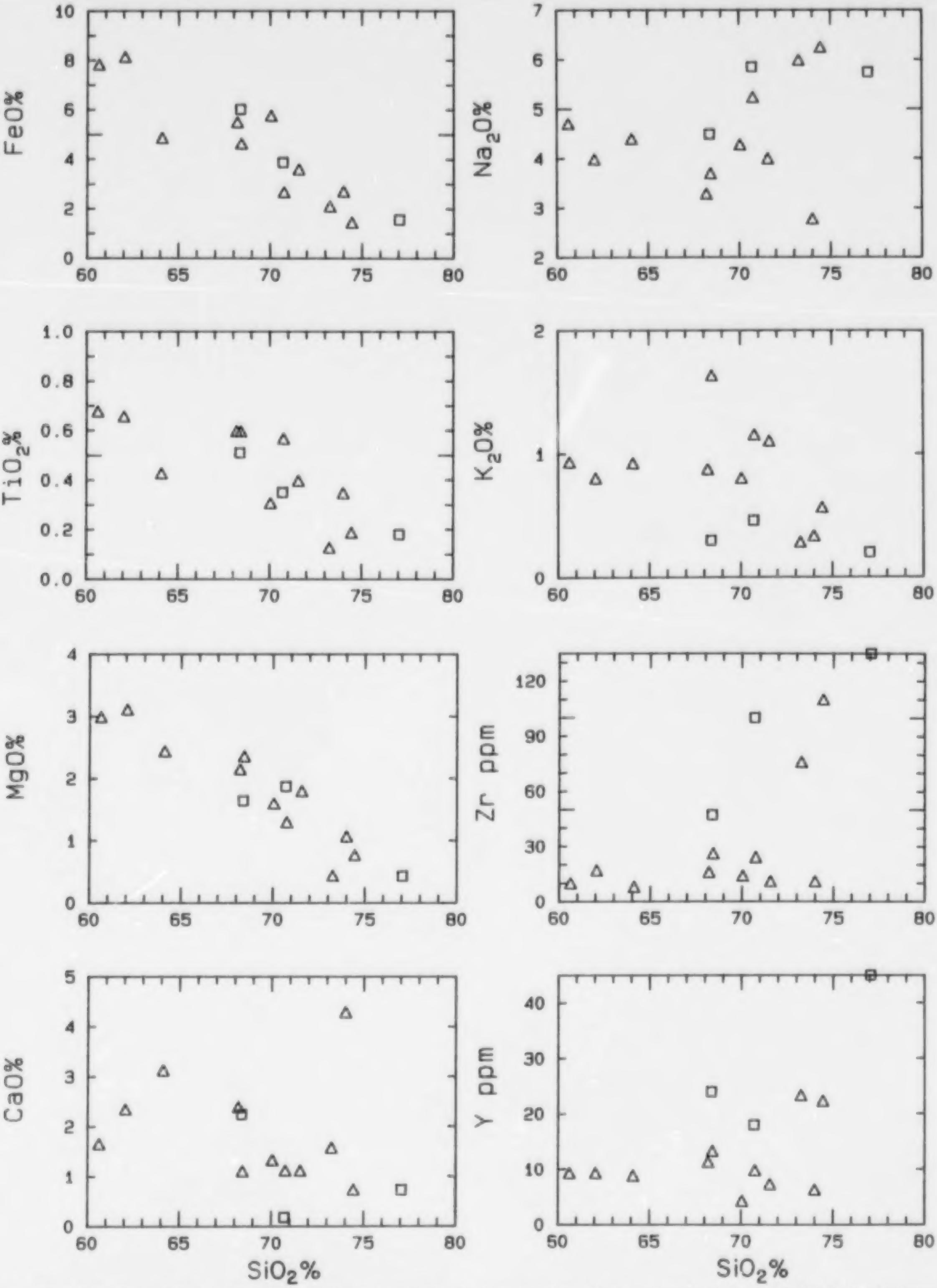

Figure 19. *Selection of Harker diagrams displaying variation between major oxides and trace elements and SiO_2 in plagiogranite of the Gander River Complex. Triangles are coarse grained, and squares are porphyritic plagiogranites.*

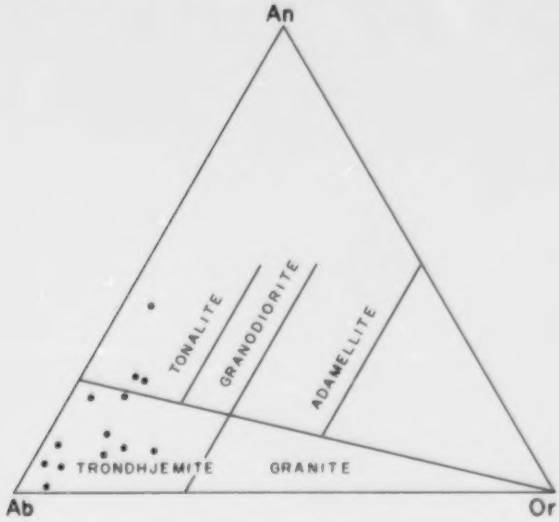

Figure 20. *Normative Ab–An–Or diagram (after O'Connor, 1965) for plagiogranite of the Gander River Complex.*

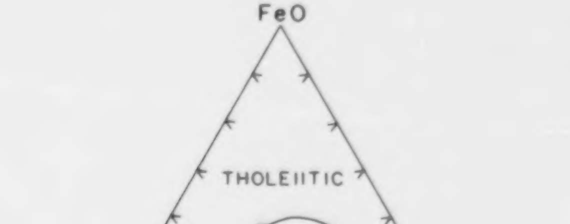

Figure 21. *The AFM plot for trondhjemites of the Gander River Complex. Closed squares are oceanic plagiogranites (Coleman and Donato, 1979). Triangles are coarse grained, and squares are porphyritic plagiogranites.*

arc-related Little Port Complex. He noted that the former have relatively high abundances of the incompatible trace elements (e.g., 64 ppm Y in the Bay of Islands complex compared to 21 ppm Y in the Little Port Complex), > 6 percent Na_2O and Rb/Sr ratios approximately 0.05; trondhjemites of the

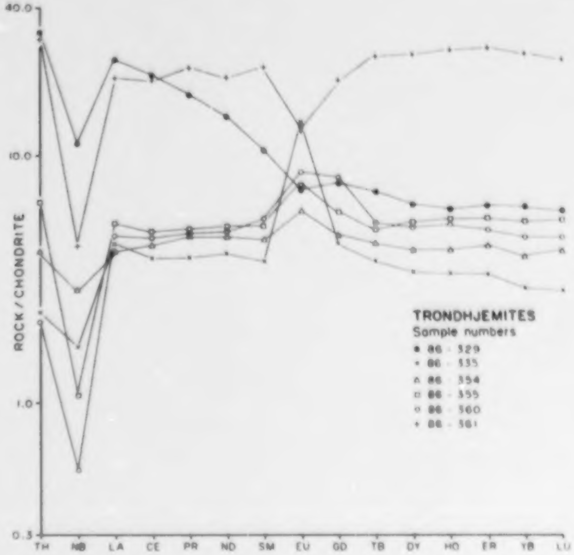

Figure 22. *Partial extended REE plot for trondhjemites of the Gander River Complex.*

Little Port Complex contain approximately 5 percent Na_2O, have Rb/Sr ratios of 0.1, approximately, and have low incompatible-element abundances. The island-arc-related Twillingate trondhjemite (Payne and Strong, 1979) shares similar chemical features with the Little Port Complex. Malpas (1979) also noted that trondhjemite of the Little Port Complex is typically cataclastically deformed, is not associated with intermediate rocks such as granodiorites and forms larger intrusive bodies or small anatectic patches within amphibolites.

Trondhjemites from the Gander River Complex have low incompatible-element abundances, approximately 5 percent Na_2O and Rb/Sr ratios of approximately 0.1. Therefore, they show similar chemical features to both the Little Port Complex and the Twillingate Pluton (Table 3). The Zr and Y abundances are significantly higher in the ophiolitic Bay of Islands and Visnes plagiogranites. Field relationships as displayed by the felsic rocks of this study are also similar to those documented for the Little Port and Twillingate complexes, although anatectic patches are not developed. In Figure 23, some of these chemical similarities are illustrated. The Zr and Y levels for some Gander River Complex trondhjemites fall within the range defined by the Little Port and Twillingate complexes, but the majority are slightly lower than those for the Little Port Complex. On a Rb versus Sr plot, trondhjemites of this study fall approximately midway between the field of oceanic plagiogranite and continental trondhjemite (Figure 24). However, there is substantial overlap with the fields defined by samples from the Little

Table 3. Average element values of trondhjemite from the Gander River Complex, compared to published trondhjemite analyses from various sources

	Gander River Complex (14)		A	B	C	Visnes	B. of I.
SiO_2	69.53	4.5 = SD	71.42	74.45	73.1	73.50	66.6
Al_2O_3	13.50	1.3	13.56	13.02	13.97	12.64	15.90
Fe_2O_3	-	-	0.81	2.62*	0.65	3.76	1.16
FeO	4.28*	2.07	2.09	-	3.81	0.48	1.44
MgO	1.68	0.82	0.95	0.28	1.28	0.24	0.93
CaO	1.68	1.03	2.22	1.85	2.27	4.28	3.7
Na_2O	4.59	1.02	4.97	5.03	4.58	4.73	7.32
K_2O	0.73	0.39	0.70	0.47	0.35	0.13	0.33
TiO_2	0.42	0.17	0.23	0.22	0.34	0.32	0.39
MnO	0.07	0.03	0.12	0.07	0.09	0.06	0.04
P_2O_5	0.07	0.04	0.10	0.01	0.06	0.07	.09
Cr	6.0	16.0	8.0	-	5.0	18.0	8.0
Ni	4.0	7.0	43.0	-	1.0	4.0	5.0
Sc	23.0	10.0	-	-	-		
V	72.0	63.0	-	-	34.0	18.0	26.0
Cu	19.0	27.0	-	17.0	16.0	128.0	13.0
Pb	1.0	1.0	-	3.0	-	-	1.0
Zn	44.0	16.0	-	39.0	44.0	7.0	41.0
Rb	14.0	7.0	12.0	10.0	5.0	-	4.7
Ba	540.0	361.0	68.0	74.0	115.0	-	173.0
Sr	101.0	47.0	129.0	97.0	103.0	233.0	100.0
Ga	5.0	3.0	-	14.0	10.0	-	21.0
Nb**	1.15	0.83	6.0	5.0	1.0	11.0	8.0
Hf	0.69	0.68	-	-	-	-	
Zr	42.0	42.0	60.0	88.0	45.0	590.0	195.0
Y	15.0	10.0	21.0	-	32.0	116.0	64.0
Th**	0.637	0.636	-	-	-	-	

* = Total Iron ** Nb and Th: Average of 6 values determined by ICP at Memorial University of Newfoundland

SD = Standard Deviation A = Little Port Complex (Average of 10 samples) (Malpas, 1979); B = Twillingate Pluton (Average of 33 samples) (Payne and Strong, 1979); C = Pipestone Pond Complex (Average of 7 samples) (Swinden, 1987); Visnes = Visnes Plagiogranite (Pedersen and Malpas, 1984). Average of 12 samples; B. of I. = Bay of Islands (Malpas, 1979). Average of 3 samples.

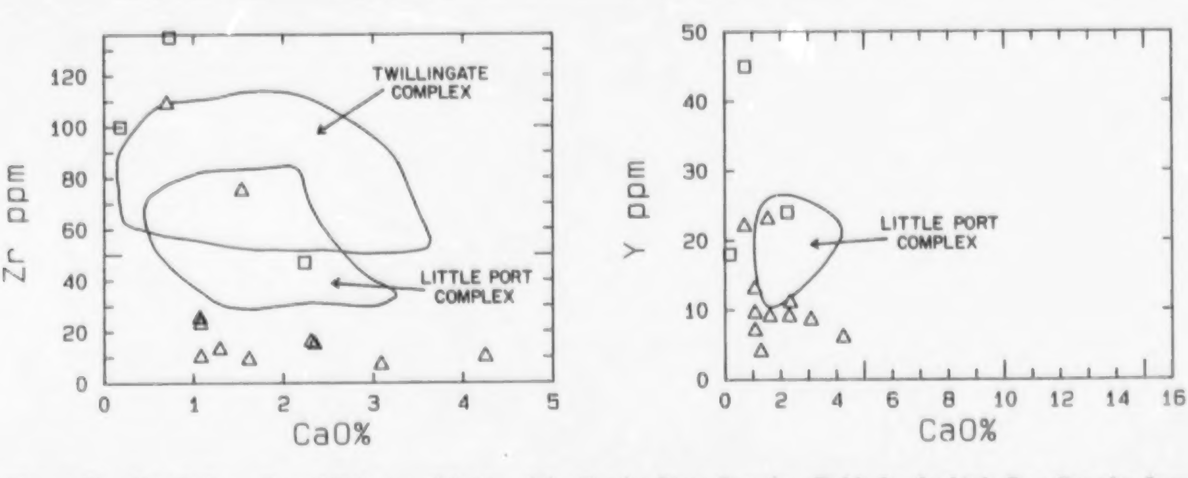

Figure 23. *The CaO vs. Zr and Y for trondhjemite of the Gander River Complex. Fields for the Little Port Complex from Malpas (1979); field from Twillingate Complex from Payne and Strong (1979).*

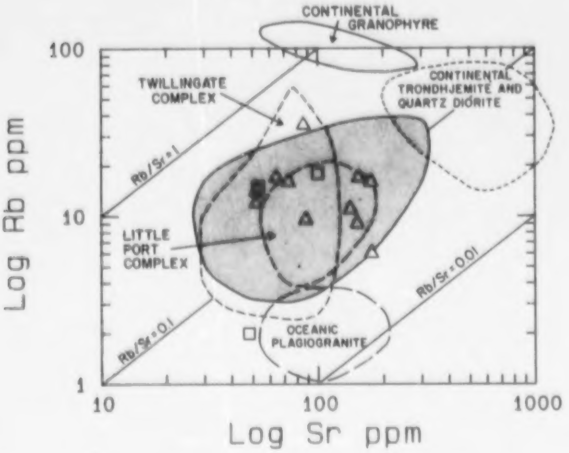

Figure 24. *The Rb vs. Sr for trondhjemite of the Gander River Complex. Fields are–Little Port Complex (Malpas, 1979), Twillingate Complex (Payne and Strong, 1979), continental granophyre, continental trondhjemite and quartz diorite, oceanic plagiogranite (Coleman and Peterman, 1976); grey area denotes field of arc-related trondhjemite and high* SiO_2*, low-K rhyolite (Swinden, 1988).*

Port Complex and the Twillingate Pluton; all three fields fall within the field of arc-related trondhjemites and high-silica, low K_2O rhyolites (taken from Swinden, 1988).

Although Zr, Y, Sr and Rb abundances are very similar to those of other trondhjemites, Ba values in the Gander River Complex range from <100 up to 1242 ppm and this element is, therefore, very enriched compared to Ba values in other trondhjemite suites.

Genesis of the Trondhjemites

The very low abundances of the incompatible elements Zr, Y, Nb and Rb and of K_2O and the flat REE patterns, suggest that the felsic rocks are derived from a mafic source rather than sialic crust. Two distinct models of generation of trondhjemites, by extreme differentiation of mafic magma (Coleman and Peterman, 1974; Malpas, 1979; Pederson and Malpas, 1984) or by partial melting of mafic or meta mafic rocks (Arth and Barker, 1976; Malpas, 1979; Payne and Strong, 1979), have been proposed.

Many features of the trondhjemitic rocks suggest generation by partial melting of mafic rocks:

1) absence of rocks of intermediate composition;
2) low incompatible-element abundances; despite the low levels of these same elements in the associated mafic rocks of the Gander River Complex, extreme differentiation would tend to raise significantly their relative abundances;
3) the absence of a negative correlation between Zr and Y and SiO_2 argues against differentiation since the fractionation of phases such as Fe–Ti oxides and zircon would result in decreasing Zr and Y with decreasing TiO_2;
4) trondhjemites are typically associated with gabbros in the complex suggesting a genetic link; Barker *et al.* (1976), on the basis of a study of Precambrian trondhjemites in the USA, suggested that low-alumina trondhjemites (those of this study are predominantly low alumina) are derived by partial melting of amphibolite and hornblende-bearing gabbro;
5) REE patterns of trondhjemites in the complex do not support derivation from the associated mafic rocks by differentiation. The REE abundance levels of the trondhjemites are as low or are lower than those of the mafic rocks;
6) although Ba values are apparently anomalously high for the trondhjemites, they are in fact very similar to the Ba abundances of the mafic rocks; this feature again suggests partial melting rather than differentiation, since differentiation would have significantly elevated the Ba levels above those of the mafic rocks; and
7) the similarity both in chemistry and in some critical field relationships between trondhjemites of this study and those from the Little Port Complex and the Twillingate Pluton, both of which are interpreted as partial melts of low K_2O tholeiites in the basal parts of an island-arc.

DAVIDSVILLE GROUP

Geochemical analyses of 18 samples of sedimentary rocks from the Davidsville Group are tabulated in Appendix 2, Table 16. Shale and sandstone are not distinguished as their chemical differences are negligible. Ranges and means of major oxides and trace elements are described here and their general trends illustrated in variation diagrams (Figure 25). Precision and accuracy of results are presented in Appendix 2.

The SiO_2 values, ranging from 48 to 84 percent, are lowest in siltstone and pelitic rocks and are highest in fine-grained, rarely cherty, sandstone. The Al_2O_3 values range from 7 to 17.4 percent; the higher values are in fine-grained pelitic rocks, whereas the lowest values occur in highly siliceous rocks. The FeO (total iron) values range from 2.4 to 8.8 percent and MgO from 1.8 to 10.4 percent. CaO ranges from 0.13 to 6.6 percent and averages 1.6 percent.

The Cr values range from 27 to 1110 ppm with a mean of 300 ppm and the Ni values vary sympathetically with Cr ranging from 18 to 373 ppm, averaging 120 ppm. Sample # 86-800 (Appendix 2, Table 16) represents the Middle Ordovician limestone (Unit 7) that unconformably overlies ultramafic rock on the northwest shore of Weir's Pond. The high values of Cr and Ni reflect abundant detritus of ultramafic origin in this sample. Sample # 87-851 (Appendix 2, Table 16) represents the chromite-bearing sandstone of Unit 5 containing fauna of late Arenig to early Llanvirn age.

In the SiO_2 versus Al_2O_3 and MgO plots (Figure 25), the oxides show negative correlation, as would be expected

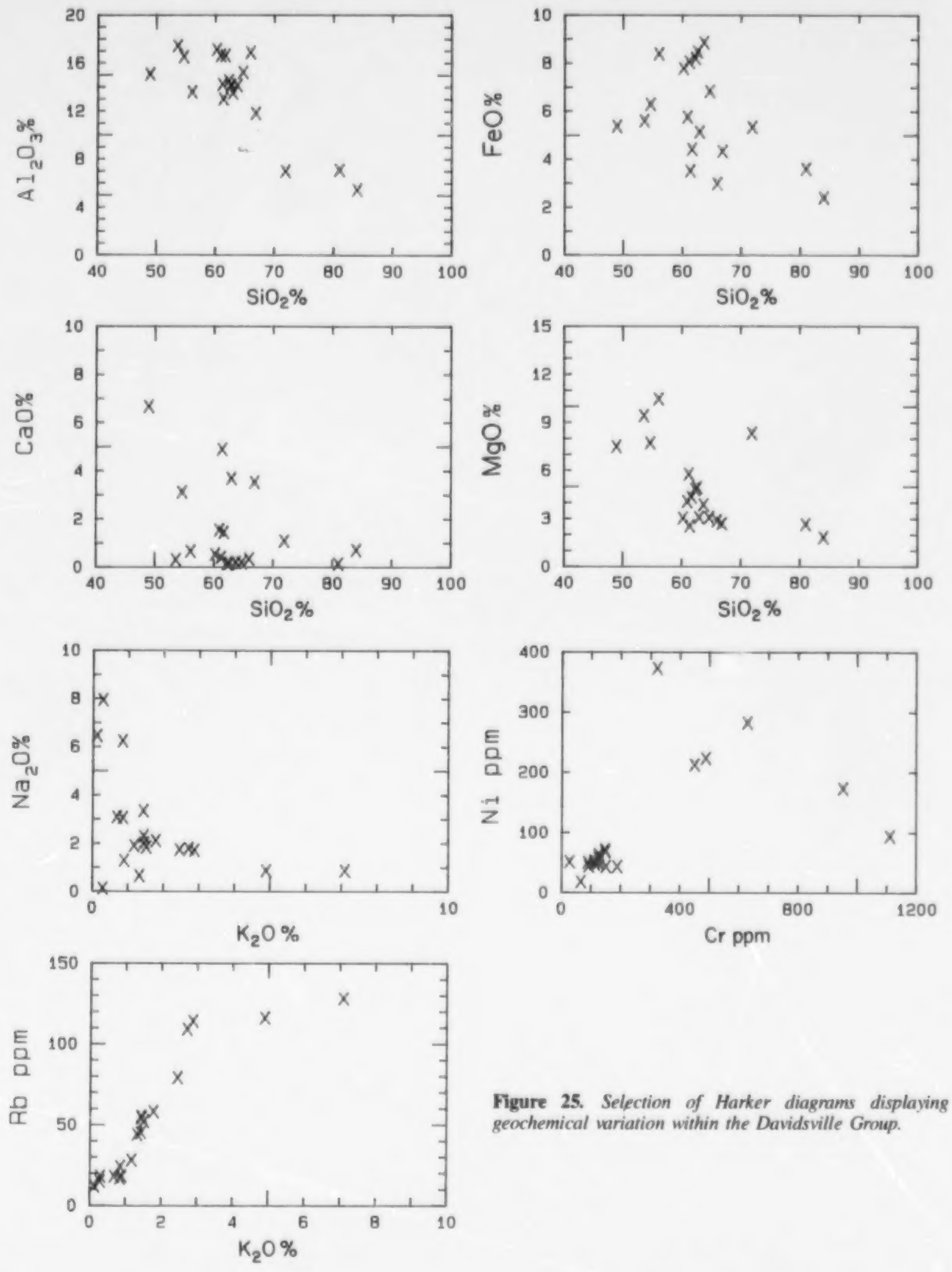

Figure 25. *Selection of Harker diagrams displaying geochemical variation within the Davidsville Group.*

in a mixture of quartz-rich and quartz-poor sedimentary rocks. On the SiO_2 versus FeO plot, points are more scattered but the negative correlation is still discernible.

The Na_2O versus K_2O plot exhibits an ion exchange or enrichment–depletion pattern; breaks in the trend at intermediate levels of K_2O and Na_2O may reflect a sampling bias. Since there is no evidence for alteration in these rocks, the trend is interpreted to be reflecting an ion exchange. Rubidium and K_2O show an excellent positive correlation. Those samples having anomalously high Na_2O and correspondingly low K_2O and Rb, are white-weathering, fine-grained, thin sandstone layers interbedded with pebbly sandstone and conglomerate of Unit 6, in the southwest near Route 330; they may represent tuffaceous sedimentary rocks. Two samples contain high K_2O values; one (5 percent K_2O) is representative of Unit 5 and is also characterized by high Cr (735 ppm). Chromite grains are abundant and several microcline grains were noted in thin section. The second sample (containing 7 percent K_2O) is a fine-grained sandstone clast separated from a cobble conglomerate of Unit 6; this sample also has the highest Ba (3670 ppm) and Rb (128 ppm) of those sedimentary Davidsville Group rocks analyzed in this study.

JONATHAN'S POND FORMATION

Appendix 2, Table 17a presents a list of analyses of sandstone, pelite, a calc-silicate and a coticule rock from the Jonathan's Pond Formation. Analyses of concordant mafic and intermediate dykes are also listed (Appendix 2, Tables 17b and 17c).

Sample # 86-288 is anomalously high in Mn (18.4 percent) and low in SiO_2 (55.5 percent) and Ba (23 ppm) and is a coticule rock (Renard, 1878). Sample # 86-286 is rich in calc-silicate minerals and contains 7 percent CaO, anomalously low Na_2O and K_2O and high Sr (342 ppm).

Variation in abundance of the major oxides and some trace elements and inter-element relationships are illustrated by a selection of Harker diagrams (Figure 26). The SiO_2 versus TiO_2, Al_2O_3, MgO, FeO and K_2O plots all share negative correlation with increasing SiO_2. These trends are very distinct in that they display no scatter. However, the SiO_2 versus CaO (not shown) and Na_2O plots both show pronounced scatter. The Cr versus Ni plot shows a good positive correlation. The variation in CaO and Na_2O values reflects either source-region variation or alteration in the rock during diagenesis and/or low-grade regional metamorphism. It appears likely that source region variation could also have influenced values of K_2O and ferromagnesian minerals and produced scatter in plots of these oxides against SiO_2; such scatter is not in evidence in the diagrams. Thus, the variation may involve alteration of Ca–Na-bearing minerals, of which feldspars are most likely, and mobilization of these ions, after burial.

INDIAN BAY BIG POND FORMATION

Major-oxide- and trace-element analyses of sandstone and pelite of the Indian Bay Big Pond Formation are presented in Appendix 2, Table 18. Major geochemical variations and abundance levels of oxides and trace elements in pelite and sandstone of the formation are illustrated in Figure 27. In the SiO_2 versus TiO_2 plot there is a general negative correlation, although values are somewhat scattered; TiO_2 values range from 0.36 to 0.85 percent and SiO_2 from 60 to 83.5 percent. The MgO values range from 0.31 to 4.37 percent, with most values less than 1.8 percent, and shows a negative correlation with SiO_2. The Al_2O_3 values are somewhat scattered, range from 7 to 18.5 percent, and decrease with increasing SiO_2. The Na_2O and K_2O show no systematic variation with increasing SiO_2. Most Na_2O values are less than 2.4 percent but one sample, # 87-630, contains 8 percent. (This rock appears psammitic and consists of angular quartz and feldspar fragments in an extremely fine-grained matrix.) Most K_2O values are less than 2.6 percent but one sample contains 5.8 percent, is relatively high in Al_2O_3 and low in other oxides. The CaO versus SiO_2 shows no systematic variation and most CaO values are less than 1 percent; however, two samples contain relatively high CaO, 7.4 percent and 6.2 percent and these samples also have high FeO, MgO, LOI and low SiO_2. Petrographically, they are calcareous (lithic) arenites. Both, Cr and Ni, show a positive correlation.

Some conclusions regarding the nature of these formations based on the data above are presented in the following section.

COMPARATIVE GEOCHEMISTRY OF GANDER AND DAVIDSVILLE GROUPS

Mean analyses of sandstones from the Gander and Davidsville groups are presented in Table 4 along with mean analyses of arkose and greywacke. Sandstones of the Weir's Pond Formation of the Davidsville Group are quite similar to the average greywacke, but have higher FeO, significantly higher MgO and relatively low K_2O, possibly reflecting a proximal mafic to ultramafic source. Cr and Ni are significantly enriched (compared to arkoses from Santa Ynez) and reflect a strong ultramafic component in the source provenance. Despite the generally K_2O-poor nature of the most likely source rocks for the Weir's Pond Formation (as implied by petrography and sandstone geochemistry), the pelite is K_2O- and Ba-rich compared to the average shale. This probably reflects significant mica content, either detrital muscovite or metamorphic sericite and in contrast to the sandstones, suggests that the provenance included metamorphic and granitoid rocks.

Sandstones of the Jonathan's Pond Formation of the Gander Group are relatively richer in SiO_2, FeO, MgO and Na_2O, and significantly poorer in CaO and K_2O than arkoses, with which they compare more favourably than greywackes. Sandstones of the Indian Bay Big Pond Formation of the Gander Group fall between the average analyses of arkose and greywacke. These trends probably reflect the greater abundance of lithic detritus in the Indian Bay Big Pond Formation than in the Jonathan's Pond Formation.

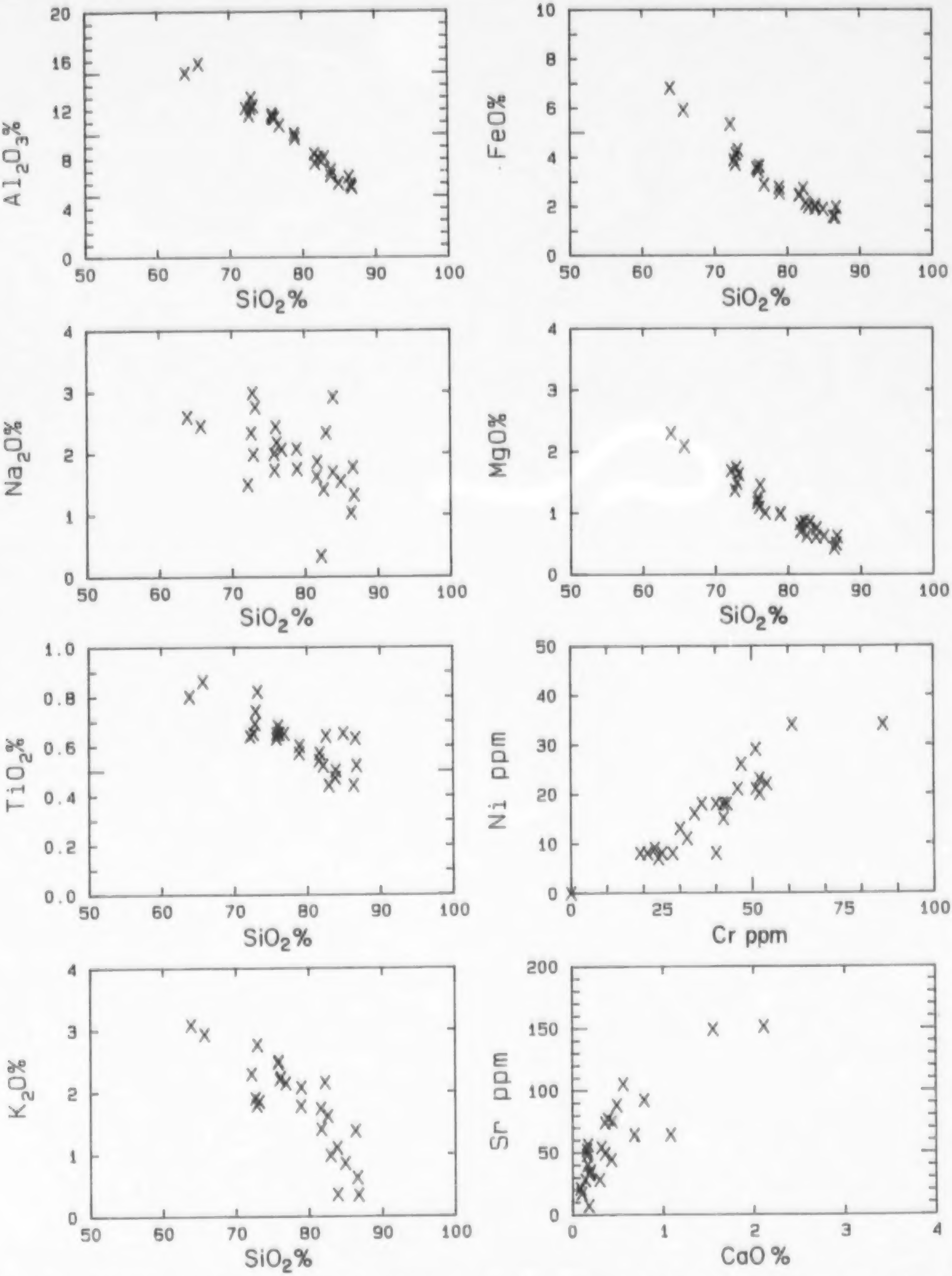

Figure 26. *Selection of Harker diagrams illustrating geochemical trends of major oxides and trace elements in rocks of the Jonathan's Pond Formation.*

Table 4. List of mean analyses of sandstone and pelite from the Gander and Davidsville groups and published means for arkose, shale and greywacke

	A	B	C	D	E	F	G	H	I	J
SiO_2	58.85	62.88	62.82	78.59	58.00	73.04	69.61	77.1	66.7	58.81
TiO_2	0.64	0.75	0.93	0.62	0.94	0.66	0.44	0.3	0.6	0.86
Al_2O_3	16.00	13.01	17.33	9.59	20.12	11.18	12.83	8.7	13.5	17.94
FeO	6.17	6.43	6.18	3.01	7.97	3.42	3.25	2.05	4.94	7.09
MnO	0.15	0.15	0.12	0.12	0.30	0.09	0.06	0.2	0.1	0.08
MgO	5.16	5.35	2.17	1.06	2.02	1.34	1.73	0.5	2.1	2.79
CaO	1.50	1.76	0.30	0.49	0.14	1.54	2.67	2.7	2.5	1.97
Na_2O	1.45	1.91	1.31	2.02	1.11	1.98	3.07	1.5	2.9	1.60
K_2O	4.22	1.61	4.21	1.65	4.67	2.09	2.75	2.8	2.0	3.58
P_2O_5	0.09	0.11	0.15	0.10	0.12	0.11	0.14	0.1	0.2	0.13
LOI	5.00	5.16	3.63	1.79	4.09	3.70	1.83	0.9	2.4	4.48
Cr	88.0	399.0	85.0	37.0	98.0	62.0	112.0			135.0
Ni	54.0	142.0	31.0	15.0	47.0	24.0	35.0			92.0
V	88.0	135.0	118.0	50.0	141.0	71.0				
Cu	15.0	26.0	13.0	8.0	24.0	17.0	12.0			48.0
Pb	6.0	6.0	9.0	8.0	13.0	10.0				
Zn	84.0	82.0	95.0	48.0	112.0	55.0	49.0			144.0
Rb	177.0	49.0	182.0	61.0	202.0	85.0	108.0			251.0
Ba	1493.0	396.0	894.0	290.0	687.0	308.0	753.0			632.0
Sr	155.0	89.0	46.0	64.0	62.0	82.0				
Ga	19.0	15.0	24.0	5.0	30.0	17.0	16.0			24.0
Nb	11.0	5.0	17.0	10.0	14.0	11.0				
Zr	136.0	130.0	129.0	137.0	136.0	136.0	191.0			173.0
Y	13.0	16.0	18.0	17.0	13.0	15.0	30.0			43.0
Th	13.0	15.0	10.0	6.0	9.0	8.0				

A and B – Davidsville Group: pelite (3 analyses) and sandstone (12 analyses); C and D – Jonathan's Pond Formation: pelite (3 analyses) and psammite (19 analyses); E and F – Indian Bay Big Pond Formation: pelite (2 analyses) and sandstone (12 analyses); G – Average of 26 arkoses (Van De Kamp *et al.*, 1976); H – Average arkose (Pettijohn, 1963); I – Average greywacke (Pettijohn, 1963); J – Average of 13 shale samples from Santa Ynez Mountains (Van De Kamp *et al.*, 1976).

Both, K_2O and Na_2O contents in Weir's Pond and the Jonathan's Pond formations are similar, but otherwise the two units are markedly different. Average Cr and Ni values in Jonathan's Pond Formation sandstones are low and Cr levels are similar to reported values of about 27 ppm in modern sands and average sandstone (Shiraki, 1978). Sandstones of the Indian Bay Big Pond Formation fall somewhat between the means of sandstones from the Weir's Pond and the Jonathan's Pond formations. The Cr values in the Indian Bay Big Pond Formation average 62 and range up to 120 ppm (detrital chromite was also noted in thin section), thus, indicating an ultramafic source. This chromite may be first cycle for the following reasons:

1) the general nature of lithic fragments in the Indian Bay Big Pond Formation indicate first-cycle origin;

2) the absence of chromite in the Jonathan's Pond Formation; this observation coupled with the interpretation in this study, that the Jonathan's Pond and Indian Bay Big Pond formations are conformable, suggests that chromite represents a new (additional) provenance; and

3) the presence of volcanic fragments in the Indian Bay Big Pond Formation.

The suggested first-cycle nature of much of the detritus in the Indian Bay Big Pond Formation contrasts with the multicycle nature of the Jonathan's Pond Formation as implied by the presence of zircon grains ranging from Cambrian to Archaean (see Geochronology section).

In Figure 28, all sandstone analyses from the Gander and Davidsville groups are compared to five sedimentary fields based on Na_2O/K_2O and SiO_2/Al_2O_3 ratios. Almost all of the Davidsville Group fall in the greywacke field and are generally distinct from those of the Gander Group, most of

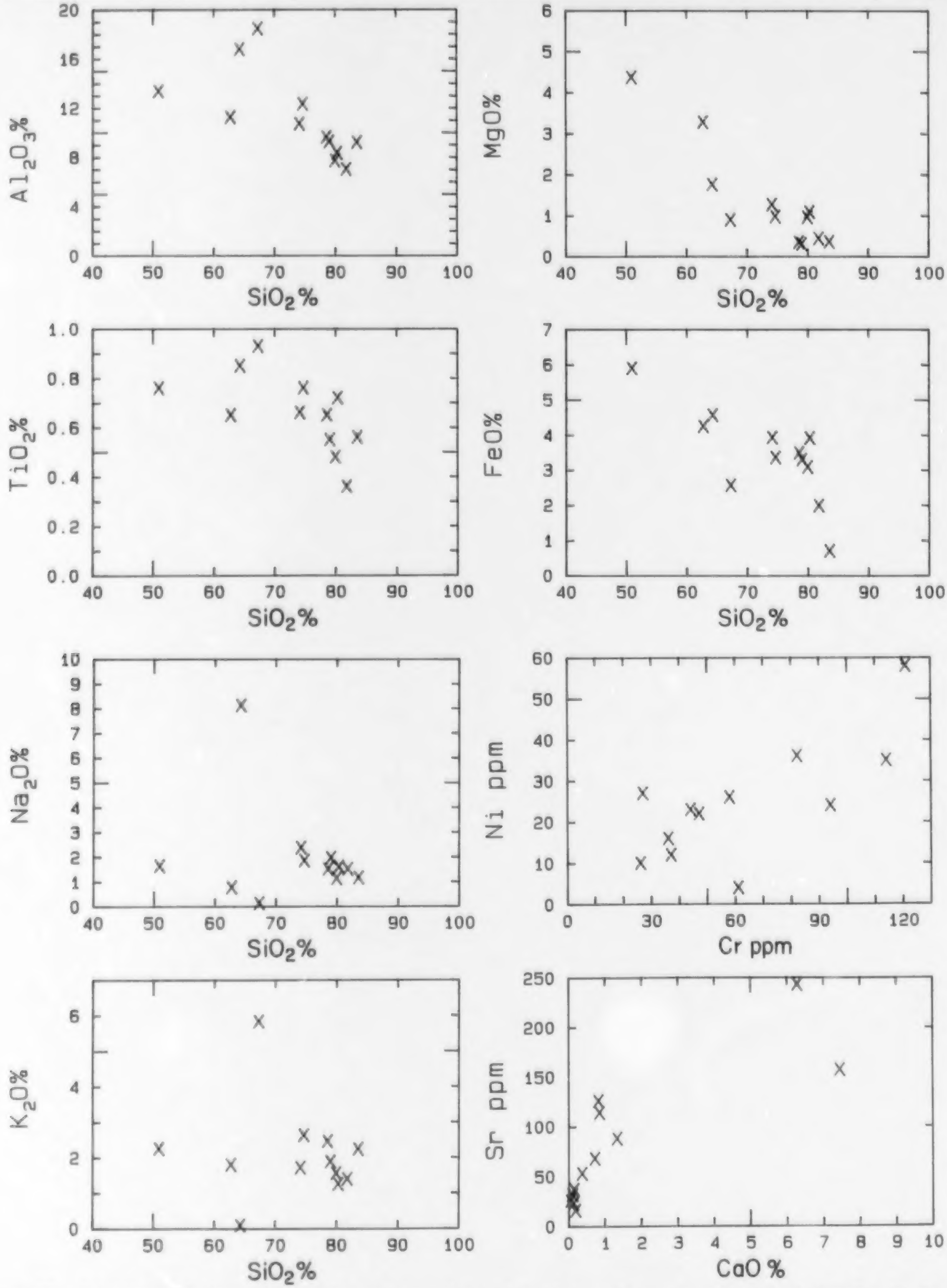

Figure 27. *Selection of Harker diagrams illustrating geochemical trends in sedimentary rocks of the Indian Bay Big Pond Formation.*

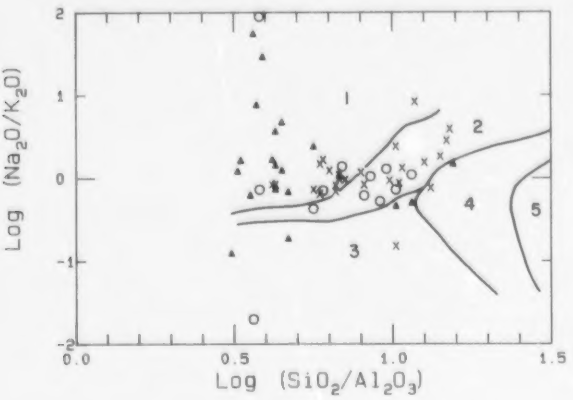

Figure 28. *Comparative plot of sandstones from Gander and Davidsville groups. Solid triangles–Davidsville Group; X–Indian Bay Big Pond Formation; O–Jonathan's Pond Formation. Fields are 1) greywacke, 2) lithic arenite, 3) arkose, 4) subarkose, 5) sublithic arenite. Fields from Pettijohn* et al. *(1973).*

which fall in the lithic arenite field. The majority of sandstones from the Indian Bay Big Pond Formation are lithic arenite, however, sandstones from the Jonathan's Pond Formation are evenly split between the field of lithic arenite and greywacke.

On the petrographic discriminant plot of Zuffa (1979), samples from the Weir's Pond Formation fall within the sublitharenite, subarkose and quartz arenite field (Figure 29). One sample, a psammite clast in conglomerate, plots in the litharenite field. The abundance of this particular type of clast in the exposure indicates a relatively nearby source. It is compositionally similar to sandstones of the Jonathan's Pond Formation and, therefore, could possibly be derived from that formation. This is discussed in a later section on Provenance.

Samples from the Indian Bay Big Pond Formation show the same scatter as those in the Davidsville Group. The four samples from the Jonathan's Pond Formation fall in the sublitharenite and subarkose fields. The small number of samples involved in this analysis preclude much meaningful interpretation. However, the results are essentially similar to those defined by the geochemical plots.

GEOCHEMISTRY OF THE OCEAN POND AND DEADMAN'S BAY GRANITES

Geochemical analyses of twenty one samples from the Deadman's Bay Granite, three samples of the Ocean Pond

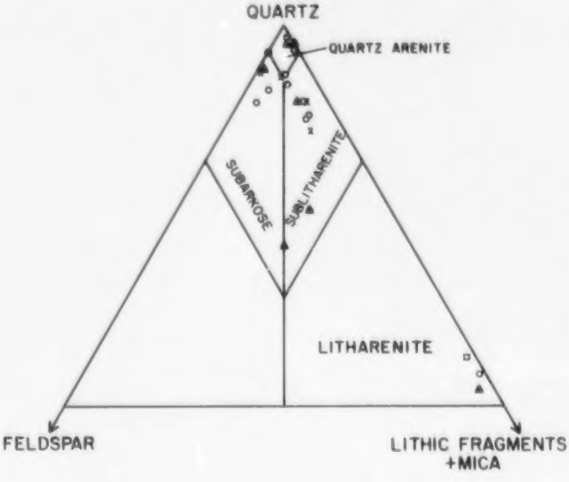

Figure 29. *Petrography-based discriminant plot of Zuffa (1979) showing results of point counted samples from Gander and Davidsville groups. Solid triangles–Davidsville Group; X–Indian Bay Big Pond Formation; O–Jonathan's Pond Formation. Fields are 1) greywacke, 2) lithic arenite, 3) arkose, 4) subarkose, 5) sublithic arenite. Fields from Pettijohn* et al. *(1973).*

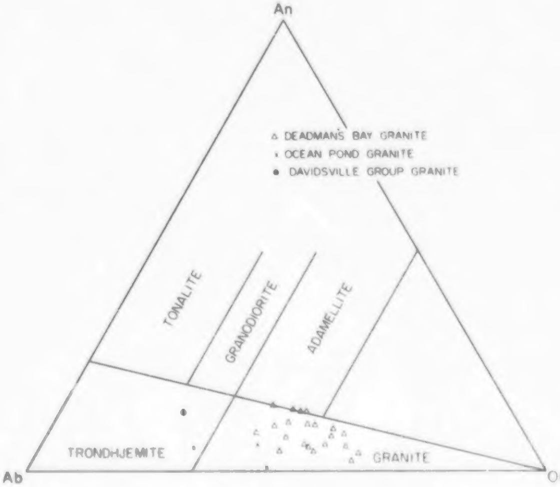

Figure 30. *Normative Ab–An–Or diagram (after O'Connor, 1965) for Ocean Pond and Deadman's Bay granites and Unit 18.*

Granite and one from Unit 18, are listed in Appendix 2, Table 19. The CIPW norms for all samples are listed in Appendix 2, Table 20 and normative orthoclase, albite and anorthite values are shown on Figure 30; all samples of the Deadman's Bay and two of the Ocean Pond granites fall in the granite field, however, one sample of the Ocean Pond

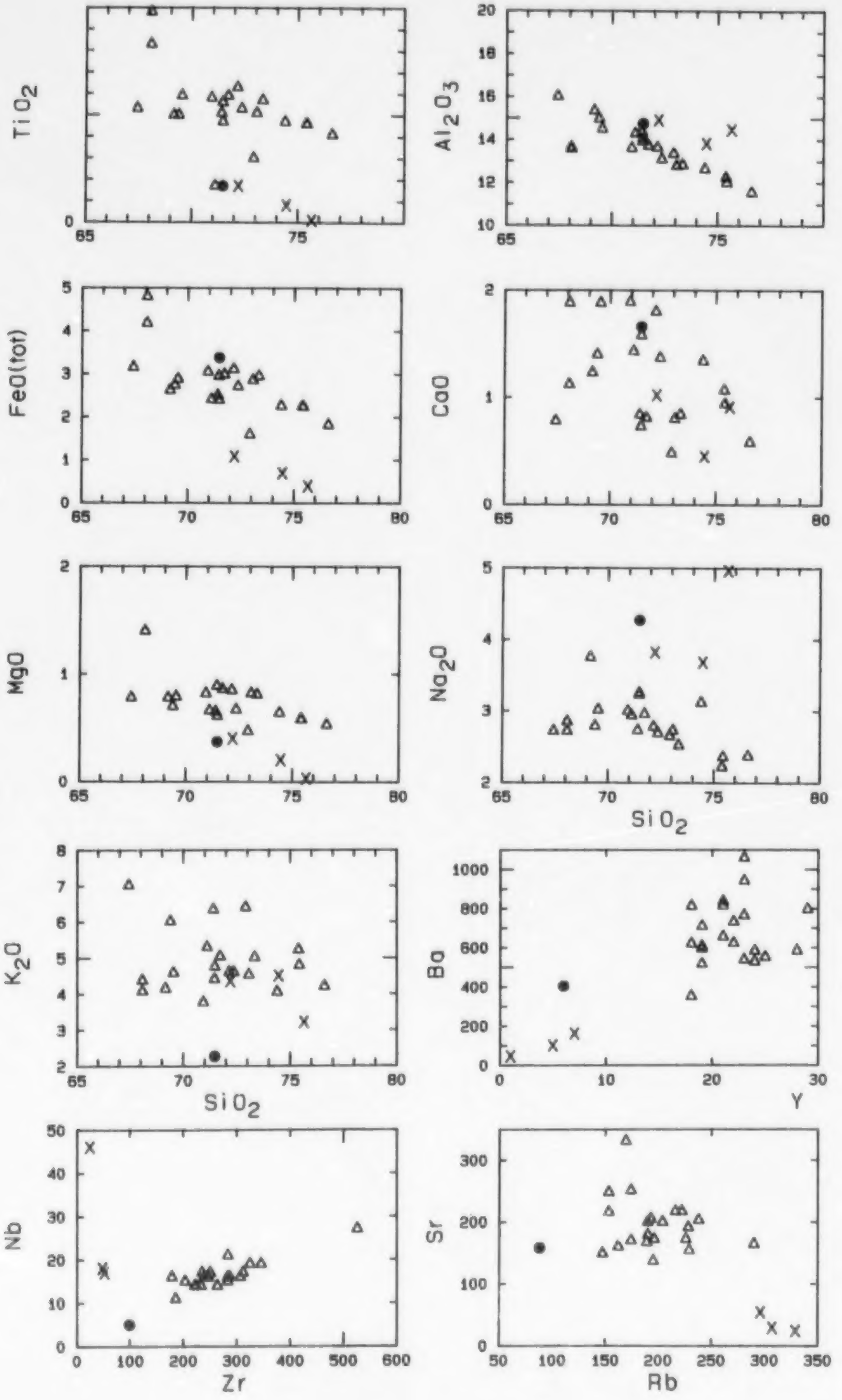

Figure 31. *Selected Harker diagrams illustrating geochemical trends in major and trace elements of Ocean Pond Granite* (x) *and Deadman's Bay Granite (open triangle) and Unit 18 (closed circle).*

Granite and the granite in the Davidsville Group plot as trondhjemites. As Appendix 2, Table 20 shows, all the granites are peraluminous having an agpaiitic index of approximately 0.75. The IS ratio is just greater than 1 and all the granites are S-type.

A suite of Harker diagrams is shown on Figure 31 to illustrate the variation in major oxides and in some trace elements between the three granites. In all plots except CaO and K_2O, which show scatter, there is a clear separation between the three granites. The Ocean Pond Granite is poorer in total iron, MgO, TiO_2 and Zr and markedly poorer in Y, Ba and Sr than the Deadman's Bay Granite. Although the K_2O values in the Ocean Pond Granite are similar to those of the Deadman's Bay, Rb, which normally varies sympathetically with K_2O, is significantly higher in the former. The granite that intrudes the Davidsville Group is significantly low in K_2O, Rb, Ba and relatively rich in Na_2O and CaO, hence its classification as trondhjemite. This granite is also low in the incompatible elements Y, Zr and Nb and although low in MgO, its total iron is high reflecting the abundant pyrite present.

GEOCHRONOLOGY

Both Ar–Ar and U–Pb dating methods were used in this study in an attempt to obtain cooling and emplacement ages, respectively, of selected samples from the map area. Several samples of pegmatitic gabbro and trondhjemite from the Gander River Complex were crushed at the Geology Department, Royal Ontario Museum to extract zircons but without success. Single titanite and zircon crystals were separated from a granule psammite from the Jonathan's Pond Formation and dated by the U–Pb method in order to elucidate the age of the source region. This is part of a continuing geochronological project (initiated by Tom Krogh at the Royal Ontario Museum) on provenance studies, to date single zircons from samples representing important units in the Avalon Zone and the Central Mobile Belt. One of the main objectives of the Ar–Ar dating is to obtain cooling ages on the regional metamorphism in the north central part of the area. Mica cooling ages were also obtained from mineral separates of the Ocean Pond and Deadman's Bay granites. Information on the samples dated is compiled in Table 5.

$^{40}Ar-^{39}Ar$

The $^{40}Ar-^{39}Ar$ incremental release ages were determined for eight muscovite, three biotite and one hornblende mineral concentrates from metasedimentary and igneous rocks in the Weir's Pond area. The age determinations were carried out by Dan Lux of the University of Maine at Orono. The analytical data are presented in Appendix 3, Table 1; and the technique (Dan Lux, personal communication, 1989) is described briefly here. The spectra are illustrated on Figures 32 to 35 and their locations are shown on Figure 36.

The $^{40}Ar-^{39}Ar$ incremental release spectra allow cooling ages to be determined for various potassium-bearing minerals. These ages date the approximate time at which the minerals passed through their closure temperatures, i.e., the temperature at which Ar ceases to diffuse through the crystal lattice. In the case of rapidly cooled rocks, the crystallization and cooling ages converge. Two types of ages, plateau and total gas, are derived from the incremental release spectra. A plateau age is the mean value of concordant gas fractions, which comprise more than 50 percent of the gas evolved based on 2 sigma analytical uncertainties. A total-gas age is determined by weighting each age and associated uncertainty, based on the amount of $^{39}Ar_K$ present in each increment, and averaging.

Sample Description

Gander Group

Biotite Zone

Three pelite samples (#'s 86-191, 86-204 and 86-253) were collected from the biotite zone of regional metamorphism in the central part of the Jonathan's Pond Formation (Figure 36) for Ar–Ar analysis of biotite and muscovite. Sample # 86-191 is a fine-grained semipelitic rock consisting of mica- and quartz-rich layers. The principal foliation is defined by muscovite, the predominant mica and is overprinted by disseminated porphyroblasts of biotite. Sample # 86-204 is a phyllite containing abundant fine-grained muscovite defining the main foliation and overprinted by widespread biotite porphyroblasts. Growth of the biotite predated a strong crenulation of the foliation. Sample # 86-253 is similar to # 86-204 but coarse-grained chlorite is abundant and biotite occurs in minor amounts.

Sillimanite Zone

Sample # 87-839 is a semipelitic rock from the regional sillimanite zone, collected approximately 4 km northwest of the Deadman's Bay Granite for Ar–Ar analysis of muscovite. The rock comprises granoblastic quartz, plagioclase and coarse porphyroblastic muscovite; sillimanite needles occur as inclusions in quartz. A fine-grained equigranular, muscovite, biotite granite, which is slightly foliated, intrudes the semipelite.

Ocean Pond and Deadman's Bay Granites

Sample # 87-847 was collected from an exposure of the Ocean Pond Granite immediately south of Ocean Pond and sample # 86-302 was collected from a muscovite-rich pegmatite 3 km southwest of the granite, for Ar–Ar analyses of muscovite. The pegmatite is situated in the garnet zone and is spatially and mineralogically related to the granite. Sample # 87-846 was collected near the west side of Ten Mile Pond, from the Deadman's Bay Granite, for Ar–Ar analysis of biotite.

Table 5. List of samples dated by U–Pb and Ar–Ar methods and their location

Sample #	Rock Type	Mineral	Grid Reference	Method	Age Ma.
86-172	Sandstone (D)	Muscovite	843583	Ar–Ar	410 (T.G.)
86-191	Pelite (G)	Muscovite	967412	Ar–Ar	392 (T.G.) 394 ± 6 (P)
86-191	Pelite (G)	Biotite	967412	Ar–Ar	396 (T.G.) 398 ± 5 (P)
86-204	Pelite (G)	Muscovite	972433	Ar–Ar	374 (T.G.) 378 ± 4 (P)
86-204	Pelite (G)	Biotite	972433	Ar–Ar	398 (T.G.)
86-253	Pelite (G)	Muscovite	966450	Ar–Ar	390 (T.G.) 391 ± 4 (P)
86-269	Granite (DAV)	Muscovite	829568	Ar–Ar	426 (T.G.) 427 ± 7 (P)
86-302	Pegmatite (OP)	Muscovite	009475	Ar–Ar	389 (T.G.) 390 ± 7 (P)
87-847	Granite (OP)	Muscovite	029493	Ar–Ar	397 (T.G.) 398 ± 5 (P)
87-839	Schist (G)	Muscovite	101571	Ar–Ar	396 (T.G.) 397 ± 5 (P)
87-846	Granite (DMB)	Biotite	138510	Ar–Ar	405 (T.G.)
87-809	Gabbro (GRC)	Hornblende	856547	Ar–Ar	520 (T.G.)
86-187	Sandstone (G)	Zircons	830513	U–Pb	549-2717 Ma
86-187	Sandstone (G)	Titanite	830513	U–Pb	530-545 Ma

G = Gander Group; D = Davidsville Group; GRC = Gander River Complex; DMB = Deadman's Bay Granite; OP = Ocean Pond Granite; DAV = Unit 18; T.G. = Total Gas Age; P = Plateau Age.

Davidsville Group and Gander River Complex

Sample # 86-172 was collected from the Hunts Cove Formation of the Davidsville Group for Ar–Ar analysis of muscovite. The sample represents a fine-grained sandstone exposure located several kilometres north of Weir's Pond and contains abundant detrital muscovite up to 0.5 mm long. Sample # 87-809 was collected from an exposure of hornblende gabbro west of Weir's Pond, of the Gander River Complex, for Ar–Ar analysis of hornblende. The hornblende is pleochroic from light-brown to green although some grains are pale-green. Hornblende crystals range up to 3 mm across and some show undulose extinction. Feldspars are partially sericitized.

Results

Gander Group

Muscovite

All muscovite spectra display good plateaus although initial increments in each suggest some Ar loss, which is less than 10 percent of total Ar liberated. Sample #'s 86-191 and 86-253 have overlapping total-gas ages of 391.6 ± 6.8 and 390.17 ± 4.13 Ma, respectively, and overlapping plateau ages of 394 (± 6) and 391 (± 4), respectively. However, sample # 86-204, although having a good plateau, is approximately

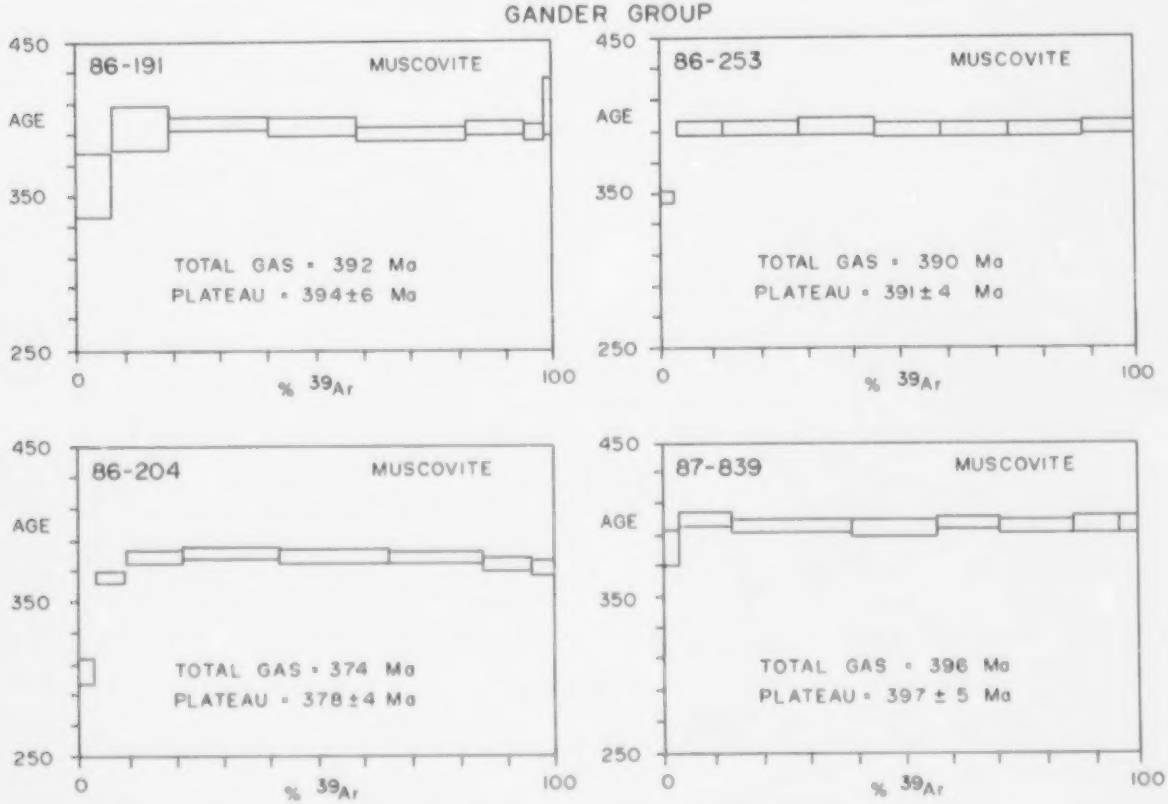

Figure 32. *The $^{40}Ar-^{39}Ar$ age spectra on muscovite from the Jonathan's Pond Formation, Ocean Pond area.*

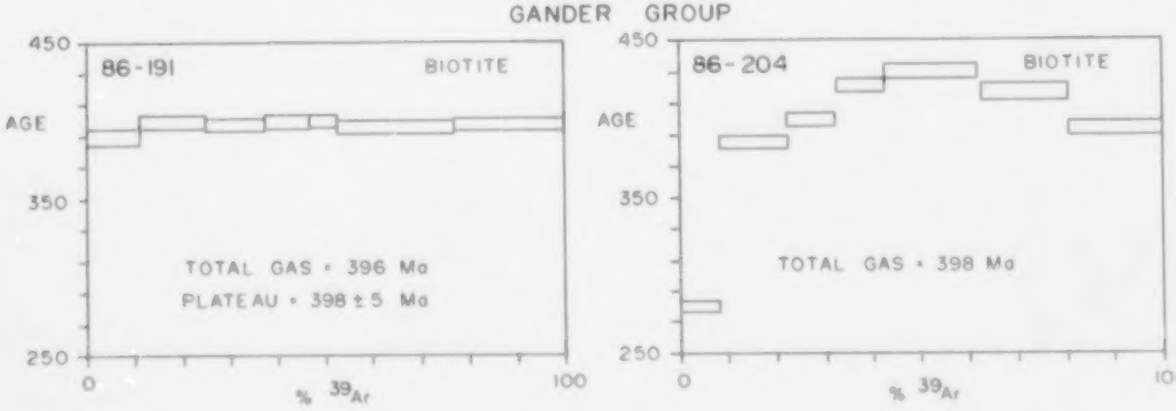

Figure 33. *The $^{40}Ar-^{39}Ar$ age spectra on biotite from the Jonathan's Pond Formation, Ocean Pond area.*

20 Ma younger than the others. Possible reasons for this difference in cooling ages are discussed in the Summary section below.

The muscovite spectra of the sillimanite zone sample gives a plateau age of 397 ± 5 Ma and a total-gas age of 396.4 ± 4.6 Ma.

Biotite

The $^{40}Ar-^{39}Ar$ age spectra, determined from two biotite concentrates from sample #'s 86-191 and 86-204, are shown on Figure 33. The spectrum for sample # 86-191 has a plateau age of 398 ± 5 and a total-gas age of 396.3 ± 4.2 Ma. Sample # 86-204 has a discordant hump-shaped spectrum and gives

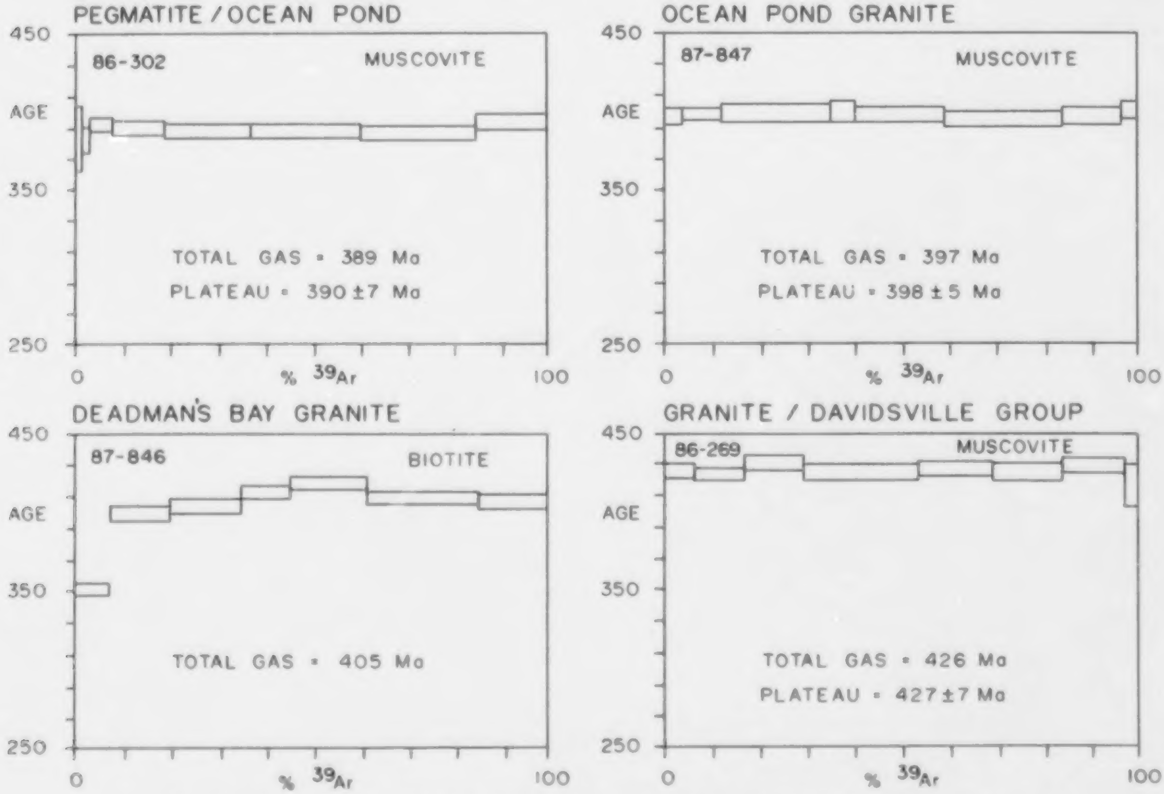

Figure 34. *The $^{40}Ar-^{39}Ar$ age spectra on granites within the Weir's Pond map area.*

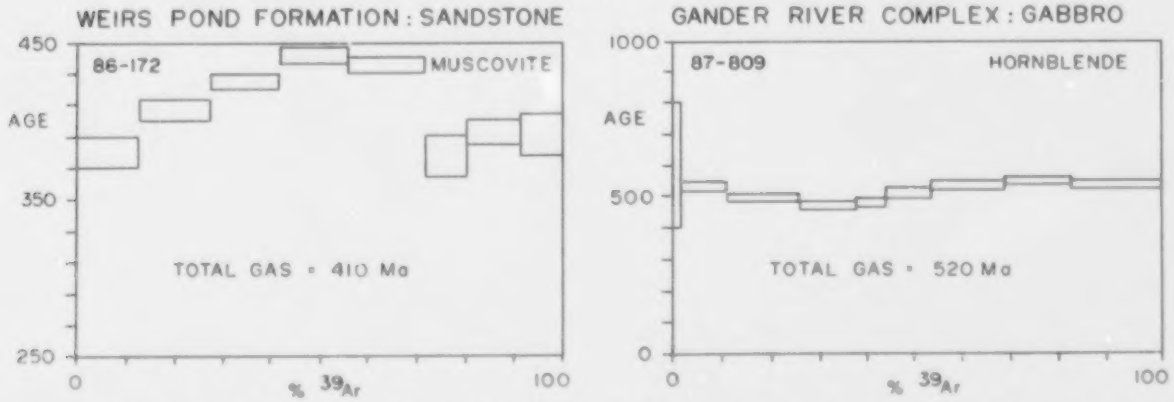

Figure 35. *The $^{40}Ar-^{39}Ar$ age spectra on detrital muscovite from a Davidsville Group sandstone and on hornblende from a gabbro of the Gander River Complex.*

a total-gas age of 398 ± 4 Ma. The low temperature part of the spectrum records an anomalously young age, but, since the initial gas fraction represents only 8 percent of the total gas liberated, this has little significance.

Ocean Pond Granite

The muscovite age spectrum for the granite (sample # 87-847) is quite flat with a plateau age of 398 ± 5 Ma and a total gas age of 397.1 ± 4.7 Ma (Figure 34) and has a slightly younger total-gas age of 389 ± 4 and a plateau age of 390 ± 7 Ma than the granite.

Deadman's Bay Granite

The age spectrum for the biotite is hump-shaped and the first gas fraction represents 7 percent of the total Ar liberated (Figure 34). The remaining increments are slightly discordant and a plateau is absent; the total-gas age is 405 ± 4 Ma.

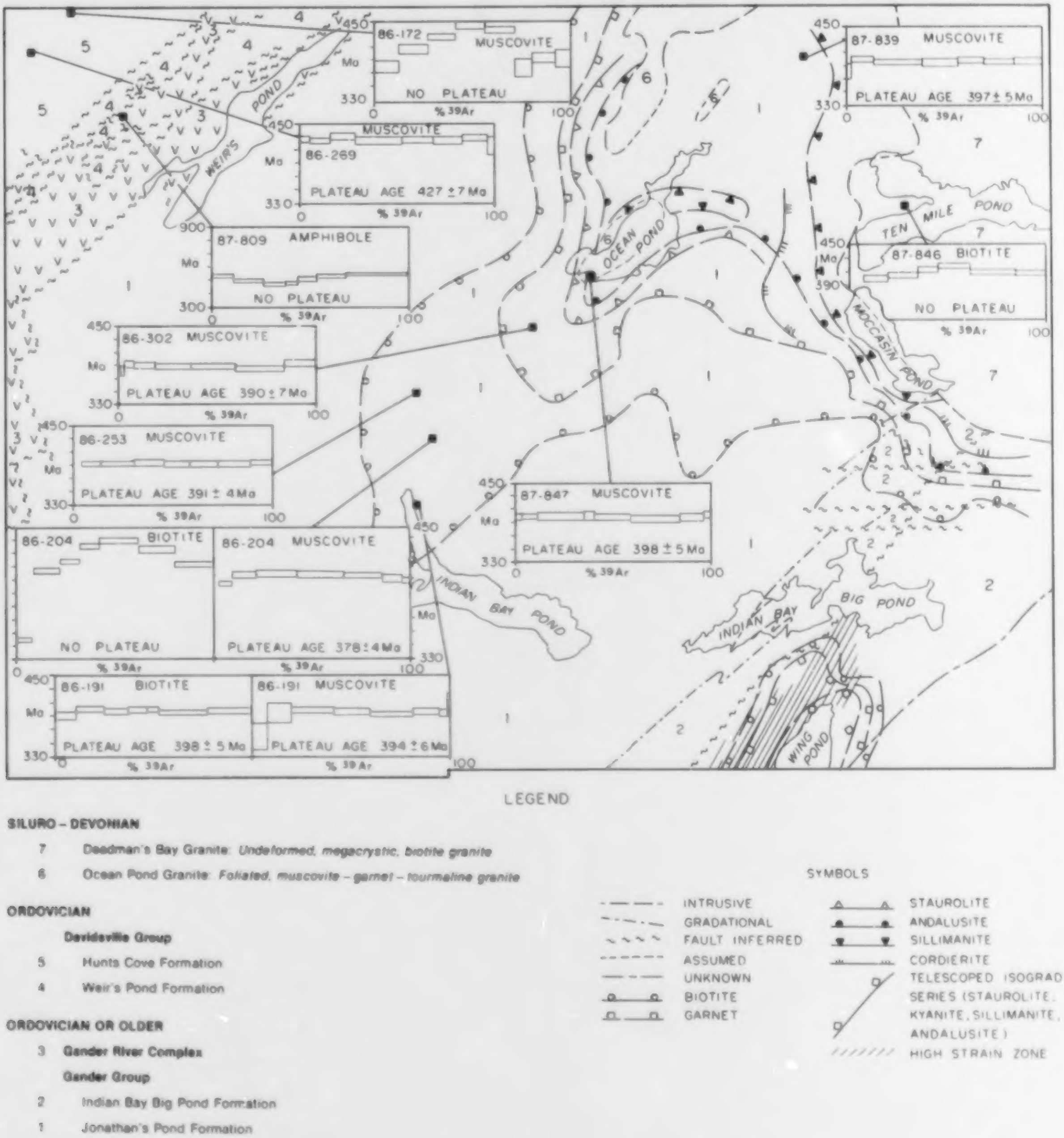
86-172 MUSCOVITE
NO PLATEAU
86-269 MUSCOVITE
PLATEAU AGE 427 ± 7 Ma
87-809 AMPHIBOLE
NO PLATEAU
86-302 MUSCOVITE
PLATEAU AGE 390 ± 7 Ma
86-253 MUSCOVITE
PLATEAU AGE 391 ± 4 Ma
86-204 BIOTITE
NO PLATEAU
86-204 MUSCOVITE
PLATEAU AGE 378 ± 4 Ma
86-191 BIOTITE
PLATEAU AGE 398 ± 5 Ma
86-191 MUSCOVITE
PLATEAU AGE 394 ± 6 Ma
87-847 MUSCOVITE
PLATEAU AGE 398 ± 5 Ma
87-839 MUSCOVITE
PLATEAU AGE 397 ± 5 Ma
87-846 BIOTITE
NO PLATEAU
Ma
% 39Ar
WEIR'S POND
OCEAN POND
TEN MILE POND
MOCCASIN POND
INDIAN BAY POND
INDIAN BAY BIG POND
WING POND
LEGEND
SILURO – DEVONIAN
7 Deadman's Bay Granite: Undeformed, megacrystic, biotite granite
6 Ocean Pond Granite: Foliated, muscovite – garnet – tourmaline granite
ORDOVICIAN
Davidsville Group
5 Hunts Cove Formation
4 Weir's Pond Formation
ORDOVICIAN OR OLDER
3 Gander River Complex
Gander Group
2 Indian Bay Big Pond Formation
1 Jonathan's Pond Formation
SYMBOLS
INTRUSIVE
GRADATIONAL
FAULT INFERRED
ASSUMED
UNKNOWN
BIOTITE
GARNET
STAUROLITE
ANDALUSITE
SILLIMANITE
CORDIERITE
TELESCOPED ISOGRAD SERIES (STAUROLITE, KYANITE, SILLIMANITE, ANDALUSITE)
HIGH STRAIN ZONE

Figure 36. *The $^{40}Ar-^{39}Ar$ spectra and their locations in the Weir's Pond map area.*

Davidsville Group

The spectrum for the sandstone sample is quite disturbed and gives a total-gas age of 409.7 ± 7.6 Ma (Figure 35). All fossil ages in the Davidsville Group are Caradocian or older and, therefore, this Late Silurian age for the muscovite suggests resetting during some Silurian thermal event.

Gander River Complex

The spectrum (Figure 35) is saddle-shaped and indicates excess ^{40}Ar, thus, the minimum age (473 ± 15 Ma) may represent a maximum age for the rock (Dan Lux, personal communication, 1988). The oldest overlying sandstones containing chromite detritus is late Arenig (480-475 Ma, approximately; time scale of Haq and van Eysinga, 1987) and implies that the Complex had to have been exhumed by approximately 480 Ma and actively shedding detritus. The Ar–Ar hornblende age, therefore, is in general agreement with the geological relationships, but does not allow a more precise age to be placed on the Complex.

Summary of Ar–Ar Results

The Ar–Ar spectra on muscovite and biotite, from the biotite zone of regional metamorphism in the Gander Group, indicate cooling through greenschist-facies conditions during the late Lower to Middle Devonian and overlap Ar–Ar ages of muscovite from the regional sillimanite zone, the Ocean Pond Granite and an associated pegmatite. The younger cooling age on the latter suggests that the pegmatite intruded the metasediments slightly later than the granite or that the pegmatite (and aureole) cooled slower than the granite. The latter appears unlikely, since the granite was the heat source and, therefore, would have cooled slower than the country rock.

The muscovite age on sample # 86-204 is younger than the remaining muscovite spectra. The reason for this discrepancy is not clear and can only be surmized. The fine-grained nature of the muscovite in sample # 86-204 (< 0.1 mm) may have effectively lowered the closure temperature of the muscovite. However, muscovite in sample # 86-253 is also fine-grained but its age is consistent with the other muscovite ages.

Several of the biotite samples show discordant spectra possibly due to excess Ar. Biotite has a lower closure temperature (280 ± 40°C, Harrison and McDougall, 1980) than muscovite (350° approximately, Harrison and McDougall, op. cit.) and the fact that the biotite age is slightly older than the muscovite suggests that the biotite contained excess Ar. Biotite has been shown (Dallmeyer and Rivers, 1983) to contain excess Ar that is thermally indistinguishable from radiogenic Ar.

Spectra of biotite from the Deadman's Bay Granite, detrital muscovite from the Davidsville Group and hornblende from the Gander River Complex are disturbed and the ages are geologically suspect.

U–Pb DATING OF ZIRCON AND SPHENE

Approximately 50 kg of a quartz granule sandstone from the Jonathan's Pond Formation (957489) were collected for U–Pb dating of zircon and sphene. The age determinations were carried out by Tom Krogh at the Royal Ontario Museum. Individual ages were acquired for twelve single zircon and six single sphene grains from the rock.

Results

The U–Pb zircon and sphene ages are listed in Tables 6 and 7 and are plotted on concordia diagrams on Figures 37 and 38. The ($^{238}U-^{206}Pb$ zircon ages range from 2717 to

Table 6: The U–Pb and Pb–Pb ages from single zircon grains, separated from a quartz granule sandstone of the Jonathan's Pond Formation

	AGE MA		
Grain/Batch	$^{206}Pb/^{238}U$	$^{207}Pb/^{235}U$	$^{207}Pb/^{206}Pb$
1/1	1347	1356	1370
2/1	2284	2351	2409
3/1	1858	1951	2050
4/1	2324	2255	2193
6/1	2062	2061	2060
1/2	1017	1018	1021
2/2	1112	1116	1122
3/2	2717	2727	2734
4/2	549	552	566
5/2	2640	2715	2772
6/2	1215	1217	1221
1/3	1514	1533	1559

Table 7: The U–Pb and Pb–Pb ages from single sphene grains from a quartz granule sandstone of the Jonathan's Pond Formation

	AGE MA		
Grain/Batch	$^{206}Pb/^{238}U$	$^{207}Pb/^{235}U$	$^{207}Pb/^{206}Pb$
1	536	545	586
2	544	548	564
3	528	533	540
4	531	545	604
5	558	(614)	(825)
6	535	548	602

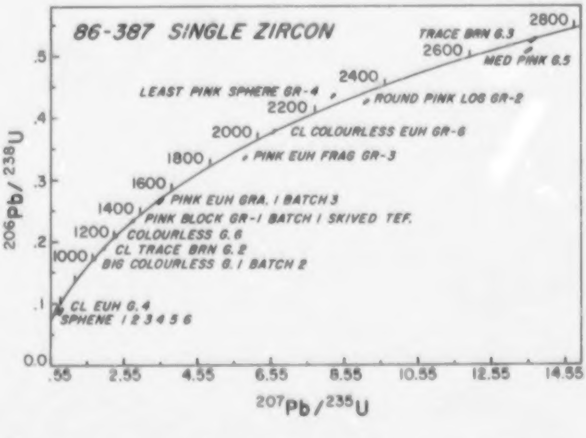

Figure 37. *Concordia plot for single zircon grains from a Jonathan's Pond Formation sandstone.*

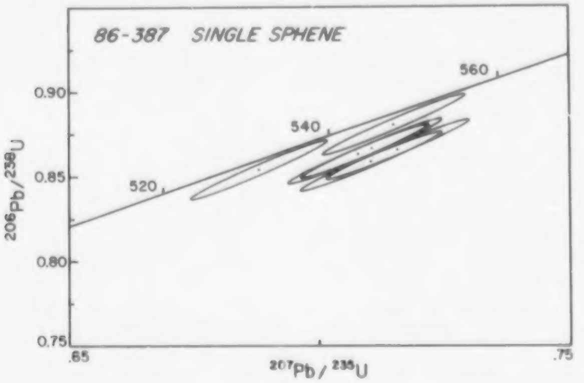

Figure 38. *Concordia plot for single sphene grains from a Jonathan's Pond Formation sandstone.*

549 Ma and sphene ages cluster between 545 and 530 Ma. The sphene data corrected for common lead using model 600 Ma Pb, plot slightly to the right of concordia between 545 and 530 Ma. The sample with the smallest common lead content plots farthest to the left, hence, it is probable that another choice of common lead would shift all data to be concordant between 545 and 530 Ma. This is also supported by the fact that grain 5, which has a very large common lead correction, plots off the figure to the right (T. Krogh, written communication, 1988).

Discussion

Although the small number of analyzed grains precludes any definitive comparison with other areas, some points can be made. Four of the twelve zircon grains fall in the 1347 to 1017 Ma time span and the remainder range up to 2717 Ma with no apparent concentration at any special age. These ages imply that the sediments were not locally derived from Cambro-Ordovician volcanic and sedimentary rocks of the Dunnage Zone. The time span covered by dated rocks in the Avalon Zone ranges from late Precambrian (760 to 570 Ma) volcanic, plutonic and sedimentary rocks to overlying Cambro-Ordovician strata (O'Brien *et al.*, 1988). Only the youngest zircon fits this range. No single zircon analyses have yet been carried out on sedimentary rocks of the Avalon Zone and the possibility, therefore, that sedimentary rocks of the Avalon Zone were selectively recycled to form the Jonathan's Pond Formation, cannot be ruled out.

Single-grain analyses of zircon from sedimentary rocks of the Ordovician Meguma Group indicate two main populations at 600 and 2300 to 2000 Ma (Krogh and Keppie, 1990), a much more restricted range than that shown by the Gander Group. Analyses of single grains from the Spruce Brook Formation in central Newfoundland, indicate a clustering of ages between 1700 and 1200 Ma and one at 2700 Ma (personal communication to Steve Colman-Sadd, 1989, T. Krogh, unpublished data): the Spruce Brook Formation has been correlated with the Gander Group by Colman-Sadd and Swinden (1984) and placed in the Gander Zone (Williams *et al.*, 1988). The similarity of ages of some of the zircons from the two formations does not support or refute the correlation.

Despite the reservations about the different origins of various types of sphene grains (see section on Petrography of the Jonathan's Pond Formation), it is believed that the sphene grains analyzed were detrital. Dr. Tom Krogh (personal communication, 1989) noted that the sphene grains selected, had frosted surfaces, characteristic of detrital grains. Also, one detrital zircon grain has an approximate age of 550 Ma, very close to that of the sphenes. The rock sample was at greenschist metamorphic grade, too low for the growth of metamorphic zircon. The clustering of the sphenes at 545 to 530 Ma suggests that all grains were derived from a single source, which is in apparent contrast with the large range of ages displayed by the zircon. However, if the source area was affected by a regional metamorphic event in the 550 to 530 Ma period, all the titanite could have been reset to this age. Alternatively, the sphenes may have been derived from granitoid bodies (body) of this age, implying an episode of granitic intrusion. Regardless of the precise nature of the source rocks, the detrital titanite imply a volcanic or magmatic event at 545 to 530 Ma, subsequent exhumation of the source rock, and erosion into the Gander Group in pre Early Ordovician times. The presence of detrital sphene of 545 to 530 Ma in psammitic rocks of the Jonathan's Pond Formation, implies that the Gander Group is no older than this Middle Cambrian age.

SEDIMENTOLOGY

PROVENANCE OF THE DAVIDSVILLE GROUP

The petrographic composition of the conglomerate and coarse-grained sandstone (Units 5 and 6), indicates that coarse- to fine-grained and porphyritic trondhjemite formed one of the principal sources of the detritus. A considerable proportion of the quartzofeldspathic material is of first-cycle origin, as it must have originated through disintegration of the plagiogranitic and volcanic rocks, which are present as lithic fragments. The monomictic nature of some conglomerate beds implies that exposures of the plagiogranite, either subaerial or submarine, were very close to the depositional basin. There is also a subordinate volcanogenic component of intermediate to rhyodacitic composition, exhibiting trachytic and spherulitic textures, but it is unclear whether this material, largely extrusive, can be genetically linked to coarser grained trondhjemitic rocks now exposed in the Gander River Complex.

Gabbro forms an important component of the source terrain but based on the relative proportions in the conglomerate, is subordinate to trondhjemite. Although gabbro pebbles and cobbles are common, individual crystals of hornblende or pyroxene are rare, suggesting that individual mineral grains degraded during sedimentation processes.

The significant proportion of chromite detritus implies that ultramafic rocks, either directly or indirectly, formed a major component of the source rocks. However, although some fine-grained, pale-green clasts may represent serpentinized material, no fresh ultramafic debris was identified in thin section. In some of the limestone of Unit 7, bright-green, fuchsitic, chromite-rich layers suggest periodic influx of material derived mainly from an ultramafic source, presumably through resedimentation processes, since no other ultramafic phases have survived. The limestone is associated with relatively mature quartz arenite, which is characterized by abundant chromite. The quartz arenite contrasts, therefore, with the conglomerate and sandstone elsewhere, in Units 5 and 6, which are characterized by, among other material, abundant plagioclase and quartz. The lack of feldspar in the rocks of Unit 7 suggests that trondhjemite either did not form an important part of their source terrain or that the feldspars were almost completely degraded during the depositional process, leaving only the quartz component. Therefore, although the trondhjemite cannot be ruled out as a source for Unit 7, the predominant quartz component, presence of tourmaline, and quartz containing abundant, randomly oriented rutile needles, are features more indicative of a continental source. The source terrain of the coarse-grained sandstone and conglomerate of Units 5 and 6 also included sedimentary rocks, which yielded greywacke, arenite and shale fragments. Some of the arenaceous clasts in the conglomerate are very similar to psammite from the Jonathan's Pond Formation. Because of the absence of a reasonable age for the formation, it cannot be ruled out as a source for the Davidsville Group. Fresh microcline grains in sandstone of Unit 5 in the Davidsville Group imply a granitic source.

On the north shore of Gander Lake, conglomeratic beds several metres west of strata containing late Arenig to early Llanvirn fauna, are characterized by abundant plagioclase and quartz grains in coarse-grained to porphyritic lithic clasts, and subordinate chromite. These coarse-grained rocks are, therefore, similar to monomictic conglomerate in the Weir's Pond area. However, the Gander Lake conglomerate also contains 5 to 10 percent biotite both as a separate component and as a phase within the igneous lithic fragments. The fossil age of the oldest, chromite-bearing sandstone in the Weir's Pond area is late Arenig to early Llanvirn and, by correlation with rocks of similar lithology and age on the north shore of Gander Lake, these sandstones are interpreted to pass up into conglomerate (of Unit 6). Tentative correlations between rocks throughout the Davidsville Group are shown in Figure 39. Thus, the conglomerate is inferred to be of approximately late Arenig to early Llanvirn age.

Exhumation of the igneous complex, which formed the principal source of the conglomerate, probably occurred in Arenig time. Proximal conglomeratic deposits were formed on the flanks of the complex as massive debris flows. Farther away, fine- to coarse-grained, crossbedded sandstone with pebbly lenses were deposited. In the late Llanvirn–early Llandeilo period, abundant shelly fauna thrived in relatively shallow-marine conditions possibly on the flanks of islands formed of volcanic and ultramafic rocks. This period of faunal proliferation may reflect a time of relative tectonic and volcanic quiescence. The locally crossbedded nature of the shelly limestone beds suggests that resedimentation occurred during the late Llanvirn–early Llandeilo. The limestone beds are overlain by calc-arenite and quartz arenite beds, which texturally are mature compared to conglomerate of Unit 6.

In summary, the Gander River Complex formed the principal source of detritus for the Weir's Pond Formation in late Arenig to early Llanvirn times. An important additional detrital component was derived from a continental source. Therefore, in late Arenig times an island-arc, now represented by the Gander River Complex, and a continental block lay adjacent to a sedimentary basin in which the Davidsville Group was deposited.

PROVENANCE OF THE GANDER GROUP

The detrital constituents of the Gander Group identified in this report, particularly the lithic components, indicate that the primary source of sediment was a continental block. This block included metamorphic rocks of greenschist and possibly amphibolite facies and granitoid plutons.

The calc-silicate assemblage, which occurs in many psammitic rocks, is somewhat enigmatic since it is not always possible to clearly separate detrital and metamorphic phases. In low-grade rocks, the variety in form and colour of some of the epidote grains, for example, may suggest a detrital origin. However, detailed petrographic examination of the relationships between at least some of these grains and abutting matrix mica, suggests that the epidote are secondary. Sphene varies little in colour between grains and conclusions as to whether it is detrital or low-grade metamorphic, are made reservedly. Confirmation that some of the titanite grains are detrital is given by the coincidence of the age of a single detrital zircon grain with that of titanite grains. Allanite grains may also be detrital, in which case they are most likely to have been derived from granitic rocks. The detrital calc-silicate component suggests that altered volcanic rocks and/or metamorphosed calcareous rocks formed part of the source.

The minor amount of monocrystalline quartz, which have corrosion embayments present in the sedimentary rocks of the Indian Bay Big Pond Formation, indicate a subordinate felsic volcanic source. However, the abundant volcanic and subvolcanic detritus, which appears to range from felsic to intermediate to mafic, identified in the pebble and cobble conglomerate boulders on the shore of Indian Bay Big Pond, suggests a nearby volcanic arc or island source, for these proximal deposits. Pebbles of gabbro also suggest that deeper levels of a volcano–plutonic complex were exposed. Jasper fragments may represent either interpillow material or exhalative deposits, possibly associated with a volcanic vent.

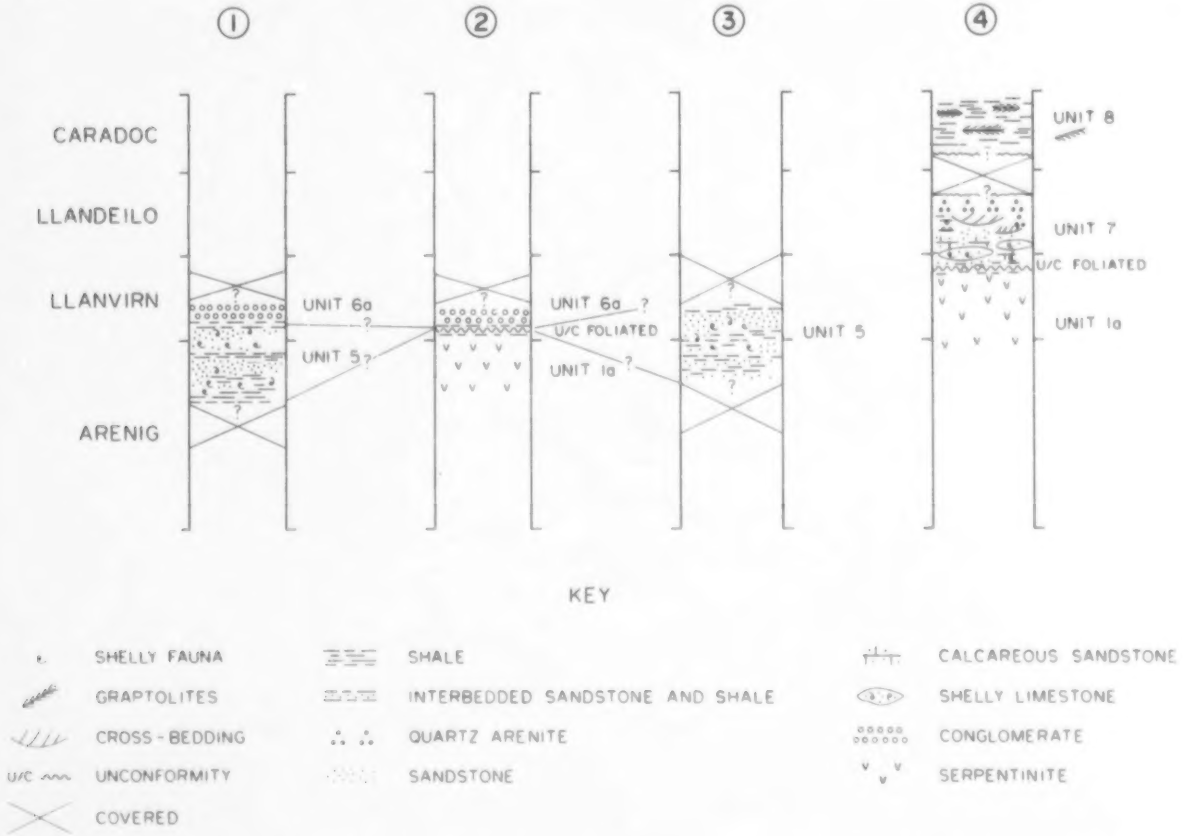
①
②
③
④
CARADOC
LLANDEILO
LLANVIRN
ARENIG
UNIT 6a
UNIT 5
UNIT 6a
U/C FOLIATED
UNIT 1a
UNIT 5
UNIT 8
UNIT 7
U/C FOLIATED
UNIT 1a
KEY
SHELLY FAUNA
GRAPTOLITES
CROSS-BEDDING
U/C UNCONFORMITY
COVERED
SHALE
INTERBEDDED SANDSTONE AND SHALE
QUARTZ ARENITE
SANDSTONE
CALCAREOUS SANDSTONE
SHELLY LIMESTONE
CONGLOMERATE
SERPENTINITE

Figure 39. *Interpretive correlations between schematic sections from various parts of the Weir's Pond Formation (Davidsville Group). The locations of these sections are shown as circled numbers on Figure 2. (See Map 90-02 for key to unit numbers).*

The presence of maroon and green shale fragments, similar to exposed rocks, may suggest that the conglomerate is an intraformational deposit. Conglomerate cobbles containing a maroon matrix, within the conglomerate, indicate repeated sedimentation cycles.

Unlike the majority of the sedimentary rocks from the Jonathan's Pond Formation, some of the psammites of the Indian Bay Big Pond Formation are exceptionally rich in lithic clasts of unmetamorphosed sedimentary rocks and metamorphic rocks. These immature sedimentary rocks appear to have formed as a result of first-cycle sedimentation, following erosion of a probable continental block containing greenschist- to amphibolite-facies metamorphic rocks and lithified clastic sedimentary rocks. This continental debris is thought to have become admixed to some extent with intrabasinal muddy sediments represented by the abundant shale and mudstone fragments. Considering the predominance of angular and subangular sand grains in the lithic graywacke, it is clear that the degree of clast roundness does not always serve as a sensitive enough indicator of recycling.

STRUCTURE

The structural histories of the Gander River Complex and Davidsville Group are not markedly different, but they are substantially different to that of the Gander Group. Hence, all three are described separately for clarity.

GANDER RIVER COMPLEX

The effects of deformation on the rocks of the Gander River Complex are heterogeneous. Unaltered or slightly altered ultramafic rocks and gabbros generally show few effects of deformation but locally contain a weakly developed foliation, which is parallel to the regional northeast-striking fabric. In places, gabbros do exhibit a well-developed penetrative foliation defined by elongate amphibole and plagioclase feldspar. A similar foliation is present in some gabbro cobbles in conglomerate in the Weir's Pond Formation. Locally, a high-strain foliation is developed in gabbro (Plate 21) in an exposure in a quarry beside Route 330. It is a heterogeneously developed shear-band foliation that implies a sinistral component of simple shear, sub-parallel to the plane of the regional fabric.

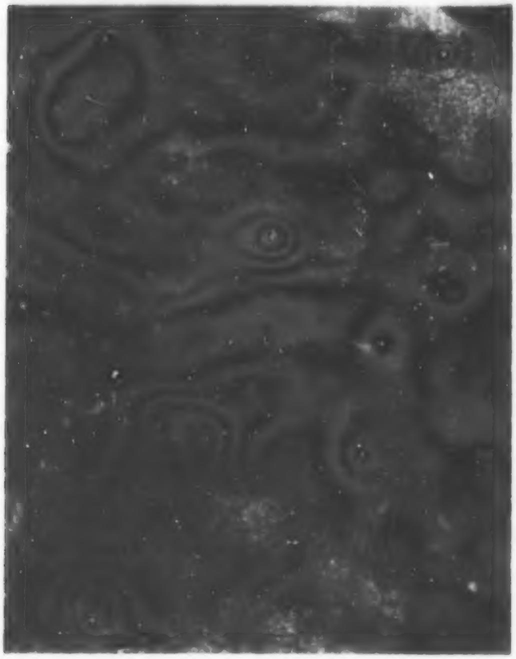

Plate 21. *Shear-band foliation in medium-grained gabbro of the Gander River Complex; pencil points southwestward.*

Trondhjemite, mafic volcanic and volcaniclastic rocks also exhibit the regional fabric. Quartz and feldspar show limited elongation and mafic blocks in trondhjemite are commonly aligned parallel to the fabric.

Metamorphosed ultramafic rocks containing talc ± carbonate ± serpentine exhibit a well-developed steep foliation, parallel to the regional fabric. Regional variations in its attitude suggest some later modification, and southwest of Route 330, an open fold of the foliation in talc-rich rocks has a sub-horizontal fold axis. Plate 22 illustrates brittle, late deformation within serpentinized rocks approximately 1 km east of Route 330. In the southwest of the area, near Weir's Brook, altered ultramafic rocks are heterogeneously and locally highly strained (Plate 23). Irregular, but generally ellipsoidal-shaped, low-strain serpentinite blocks are separated by higher strain, intensely foliated zones of variable width. This fabric is locally shallowly dipping and has probably been modified by later (post high-strain) deformation.

Microfabrics

Plate 22. *Late brittle folding of an earlier foliation in ultramafic rock of the Gander River Complex.*

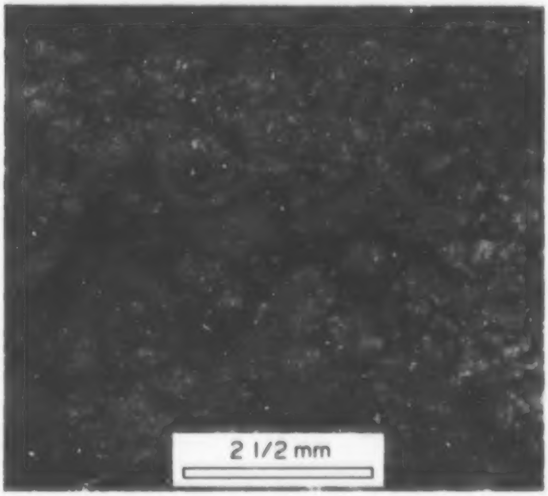

Plate 23. *High-strain foliation in altered ultramafic rocks of the Gander River Complex. (Scale bar is approximately 2.5 mm).*

Because of the incompetent nature of most of the metamorphic assemblage, rocks of the Gander River Complex have tended to deform relatively easily. Serpentine-rich rocks in particular are intensely foliated in places. Although carbonate-rich rocks do exhibit a foliation in some sections, the carbonate recrystallizes with ease and, therefore, tends not to record its deformational history. Talc-rich rocks are typically foliated in rock exposure, however, in thin section, the extreme fine grain size of talc obscures the fabric. A high-strain foliation is developed in rocks near the western edge of the map area, immediately south of Gander River and coincides with the western edge of the complex. Gabbroic, trondhjemitic and sedimentary rocks are involved in this high-strain zone. In thin section, lenticular to sigmoidally- and fish-shaped plagioclase (Plate 24) are aligned within a very fine-grained, intensely foliated serpentine-rich matrix. Cracks within the plagioclase crystals, which locally curve into the external foliation, imply extension along the foliation and semi-brittle behaviour. Within the matrix foliation, two fabrics are locally developed, which exhibit a C-S geometry (Berthe *et al.*, 1979). These textures suggest that the rocks have undergone some simple shear (Simpson and Schmid, 1983; Lister and Snoke, 1984). This high-strain zone is coincident with the approximate western limit of exposure of rocks of the Gander River Complex and it may define a major boundary between the latter and surrounding sedimentary rocks.

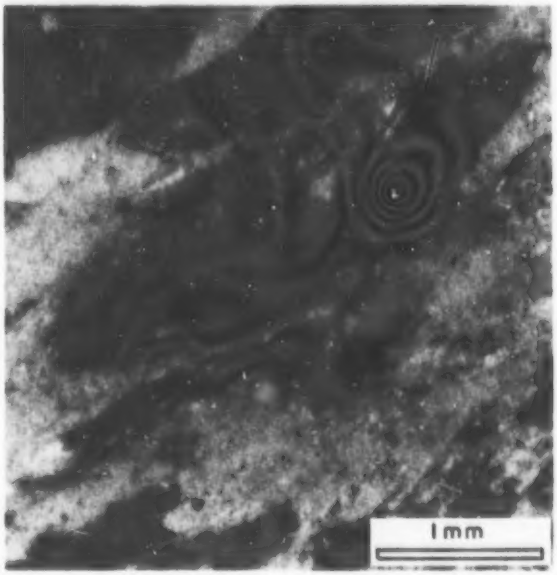

Plate 24. *Photomicrograph of high-strain foliation in conglomeratic or trondhjemitic rock from the western margin of the Gander River Complex (scale bar represents one millimetre).*

DAVIDSVILLE GROUP

Sedimentary rocks of the Davidsville Group contain one penetrative slaty cleavage, designated S_1, which strikes northeast and generally dips steeply northwest (Figure 40). The F_1 folds were rarely observed; however, where present, they plunge at various angles northeastward or southwestward. The slaty cleavage is folded by heterogeneously developed, mesoscopic structures such as chevron folds and kink bands.

The degree to which the regional foliation is developed varies between exposures. Plate 6 shows a bedded conglomerate (Subunit 6a) with a poorly developed cleavage, whereas a massive conglomerate with an intense fabric and shear band foliation is illustrated in Plate 25. Many of the trondhjemitic clasts are parallel to the foliation and some have weakly developed asymmetric tails. Such features suggest localized, non-coaxial deformation in the sedimentary rocks. A moderately southwestward-plunging pebble lineation is locally present in the more strongly foliated, coarse-grained rocks.

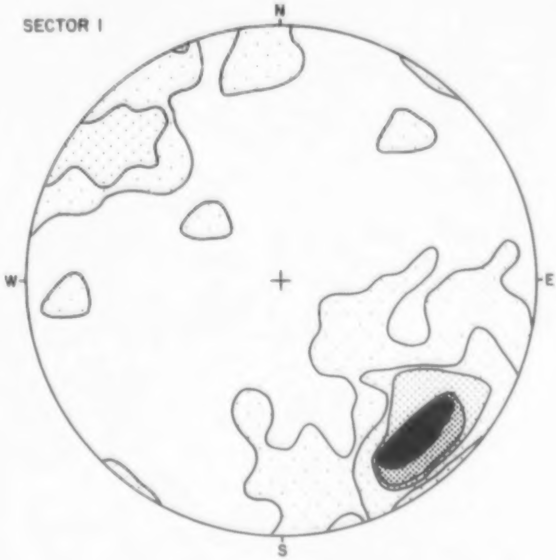

Figure 40. *Contoured plot of poles to regional foliation in the Davidsville Group. Contour intervals are at 1, 3, 6, 9 and 12 percent per 1 percent area. The total number of measurements is 94.*

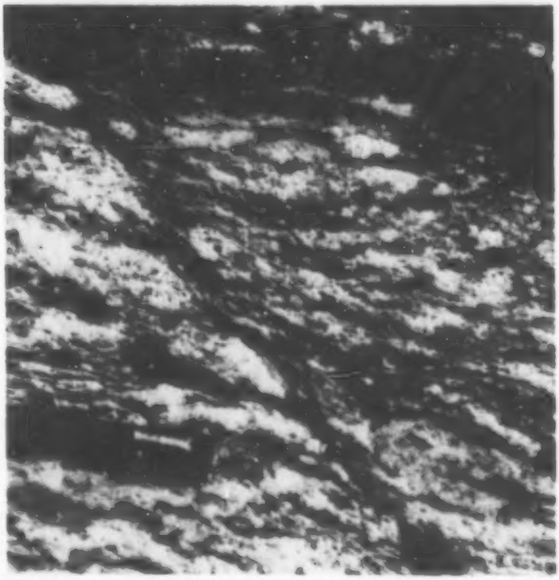

Plate 25. *Intensely foliated conglomerate of subunit 6a, Weir's Pond Formation, Davidsville Group; the shear band implies a dextral sense of shear.*

Microfabrics

In those samples in which the foliation is most intensely developed, fine-grained chlorite and sericite in the conglomerate matrix, in siltstone and in metamorphosed ultramafic clasts, define the fabric. The grain size of the micas tends to be slightly coarser in these strongly foliated rocks than in poorly foliated rocks. The matrix foliation or micaceous clasts commonly wrap around 'hard' detrital grains or clasts. Inequant grains are aligned parallel to the fabric and occasionally mica beards join adjacent grains. Locally, chromite and feldspar grains are broken and displaced along the foliation and cracks within the grains are filled by chlorite. The fabric appears to be predominantly a flattening foliation since only rarely is there evidence, in the form of fish-shaped grains and asymmetric pressure shadows, for simple shear. Solution seams, filled with opaque material, commonly parallel the foliation.

GANDER GROUP

In most exposures, rocks of the Gander Group exhibit the effects of two stages of deformation (Plate 26). The S_1 fabric is the oldest recognized fabric in the area and is either a mimetically recrystallized, bedding-parallel compaction fabric or a tectonic fabric, unrelated to a major deformational event. In hand specimen, the S_1 fabric is locally observed in pelite and semipelite.

Plate 26. *Two phases of deformation affect rocks throughout much of the Gander Group.*

D_2 Deformation

Throughout the Gander Group, the principal tectonic fabric, S_2, is a penetrative foliation axial planar to isoclinal F_2 folds. In psammitic rocks, S_2 is a spaced solution seam cleavage, which is typically anastomosing and discontinuous (Plate 27). In pelite and semipelite, S_2 is normally a well-defined slaty cleavage or penetrative crenulation. The S_2 foliation is ubiquitous and is typically anastomosing on microscopic and mesoscopic scales. The anastomosing nature of S_2 seams in psammitic and semipelitic rocks is at least locally, due to the preservation of a relict S_1. Therefore, S_2 is a composite fabric, formed from complete or partial transposition of S_1 and the newly developed axial-planar S_2 foliation.

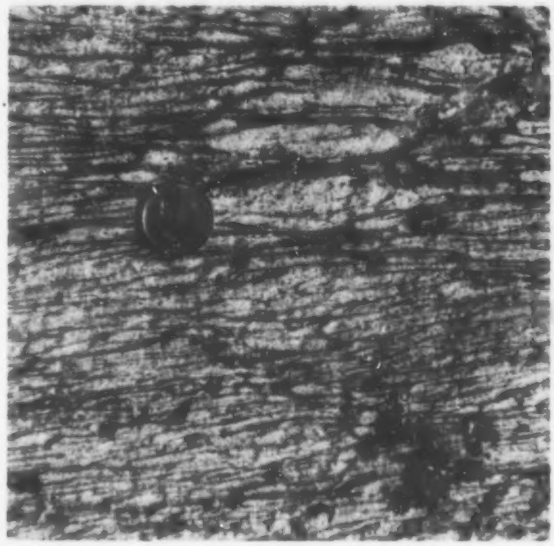

Plate 27. *Spaced, solution-seam cleavage (S_2) typically developed in psammite and quartzite of the Jonathan's Pond Formation.*

The S_2 solution seams in psammite are normally 1 mm thick or less and are discontinuous. The quartzose lithons between the seams vary from approximately 4 to 10 mm thick in hand specimens; a finer layering is present in thin section. Refraction of S_2 is very pronounced in multilayered, ungraded psammite–pelite sequences that typically display sharp planar contacts between beds.

In order to best illustrate the local variation in the attitude of foliations and lineations, the map area is subdivided into four sectors (Figure 41). Sector 1 includes foliation measurements from the Davidsville Group and the Gander River Complex, which occur exclusively in the northwestern part of the map area (Figure 40) and have been discussed previously. Sector 2 demarcates an area of steeply, south-southeast-inclined S_2 foliations, which strike north to north-northeast (Figure 42). In sector 3, S_2 foliation dips range widely, from shallow near Indian Bay Pond to moderate farther north, and steep near the Deadman's Bay Granite (Figure 42).

Variably dipping, north- to northeast-striking, spaced to slaty S_2 foliation, is axial planar to isoclinal F_2 folds, which

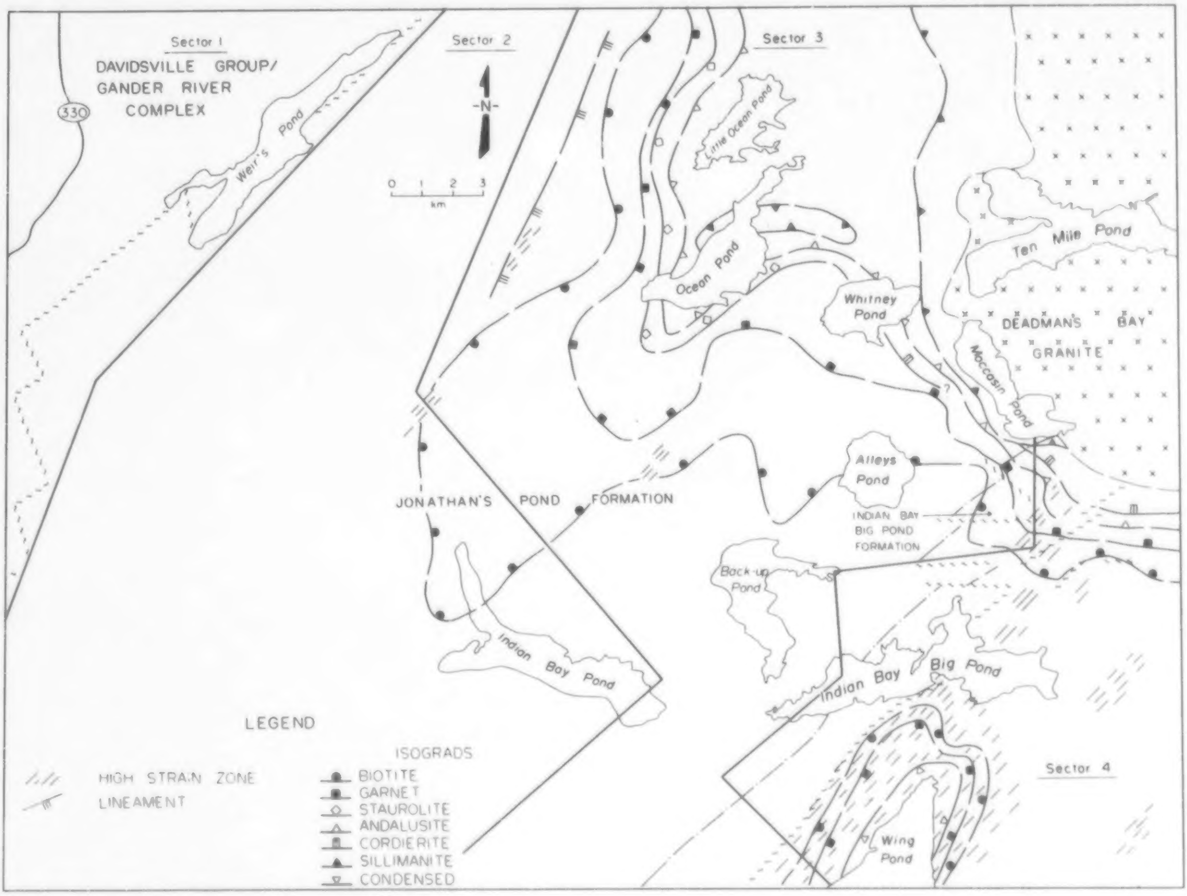
Sector 1
DAVIDSVILLE GROUP/
GANDER RIVER
COMPLEX
330
Weir's Pond
Sector 2
-N-
0 1 2 3
km
Sector 3
Little Ocean Pond
Ocean Pond
Whitney Pond
Ten Mile Pond
DEADMAN'S BAY
GRANITE
Moccasin Pond
Alleys Pond
INDIAN BAY
BIG POND
FORMATION
JONATHAN'S POND FORMATION
Back-up Pond
Indian Bay Pond
Indian Bay Big Pond
Wing Pond
Sector 4
LEGEND
HIGH STRAIN ZONE
LINEAMENT
ISOGRADS
BIOTITE
GARNET
STAUROLITE
ANDALUSITE
CORDIERITE
SILLIMANITE
CONDENSED

Figure 41. *Simplified geological map of Weir's Pond map area, showing 4 sectors, defined for ease of representation of structural data.*

are present in many exposures (Plate 28) of the Gander Group. A contoured plot of F_2 fold axes, which fall on a rough girdle on a northwesterly dipping plane, shows the predominance of shallow to moderately southwest-plunging minor folds in sectors 2 and 3 (Figure 42). The L_2 stretching lineations on the S_2 fabric are rarely observed. However, in two locations (G.R. 950457 and G.R. 976503), L_2 stretching lineations are present. The latter location, 5 km west of the south end of Ocean Pond, lies on a very strong topographic lineament (shown on Map 90-2) produced by a chain of narrow ponds. The other location lies farther south, approximately along strike, and therefore, may define the continuation of this same lineament (which is not as well-defined in the area of the second sample. The stretching lineations lie on the S_2 foliation and plunge moderately westward. The lineations are approximately parallel to F_2 fold axes in this area (see Map 90-02). The two measurements are plotted (Figure 42) and they fall on the girdle defined by the F_2 fold axes. Microscopically, L_2 is defined by elongate pressure shadows adjacent to porphyroclasts of quartz and feldspar. Although recrystallization is complete in the rocks containing the L_2 lineation, concordant quartz lenticles and veins and minor shear bands occur and suggest that the foliation is high strain.

D_3 Deformation

The regional S_2 fabric is folded about upright to slightly inclined, open to tight, microscopic to mesoscopic F_3 folds (Plate 26). The S_2 fabric near Indian Bay Pond (sector 3) is shallow to subhorizontal and is folded about very open F_3 folds with metre-scale amplitudes and wavelengths ranging from a metre to tens of metres. The F_3 folds are most commonly developed as F_3 crenulations that locally have an associated S_3 crenulation cleavage (Plate 29). The S_3 foliation has a predominant north-northeastward strike and dips steeply. The S-pole diagrams (Figure 43) illustrate the local variability in S_3 across the area. In the central parts of the map area, a subhorizontal, crenulation lineation is very well developed (Plate 30) and lies parallel to F_3 fold axes. Throughout sector 2, the L_3 lineations define a good point maximum, plunging shallowly either to the north-northeast or south-southwest. In sector 3, there is slightly more variability in the amount of plunge of L_3 but the azimuths still define a similar point maximum, as in sector 2 (Figure 44).

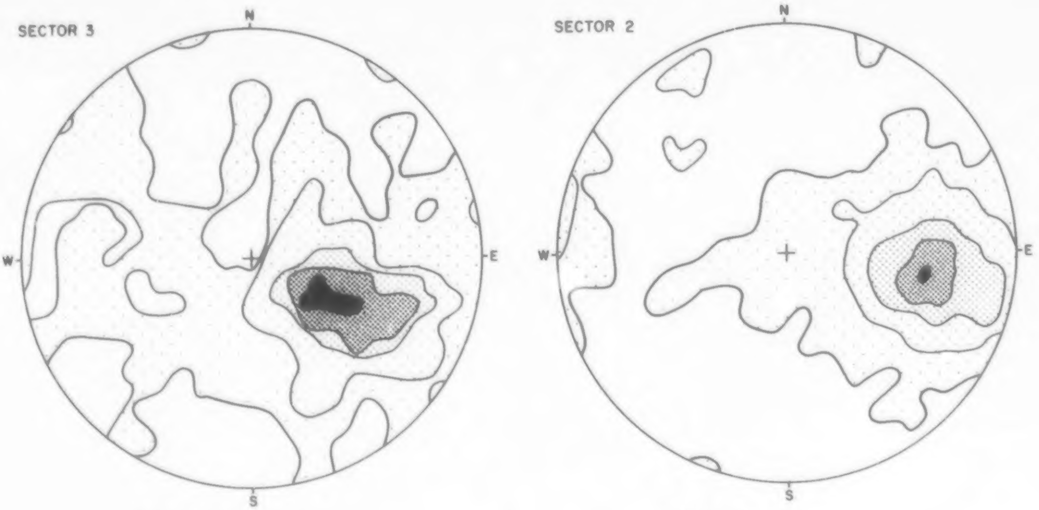

POLES TO S_2
C.I. AT 0.3, 1.5, 4.2, 6.0, 8.1 %
335 POINTS

FOLES TO S_2
C.I. AT 0.4, 2.4, 6.3, 10.3, 12.3%
253 POINTS

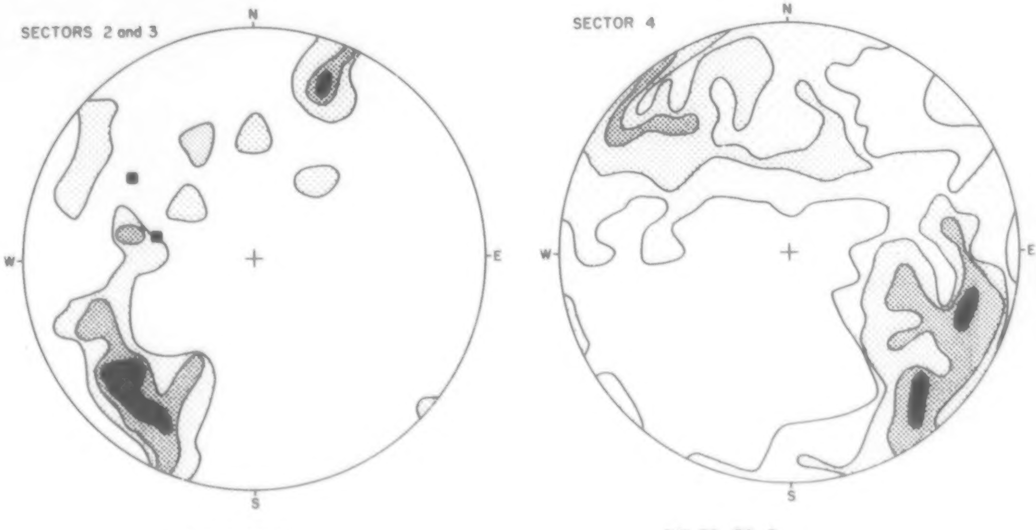

F_2 FOLD AXES
C.I. AT 3.1, 6.2, 9.3%
32 POINTS

POLES TO S_2
C.I. AT 0.5, 2.0, 3.8, 5.7, 8.5%
234 POINTS

Figure 42. *Contoured stereoplots of poles to S_2 as well as F_2 fold axes for the Gander Group. C.I. = Contour intervals (at x percent per 1 percent area). Two L_2 measurements (filled squares) taken east of Harveys Pond, are also plotted with F_2 fold axes.*

The intensity with which folds and lineations associated with D_3 are developed, is variable throughout the area. South and west of Indian Bay Pond, F_3 folds and L_3 lineations are scarce. In the southeast of the map area in sector 4, most late folds (generation uncertain) are moderately to steeply, southwest-plunging and lie closest to the regional plunge of the F_3 folds. These late folds are typically asymmetric, are either Z- or S-shaped and, therefore, do not display the same style as F_3 folds farther northwest. This area is underlain by highly strained rocks of the Wing Pond area (see following section) and these fold structures may be related to this high-strain event. The D_3 structures are best developed north of Indian Bay Pond, where they occur in an area coincident with, but more extensive than, the area that is regionally

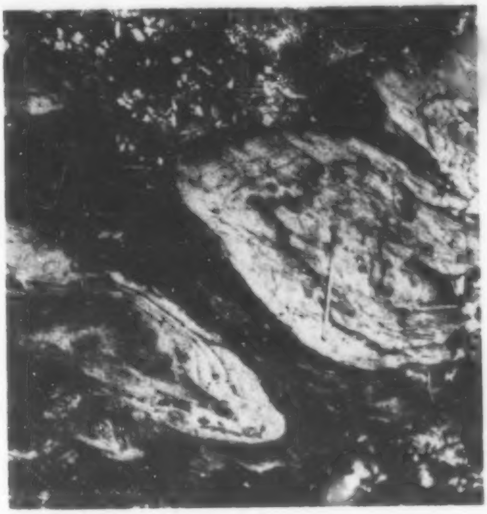

Plate 28. *Isoclinal F$_2$ folds with associated axial-planar spaced solution-seam cleavage (S$_2$) in psammite and slaty cleavage in pelite; Jonathan's Pond Formation.*

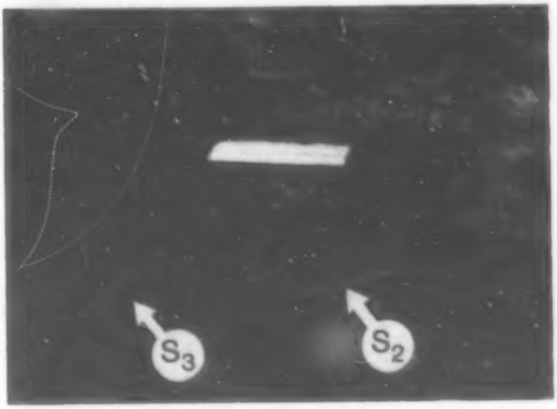

Plate 29. *Poor to incipient development of axial-planar cleavage (S$_3$) to slightly asymmetric F$_3$ folds in Jonathan's Pond Formation semipelite.*

metamorphosed (i.e., at biotite grade and higher; the Ocean Pond area of Figure 3). In areas peripheral to the Deadman's Bay Granite, D$_3$ structures are not well-defined.

Post D$_3$ Deformation

Late brittle deformation effects are represented by kink bands, which are common thoughout the area and locally occur as conjugate sets.

Sector 4 is located in the southeast of the map area, where it demarcates a northeasterly striking belt of steeply northwest- and southeast-dipping foliations. North-striking, steeply east- or west-dipping foliations are also present, mostly east of Wing Pond and immediately northwest of First Pond. Reference to Figure 42 shows that a girdle can be drawn through the S-poles for sector 4, suggesting folding (generation uncertain) around a moderately southwesterly plunging fold axis, in that region. This latter figure includes S-poles to the steep high-strain fabric developed near Wing Pond and northward and S$_2$. The high-strain and S$_2$ foliations are approximately coplanar in this area and therefore, are not readily separated in this sector. However, the timing of the development of the high-strain zone, relative to D$_2$ and D$_3$, is not known.

High Strain Zones

The best exposed high-strain zone is located near Wing Pond (Plate 31). It is 4 to 5 km at the widest part and extends from the southern edge of the map area northeastward to Indian Bay Big Pond where it appears to narrow. North of Indian Bay Big Pond, the high-strain zone anastomoses and the high-strain foliation appears to be heterogeneously developed. Plate 32 illustrates a chert horizon within the Indian Bay Big Pond Formation that is highly strained; elliptical-shaped low-strain augen of fine-grained quartz are separated by intensely foliated zones, millimetres to centimetres wide. Much of the southeastern margin of the Indian Bay Big Pond Formation appears to coincide with the high-strain zone.

The rocks in the Wing Pond area are phyllonites in the low-grade metamorphic zones and platy schists in the higher grade zones adjacent to the pond. Concordant and complexly folded quartz veins are profusely developed in pelitic rocks (Plate 31). A northeast-striking, steeply dipping foliation is intensely developed, marked by numerous quartz lenticles or platelets. Rootless intrafolial folds are common and, in places, fold axes curve through 90 degrees. It is not clear if a single generation of folds is present or whether the folds having curvilinear axes are due to interference created by superimposed folding episodes. Late asymmetric folds of the high-strain fabric are ubiquitous and appear to have consistent vergences east of Wing Pond where they imply a major antiformal structure to the northwest. Crenulations associated with this late deformation have obscured earlier kinematic indicators in the zone.

The southeastern contact of the Indian Bay Big Pond Formation with the southeastern belt of the Jonathan's Pond Formation is nowhere clearly exposed in the map area. However, the Wing Pond shear zone occurs immediately southeast of rocks assigned to the Indian Bay Big Pond Formation. This is clearly demonstrated southeast of Southern Pond. North of Indian Bay Big Pond, highly strained rocks occur within the Indian Bay Big Pond Formation and the southeastern contact of this formation is interpreted to lie within the high-strain zone. The Wing Pond high-strain zone is, therefore, interpreted here to define the contact between the Indian Bay Big Pond Formation and the southeast belt of the Jonathan's Pond Formation.

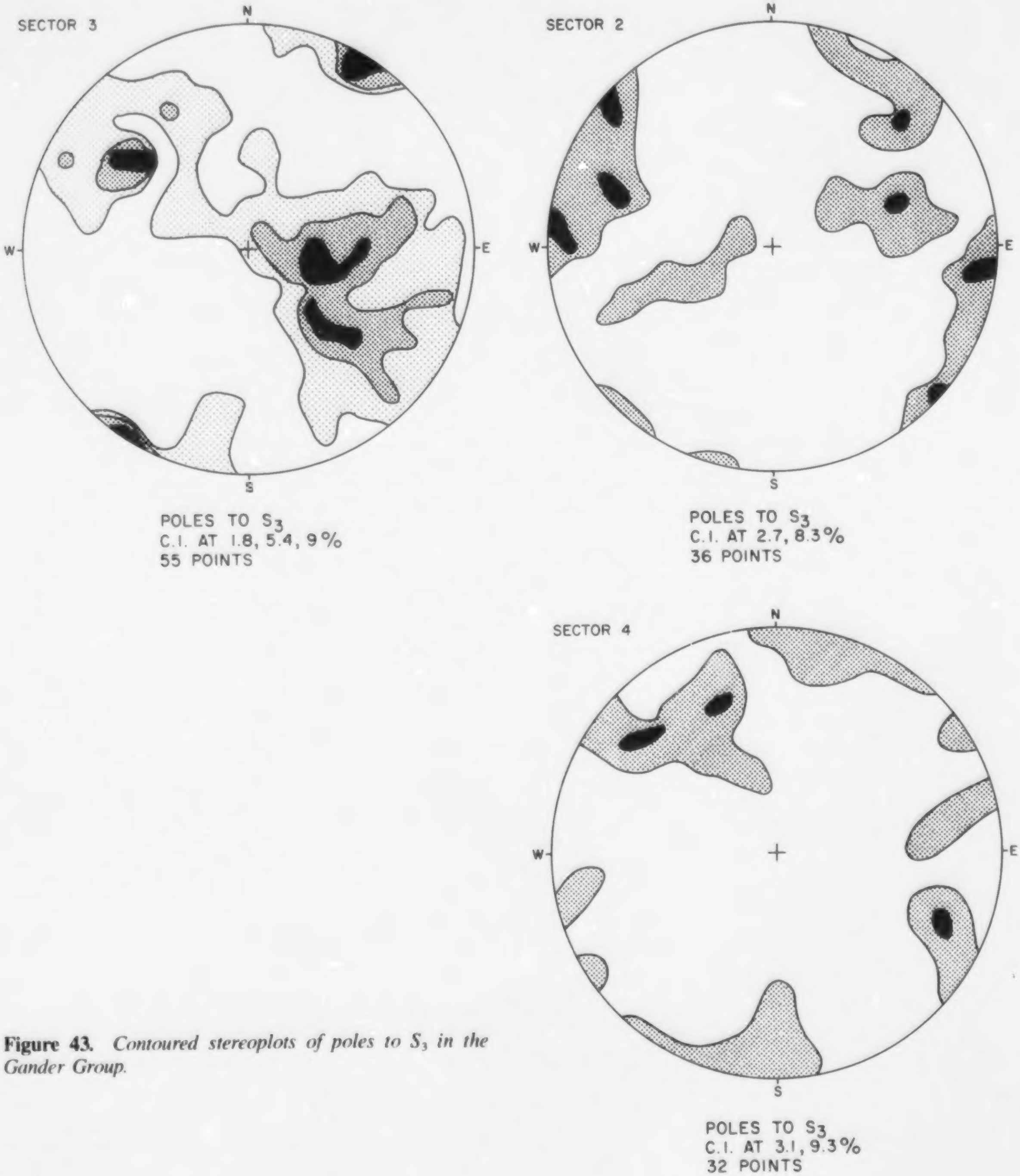

Figure 43. *Contoured stereoplots of poles to S_3 in the Gander Group.*

Elsewhere, in the Gander Group, highly strained rocks occur locally. For example, approximately 6 km west of Ocean Pond (976503), a very finely laminated quartzite contains numerous concordant quartz veinlets, complexly and isoclinally folded quartz lenticles and intrafolial folds (Plate 33). The quartz in the veins and lenticles has recrystallized to a granular mosaic of polygonal grains. However, in the intervening layers, the extremely fine-grained quartz occurs with fine-grained opaque material, forming 15 to 25 percent of these layers. Approximately 50 percent of the rock has

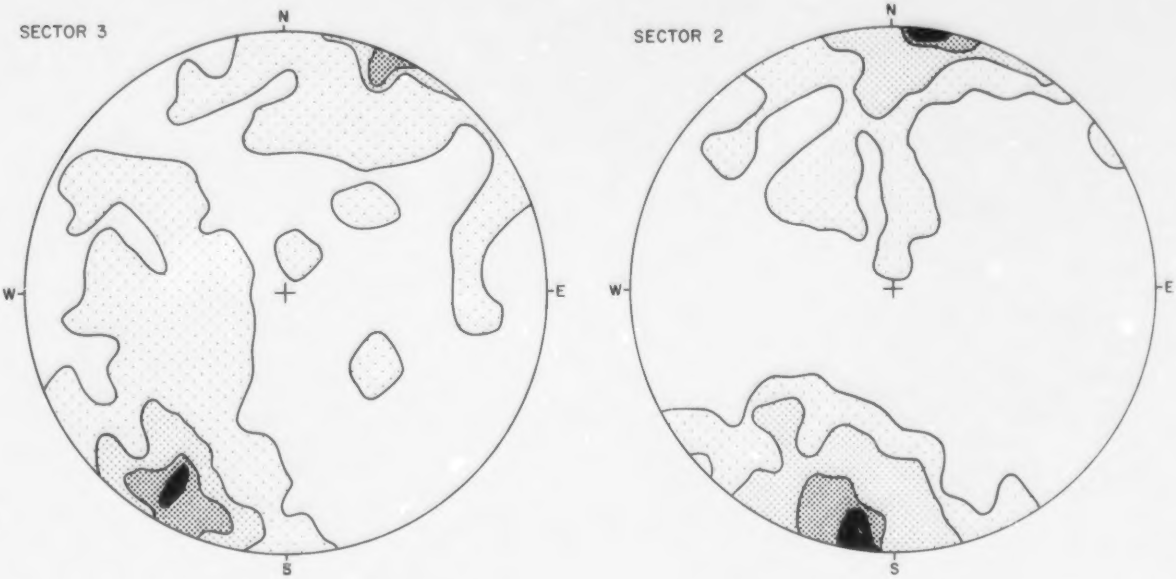

F_3 FOLD AXES, L_3 LINEATIONS
C.I. AT 0.7, 5.0, 8.6, 15.1%
144 POINTS

F_3 FOLD AXES, L_3 LINEATIONS
C.I. AT 1, 3, 9, 14, 17%
100 POINTS

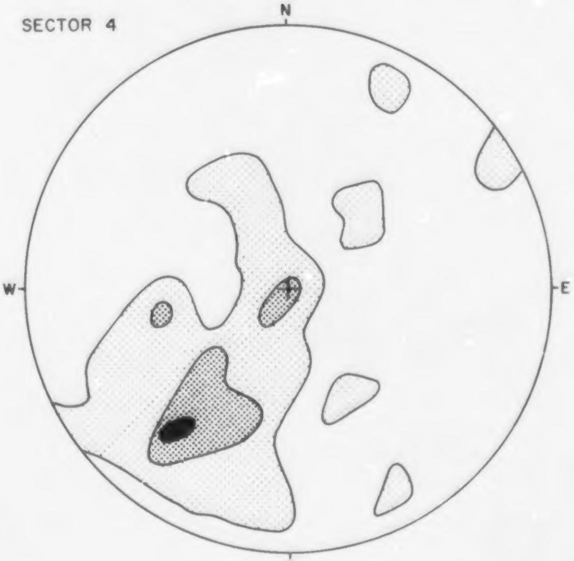

F_3 FOLD AXES, L_3 LINEATIONS
C.I. AT 1.7, 7.1, 12.5%
56 POINTS

Figure 44. *Contoured stereoplots of F_3 fold axes and L_3 lineations in the Gander Group.*

recrystallized and, therefore, it is more appropriately called a blastomylonite. The sample location coincides with a very strong lineament, defined by a chain of narrow lakes, which extend parallel to the local north-northeast strike for a minimum distance of 10 km. Approximately 5 km to the southwest, a rock of similar composition is also blastomylonitic and appears to lie along the on-strike extension of this lineament. It is likely that this lineament

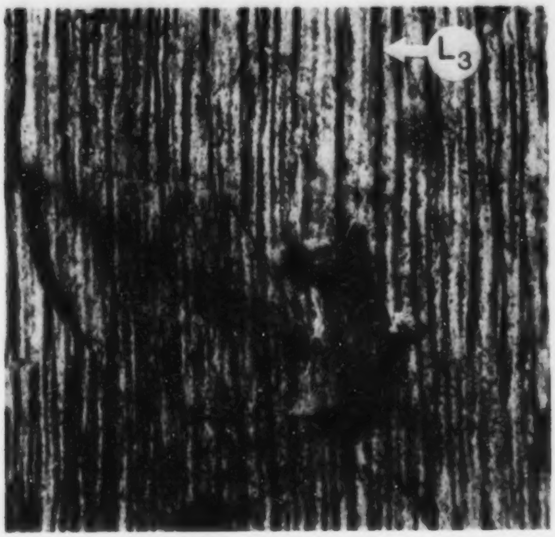

Plate 30. *Crenulation lineation (L_3) in pelite of the Jonathan's Pond Formation, Ocean Pond area. (Note blueberry for scale).*

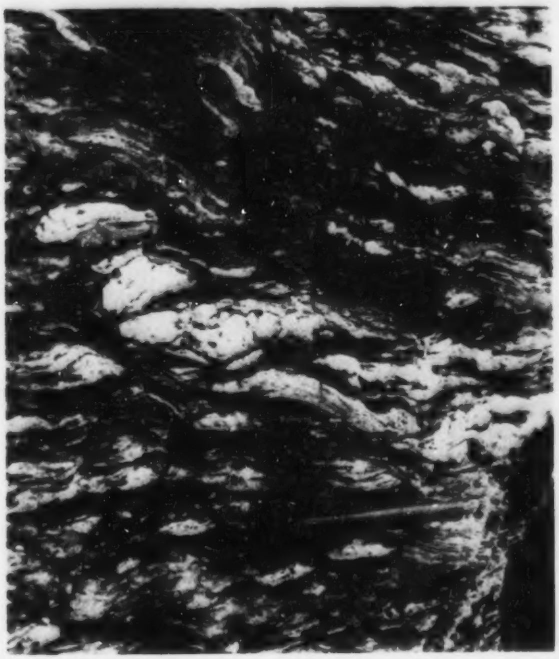

Plate 31. *High-strain zone near Wing Pond is developed in predominantly pelitic rock types which characteristically contain profuse quartz veins.*

probably defines a ductile fault within the Jonathan's Pond Formation.

A schist sample, collected from an exposure 3.5 km northwest of Back-Up Pond (G.R. 026441), contains porphyroblastic biotite, up to 3 mm across, in a well-developed, fine-grained muscovite foliation. Biotite is elongate on the schistosity and displays a fish-shape locally. Some biotite grains contain helicitic, inclusion trails, which curve continuously into the high-strain, matrix foliation. Some of this syntectonic biotite has variably developed

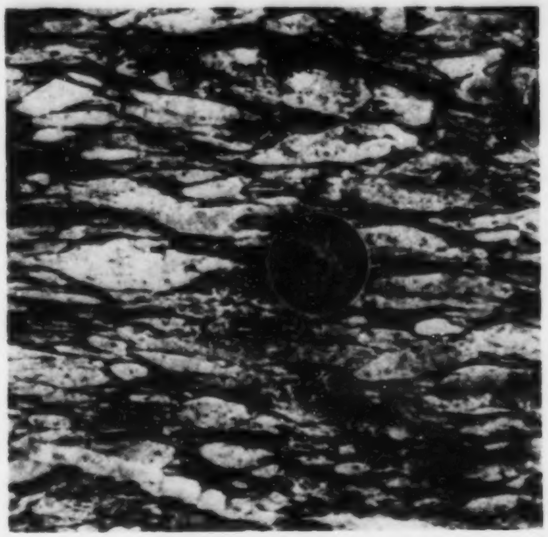

Plate 32. *Anastomosing high-strain foliation in chert of the Indian Bay Big Pond Formation.*

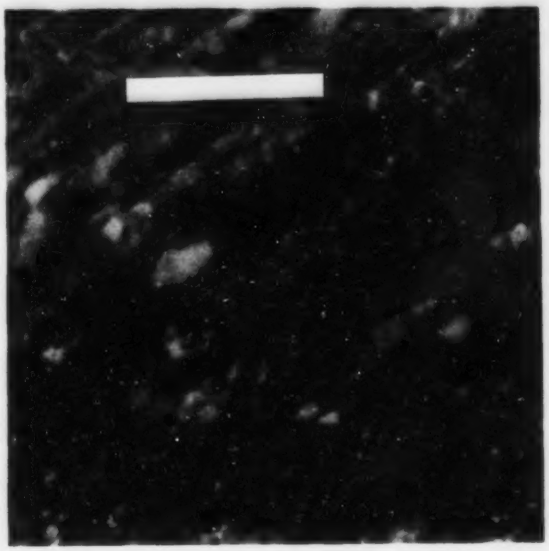

Plate 33. *Photomicrograph of high-strain foliation in quartzitic rock, characterized by intrafolial folds (of quartz lenticles); Jonathan's Pond Formation, west of Ocean Pond. (Scale bar = 1 mm).*

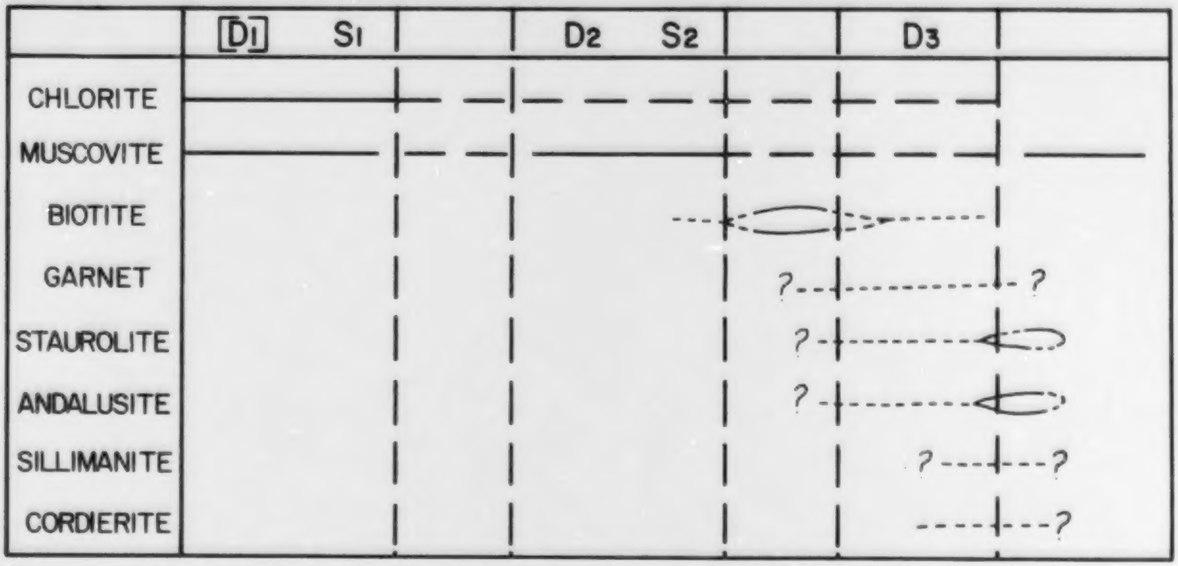

Figure 45. *Relationship between porphyroblastesis and timing of deformational phases in the Ocean Pond area, Gander Group.*

pressure shadows. Nevertheless, much of the biotite does not form augen in the high-strain foliation and is at least partly posttectonic.

Although the high-strain foliations in the Gander Group are parallel to sub-parallel to the regional S_2 foliations, their relationships are uncertain. As seen in the Ocean Pond area, the effect of the D_3 event is to produce open upright folds, i.e., to steepen earlier flat-lying or shallowly dipping structures, through west-northwest to east-southeast shortening. This shortening could have occurred in conjunction with shearing in the high strain zones.

Microfabrics

Ocean Pond Area

Relationships between porphyroblastesis and timing of fabric development in the Ocean Pond area is summarized in Figure 45.

Chlorite, Biotite and Garnet Zones

In most semipelitic and pelitic rocks, S_2 is folded by symmetric to asymmetric F_3 folds produced during the regional D_3 deformation. Microscopic F_3 crenulations are second-order structures associated with sub-horizontal, open folds and crenulations on a mesoscopic scale.

In psammitic rocks of the chlorite to garnet zones, S_1 is mineralogically defined by chlorite and muscovite and rarely by dissolution-elongated quartz, ranging from less than 0.05 to 0.2 mm long. Where the psammite is sufficiently mica-rich, the S_1 fabric is preserved in microlithons separating the S_2 seams. S_2 is typically defined by pressure solution seams, 0.05 to 1 mm wide and spaced approximately 0.3 to 0.6 mm apart, which comprise fine-grained white mica, chlorite, sphene, opaque minerals and locally calcite. Mica laths in S_1 are approximately the same grain size as in S_2. The S_2 seams are locally marked by limonitic opaque seams, up to 0.01 mm wide, which wrap around clastic grains. The F_3 crenulation folds are quite heterogeneously developed and vary from open, symmetric microfolds to tight, asymmetric crenulations. The former have no associated axial–planar cleavage whereas in the latter, a crenulation cleavage, S_3, is defined by microlithons, 0.2 mm across or less, in which the mica laths lie at a high angle to the S_2 fabric. The central parts of the microlithons have a discontinuous concentration of fine-grained opaque material, sphene and quartz. Muscovite laths bent around the F_3 fold hinges, typically, have not annealed and little if any neocrystallization has occurred parallel to the S_3 seams.

In semipelitic and pelitic rocks, the relationships between S_1 and S_2 are well-defined (Plate 34). Although S_2 is invariably the main tectonic foliation, a relict S_1 is preserved in the following microstructural locations–1) in elongate lenses 0.2 mm thick or less and 1 mm long or less in S_2, as an oblique fabric, locally associated with rare relict F_1 intrafolial folds; 2) as an oblique fabric in quartzose lithons; 3) in pressure shadow regions; and 4) in several samples, quartzose knots, 0.3 to 0.5 mm across, contain a fabric, which remains parallel between the knots, and oblique to the matrix foliation. The oblique S_2 fabric is generally at high angle, 70 to 90° to S_1 in pelitic rocks.

The S_1 fabric is defined by chlorite and muscovite in approximately equal proportions. These minerals gradually increase in grain size from < 0.1 to 0.3 mm, as metamorphic grade increases from chlorite to garnet. The same minerals define S_2, but muscovite usually predominates over chlorite and the latter decreases in abundance toward higher grades.

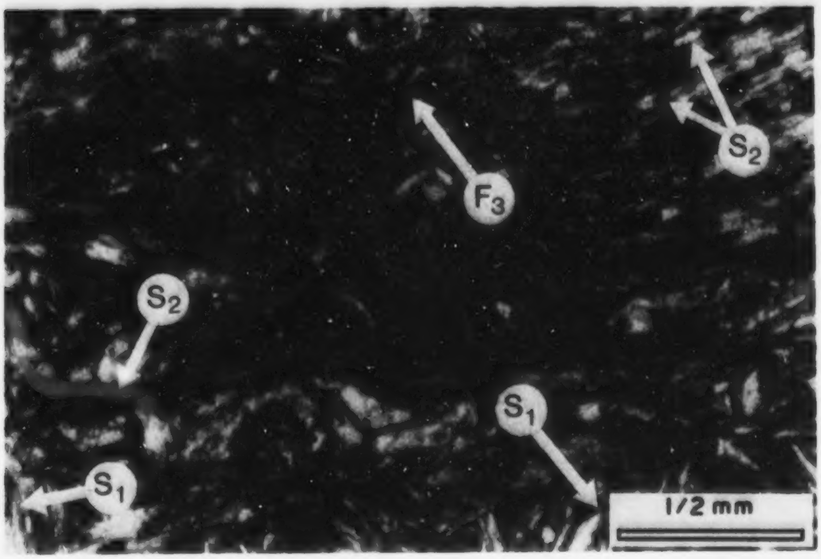

Plate 34. *Photomicrograph showing relationship between S_1, the earliest defined foliation (runs north-south in plate), S_2 the principal regional foliation (runs east-west) and F_3 microfolds; Jonathan's Pond Formation near Ocean Pond. (Scale bar is 0.5 mm approximately).*

In some semipelitic and pelitic rocks, S_2 defined by mica and elongate quartz appears to be a higher strain fabric than normal and wraps around porphyroclasts of quartz and feldspar. The porphyroclasts are either relict clastic or early metamorphic grains and have generally symmetrical pressure shadows, which contain granoblastic polygonal quartz. Opaque material is elongate in S_2 and quartz grains within this fabric are typically elongate and may have aspect ratios up to 1:8. In some semipelitic rocks, numerous elongate lenses or platelets of polygonized quartz occur with well-defined S_2-parallel grain boundaries, commonly accentuated by less than 0.01-mm-wide mica layer. Internal boundaries are sutured and blurred. In addition, inequant quartz and feldspar grains are parallel to sub-parallel to muscovite and chlorite in S_2 and exhibit little if any evidence for rotational strain. Quartz is very rarely elongated parallel to S_1.

In pelitic rocks of the biotite and garnet zones, S_2 seams contain only muscovite and opaque minerals and some sphene locally.

Biotite poikiloblasts, in which an included mineral fabric (S_i) is preserved, always overprint both S_1 and S_2 (Plate 35). The S_1 is normally defined by fine-grained quartz, muscovite and opaque inclusions and is typically continuous with S_2, the external matrix fabric (S_e). In places, muscovite laths that are coarser grained than the external foliation overprint S_2 but are overgrown by even coarser grained biotite.

The relationship between the timing of biotite growth and the development of F_3 crenulations is more complex. Nowhere does biotite clearly overprint the S_3 fabric. However, at the margin of approximately 20 percent of the biotite grains examined, S_i curves to match a corresponding curvature of S_2 by F_3 microcrenulations in the matrix. Locally, biotite laths have preferentially grown parallel to asymmetric F_3 microfolds. Elsewhere, in the matrix, biotite laths are bent around F_3 folds. Thus, biotite growth, which is post D_2, occurred before and synchronously with the early stages of D_3 deformation. The very localized and minor development of augen of biotite in S_2 may be due to strain during D_3. Locally, biotite grains and inclusions are sharply truncated against S_3 suggesting some dissolution along this fabric seam. In a few places, S_3 seams are deflected around or terminate at biotite porphyroblasts.

Garnet porphyroblasts have a poorly to moderately developed internal fabric (S_i), which is typically straight or gently curvilinear and continuous with S_e (S_2). Garnet overprints biotite although its relationship to the F_3 microfolds is not evident. Nonetheless, garnet is assumed to have the same relationships to the regional fabrics, S_1, S_2 and S_3 foliations as does biotite. Magnetite porphyroblasts, which do not contain inclusion trails, also present similar relations to the regionally developed foliations as biotite and garnet.

Staurolite, Andalusite and Sillimanite Zones

Staurolite and andalusite typically contain an S_i defined by elongate quartz, opaque minerals and muscovite. They also contain randomly oriented porphyroblasts of biotite, garnet and less commonly, coarse muscovite. Helicitic trails in staurolite and andalusite are straight, curved or crenulated. As in the case of biotite, the aluminosilicates overprint the S_1 and S_2 foliations. However, unlike biotite, they overprint crenulated S_2 in places. Locally, they appear to be folded around F_3 folds. Thus, staurolite and andalusite developed after S_2 and either experienced continuous growth throughout D_3 or, resumed growth after D_3. However, these minerals do not apparently form augen in S_3, suggesting simultaneous cessation of growth and fabric (S_3) development or posttectonic growth. There is very limited growth of

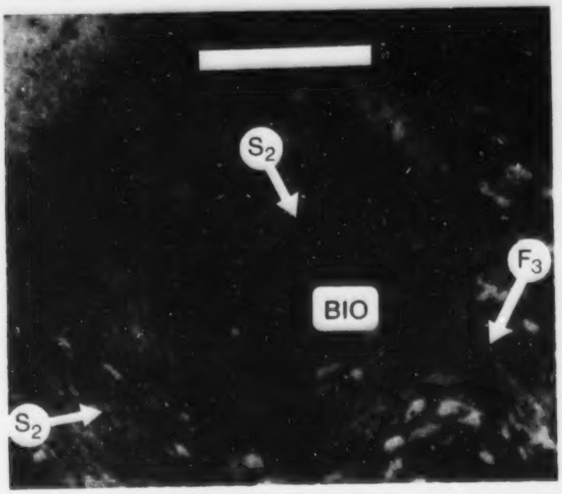

Plate 35. *Photomicrograph of biotite porphyroblast overprinting S_2 foliation defined mostly by fine-grained muscovite. (Scale bar is 1 mm approximately).*

metamorphic minerals axial planar to F_3 folds suggesting posttectonic rather than syntectonic growth.

Fibrolite and sillimanite developed after the growth of andalusite and, therefore, probably have similar relationships to D_3 as outlined above. Quartz and feldspar in the higher grade parts of the andalusite zone and in the sillimanite zone rarely exhibit a tectonic elongation, but are almost invariably granoblastic or polygonal.

In much of the eastern part of the sillimanite zone, the rocks are characterized by poorly preserved tectonic foliations and locally are hornfelses. From the northern part of the Ocean Pond sillimanite zone to Moccasin Pond, most rocks are characterized by coarse porphyroblastic muscovite, up to 3 mm across. This contrasts with the relatively fine- to medium-grained muscovite, up to 0.6 mm across, which defines S_2 elsewhere. The porphyroblastic muscovite contains inclusions of sillimanite and biotite and is, therefore, considered to have formed relatively late in the metamorphic history of this area.

In one sample, a high-strain fabric involving sillimanite is developed (Plate 36). Both fibrolite and sillimanite are strongly aligned in foliae, which are evident in hand specimen and are clearly crenulated. The sillimanite foliae are variable in width up to a maximum of 1 mm and thicker foliae split and anastomose around single or aggregate quartz grains and biotite. Some of the quartz grains enveloped by sillimanite have aspect ratios of 15:1, are en echelon and strained. Biotite grains enveloped by the aluminosilicate locally have fish shapes suggesting non-coaxial deformation. Within the wider sillimanite foliae, subfoliae anastomose and bend into the main fabric. The morphology of the sillimanite within the foliae contrasts markedly with that within quartz away from the foliae, which is random.

In at least one highly strained sample from the biotite zone of the Ocean Pond area, biotite with muscovite is a foliation-forming phase in a blastomylonitic schist. Quartz grains are ribboned and have not recrystallized. Single biotite grains and aggregates are locally fish-shaped and the biotite foliation is asymmetrically crenulated. These textures, in which biotite is synkinematic, contrast with the usual relationship of biotite to the foliations outlined above and imply that the high-strain foliation during D_3.

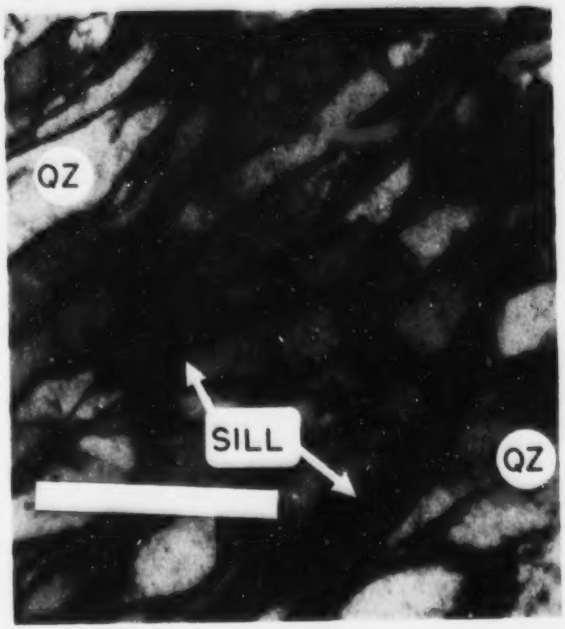

Plate 36. *Photomicrograph showing high-strain foliation developed in sillimanite-zone rock of the Ocean Pond area, Gander Group. (Scale bar is 1 mm approximately).*

Calc-Silicate-Rich Rocks and Amphibolites

These rocks generally contain a banding defined by alternating layers of different mineralogy. The metamorphic mineral assemblages exhibit no effects of D_2 or D_3

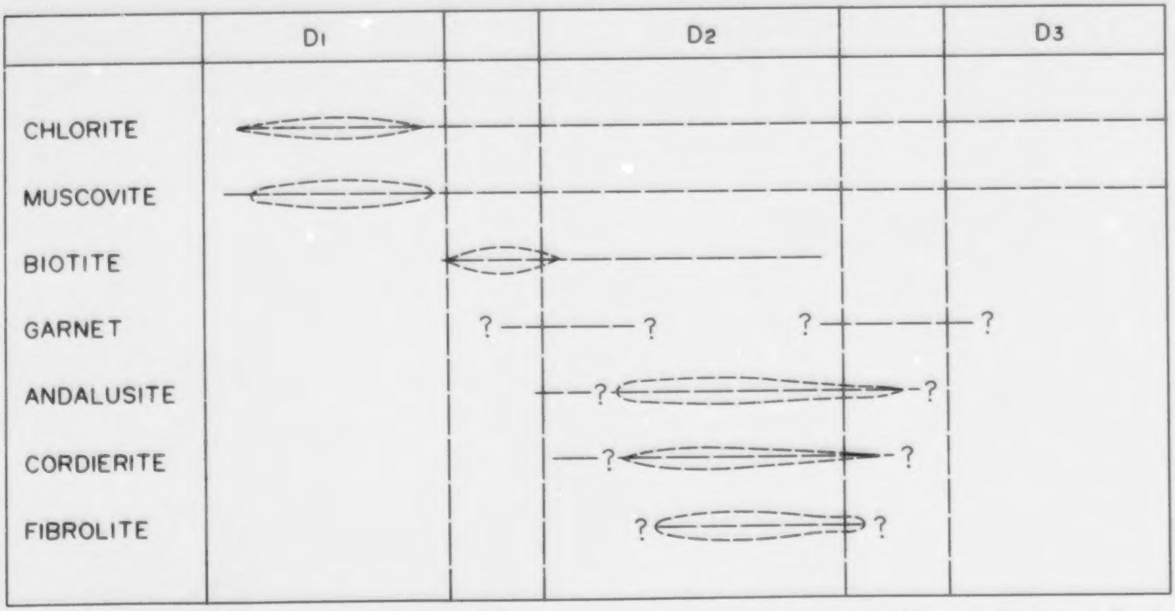

Figure 46. *Relationship between porphyroblastesis and timing of deformational phases in the Moccasin Pond area, Gander Group.*

deformation and textural characteristics, e.g., hornblende rosettes, imply static growth.

Moccasin Pond Area

The relationship between porphyroblastesis and the development of tectonic fabrics in the Moccasin Pond area is shown in Figure 46. Exposures are poor in the Moccasin Pond area and because of localized development of hornfelses, the relationships between regional deformation and metamorphism are not as clearly defined as in the Ocean Pond area. In the Moccasin Pond area, biotite is a principal component defining the main fabric, whereas in the Ocean Pond area, biotite rarely is a foliation-forming mineral. Thus, the deformational phases as discriminated in thin section and illustrated in Figure 46 are for this area alone.

Southward, from the vicinity of the north end of Moccasin Pond, the textural characteristics of the metasedimentary rocks contrast with those exhibited by the rocks around Ocean Pond. The principal difference is in their relative grain size and in microfabric–porphyroblast relationships. The rocks are typically fine grained in the biotite and garnet zones of the Moccasin Pond area.

A very fine-grained, poorly developed, chlorite–muscovite foliation is the oldest fabric observed in most thin sections and is designated S_1. In rocks that preserve a better than average 'textural memory' of the metamorphic and structural history, fine-grained, randomly oriented biotite overgrows this chlorite–muscovite foliation. After the growth of biotite, the rocks were deformed during D_2 and the early foliation was crenulated. The biotite and crenulated foliation were, in turn, overprinted by pseudomorphs (after ?andalusite and/or cordierite) and near the Deadman's Bay Granite, by both andalusite and cordierite porphyroblasts, which have mostly survived the extensive retrogression affecting these rocks. The only evidence for S_1 is preserved in porphyroblasts. This foliation is either straight, crenulated or locally curved at the margins of the porphyroblasts so that it swings into parallelism with Se. In some porphyroblasts, a weak alignment of biotite may be due to mimetic crystallization. After cessation of porphyroblast growth and before retrogression, the rocks were intensely deformed during the main part of the D_2 deformation and the main foliation was formed by transposition of the early fabric and rotation of biotite.

Growth of andalusite and D_2 deformation occurred synchronously but deformation, at least locally, continued after growth of the porphyroblasts, since the the main foliation is strong around pseudomorphs and porphyroblasts of andalusite and cordierite form augen in it. Garnet, granoblastic K-feldspar and quartz locally overprint the biotite foliation, S_2, which is gently folded by a late crenulation.

Wing Pond Area

In the Wing Pond area, the metamorphic mineral assemblages exhibit the effects of high-strain deformation (Plate 37). The lower grade rocks are muscovite ± biotite schists, commonly containing retrograde chlorite. Syntectonic muscovite and biotite define the main foliation. Individual mica grains, particularly muscovite, are up to 2 to 3 mm long by 0.05 mm across or less. Asymmetric, fish-shaped biotite and chlorite porphyroblasts, up to 3 mm across, are common and are elongated along the foliation. Fish-shaped lenticular aggregates of mica, up to several centimetres long and 0.1 mm wide or less, are also common. Magnetite anhedra and rarely garnet, are broken and displaced along the foliation and some have en echelon shapes; cracks between the broken grains are filled with quartz and/or chlorite. Shear bands are a common feature in some samples. Concordant quartz lenticles or platelets and veins, up to several centimetres long and typically less than 0.1 mm wide, are widespread. The quartz is granoblastic in most places but rarely elongate individual cystals are preserved with aspect ratios of up to 10:1. The foliation and concordant quartz veins are isoclinally folded and isolated rootless folds occur locally. In quartzose rocks that have undergone extensive recystallization, the quartz is mostly granoblastic. However, porphyroclasts of quartz, and in places perthite, occur with symmetrical pressure fringes. Feldspar is broken and displaced along the foliation.

Plate 37. *Photomicrograph showing high-strain foliation, defined mostly by syntectonic muscovite, parallel to quartz lenticles in Wing Pond area, Gander Group. (Scale bar is 1 mm approximately).*

High-strain fabrics defined by muscovite and biotite, locally retrogressed to chlorite, are also developed in the higher grade rocks where the metastable assemblage kyanite–staurolite–andalusite–sillimanite–garnet–biotite is present. Various combinations of fractured and strained kyanite, staurolite and andalusite occur in low-strain augen. In places, anastomosing subfoliae associated with the high-strain fabric cut across the low-strain augen and the disparate parts of the augen are displaced along the foliation.

In some low-strain augen, anastomosing seams of fibrolitic sillimanite 0.01 mm wide or less, replace parts of kyanite and staurolite grains. Elsewhere, seams of fibrolitic sillimanite are enclosed in syntectonic muscovite and biotite. In some samples, andalusite porphyroblasts include microfolds defined only by sillimanite (Plate 38). This feature suggests that the andalusite is later than the sillimanite. The andalusite does not overprint the high-strain fabric. Inclusion trails in garnet are straight and poorly developed and in most cases, the S_i (which is possibly earlier increments of the high-strain foliation) are continuous with Se. Elsewhere, sub-idiomorphic garnets have overgrown the high-strain foliation.

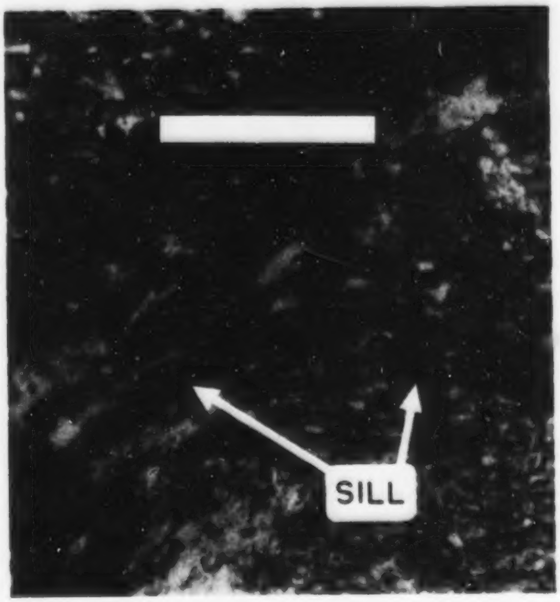

Plate 38. *Photomicrograph showing microfolds in andalusite defined by sillimanite, Wing Pond high strain zone, Gander Group. (Scale bar is 1 mm approximately).*

Between the garnet zone and rocks containing andalusite–sillimanite–kyanite–staurolite–biotite ± garnet near Wing Pond, a sequence of isograds reflecting increasing metamorphic grade were not observed. The transition from sub-biotite grade to higher grade occurs over less than 1 km at the north end of Wing Pond and indicates that several isograds are condensed within this narrow cross-strike distance. The coincidence of the higher grade metamorphism and the shear zone suggests that rapid but variable amounts of uplift occurred in the zone and resulted in the juxtaposition of isograds.

The present study merely documents the existence of this zone and some of its main features. Full delineation of the shear zone and its relationship with the metamorphism require a detailed and combined structural and metamorphic study. Within the context of types of metamorphism in the northeastern Gander Zone, the zone is unusual in that it contains kyanite and is not associated with voluminous granites.

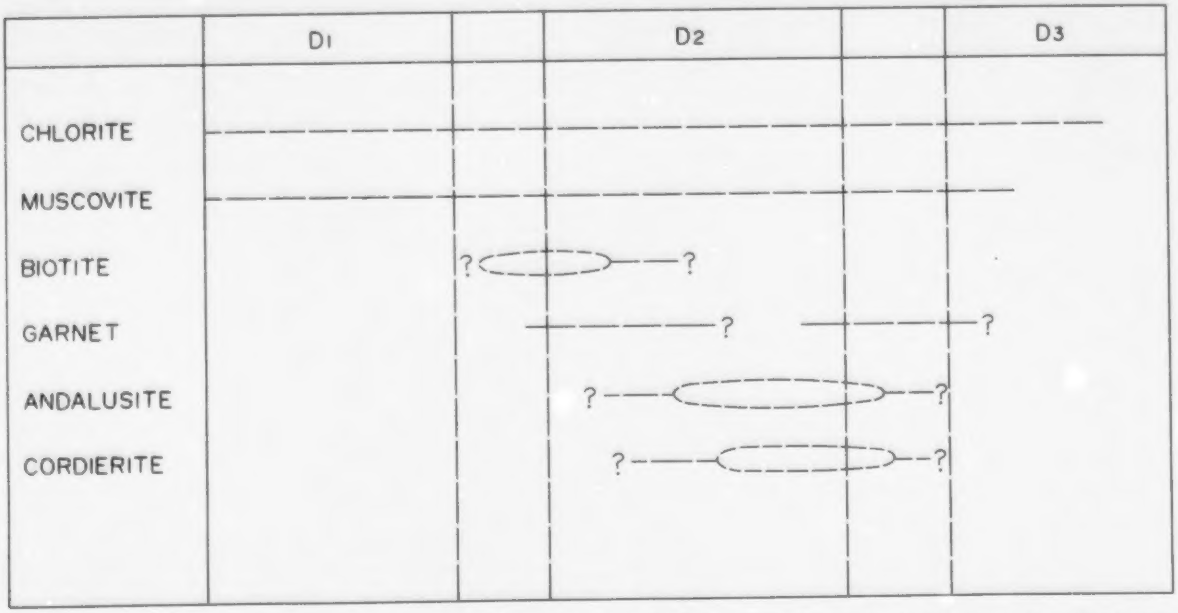

Figure 47. *Relationship between porphyroblastesis and timing of deformational phases in the Big Bear Cove Pond area, Gander Group.*

Big Bear Cove Pond Area

The relationships between porphyroblastesis and timing of fabric development in the Big Bear Cove Pond area is illustrated in Figure 47. The weakly preserved, oldest fabric S_1 is defined by fine-grained chlorite and muscovite. The S_1 foliation was subsequently crenulated by F_2. Fine-grained, non-schistose biotite typically overprints the chlorite–muscovite foliation but its growth relative to the crenulation development is uncertain because of its fine grain size. The S_1 foliation relationships are best preserved in cordierite and andalusite porphyroblasts and in sericite pseudomorphs after one or both of these two phases.

In most samples, the matrix S_2 foliation is composite and comprises the transposed S_1 chlorite–muscovite foliation as well as realigned biotite. Andalusite and cordierite overprint the F_2 crenulations of the S_1 foliation. In places, porphyroblastesis occurred statically. In other locations, the porphyroblasts form distinct augen and, therefore, S_2 continued to develop after porphyroblast growth. Weakly developed, late, open microfolds heterogeneously affect the main S_2 fabric.

Midway between Big Bear Cove Pond and Moccasin Pond, close to the Deadman's Bay Granite, tectonic fabrics are generally absent, although a compositional banding is defined locally by quartz-rich and pelitic layers. The rocks are equigranular and relatively coarse-grained hornfelses in which individual grains are up to 1 mm across. The quartz is granoblastic and 120°-triple junctions are commonly developed. One sample contains coarse andalusite, biotite, primary muscovite and has approximately 20 modal percent K-feldspar, some of which is microcline. Graphic intergrowths of quartz amd plagioclase occur rarely in the rock, adjacent to granoblastic K-feldspar. In places, andalusite is preserved as small relics within sericite pseudomorphs. Some of the white mica is fine grained and plumose in the matrix and also forms coarser grained porphyroblasts up to 1 mm across, which contain inclusions of biotite. These rocks are hornfelses related to the intrusion of the Deadman's Bay Granite.

STRUCTURAL SYNOPSIS

In the Weir's Pond area, rocks of the Gander River Complex and the Davidsville Group contain one main foliation axial planar to tight folds, which occur locally. Rocks of the Gander Group exhibit the effects of two main phases of deformation (D_2 and D_3) and a cryptic foliation (S_1), which may or may may not be related to a phase of deformation. The principal foliation, S_2, in the Gander Group is axial planar to isoclinal folds and strikes north to north-northeast, whereas the main foliation in the Davidsville Group and Gander River Complex, strikes northeast. This obliquity in structural trends is paralleled by two positive aeromagnetic anomaly belts, one produced by the Gander River Complex and the second, in the middle of the Gander Group, termed the Ocean Pond anomaly belt (Miller and Weir, 1982). These two belts appear to intersect in the Carmanville map area, northeast of Weir's Pond, a location where the Gander River Complex is absent. The parallelism of the Ocean Pond anomaly belt and the principal foliation, S_2, in the Gander Group, suggest that the origin of these two features is linked. A second, subparallel negative aeromagnetic anomaly belt is coincident with positive residual gravity anomalies and was termed the Indian Bay Big Pond thrust belt by Miller (1988).

A positive magnetic belt immediately to the east of the low is similar in intensity to that produced by the Gander River Complex and is coincident with gabbroic intrusions on the surface and the Wing Pond shear zone. The Ocean Pond anomaly belt was modelled by Miller (1988) (also using gravity data) as being produced by near-surface granitic rocks underlain by a mafic to ultramafic block. Although the intensity of the Ocean Pond anomaly belt is lower than that of the Gander River Complex, the presence of an exposed sliver of ultramafic and gabbroic rock (Unit 17, *this report*) coincident with the eastern edge of the anomaly, apparently lends support to Miller's (1988) theory that the anomaly partly represents ultramafic rock. Miller (1988) concluded that the Indian Bay Big Pond thrust belt (initially suggested by Wonderley and Neuman (1984)) contained the easternmost occurrence of Dunnage Zone mafic and ultramafic rocks.

The method of emplacement of the inferred mafic–ultramafic blocks is unclear, although Miller (1988) concluded that they represent thrust sheets in which Gander River Complex type rocks had been emplaced into the Gander Zone. The presence of the blocks has important implications for the allochthonous or autochthonous nature of the Gander Group. Fryer *et al.* (1989) have shown that granitoid rocks of the Gander and eastern Dunnage zones are derived from rocks that have identical isotopic characteristics to the Hare Bay Gneiss in the eastern Gander Zone. They concluded that there is no evidence of any mafic–ultramafic component in the source rocks of the granitoids of the northeastern Gander Zone. This suggests that the ultramafic rocks are not indicative of basement to the Gander Group, or at least basement to the eastern Gander Zone. If these ultramafic rocks were confined to the western side of the Gander Zone, then isotopic characteristics of granitoid rocks of the eastern Gander Zone would not reflect an ultramafic component.

If the anomaly belts are reflecting mafic–ultramafic rocks, then, they must have been emplaced tectonically. This conclusion is indirectly supported by the absence of metamorphic effects in the surface rocks, which might be related to a north-northeast-striking thermal high, i.e., associated with a hot igneous intrusion. Since the evidence presented in this report indicates that major deformation occurred prior to granite petrogenesis, and since any tectonic emplacement of mafic–ultramafic rocks would probably involve major deformation, this implies that the mafic–ultramafic rocks were emplaced prior to the metamorphism and generation of granites. The parallelism of the north-northeast S_2 structural grain and the north-northeast strike of the anomaly belt supports emplacement in the Gander Group during D_2.

Plutons such as the Deadman's Bay and Ocean Pond granites do not contain ultramafic xenoliths or other evidence that they rose through ultramafic rocks or were formed by melting of source rocks, which included ultramafic rocks. However, Miller (1988) pointed out that there are cobalt and nickel anomalies (in lake sediments) along the western margin of the extension of the Indian Bay Big Pond thrust belt through the Deadmans Bay Granite. Similarly, evidence for involvement of ultramafic rocks in the genesis of the Gander Lake Granite has not been documented, even though this granite lies directly on the Ocean Pond anomaly belt. Colour-shaded relief maps of the aeromagnetic data (G. Kilfoil, personal communication, 1989) show that the anomalies associated with the Ocean Pond plutons lie off the main trend of the positive aeromagnetic anomaly. Also, the occurrence of ultramafic rocks along these belts tends to be discontinuous. Thus, the granites now exposed may not have risen through ultramafic rocks. Indeed, the presence of tourmaline-bearing pegmatitic patches in the gabbroic part of Unit 17 suggests involvement of sialic crust in its origin. The absence of evidence for the ultramafic rocks in the Ocean Pond Granite in the form of xenoliths, suggests the aeromagnetic anomaly is due to some non-mafic source, for instance magnetite-rich sedimentary horizons in the Gander Group (or its basement) or magnetite-rich granite.

The presence of two tectonically emplaced ultramafic blocks in the Gander Group suggests the Gander Group may have been deposited close to a continent-ocean interface and become tectonically imbricated with slices of the ocean floor during closure of Iapetus. In such a model, the Gander Group could remain close to its original depositional setting. However, the postulated existence of these two mafic–ultramafic anomaly belts and the presence of Unit 17 is difficult to reconcile with an autochthonous Gander Group, and it seems more reasonable to suggest that the Gander Group is allochthonous.

Structural features of the Gander Group contrast with those of the Gander River Complex–Davidsville Group and imply a longer, more protracted deformational history in the former. The non-parallelism of major structural and aeromagnetic trends in the rocks east and west of Weir's Pond, substantiates this dichotomy in the deformational history.

One of the characteristic features of the relationship between the Gander River Complex and the Davidsville Group is their complex structural imbrication. This contrasts with the Jonathan's Pond Formation, which, in the map area at least, is not structurally imbricated with either the Davidsville Group or the Gander River Complex (there are interbedded black shales and grey-green sandstones in the western part of the Jonathan's Pond Formation, but these are interpreted to be part of that formation). The inference from this observation is that major structural imbrication of the Davidsville Group and Gander River Complex, occurred prior to their juxtapositioning with the Gander Group. This is a reasonable inference, since the absence of detritus from the Gander River Complex, in the Gander Group (specifically the Indian Bay Big Pond Formation, which is tentatively placed at the top of the Gander Group) indicates that the two were not adjacent. Therefore, early deformation resulting in the exhumation of the Gander River Complex and its imbrication with the Davidsville Group need not have affected the Gander Group. Juxtapositioning of the Gander Group with rocks to the west may have occurred by transcurrent motion along the strike of the Gander River Complex. A northeast-striking, locally developed high-strain fabric in the Weir's

Pond area suggests transcurrent motion and is supported by the work of Piasecki (1988) who concluded that Dunnage Zone rocks moved over the Gander Zone in a southwesterly direction. Other shear zones described in the Weir's Pond map area (e.g., the Wing Pond shear zone) may have developed contemporaneously. Therefore, shear zones described in this report, and also that by Piasecki (1988) and by Hanmer (1981) may all be correlative structures. Hanmer (1981) described these shear zones as Acadian in age.

The structural incorporation of the ultramafic–mafic blocks in the Gander Zone may have occurred contemporaneously with juxtapositioning of the Gander Group and Gander River Complex as implied by Miller (1988) during the principal deformation (D_2) of the Gander Group. However, the obliquity of the structural and aeromagnetic trends described above, need to be reconciled to this interpretation.

The D_2 deformation produced isoclinal folds, recumbent in structural flat belts and reclined in structural steep belts. Near Harveys Pond, these fold axes plunge moderately westward and are parallel to stretching lineations, which were observed in the same area. McGonigal (1973) concluded on the basis of his work near Gander Lake that these F_2 folds were overturned to the southeast on a macroscopic scale, suggesting tectonic transport in this direction, which agrees with the stretching lineations in the Harvey's Pond area.

METAMORPHIC HISTORY

METAMORPHISM OF THE GANDER RIVER COMPLEX

Ultramafic rocks exhibit the effects of a very heterogeneous low-grade metamorphism. Most of the partially metamorphosed ultramafic rocks contain relict igneous mineralogy, typically clinopyroxene and an alteration assemblage, which consists predominantly of antigorite, magnetite and, in some samples, minor talc. In most ultramafic rocks that are completely altered, the metamorphic assemblage consists of variable proportions of antigorite, talc, magnesite, ± dolomite, quartz and magnetite. These general observations suggest that the alteration process involved hydration locally, producing serpentine mostly, whereas elsewhere the fluid contained H_2O and CO_2, producing magnesite- (± dolomite-) bearing assemblages. The common observation that antigorite is replaced by carbonate (in intensely altered rocks) indicates that these processes were sequential, at least in some rocks.

The most common mineral parageneses, which generally appear to be in equilibrium are (dolomite may also be be present in assemblages containing magnesite)

Antigorite–Talc–Magnesite
Antigorite–Magnesite

Sample # 86-77 for example, contains antigorite, magnesite, talc and disseminated magnetite xenomorphs as well as relict chromite anhedra. Antigorite and magnesite are in approximately equal modal proportions, whereas talc forms less than 10 modal percent of the rock. The magnesite occurs both in intersecting veins and as aggregates of xenomorphic crystals, which have replaced antigorite. Carbonate grain boundaries in contact with antigorite are generally sharp. Small patches of talc are widespread and have also replaced antigorite. Locally, where magnesite and talc are in contact, the magnesite has sharp grain boundaries.

Other less commonly occurring assemblages are

Magnesite–Talc–Quartz
Antigorite–Talc
Magnesite–Talc
Magnesite–Quartz

Descriptions of the three-phase assemblage, magnesite, talc and quartz as they occur in sample #'s 86-114 and 86-266 serve to illustrate some variation in equilibrium relations between these minerals. In sample # 86-114, magnesite occurs as a coarse-grained granular mosaic and forms approximately 70 modal percent of the rock. Quartz and talc form irregular patches within the magnesite mosaic and talc is subordinate in modal proportions. Some quartz xenomorphs are clouded with a fine opaque dust. In places, the quartz is polygonal and displays 120° triple junctions. Commonly, talc forms a narrow rim between the carbonate and quartz where quartz is not rimmed by opaque, and locally, magnesite inclusions in quartz are completely rimmed by talc. In sample # 86-266, talc and carbonate occur in approximately equal modal proportions, whereas quartz forms less than 10 modal percent of the rock. All three minerals are in mutual contact, however, in contrast to sample # 86-114, the carbonate and quartz are not reacting to form talc.

Some possible reactions occurring in the ultramafic rocks, which are indicated by the equilibrium assemblages, are illustrated in Figure 48. The assemblage serpentine–talc–carbonate, in which serpentine is commonly partially replaced by talc and carbonate, and the sub-assemblage talc–carbonate, suggest that the reaction

$$2\ \text{Serpentine} + 3\ CO_2 = 1\ \text{Talc} + 3\ \text{Magnesite} + 3\ H_2O \ldots\ldots 1$$

(Winkler, 1979)

has taken place. This reaction constrains the metamorphic temperatures to between 310°C and 500°C and indicates relatively low values of XCO_2 (5 mol percent or less, from Figure 11-2, page 157, Winkler 1979).

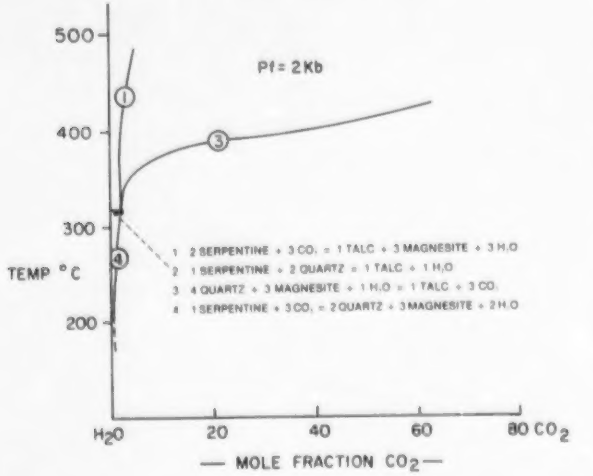

Figure 48. *Isobaric equilibrium curves of reactions relevant to the metamorphic mineral assemblages in the Gander River Complex; (part reproduction of Figure 11-2, page 157 in Winkler, 1979).*

The subassemblage talc + serpentine suggests that the reaction

Serpentine + 2 Quartz = 1 Talc + 1 H_2O 2
(Winkler, 1979)

may have occurred and that the quartz has been consumed. The assemblage talc + magnesite + quartz in some samples suggests that the reaction

4 Quartz + 3 Magnesite + 1 H_2O = 1 Talc + 3 CO_2 3
(Winkler, 1979)

may have been operative. In one sample (86-114) the common occurrence of talc between quartz and magnesite suggests that this reaction has occurred, however, in several other samples with this assemblage, textural relationships do not support operation of the reaction.

The assemblage magnesite and quartz suggests that that reaction

1 Serpentine + 3 CO_2 = 2 Quartz + 3 Magnesite + 2 H_2O 4
(Winkler, 1979)

may have occurred.

Reactions 1, 2, 3 and 4 are plotted on a T−X diagram for Pfluid (= Plithostatic) = 2 kbars (from Winkler, 1979). The presence of antigorite in some samples, magnesite in others (with antigorite absent) and the replacement of antigorite by magnesite implies that XCO_2 in the fluid phase was not constant either spatially or temporally.

Winkler (1979) notes that quartz, which occurs in several assemblages, is only to be expected at temperatures lower than that at which reaction 2 takes place (320°C from Figure 1, Winkler, 1979). However, the assemblage antigorite + quartz was not observed, suggesting that the T-X conditions for this reaction have been exceeded.

The ambivalent nature of the reactions above, as regards to constraining T-X conditions, may reflect the variation in composition of the fluids as implied by the varied nature of the assemblages produced by these fluids. However, the absence of the assemblage serpentine + quartz suggests that temperatures were above the invariant point of reactions 1, 2, 3 and 4, which occurs at approximately 320°C for Pfluid = 2 kbars and XCO_2 less than 5 mol percent. The absence of forsterite from the assemblages implies that temperatures were not very close to the high end of the range (320° to 500°C approximately) where this mineral is stabilized at low XCO_2 (Winkler, 1979).

Gabbros, diabase dykes and mafic volcanic rocks also contain low-grade (greenschist) alteration assemblages, consisting of actinolite ± clinozoisite ± epidote ± chlorite ± calcite ± sphene. Clinozoisite is defined by Winkler (1979) as diagnostic of this metamorphic grade. Prehnite occurs predominantly in veins, associated with calcite and locally clinozoisite, suggesting very low-grade metamorphic conditions. The alteration assemblages noted in trondhjemites are chlorite−albite ± actinolite ± sphene ± calcite ± epidote and are low grade.

The similar metamorphic grade of rocks in the Gander River Complex suggests that they were affected by a very heterogeneous low-grade, greenschist-facies metamorphism.

METAMORPHISM OF THE DAVIDSVILLE GROUP

Limited metamorphic effects are observed in the rocks of the Davidsville Group. In many samples, the matrix is extremely fine grained and has undergone little if any recrystallization. However, in some of the more highly deformed rocks, the pelitic matrix has recrystallized to sericite and fine-grained chlorite; neocrystallized coarser grained white mica occurs locally. In a later section (Ar−Ar Geochronology), an Ar−Ar cooling age on detrital muscovite from a sedimentary sample from the Davidsville Group, suggests some resetting and the attainment, therefore, of metamorphic temperatures possibly of the order of 300 to 350°C.

METAMORPHISM OF THE JONATHAN'S POND FORMATION, GANDER GROUP

The field observations presented in this section mostly pertain to that part of the Jonathan's Pond Formation at biotite grade or higher. For the purposes of describing the variable metamorphic assemblages and textures, three areas are defined (Figure 3), viz. Ocean Pond, Moccasin Pond and Wing Pond and treated separately. The chlorite zone lies outside of the areas specified above.

Chlorite Zone

In the chlorite zone, chlorite occurs in all rock types but is most abundant in the pelitic and semipelitic rocks. Chlorite porphyroblasts up to 2 mm across, occur locally. The most common metamorphic assemblage is chlorite and fine-grained white mica. The rocks are fine grained and typically have a sericitic sheen.

Ocean Pond Area

Psammitic, Semipelitic and Pelitic Rocks

Flecks of biotite, 1 mm across, become abundant in pelite and semipelite, in the lower grade parts of the biotite zone and increase in size from 4 to 5 mm across at higher grades. In more schistose rocks, the biotite forms seams that locally intersect; the seams are approximately 4 mm wide and are oblique to the main foliation. Biotite grains typically display a random pattern of distribution relative to the main penetrative foliation.

Garnets are typically red to brownish red and occur commonly southwest and northeast of Ocean Pond. However, southeastward, between Ocean Pond and Moccasin Pond, only three occurrences of garnet were observed. Generally, the mineral does not form more than 10 percent of the rock, in contrast to biotite, which may form 50 percent. Idiomorphic garnet crystals range up to 5 mm across. Throughout all of the biotite zone and much of the garnet zone, the pelitic and semipelitic rocks display a sericitic sheen and are phyllitic near the higher grade side of the garnet zone.

Although the andalusite isograd was mapped on the lower grade side of staurolite, andalusite partially encloses staurolite in places. Andalusite occurs as pink or pinkish-grey prismatic crystals, which are 4 cm or less in pelites and schists, but 6 cm or less where associated with vein quartz. The crystals are randomly oriented and form up to 50 percent of the rock. Biotite, muscovite and quartz are typically associated with andalusite, whereas garnet and staurolite occur locally. In the andalusite zone and especially the sillimanite zone, the pelitic rocks become coarsely schistose around and northeast of Ocean Pond.

Staurolite has a very restricted occurrence, principally around Ocean Pond and does not occur south of Whitney Pond. It is commonly associated with andalusite and forms dark, honey-brown, euhedral to subhedral crystals up to 2 cm across. They grow in generally random orientation and rarely form more than 15 percent of the rock. In all but one occurrence (south of Ocean Pond, cf., Map 90-04), staurolite is associated with garnet and andalusite (quartz, biotite and muscovite are ubiquitous). Staurolite was not found in association with sillimanite–fibrolite.

Four to five km east of Ocean and Little Ocean ponds, sillimanite occurs as small, grey bladed crystals, < 2 mm long, in pelitic to semipelitic schists. Adjacent to the Deadman's Bay Granite, sillimanite is bluish grey and fibrolitic knots, 4 to 8 mm across, form 50 to 70 percent of some schists. The schists are characteristically rugged weathering, as the sillimanite knots stand out in sharp, positive relief. Andalusite coexists with sillimanite in a transition zone that is normally several hundred metres wide, but which extends up to 1.5 km wide locally (cf., Map 90-04). In the western part of the sillimanite zone, fibrolite–sillimanite knots completely or partially envelope andalusite. Andalusite is absent north of Ten Mile Pond within 2 to 3 km of the Deadman's Bay Granite, but west of and south of the north arm of the pond, sillimanite and andalusite coexist up to the margin of the granite. Sillimanite-bearing rocks in the northeast, within 3 km of the Deadman's Bay Granite, are characterized by coarse porphyroblastic muscovite. Tectonic fabrics are only vaguely defined or are totally absent and these rocks appear to have been statically recrystallized. The sillimanite zone narrows and is pinched out southward by the Deadman's Bay Granite.

A profuse network of quartz veins cuts some sillimanite-bearing rocks, near the Deadman's Bay Granite and results in chaotic-looking exposures (Plate 39). The quartz veins are normally no more than 10 cm thick and have haloes of silicified country rock; both veins and haloes weather positively. Some of these quartz veins appear to initiate locally in quartzitic layers. Within the same exposures, thin, incompetent sillimanite schist layers intercalated with psammitic beds are locally disrupted. The isolated, sillimanite-rich pods, which have relatively soft, negatively weathering rinds, stand out in positive relief (Plate 40).

Irregular, unfoliated, concordant pegmatitic pods and veins occur in semipelitic and pelitic layers but do not form more than 10 percent of the rock in the sillimanite zone. Some of these pegmatitic bodies have narrow biotite-rich selvedges and may represent partial melt products. Quartz–feldspar segregations, 1 to 10 cm thick, are generally coarse grained in the centre and finer grained toward the margins where they appear to grade into the host. Localized segregation of biotite-rich and quartzofeldspathic layers produce an incipient gneissic banding.

Calc-Silicate-Rich Rocks

The concentric colour zoning of calc-silicate layers and lenses is very distinctive at garnet and higher grades (Plate 41). The central part of the lens is light-coloured, comprising quartz, feldspar, epidote and garnet. The outer part of the lenses are actinolite- or hornblende-rich. The garnets range up to 4 mm across and amphiboles are approximately 6 mm or less. At sillimanite grade, calc-silicate lenses are, generally, more melanocratic due to an increase in amphibole component. It was not possible in the field to map out isograds based on calc-silicate index minerals.

Plate 39. *Random network of thin quartz veins that crisscross exposures of the sillimanite zone (Jonathan's Pond Formation) close to the Deadman's Bay Granite, west and north of Ten Mile pond.*

Plate 40. *Disaggregated, sillimanite-rich pelitic layers within quartz-veined psammitic 'matrix', northwest of Ten Mile Pond, Jonathan's Pond Formation.*

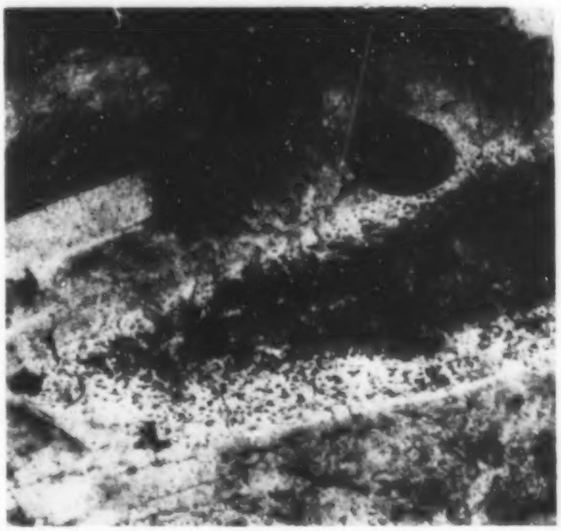

Plate 41. *Part of a calc-silicate lens in the Ocean Pond area, Jonathan's Pond Formation.*

Mafic Intrusive Bodies

In biotite and higher grade areas, mafic bodies are very dark-green to black, medium- to coarse-grained amphibolites.

Moccasin Pond Area

West of Moccasin Pond, pelite and semipelite are nonschistose within approximately 1 km of the Deadman's Bay Granite. White-weathering porphyroblasts of a dark mineral, possibly cordierite, 2 to 5 mm across, grow randomly and profusely in pelitic rocks south of Whitney Pond, and locally produce spotted pelites. The matrix to the porphyroblasts is typically very fine-grained mica. Exposures are not as good in this area as farther northwest and mineral isograds are not as well-defined.

Wing Pond Area

A sharp increase in metamorphic grade occurs in the vicinity of Wing Pond. In the lower grade parts, the rocks are coarse grained, muscovite-rich and schistose. Identification of both biotite and garnet zones is based on rare occurrences of these minerals. Andalusite crystals, several centimetres long, occur in several exposures close to Wing Pond. Coarse-grained kyanite was noted in one exposure on the northern side of the pond. Eastward from Southern Pond, most of the exposures within this zone are predominantly grey-green pelite and semipelite. Conformable granitic bodies occur in some schist exposures on the shores of Wing Pond and are spatially related to this higher grade metamorphism. They are 1 m or less thick and contain an intense, high-strain foliation.

METAMORPHISM OF THE INDIAN BAY BIG POND FORMATION, GANDER GROUP

The following description applies to those rocks in the northern part of the Indian Bay Big Pond Formation, in the Big Bear Cove Pond area. Biotite, garnet, andalusite and cordierite isograds are defined and roughly parallel the margin of the Deadman's Bay Granite. This area is distinguished from the other areas to the northwest by the absence of sillimanite.

Biotite Zone

In the biotite zone, biotite is generally fine grained, ranging up to approximately 0.5 mm across. In semipelitic rocks, the biotite forms felted masses restricted to pelitic layers, whereas in psammitic rocks, it is widely disseminated in trace amounts. Fine-grained muscovite and quartz are ubiquitous.

Garnet Zone

Garnet occurs locally in this zone as idiomorphic crystals up to 0.5 mm across. The typical assemblage is garnet, biotite, muscovite and quartz. As in the Moccasin Pond area, grey porphyroblasts, up to 4 mm across, are present in both the biotite and garnet zones. It is not clear what these minerals are, but both andalusite and cordierite are possible candidates.

Andalusite Zone

Andalusite occurs in four localities in the andalusite zone, invariably coexisting with biotite, but with garnet also in two samples; muscovite and quartz are ubiquitous. Andalusite is profuse in places and crystals range up to 3 cm but are typically less than 1 cm. Some samples are rich in tourmaline.

A calc-silicate-rich rock sampled in this zone contained the assemblage epidote, actinolite and hornblende.

Cordierite Zone

Cordierite occurs in four samples from this zone. All samples contain biotite, muscovite and quartz. Andalusite is present in two samples and andalusite and garnet are present in one sample. The complete assemblage in the latter sample is cordierite–andalusite–garnet–biotite.

METAMORPHIC ASSEMBLAGES AND REACTIONS IN THE GANDER GROUP

General Description

Although metamorphic conditions vary between the Ocean Pond, Moccasin Pond, Big Bear Cove Pond and Wing Pond areas, the assemblages in the chlorite, biotite and garnet zones are similar in all areas and are discussed first and then the higher grade parts of the various areas are treated separately. The ubiquitous assemblage in the chlorite zone, consists of chlorite, muscovite and quartz. Chlorite occurs in several modes, as a very fine-grained fabric-forming mineral, as porphyroblasts containing abundant opaque inclusions, and as vein-forming material along with quartz. At the biotite isograd, possible biotite-forming reactions include

Phengite + Chlorite = Biotite + Al-richer Chlorite + Quartz..............................5
(Turner, 1948)

Phengite + Al-poor Chlorite = Muscovite + Al-richer Chlorite + Biotite + Quartz + H_2O..6
(Kamineni and Carrara, 1973)

Chlorite + K-Feldspar = Biotite + Muscovite + Quartz + H_2O..............................7
(Thompson and Norton, 1968)

The ubiquitous assemblage in the biotite zone, is biotite–muscovite–chlorite–quartz + plagioclase. Fine-grained garnet crystals, which occur as inclusions in biotite porphyroblasts in the biotite zone, are likely to be Mn-rich and to have formed at low temperatures and pressures (Winkler, 1979).

Thompson and Norton (1968) suggest the following reaction to produce garnet

Chlorite + Muscovite + Quartz = Almandine + Biotite + H_2O..............................8

Another reaction, (See Winkler, 1979, page 221) has also been proposed to account for the source of the Ca in garnet

Chlorite + An component of Oligoclase = Almandine + Al-richer Chlorite + Quartz + H_2O...9

Epidote is common in rocks of the Gander Group and may promote the following reaction

Chlorite + Muscovite + Epidote = Almandine + Biotite + H_2O..............................10
(See Winkler, 1979, page 220)

The most common assemblage in the garnet zone is garnet–biotite–chlorite–muscovite–quartz ± plagioclase. Coarse-grained garnet is common in the Ocean Pond area but farther south near Moccasin Pond and Big Bear Cove Pond, garnet grains are very small or absent.

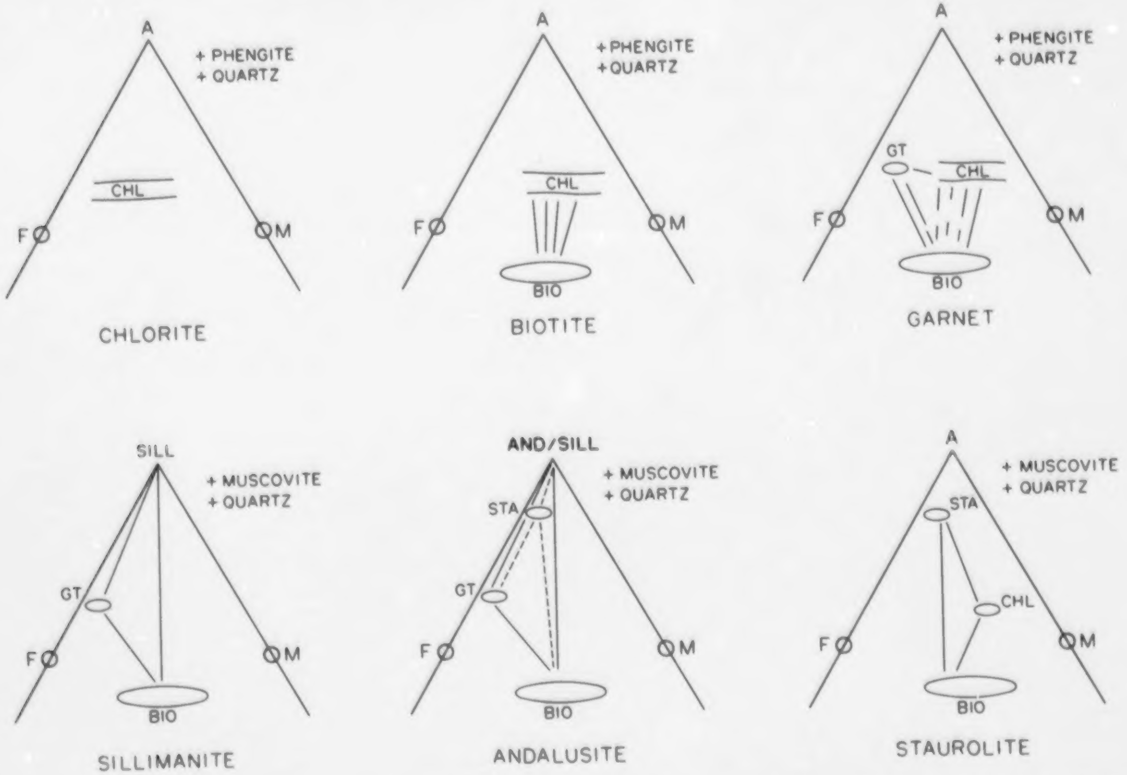

Figure 49. *Schematic AFM diagrams (from Winkler, 1979) depicting the mineral assemblages in the Ocean Pond area, Jonathan's Pond Formation. Prograde reactions that occurred in the study area may not necessarily have involved the exact assemblages shown here. BIO–Biotite, CHL–Chlorite, GT–Garnet, SILL–Sillimanite, STA–Staurolite, AND–Andalusite.*

Ocean Pond Area

The first appearance of staurolite and andalusite appear to be approximately coincident in the field. However, staurolite mostly occurs as inclusions in andalusite. In one instance, 1 km southwest of Ocean Pond, staurolite coexists with biotite and chlorite and andalusite is absent. This assemblage is shown schematically in Figure 49, but it is not clear if it represents the stable equilibrium assemblage of the staurolite zone. The appearance of staurolite is diagnostic of the transition from greenschist- to amphibolite-facies metamorphism (Winkler, 1979). Possible staurolite-producing reactions include

Chlorite + Muscovite = Staurolite + Biotite +
Quartz + H_2O.................................. 11
(Hoschek, 1969)

Chlorite + Muscovite + Almandine = Staurolite
+ Biotite + Quartz + H_2O.................. 12
(See Winkler, 1979, page 223)

Reaction 11 is more likely as garnet is absent from the assemblage observed. Winkler (1979) points out that chlorite–muscovite–staurolite coexist within a narrow temperature range close to the transition between amphibolite- and greenschist-facies metamorphism and that the paragenesis is diagnostic of a low-temperature zone within the medium-grade zone of metamorphism. Reaction 11 takes place at 520° ± 10°C at 2 kb H_2O pressure and 540° ± 15°C at 4 Kb H_2O pressure (Hoschek, 1969).

Immediately east of the staurolite isograd, andalusite first appears. Close to the staurolite zone, all of the andalusite-bearing assemblages also contain garnet, biotite and staurolite. Chlorite is present in many of the samples, predominantly as a retrogression product of biotite, but some of it appears to be primary. In these low-variance assemblages, the occurrence of staurolite as inclusions in andalusite indicates that staurolite is a metastable phase.

One possible reaction that may have occurred at the staurolite–andalusite boundary is

Mg-rich Chlorite + Staurolite + Muscovite +
Quartz = Biotite + Andalusite + H_2O..... 13
(Thompson and Norton, 1968)

This accords with the petrographic observation of andalusite coexisting with abundant biotite and staurolite relicts in andalusite. In the andalusite zone, the assemblage andalusite–biotite–garnet (Figure 49) is one of the commonest and suggests that the terminal discontinuous reaction

Staurolite + Muscovite + Quartz = Andalusite
+ Garnet + Biotite + H_2O.................. 14
(Thompson, 1976)

has occurred. The univariant curve for this reaction is shown on Figure 50. Since the reaction has occurred in the stability of andalusite, it implies that pressure is less than 3.1 Kb. Other possible reactions leading to the disappearance of staurolite are

Staurolite + Muscovite + Quartz = Al_2SiO_5 +
Biotite + H_2O.................................. 15
(Winkler, 1979)

Staurolite + Sodic Muscovite + Quartz =
Al_2SiO_5 + Biotite + K-richer Muscovite +
Albite + Almandine + H_2O................. 16
(See Winkler, 1979, page 228)

Since muscovite is present in all of the staurolite-bearing rocks, it is likely that one or all of these reactions were operative and that staurolite was 'reacted-out' of these rocks relatively early. However, close to the staurolite–andalusite zone boundary, on the higher temperature side, chlorite and staurolite appear to be relict phases and imply that the chlorite + staurolite consuming reaction (Reaction 13) has not gone to completion. Reaction 15 (curve 3 on Figure 50) has been investigated by Hoschek (1969) who showed that it occurs at 575° ± 15°C at 2 kbar H_2O pressure and 675° ± 15°C at 5.5 kbar H_2O pressure. On the high-temperature side of reaction 14, the assemblage staurolite–biotite–garnet can be stable, in the absence of muscovite, (Figure 14-9, page 226, Winkler, 1979) and one occurrence of this assemblage was noted in the andalusite zone northeast of Ocean Pond.

Near Ocean Pond, four samples were found containing the assemblage andalusite (with staurolite inclusions)–biotite–garnet–fibrolite–muscovite–quartz; the fibrolite rims had partially replaced the andalusite. An isolated occurrence of the same assemblage occurs near the south end of Little Ocean Pond. This paragenesis suggests that the rock records the P-T conditions at the point of intersection of curve 2 and the andalusite to sillimanite transition on Figure 50, i.e., approximately 550°C and 3.1 kbar. Electron microprobe analyses of the various phases are required to place better constraints on P-T conditions.

North of Ocean Pond, the andalusite zone is wide, up to 7 km, perhaps suggesting a shallowly dipping isograd. This contrasts with the narrow staurolite and andalusite zones around Ocean Pond, suggesting either variable P-T conditions or change in attitude of the geothermal gradient near the Ocean Pond Granite.

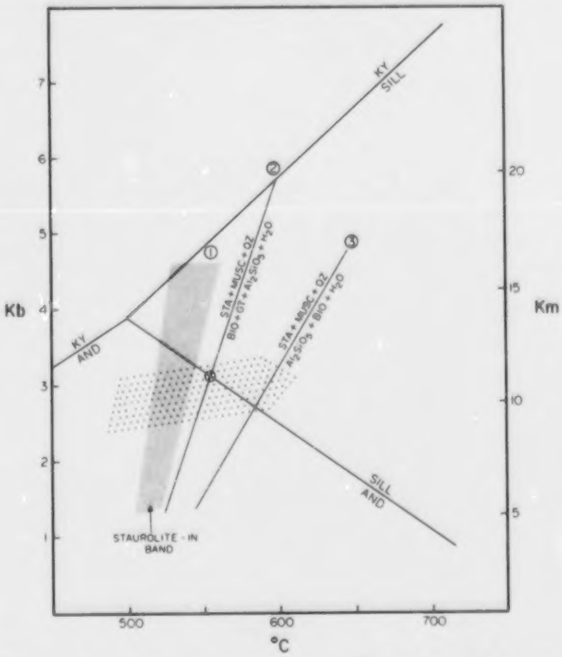

Figure 50. *Pressure–temperature grid inferred from mineral assemblages in the Ocean Pond area. Curve (1) staurolite-in-reaction band from Winkler (1979); Curve (2) staurolite breakdown in presence of muscovite and quartz; unpublished curve from Carmichael (personal communication to T. Rivers, 1990); Curve (3) from Hoschek (1969); Curve (4) from Winkler (1979). Stippled band represents a geothermal gradient of 100°C per km.*

The first occurrence of sillimanite defines the first sillimanite isograd and is usually defined by fibrolite. Fibrolite occurs near Ocean Pond and Little Ocean Pond and outlines localized metamorphic culminations, which appear to be separate from the main sillimanite zone west of Ten Mile Pond; the lack of continuity may be due to insufficient sampling in specific areas or to irregular (or folded) topography on the isograd surface.

Northwest of Ten Mile Pond, the most easterly of the rare staurolite occurrences is 3 km west of the andalusite to sillimanite transition. Fibrolitic sillimanite initially coexists with andalusite, in a zone up to 2 km wide, in the sillimanite zone. Studies by Kerrick and Speer (1988) have shown that minor-element partitioning, especially of Fe, between andalusite and sillimanite is an important factor in the bivariant behaviour and leads to a relatively wide zone of andalusite–sillimanite coexistence. The parageneses sillimanite–biotite, sillimanite–biotite–garnet, sillimanite–biotite–andalusite and sillimanite–andalusite–biotite–garnet are present. West and northwest of Ten Mile Pond, fibrolite is replaced by sillimanite. At one locality, north of Ten Mile Pond, a raft of metasedimentary rock, 1 km inside the Deadman's Bay Granite, contains the assemblage sillimanite–biotite.

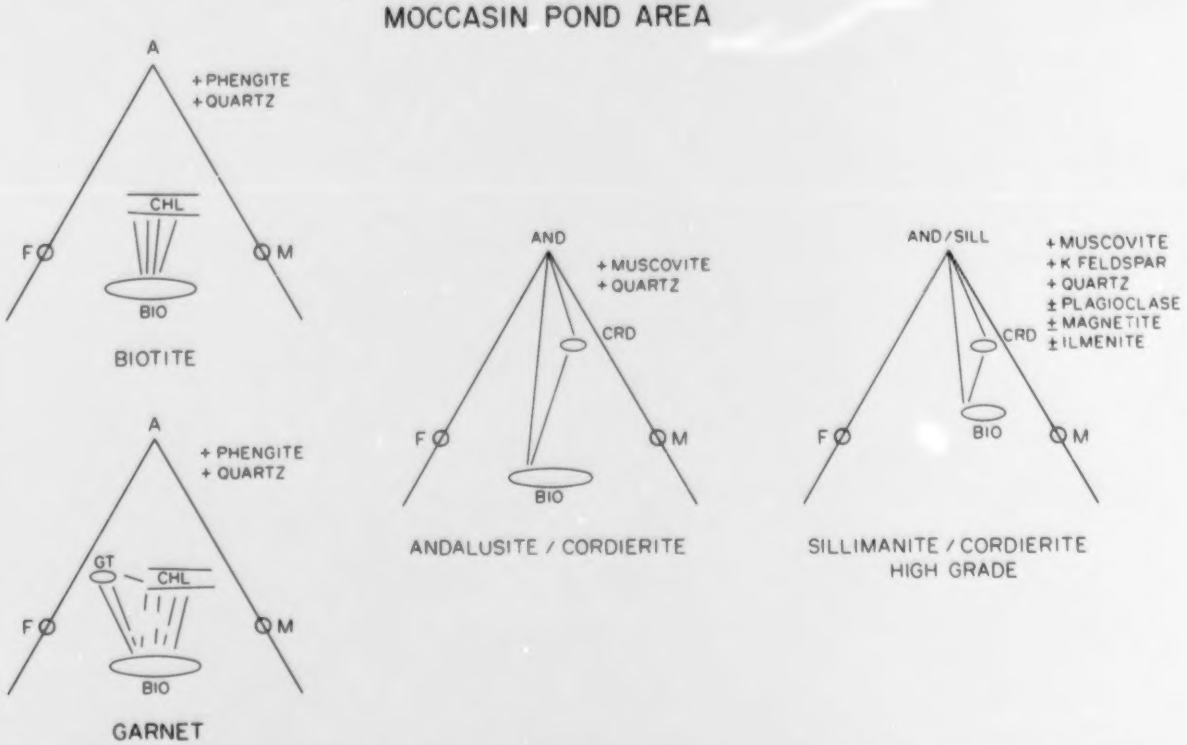

Figure 51. *Schematic AFM diagrams (Winkler, 1979) depicting the mineral assemblages west of Moccasin Pond, Gander Group.*

Moccasin Pond Area

Northwest of Moccasin Pond, the isograds swing from a northeasterly trend to a southward trend and parallel the margin of the Deadmans Bay Granite. Biotite, garnet, cordierite, andalusite and sillimanite isograds are defined west of Moccasin Pond. Relevant reactions have already been described for the lower grade parts.

Two occurrences of cordierite in the andalusite zone near Whitney Pond are recorded; the assemblage is cordierite–andalusite–biotite–muscovite–quartz (Figure 51). The most common reaction producing cordierite is interpreted to have been

Chlorite + Muscovite + Quartz = Cordierite + Biotite + Al_2SiO_5 + H_2O..................17

(curve 1 on Figure 52), which occurs at approximately 525° ± 10°C at 2 Kb H_2O pressure and 555° ± 10°C at 4 Kb H_2O pressure (See Winkler, 1979, page 77). Winkler (1979) points out that the staurolite- and cordierite-forming reactions take place at approximately the same P-T conditions and the cordierite isograd is shown on the low-temperature side of the andalusite isograd. Although cordierite–chlorite assemblages were not recorded, sericite pseudomorphs are common in rocks on the lower grade side of the cordierite zone and these may be after cordierite. Based on Reaction 12, cordierite and andalusite may appear simultaneously.

Fibrolite is the predominant form of sillimanite in the area. South of Moccasin Pond, the sillimanite isograd is intersected by the Deadmans Bay Granite. In the sillimanite zone, two samples contain the assemblage K-feldspar–biotite–cordierite–andalusite–fibrolite–muscovite–quartz (Figure 51). Although much of the muscovite appears primary, some grains are very resorbed and are probably unstable. The coexistence of K-feldspar and sillimanite is diagnostic of the second sillimanite isograd (Thompson and Norton, 1968) and marks the transition from medium- to high-grade metamorphism. The most likely K-feldspar-forming reactions include

Muscovite + Quartz = K-feldspar + Sillimanite + H_2O...18

(Curve 3 on Figure 52) (Winkler, 1979). This reaction occurs at 620° ± 10°C at 2 kbar and 655° ± 10° at 3 kbar and takes place at lower temperatures than anatexis, which is in agreement with the absence of melt in the rock. The persistence of biotite and muscovite up to the peak temperature zones implies that water activity was high.

In cordierite-bearing rocks, the following reaction is important

Muscovite + Biotite + Quartz = K-feldspar + Cordierite + H_2O................................19
(Winkler, 1979)

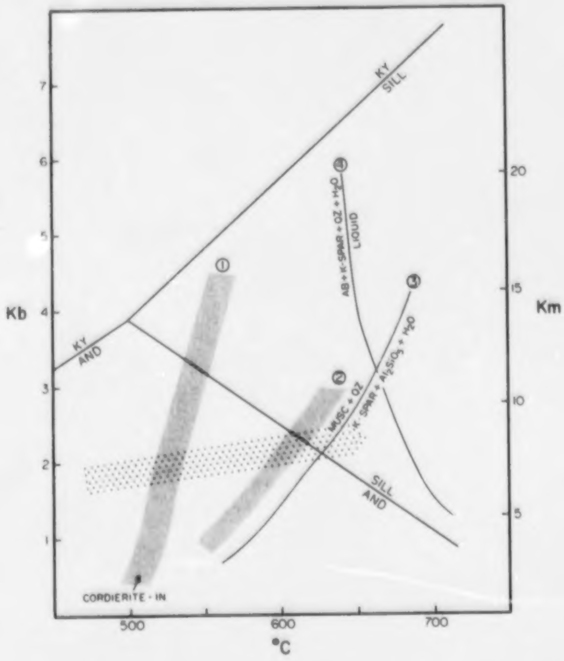

Figure 52. *Pressure–temperature grid inferred from mineral assemblages in the Moccasin Pond area. Curves 1 to 4 from Winkler (1979). Stippled band represents a geothermal gradient of 100°C per km.*

K-feldspar and cordierite commonly occur in apparently stable contact in two samples. Cordierite completely encloses andalusite in places and more rarely has inclusions of sillimanite; K-feldspar also contains sillimanite inclusions. Much of the biotite in contact with cordierite and K-feldspar appears stable. The combination of reactions 18 and 19 occurs at 600° ± 10°C at 2 kbar and 635° ± 10°C at 3 kbar (Winkler, 1979); P-T conditions for this combination are shown by the grey band (curve 2) on Figure 52.

In both samples, andalusite is partly replaced by fibrolitic sillimanite. The P-T conditions indicated by the assemblage are, therefore, closely constrained to the intersection points of curves 2 and 3 with the sillimanite to andalusite transition on Figure 52, which lies at approximately 625°C at 2 kbar. This implies that peak metamorphic conditions as recorded in this zone are approximately 1 kbar less than those defined for the Ocean Pond area; this pressure differential corresponds to a difference in depth of approximately 4 km. This difference is interpreted to result from the metamorphism around the Deadman's Bay Granite occurring at a shallower level in the crust than that in the Ocean Pond area.

Big Bear Cove Pond Area

In the Big Bear Cove Pond area, low-grade pelitic rocks contain similar mineralogy to that observed in the Ocean Pond area. Thus, biotite- and garnet-forming reactions probably involve the same reactants. Rocks downgrade from andalusite contain biotite–chlorite–muscovite suggesting the following reaction

Chlorite + Muscovite + Quartz = Andalusite
+ Biotite + H_2O..................................20
Thompson and Norton (1968)

The sub-assemblages in the andalusite zone are andalusite–biotite and andalusite–biotite–garnet. Andalusite locally encloses biotite and garnet. Chlorite is abundant in some sections but much if not all of it, is retrograde (from biotite).

Between Moccasin Pond and Big Bear Cove Pond, cordierite is apparently absent. South of Big Bear Cove Pond, the andalusite isograd occurs prior to (at lower T and P) than cordierite (Figure 53), apparently reversing the previous (interpreted) order of appearance of these two minerals. In the cordierite zone, four samples contain cordierite and the assemblages are, cordierite–biotite, cordierite–andalusite–biotite and cordierite–andalusite–biotite–garnet. Cordierite locally replaces biotite in biotite-rich layers. Primary chlorite was not seen. Equilibrium relationships between cordierite and andalusite are unknown since the two minerals are not seen in contact.

The assemblage cordierite–andalusite–biotite–garnet occurs in only one sample; none of the minerals are obviously in disequilibrium (although all phases were seen in contact with each other). Winkler (1979) notes that the assemblage cordierite–garnet–sillimanite–biotite–muscovite–quartz ± plagioclase is diagnostic of the cordierite–almandine zone of medium-grade metamorphism, which is a special high-temperature zone. However, he notes that andalusite may be the stable aluminosilicate polymorph and such an assemblage has been observed in the Abukuma region of Japan. This latter region was metamorphosed at approximate pressures of 3 Kb. Sillimanite does not occur in the Big Bear Cove Pond area and constrains the temperatures to less than 560°C at 3 kbar and less than 635°C at 2 kbar. More samples containing this assemblage need to be examined to study the phase relationships properly.

One kilometer west of Big Bear Cove Pond (within several hundred metres of the contact with the Deadman's Bay Granite) the assemblage andalusite–biotite–K-feldspar occurs. Primary muscovite is still present and suggests that P-T conditions are close to the univariant curve for reaction 13. Cordierite is absent (possibly because of bulk compositional constraints) and the andalusite–sillimanite transition has not been reached. The assemblage suggests that reaction 13 has occurred within the andalusite zone (indicating slightly lower pressure).

Aureole of the Deadman's Bay Granite

Textural considerations and the metamorphic mineral assemblages that are developed in the Moccasin Pond–Big

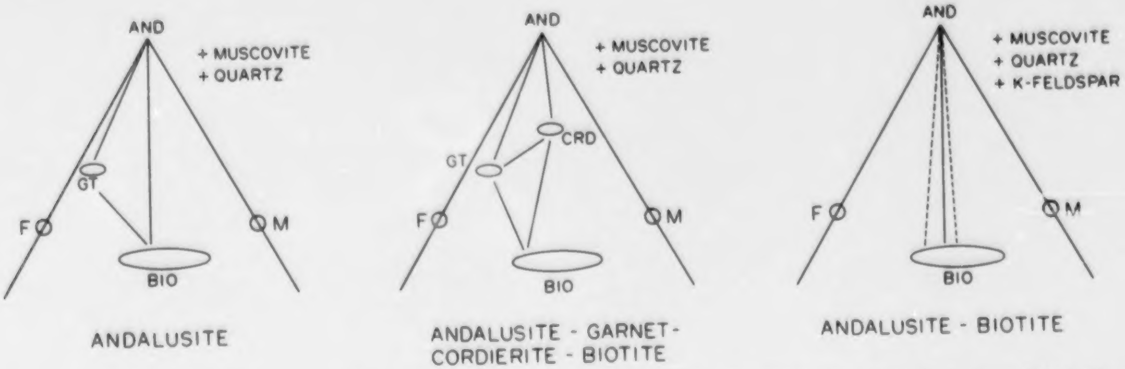

Figure 53. *Schematic AFM diagrams (Winkler, 1979) depicting mineral assemblages north of Big Bear Cove Pond, Gander Group.*

Bear Cove Pond area, suggest that the rocks record the thermal overprint of the Deadman's Bay Granite. The isograds are approximately parallel to the margin of the granite. The rocks are statically recrystallized, particularly close to the granite, whereas in the outer and middle parts of the aureole, some porphyroblasts of andalusite and cordierite form augen within a biotite–muscovite fabric that is heterogeneously developed. The deformation that caused formation of these augen may have been synchronous with granite intrusion, even though there is no tectonic foliation in the Deadman's Bay Granite. The temporal relationships between the development of this biotite fabric and the development of the high-strain fabric at Wing Pond are uncertain. Both may be related to the same deformational event.

At Moccasin Pond, the Deadman's Bay Granite intrudes across the trace of the sillimanite isograd. In the northeast, the sequential development of andalusite, fibrolite and coarse-grained sillimanite, contrasts with the absence of sillimanite of any kind in the Moccasin Pond–Big Bear Cove Pond area. It is significant also that the sillimanite zone broadens northward. The highest temperature assemblages (cordierite–fibrolite–K-feldspar) occur (immediately north of Moccasin Pond) approximately where the regional metamorphic assemblages overlap with the contact aureole assemblages. This area is also characterized by the textural change in the metasedimentary rocks, from coarse grained in the north to fine-grained in the south.

At Moccasin Pond and southeastward, typical contact metamorphic assemblages, containing andalusite and cordierite, are developed near the margin of the Deadmans Bay Granite. West and northwest of Ten Mile Pond, these assemblages are absent and sillimanite-zone rocks close to the contact with the granite are characterized by profuse growth of late muscovite porphyroblasts. The difference in behaviour of the country rocks may be attributable to the ambient temperatures at the time of granite intrusion. In the northwest, the country rocks were already regionally metamorphosed and were cooling, based on the Ar–Ar ages. Therefore, the difference between their temperature and the temperature of intrusion of the granite would have been considerably less than that farther south near Big Bear Cove Pond, where the country rocks record no evidence of regional metamorphism higher than chlorite grade. The pressure differential recorded by the contact and the regional metamorphic assemblages, therefore, suggests that the former occurred at a level approximately 4 km higher in the crust than that of the regional metamorphism. The absence of overprint relations in the Moccasin Pond–Big Bear Cove Pond area implies that these contact-metamorphosed rocks were never at depths greater than about 8 km. The 385 Ma age (U–Pb zircon) of the Deadman's Bay Granite indicates that it crystallized after the metasedimentary rocks and Ocean Pond granite had cooled through greenschist facies conditions. The Ar–Ar cooling age of 397 ± 5 Ma, for the sillimanite-zone sample # 87-839, collected several km from the northwestern margin of the granite, shows no apparent thermal resetting attributable to the Deadman's Bay Granite.

Wing Pond Area

Near Wing Pond, part of a northeast-trending metamorphic high has been mapped. The biotite zone is defined on the occurrence of one biotite-bearing sample and the garnet zone is based on three occurrences northwest of Wing Pond. Coarse- to medium-grained muscovite (the main fabric-forming mineral) characterizes all the rocks in the area. The distinctive assemblage recorded in 5 samples (collected on the shores of, or very close to Wing Pond) contains andalusite [staurolite–kyanite–sillimanite] ± garnet–biotite–muscovite–quartz ± plagioclase. Staurolite and kyanite occur almost exclusively as armoured relics within andalusite porphyroblasts. Sillimanite also occurs as inclusions in andalusite. Kyanite and sillimanite are commonly associated (where they form inclusions in andalusite) and sillimanite invariably replaces the kyanite. Many of the textural relationships between andalusite and sillimanite are equivocal with regards to which grew first; however, locally, andalusite clearly overprints a crenulation, which in places is defined by sillimanite, implying that the andalusite is later. The textural relationships suggest that the kyanite (+ staurolite) assemblage was overprinted by a sillimanite-bearing assemblage and that both were overprinted by andalusite. Little can be deduced about the reactions that produced these minerals. Based on the inclusions in andalusite, the assemblages were probably combinations of the following minerals, staurolite–kyanite ± garnet ± biotite–muscovite–quartz–plagioclase. The suggested order of growth of the aluminosilicate minerals is kyanite–sillimanite–andalusite, which implies a P-T loop similar to that shown schematically in Figure 54. Retrogression normally associated with shear-zone development (Beach, 1980) may have produced the syntectonic muscovite, now defining the high-strain foliation. The andalusite is partly replaced by this muscovite which exhibits evidence of coaxial deformation (discussed in the structure section). There is no evidence for partial melting in the rock and this helps to constrain the P-T conditions.

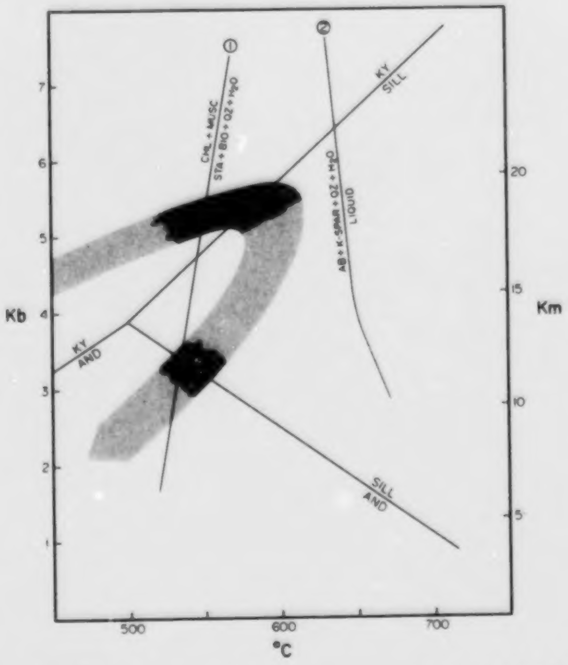

Figure 54. *Schematic pressure–temperature grid inferred from partial metamorphic assemblages in the Wing Pond area, Gander Group. The stippled band represents a possible P-T path followed by the rocks as suggested by the mineral assemblages.*

METAMORPHIC HISTORY

Although the S_1 and S_2 foliations throughout the Ocean Pond area are defined by fine-grained chlorite and muscovite and fine- to medium-grained muscovite respectively, the muscovite records an age that is the same as that of coarse-grained muscovite from the Ocean Pond Granite and the sillimanite zone. Therefore, the muscovite in the low-grade zones was recrystallized and its $^{40}Ar-^{39}Ar$ systematics were completely reset during the high T-low P regional metamorphic event. Therefore, although the D_1 and D_2 deformational events are older than the high T-low P metamorphism, as implied by andalusite and staurolite overprinting relationships, there is no record of their age in the Ar age spectra.

Microtextural relationships between biotite and the F_3 crenulation suggest that porphyroblastesis and D_3 deformation overlapped in time. At higher grades, staurolite and andalusite overprint F_3 microfolds. Therefore, the approximate age range of 400 to 390 Ma on muscovite and biotite, dates post-metamorphic cooling and suggests that the D_3 event occurred in Late Silurian–Early Devonian time. Although it is not known how long the rocks were maintained above the closure temperatures of muscovite and biotite, the fine grain size of the pelitic rocks suggests that it was for a relatively short period of time only. The similarity (within error) of the cooling ages of rocks within the biotite and sillimanite zones and granite and pegmatite indicate that rocks of different initial temperatures cooled through the closure temperatures at about the same time; this may indicate rapid uplift. Whether the cooling age approximates the age of metamorphism and the development of the D_3 deformation, must await further resolution by precise U–Pb dating.

As reference to Figure 36 will show, some of the muscovite and biotite samples were taken up to 20 km away from the Deadman's Bay Granite and, thus, are unlikely to have been affected by any localized thermal resetting due to this granite. This agrees with a U–Pb age of 385 Ma on the Deadman's Bay Granite, i.e., post-regional metamorphism. This U–Pb age also gives an independent minimum age on the D_2 event and regional metamorphism. The D_2 event is pre-regional metamorphism. Based on the work of Currie *et al.* (1979), the regional metamorphism continues northward and may cut across the Gander Group–Gander River Complex contact in the Carmanville area. Thus, tectonic juxtapositioning of these two units would have to have been completed by the Early Devonian.

The timing of development of the Wing Pond metamorphism and post-metamorphic development of the high-strain zone are unknown. The regional parallelism of the steep high-strain fabric with the S_2 foliations in the Gander Group suggests that the high-strain fabric developed (perhaps late) during D_2. If this is the case, then the kyanite–staurolite metamorphism is older than D_2 since the high-strain foliation overprints the metamorphic assemblage. If the high-strain foliation developed during D_2 then this metamorphism would have occurred prior to the high T-low P event in the Ocean Pond area. If the high-strain foliation is not a D_2 event, then the high T-low P and Wing Pond metamorphism may be approximately synchronous. This problem may be resolved by Ar–Ar dating of the syntectonic muscovite and biotite and U–Pb dating of the metamorphic zircon in the schistose and foliated granitoid rocks in the Wing Pond high-strain zone.

North of Ten Mile Pond, the absence of a distinct thermal overprint on the regional metamorphic assemblages (other than late porphyroblastic muscovite) suggests that these regionally metamorphosed rocks were still hot when intruded by the Deadman's Bay Granite (at 385 Ma). However, this appears to conflict with the conclusion above, that rocks in the sillimanite zone (3.5 km away from the Deadman's Bay Granite) cooled through greenschist-facies conditions at approximately 396 Ma. This discrepancy may be explained by combination of (?rapid) uplift associated with the intrusion of the granite and a very narrow thermal aureole around the granite.

Near Moccasin and Big Bear Cove ponds, syntectonic growth and formation of porphyroblast augen in the contact aureole suggest deformation coincident with intrusion. The foliation in the rocks is parallel to the regional S_2 foliation and also to the high-strain foliation, which heterogeneously affects the rocks in this area.

The Davidsville Group and the Gander River Complex have only been heterogeneously affected by low-grade metamorphism. Detrital muscovite in Early to Middle Ordovician sandstone has yielded a Siluro-Devonian Ar–Ar age, which suggests thermal resetting during this period. A small muscovite granite, which is interpreted to intrude the Davidsville Group (no contacts exposed), has a muscovite Ar–Ar age of 427 ± 7 Ma. The granite is undeformed, suggesting that major deformational events preceded its intrusion (because of the rheological contrast between the granite and the surrounding shales, however, the strain associated with deformational events after intrusion may have been preferentially partitioned into the shales).

LOW PRESSURE–HIGH TEMPERATURE METAMORPHISM

Several models have been proposed to explain thermal structures in low T-high P regional metamorphic belts, e.g., high-heat flow induced by large calc-alkaline intrusions in island arcs (Miyashiro, 1961), high-heat flow in areas of continental rifting (Wickham and Oxburgh, 1985), introduction at intermediate crustal levels of sheet-like igneous intrusions (Lux *et al.*, 1986), or large-scale transport of heat by fluids or melt generated in a shallow subduction zone in an ocean–continent convergence region (Sisson and Hollister, 1988). Another model (England and Thompson, 1984) based on large-scale crustal thickening and subsequent erosion, predicts that melting occurs in the lower crust as a result of crustal thickening and that P-T-t paths pass through the kyanite–sillimanite (initially) and then, andalusite fields during retrograde metamorphic conditions.

Voluminous granitoid bodies and metamorphic rocks characterize the northeastern Gander Zone. The present report does not intend to deal with the primary reasons for the development of the granitic rocks or their general relationship, whether causal or otherwise, to the metamorphic rocks. However, some conclusions based on the geology of the Weir's Pond area can be drawn, which may have regional applications.

Lux *et al.* (1986) proposed a model that attempts to explain one of the most commonly observed features in low P-high T metamorphic belts, the prograde andalusite to sillimanite transition. Based on studies of low P-high T metamorphism in New England, they suggested that granitoid magmas form in lower crustal regions characterized by normal mantle heat flow, and are emplaced as thin tabular plutons, at intermediate levels producing regional-type, contact aureoles with high T, low P metamorphic assemblages. Medium- to high-grade regional metamorphism, with maximum temperatures of 650°C and thermal gradients of 80 to 100°C km^{-1}, are predicted by their model, out to approximately 2 km from the granite sheet. Therefore, in this model, plutons were emplaced and the metamorphism is a secondary feature produced by them.

In the Ocean Pond area, although the granite bodies are only exposed in three localities near Ocean and Little Ocean ponds, several more granitic plutons have been modelled at shallow depths (J. Todd, personal communication, 1986) and the distribution of these plutons and their relationship to the isograds is shown in Figure 55. The Ocean Pond Granite is slightly discordant to the regional isograds so peak regional metamorphic conditions must have been attained prior to final emplacement of the granite. Localized cataclastic deformational features in the granite suggest it was partially solidified during intrusion. A poorly to moderately developed foliation in the granite indicates that its intrusion predated the end of regional deformation. The close spatial coincidence of the Ocean Pond Granite, and local metamorphic culminations in the Ocean Pond area, suggest a genetic relationship between the granite and the metamorphism. The plutons display a north–northeast elongation, which suggests that their emplacement was structurally controlled by the pre-existing D_2 structural grain. West of Ocean Pond, a sharp transition occurs, from biotite to sillimanite zones, across a 1.3 km width of metasedimentary rock. Since the metamorphism occurred after the D_2 event and the effects of the D_3 event are minimal, the thermal gradient across this narrow zone is of the order of 100°C km^{-1}.

A number of features of the geology of the northeastern Gander Zone are similar to those in low P, high T metamorphic belts of the New England states:

1) presence of peraluminous granite;

2) prograde andalusite to sillimanite metamorphism;

3) spatial association of the granite with the highest grade parts of the regional metamorphism;

4) absence of a distinct, narrow contact aureole immediately peripheral to exposures of the Ocean Pond Granite;

5) presence of regionally metamorphosed rocks up to 10 km from exposed granite; and

6) a thermal gradient of the order of 100°C/Km

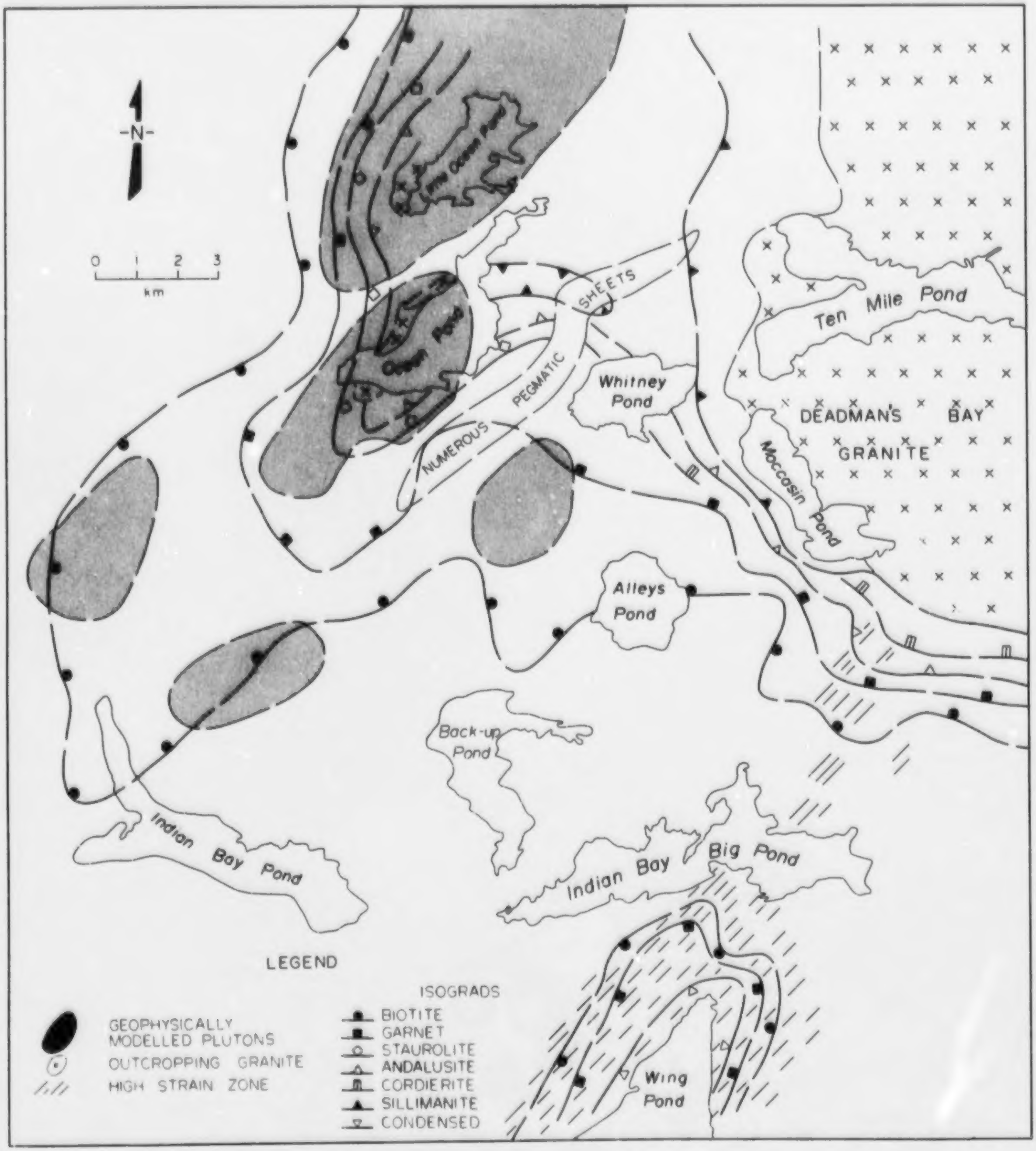
N
0 1 2 3
km
Ocean Pond
SHEETS
NUMEROUS
PEGMATIC
Whitney Pond
Ten Mile Pond
DEADMAN'S BAY GRANITE
Moccosin Pond
Alleys Pond
Back-up Pond
Indian Bay Pond
Indian Bay Big Pond
Wing Pond
LEGEND
GEOPHYSICALLY MODELLED PLUTONS
OUTCROPPING GRANITE
HIGH STRAIN ZONE
ISOGRADS
BIOTITE
GARNET
STAUROLITE
ANDALUSITE
CORDIERITE
SILLIMANITE
CONDENSED

Figure 55. *Geophysically modelled plutons (J. Todd, personal communication, 1986) and simplified geology in the Weir's Pond map area. The 'x' pattern represents areas underlain by granite.*

The model of Lux *et al.* (1986), therefore, can be used to explain the features associated with the regional metamorphism in the Ocean Pond area. Although the model also predicts prograde kyanite to sillimanite transitions, its applicability to the metamorphism in the Wing Pond area is uncertain and requires further work. In the latter area, the sequential replacement of kyanite by sillimanite and of kyanite and sillimanite by andalusite seems to suggest some decompression associated with, or followed by, synchronous formation of a northeast-striking, steep high-strain zone and replacement and formation of augen of aluminosilicates by synkinematic muscovite. Microfolds locally outlined by sillimanite and preserved in andalusite porphyroblasts, are the only record of early fabrics. The relationship between these microfolds and the mylonitic fabric is not clear but they may record the early development of this fabric. It seems clear from the spatial relationships between the metamorphic zone and the high-strain zone that the latter is responsible for uplift of the rocks containing aluminosilicate and staurolite assemblages.

The kyanite–sillimanite–staurolite assemblages suggest that the rocks experienced depths of the order of 15 km, deeper than those implied by the Ocean Pond assemblages. It is not known whether the schists in the shear zone actually represent Gander Group rocks or are unrelated.

The type of P-T loop implied by the Wing Pond assemblages, in which kyanite is initially the stable aluminosilicate polymorph, has been modelled (England and Thompson, 1984) as a result of crustal thickening by overthrusting. During thermal relaxation, sillimanite becomes stable. The stabilization of andalusite may coincide with early uplift along the major shear zone in which these metamorphic rocks are now located. What is of more regional interest is the fact that granitic magmas are also likely to have been produced as a result of such overthrusting. The Ocean Pond Granite may represent such a magma, which has risen into the upper crust to produce the high-T–low-P metamorphism. Such a model may also be applicable to other granitoid bodies in northeastern Gander Zone.

REGIONAL CHRONOLOGICAL CORRELATIONS

Sericite-bearing metavolcanic rocks from the western part of the Avalon Zone, yielded whole-rock $^{40}Ar-^{39}Ar$ spectra having plateau ages in the range 390 to 370 Ma (Dallmeyer *et al.*, 1983), which were interpreted to closely date the regional metamorphism and associated deformation in the western Avalon Zone. The $^{40}Ar/^{39}Ar$ age spectra on biotite from the Hare Bay Gneiss in the northeastern Gander Zone, record plateau ages ranging from 383 to 365 Ma (Dallmeyer *et al.*, 1981) and were interpreted to date regional post-metamorphic cooling and also to reflect a minimum date for initial tectonic activity along the Dover Fault. The Hare Bay Gneiss ages are younger than the Ar–Ar ages presented here: this may reflect protracted cooling of the higher grade rocks in the east or cooling after later plutonism around this time period (as exemplified by the Deadman's Bay Granite) or later uplift. The ages from the western Avalon Zone are more similar but are generally younger. These discrepancies may be resolved by more precise dating of peak metamorphic episodes through U–Pb dating of zircon and sphene.

In southern Newfoundland, Dunning *et al.* (1988) argued for a major Late Silurian orogeny with medium- to high-grade, regional metamorphism and deformation, combined with plutonism and volcanism. The North Bay Granite is posttectonic, dated by U–Pb at 396^{+6}_{-3} and provides a younger age limit for the orogenic event in the south. Cooling ages on biotite and muscovite from the Ocean Pond area, northeastern Gander Zone, are approximately 20 Ma younger than U–Pb peak metamorphic ages for the southern Newfoundland event and overlap the age of the North Bay Granite. As pointed out above, certain features of the Ar–Ar chronology for the Ocean Pond area, imply rapid cooling rather than a protracted cooling over 20 Ma. Therefore, the Early Devonian metamorphism in the Ocean Pond area is not readily correlatable with Silurian metamorphism on the south coast. The type of metamorphism extant at Wing Pond, characterized by kyanite, is more typical of that seen on the south coast, e.g., in the Port aux Basques Complex (O'Neill, 1985) and Bay du Nord Group (Chorlton, 1984).

In Maine, Lux *et al.* (1986) reported that most plutons in the Merrimack Synclinorium have ages that cluster at 400 Ma and 370 Ma, based on cooling ages from hornblende, biotite and muscovite. Hubacher and Lux (1987) used crosscutting plutons in Maine, to place a lower limit of 402 ± 6 Ma on the timing of Acadian folding. In this study, the data suggest synchronous development of open upright folds and metamorphism at approximately 400 Ma (assuming cooling ages are reasonably close to metamorphic ages). The main phase of deformation in the Gander Group, had a different style and was pre-metamorphic.

SYNOPSIS

PALEOTECTONIC SETTING OF THE GANDER RIVER COMPLEX

Lithological and geochemical patterns in the Gander River Complex in the Weir's Pond area, suggest that the complex is a mosaic of rock units that have been structurally juxtaposed and imbricated. Two groups of gabbros are defined and their geochemistry suggests that they are unrelated to basalt and diabase, which occur locally; the latter consistently show tholeiitic fractionation trends, indicating a common source. Chemical patterns of basalt and diabase, in particular, and of gabbros and trondhjemites in general, suggest that these rocks formed in an island-arc environment. There is some suggestion in trace and REE trends of the mafic rocks, of a MORB influence; however, a better database is required to further substantiate this.

Geochemical trends indicate formation of the trondhjemite by a process of partial melting of a mafic source. The close spatial association between mafic and felsic rock types in the Complex suggests that deeper level equivalents of the gabbroic rocks may have been the source material, which partially melted to form the trondhjemite. The gabbros as presently exposed, show no evidence of partial melting. Payne and Strong (1979) noted that the conditions required for formation of the Twillingate trondhjemite (geochemically similar to the Gander River Complex trondhjemite) require a volcanic sequence approximately 12 km thick. They argued that the high geothermal gradient necessary for melting a mafic source was generated by the heat input from voluminous basaltic magmatism at the base of such an island arc. The interpretation here, that at least some of the rocks of the Gander River Complex have island-arc affinities, suggests that a volcanic sequence of this magnitude was present. Alternative models for the formation of the trondhjemitic rocks involve melting of the basal part of the complex, induced by high-heat flow in an area of rifting. This may involve either arc or back-arc rifting. If the suggestion of a MORB influence in the mafic chemistry is substantiated, then this model may be applicable.

The present spatial association of gabbro, locally cut by diabase dykes, pillowed and massive basalts, trondhjemite, clinopyroxenite and altered rocks of dunitic to harzburgitic composition, suggests that the Gander River Complex represents remnants of an island-arc complex built on an oceanic substrate. The complex can, therefore, be considered to represent remnants of an ophiolite as concluded by Kennedy (1975) and Currie *et al.* (1979). Chromite and volcanic detritus in Unit 5 of the Davidsville Group is considered to represent the earliest evidence of exhumation of the complex. Farther north, the Carmanville ophiolitic melange has been interpreted (Pajari *et al.*, 1979) to contain various units of the complex incorporated into a sedimentary matrix. Although no large-scale comparisons can be made between the Carmanville melange and rocks in the Weir's Pond area, locally, scattered boulders of gabbro and/or ultramafic rock occur in a black shale matrix adjacent to the large trondhjemite exposure on Route 330. The method of emplacement of the trondhjemite itself into the black shale is unknown and it may represent a large olistolith.

DEPOSITIONAL SETTING OF THE GANDER AND DAVIDSVILLE GROUPS

The depositional setting of the psammite and pelite of the Jonathans Pond Formation is uncertain (O'Neill and Knight, 1988). Abrupt contacts between well-sorted psammite and pelite are characteristic and suggest that each psammite bed represents a distinct event when mud was transported into the depositional basin. The rare occurrences of massive graded beds suggest deposition from a turbidity current or liquified sand flow. The best-exposed psammite beds are commonly characterized by a planar, thin stratification. Such units can occur at the beach face or in washover fans in siliciclastic shoreline sequences (Reinson, 1984). The stratified sands in these cases are associated with distinctive sequences of offshore to subaerial sands and muds with a predominance of cross-stratification, both of which are generally lacking in the Jonathans Pond Formation. Planar stratified sands are also common in ephemeral, sandy fluvial systems of semi-arid settings (Tunbridge, 1981). However, further evidence for a subaerial, semi-arid setting for the rocks of this formation is absent. The well-sorted, mature, quartzose nature of the psammite and the monotonous nature of the facies in the Jonathan's Pond Formatiom is suggestive of shallow-marine, near-shore or shelf environment (Pettijohn *et al.*, 1973) with a major granitic and (or) metamorphic source area. The presence of detrital sphene within these sandstones appears to be rather anomalous since sphene is generally considered to degrade easily. However, Hiscott (1978) reported rounded sphene grains in sandstones of the Tourelle Formation, which he interprets as recycled sphene. Therefore, this mineral may not be as easily broken down as is commonly thought.

The significance of the ubiquitous mafic intrusive bodies is not known and awaits further resolution geochemically.

McGonigal (1973), Kennedy and McGonigal (1972), Pickerill *et al.* (1978), and Blackwood (1982) have interpreted the Gander Group (*sensu lato*) as a continental rise or shelf deposit. Results of the present study, although not environment-specific, support these previous conclusions. The absence of fossils from the Jonathan's Pond Formation may indicate a paucity of marine life or considerable distance from land.

The depositional setting of the Indian Bay Big Pond Formation is also uncertain. Relationships between key units are not exposed and some important rock types are defined only by their occurrence as boulders on the shores of Indian Bay Big Pond. Because of the close spatial relationship of all the units and their occurrence together in one restricted geographic area, it seems reasonable to assume that most if not all of these units were originally deposited close together. The intercalation of the black pelite with the grey psammite, marking the northwestern gradational contact with the Jonathan's Pond Formation, indicates a relatively rapid change in the sedimentation. Black pelite indicates anoxic conditions, which commonly develop in restricted marine basins (including ocean basins), but can also form in estuarine or tidal-flat deposits.

If the volcanic and intrusive rocks elsewhere in the formation are an integral part of the formation, they indicate that volcanism was approximately contemporaneous with the black shale deposition. The presence of a chert band, of possible exhalative origin, interbedded with the black pelite also argues for volcanism coincident with the black pelite deposition. Maroon psammite and maroon siltstone interbedded with grey psammite and rare black pelite in the southeastern part of the formation, near Indian Bay Big Pond, suggest a fundamental change in redox conditions of the depositional environment, from an anoxic, carbon-rich, restricted basin to an oxidizing environment. The change from black to red in shale colour indicates a change from high (0.8 to 1.0 mole fraction) Fe^{2+}/Fe^{3+} to very low (0 to 0.3 mole fraction), accompanied by a decrease in organic carbon content (Potter *et al.*, 1980). Oxidizing conditions suggest shallow-water deposition, which is also implied by well-preserved (commonly whole) fossils in boulders that are interpreted to be derived from this particular subunit.

In New Brunswick, the Miramichi Zone, mostly comprising a northeast-trending Cambro-Ordovician belt of sedimentary and volcanic rocks termed the Tetagouche Group, has been correlated with the Gander Zone (Rast *et al.*, 1976; Williams, 1978). The southern and structurally lower part of the Tetagouche Group principally comprises alternating quartzite and semipelite beds (Skinner, 1974; Fyfe, 1982), which have been interpreted as continental rise or slope deposits (Ruitenberg *et al.*, 1977). Conodonts and shallow water, shelly fauna in calcareous, tuffaceous phyllite that are close to the contact with the overlying silicic volcanic rocks indicate an Arenig age (Neuman, 1984; Nowlan, 1981). In Maine, the Shin Brook Formation (Neuman, 1964) is a late Arenig sequence of volcaniclastic rocks, which overlie polydeformed slate and quartzite of the Cambro-Ordovician Grand Pitch Formation (Neuman, 1984). Correlation between these rocks in New Brunswick and Maine, and the Gander Group, supports the interpretation that the Indian Bay Big Pond Formation is at the stratigraphic top of the Gander Group.

Lithological diversity within the basal division of the Davidsville Group, (the Weir's Pond Formation), indicates unstable tectonic conditions from the late Arenig to the Caradoc. The presence of volcanic debris and chromite in late Arenig sandstone implies that the Gander River Complex had been exhumed and was being actively eroded. The only source for abundant chromite detritus is the cumulate zones of layered ultramafic complexes and ophiolites (Stanton, 1972; Hiscott, 1978). This scenario has important implications for timing of deformation in eastern Newfoundland. On the western margin, chromite detritus occurs in the Arenig Eagle River Formation (Botsford, 1987) and the late Arenig Tourelle Formation of eastern Quebec (Hiscott, 1978). However, the late Arenig sandstone of the Weir's Pond Formation also contains much quartz and fresh microcline, the latter, at least, implying direct derivation from a continental granitic source. These late Arenig sandstones are inferred to be overlain by massive conglomerates, signalling rapid deposition by debris flows off a proximal Gander River Complex. The monomictic nature of some plagiogranite-rich deposits implies a depositional environment restricted to gorges cutting through these rocks. Other channels accessed a more diverse suite of ultramafic to felsic plutonic rocks. Some conglomerate beds contain abundant sedimentary and metasedimentary clasts as well as ultramafic to felsic clasts. These clasts, consisting of black shale, siltstone and sandstone and fragments of low-metamorphic grade, suggest derivation from a continenal block such as that now represented by the Gander Zone. Any tectonic model for the eastern margin of Iapetus must include a depositional basin, which has simultaneous access to a continental source and an exhumed island arc and its basal ophiolitic sequence from the late Arenig onward. Two different end-members models are presented here and then compared to previous workers' models:

1) The island arc and its basal ophiolitic substrate were thrust up onto the eastern continental margin, before or in the late Arenig; and
2) that an island arc developed and that both it and ultramafic rocks, which may have formed a substrate to the arc, became available for erosion into an adjacent back-arc basin, which was flanked on the other side by a continental source.

Initially, in the late Arenig–early Llanvirn, as implied by Unit 5 of the Weir's Pond Formation, detritus from a continental source was important. There are no paleocurrent directions available for the Davidsville Group and no direct evidence for the relative paleogeographic positions of the depositional basin relative to the volcanic arc and continental source.

Model 1 suggests up-thrusting of the Gander River Complex in the Arenig; such deformation would be contemporary with the Taconian Orogeny in western Newfoundland. Previous geological studies in eastern Newfoundland have not, to date, uncovered evidence for Taconian deformation. As Hiscott (1978) has emphasized, however, petrographic studies of sandstones are an important aid to tectonic modelling, in that they provide a link to paleotectonic settings for which other evidence is lacking. Based on petrographic data of this study, the only evidence for Arenig deformation is that implied by exhumation of the Gander River Complex. Currie *et al.* (1979) interpreted the ultramafic and volcanic rocks (their Units 1 and 2) to represent remnants of oceanic crust, which were 'thrust over the toe of the continental slope' in the Llanvirn–Llandeilo period, based on the unconformity of this age between limestone and serpentinite on Weir's Pond. The continental slope deposits are represented by the on-strike extension of the Jonathan's Pond Formation. In their model, the Avalon Platform formed the stable craton to the east. Colman-Sadd (1980) in contrast to Currie *et al.* (1979), stated that the unconformity between serpentinite and limestone could have formed on oceanic crust before thrusting and been rafted into place during the Acadian deformation. In model 2, obduction is not necessarily a prerequisite and the ultramafic rocks may have been exhumed along a transform fault (Blackwood, 1982).

Both of the models above assume that the Gander Group and continental source lay to the east; however, this is merely based on the present-day disposition of the major geological elements of northeastern Newfoundland. Single-zircon ages from a psammite of the Jonathan's Pond Formation suggest a source containing rocks ranging in age from 2700 Ma to 570 Ma. Further studies need to be done to determine the extent to which the Laurentian or Baltic cratons acted as sources to the Jonathan's Pond Formation.

The chromite in limestone and calc-arenite of Llanvirn to Llandeilo age nonconformably overlying serpentinite at Weir's Pond, is not necessarily first cycle but may be recycled from the late Arenig to early Llanvirn chromite-bearing sandstone (Unit 5). Thus, this unconformity does not necessarily indicate major obduction at this time. In addition, no metamorphic soles at the structural base of ultramafic exposures have yet been mapped in the Gander River Complex.

ECONOMIC POTENTIAL

The recent announcement by Noranda Exploration Company Limited and Noront Resources Limited of a joint-venture agreement on the 'GRUB', whereby Noront spends 30 million dollars to 1991, emphasizes the fact that the Gander River Complex is the most promising mineral-exploration target in the area. Much of the exploration work in the Weir's Pond area has been done in the Gander River Complex and, more recently, sedimentary rocks of the Davidsville Group have also become a target. Based on the recognition in this study that mafic rocks of the complex have an island-arc affinity, the igneous complex contains potential for hosting base-metal sulphide and gold deposits similar to those in the Victoria Lake Group (Kean and Evans, 1988) where mineralization, although in felsic volcanic rocks, is partly associated with island-arc tholeiites. Extrusive felsic volcanic rocks have not been recognized in outcrop but occur commonly as detritus in conglomeratic rocks of the Davidsville Group, which are derived from the complex. Gold has been located in several places in the complex, where it is usually associated with quartz veins. Shear zones, which occur within the complex, have the ability to remobilize and concentrate gold, as in the Victoria Lake Group (Kean and Evans, 1988).

Much hydrothermal activity has affected ultramafic rocks of the complex as implied by ubiquitous networks of calcite, chlorite and locally quartz veins; conversion of primary igneous assemblages to talc, carbonate and serpentine is almost complete in many places. The carbonate and talc-rich rocks, termed listwaenites (Lobochnikov, 1936) commonly occur in ultramafic rocks and have been identified as potentially gold-bearing (Buisson and LeBlanc, 1985).

In the Davidsville Group, the small muscovite granite is noteworthy for significant (approximately 2 percent) pyrite disseminated throughout; an assay sample returned 36 ppb Au.

Although much of the Jonathan's Pond Formation is devoid of mineralization, several exposures of psammite and semipelite near the north edge of the map area contain profuse quartz veins. One quartz vein, which ranges in thickness from 1 to 10 cm, contains up to 20 percent sulphide. An assay sample returned 2.6 percent Pb, 0.17 percent Cu, 73 ppm Mo, 11.2 ppm Ag and 210 ppb Au. The quartz veins are relatively late and may be related to the Ocean Pond Granite that is exposed to the southeast.

Muscovite-rich pegmatites associated with the Ocean Pond Granite locally contain beryl. Segregations of pale-green muscovite locally occur in bands up to 10 cm thick and molybdenite specks were also noted.

Prior to 1987, the eastern part of the map area had not attracted any mineral-exploration companies because of the apparently barren and monotonous nature of the Gander Group. However, recognition of intermediate volcanic rocks in the Indian Bay Big Pond Formation in this study, considerably enhances the exploration potential of the area. A grab sample taken south of Southern Pond consisted of representative chips of pyrite-rich rock and crosscutting quartz veins. The sample assayed 2200 ppb Au. The exposure was originally thought to be related to a felsic volcanic rock (O'Neill and Knight, 1988). However, subsequent petrographic examination showed that the rock consisted of angular quartz and feldspar fragments set in an optically irresolvable matrix and its protolith remains unknown. A conglomeratic unit mapped south of this area by Blackwood (1977) suggests that the Indian Bay Big Pond Formation continues to the south. An Open File release on the distribution of gold and associated elements in the NTS 2/E map area, recently made available by the Department of Mines and Energy (Davenport and Nolan, 1988) confirms the presence of anomalous gold concentrations in this area. The release also showed that gold occurs in anomalous levels in sedimentary rocks of the Davidsville Group. Continued mapping to the south, in the Gander Lake area, by the author (O'Neill, 1990) has documented many quartz veins in the Gander Group containing anomalous gold values. These quartz veins were probably produced during the regional greenschist-facies metamorphism. They are commonly pyritiferous and locally are associated with silicification of the host rocks. The recognition of numerous shear zones in the Gander Zone is important in respect to gold concentrations. Some of the world's important gold producing mines are located in ductile shear zones. In the Golden Mile, Kalgoorlie, Australia, Boulter *et al.* (1987) document regional deformation producing anastomosing ductile shear zones in which pyrite and gold are disseminated throughout. They attribute the concentrations of gold to high-fluid flow focussed in the deforming shear zone.

The contact zone between chert and laminated black pelite of the Indian Bay Big Pond Formation, locally contains disseminated pyrite and molybdenite. A grab sample yielded 123 ppm Mo and 1.5 ppm Ag.

Although previously considered a relatively poor exploration target, the occurrences of anomalous gold in quartz veins in the Gander Group must significantly raise its potential for hosting gold deposits, particularly because of the presence of shear zones, which provide the means of concentrating gold.

MAJOR RESULTS

1. Stratigraphic subdivision of the Davidsville Group resulted in the definition of the Weir's Pond, Hunts Cove and Outflow formations. The Weir's Pond Formation is intimately associated with the Gander River Complex and only occurs unconformably overlying or structurally imbricated with igneous rocks of the Complex. Elucidation of the history of the Weir's Pond Formation is a critical part of unravelling the geological history of the Gander River Complex. The Weir's Pond Formation was spatially associated with the complex probably from late Arenig times. Structural imbrication of the Weir's Pond Formation and Gander River Complex occurred prior to final juxtaposition with the Gander Group.

2. Immobile element chemistry of mafic and felsic rocks of the Gander River Complex in the Weir's Pond area suggests an island-arc affinity. Ultramafic rocks of the complex may form remnants of an ophiolitic substrate to this complex. Ultramafic and volcanic detritus in late Arenig sandstone of the Weir's Pond formation imply that exhumation and erosion of the Complex occurred during the Arenig.

3. The contrast in structural grain (northeast in the Davidsville Group and Gander River Complex and north to north-northeast in the Gander Group) suggests that the dominant structure was imposed on the Gander Group prior to its structural juxtapositioning with the Davidsville Group and Gander River Complex. The north to north-northeast trend is paralleled by a major aeromagnetic anomaly in the northeastern Gander Zone, which is terminated by the northeastward extension of the Davidsville Group and Gander River complex.

4. The Gander Group has been divided into the Jonathan's Pond and Indian Bay Big Pond formations. The latter unit is important since it is tentatively placed at the stratigraphic top of the Gander Group and is late Arenig–early Llanvirn in age.

5. Evaluation of the detrital components of the Davidsville Group indicates that a continental block was an important constituent of its provenance from the late Arenig onward. If the Indian Bay Big Pond Formation is stratigraphically conformable with the Jonathan's Pond Formation and if the former is entirely late Arenig in age, then that implies that the end of deposition of the Gander Group coincided with deposition of the basal unit of the Davidsville Group. In this case, the Gander Group could not have formed part of the continental block adjacent to the sedimentary basin in which the Davidsville Group was laid down. If the Indian Bay Big Pond Formation is not a stratigraphically conformable succession and if it's late Arenig age does not represent the age of the top of the Gander Group, then the Gander Group (specifically the Jonathan's Pond Formation) could be much older (maximum 530 Ma, from detrital titanite). In this case, the Jonathan's Pond Formation could have been deposited, subsumed, regionally metamorphosed and uplifted to shed detritus into the basal Davidsville Group in late Arenig times. This model would also require that at least part of the Indian Bay Big Pond Formation is unconformable on the Jonathan's Pond Formation. Which of these models, if either, is correct awaits improved resolution of the age of the Gander Group.

6. The metamorphic character of the rocks in the Gander Zone does not allow a simple eastward prograde regional metamorphism to be defined. Instead, two types of metamorphism are defined; low P-high T regional metamorphism associated with the Ocean Pond Granite and low P-high T contact metamorphism associated with the Deadman's Bay Granite and medium-pressure metamorphism characterized by kyanite and exposed in a structural window at Wing Pond.

7. The Ar–Ar ages on muscovite and biotite from the Ocean Pond area, indicate that the regionally metamorphosed rocks cooled through greenschist-facies conditions in early Devonian times. This metamorphism is genetically linked to the leucocratic, S-type Ocean Pond Granite, which is interpreted as a shallow-level intrusion. The metamorphism overlapped the development of an open phase of folding (F_3), the effects of which are best developed in the central part of the Gander Group. In the eastern and western parts of the Gander Group, the regional foliation (S_2) is steep (or steep to moderate) and the effects of D_3, which was essentially an east–west shortening, was therefore minimal in these areas, merely resulting in a tightening-up of previously developed structures. The F_2 fold hinges vary in plunge from shallow to steep toward the west. This deformational phase is interpreted to be related to east-directed, recumbent folding in which the fold axes are approximately parallel to the direction of thrusting.

8. The regional metamorphism that affected the Gander Group has generated abundant quartz veins, many of which contain pyrite and some contain anomalous gold values. The recognition of numerous shear zones throughout the Gander Zone has implications for gold potential as shear zones commonly focus fluid-flow and are known to concentrate economic gold deposits in this way.

ACKNOWLEDGMENTS

During the field mapping part of this project, excellent assistance was provided by Kerry Sparkes and Chris Beer. This report has benefitted from discussions with Steve Colman-Sadd and Frank Blackwood. Sections of the manuscript were reviewed by Scott Swinden and Brian O'Brien. The report was critically read by Steve Colman-Sadd and Toby Rivers who offered many useful suggestions.

I thank Tomasz Dec for his work in point counting thin sections, tabulating the results and for discussion of the petrography. Gerry Kilfoil is thanked for providing expertise regarding geophysical anomalies in the study area, and Terry Sears for assistance with the drafting.

REFERENCES

Abbey, S.
1980: Studies in 'standard samples' for use in the general analysis of silicate rocks and minerals. Part 6: 1979 edition of 'usable' values. Geological Survey of Canada, Paper 80-14, 30 pages.

1983: Studies in 'standard samples' of silicate rocks and minerals. Geological Survey of Canada, Paper 83-15, 114 pages.

Alexander, E.C. Jr., Michelson, G.M. and Lanphere, M.A.
1978: A new ^{40}Ar/^{39}Ar dating standard. *In* Short papers of the 4th International Conference on Geochronology, Cosmochronology and Isotope Geology. *Edited by* R.E. Zartman, United States Geological Survey, Open File Report 78-701, pages 6-8.

Arth, J.G. and Barker, F.
1976: Rare-earth partitioning between hornblende and dacitic liquid and implications for the genesis of trondhjemitic-tonalitic magmas. Geology, Volume 4, pages 534-536.

Baird, D.M., Moore, J.G.G., Scott, H.S. and Walker, W.
1951: Reconnaissance geology of east central Newfoundland between Sir Charles Hamilton Sound and Baie d'Espoir. Department of Natural Resources, Mineral Development Division, Newfoundland Geological Survey, Unpublished report, 155 pages. [Nfld (73)]

Barker, F., Arth, F.G., Peterman, Z.E. and Friedman, I.
1976: The 1.7 to 1.8 b.y. old trondhjemites of southwestern Colorado and Northern New Mexico: geochemistry and depths of genesis. Geological Society of America Bulletin, Volume 87, pages 189-198.

Basaltic Volcanism Study Project (BVSP)
1981: Ocean-floor basaltic volcanism. *In* Basaltic Volcanism Study Project, Basaltic Volcanism on the Terrestrial Planets. Pergamon Press, New York, pages 132-160.

Beach, A.
1980: Retrogressive metamorphic processes in shear zones with special reference to the Lewisian Complex. Journal of Structural Geology, Volume 2, pages 257-264.

Beccaluva, L., Ohnenstetter, D., and Ohnenstetter, M.
1979: Geochemical discrimination between ocean-floor and island-arc tholeiites—application to some ophiolites. Canadian Journal of Earth Sciences, Volume 16, pages 1874-1882.

Bence, A.E. and Albee, A.L.
1968: Empirical correction factors for the electron microanalysis of silicates and oxides. Journal of Geology, Volume 76, pages 382-403.

Berger, A.R. and Naylor, R.S.
1974: Isotopic dates on zircons from the Deadmans Bay pluton, northeast Newfoundland and their geological implications. *In* Geological Association of Canada 27th Annual Meeting, Program with Abstracts, page 9.

Bergstrom, S.M., Riva, J. and Kay, M.
1974: Significance of conodonts, graptolites, and shelly faunas from the Ordovician of western and north-central Newfoundland. Canadian Journal of Earth Sciences, Volume 11, pages 1625-1660.

Berthe, D., Choukroune, P. and Jegouzo, P.
1979: Orthogneiss, mylonite and non-coaxial deformation of granites: The example of the South Armorican shear zone. Journal of Structural Geology, Volume 1, pages 31-42.

Blackwood, R.F.
1976: The relationship between the Gander and Avalon Zones in the Bonavista Bay region, Newfoundland. M.Sc. Thesis, Memorial University of Newfoundland, St. John's, 156 pages.

1977: Geology of the east half of the Gambo (2D/16) map area and the northwest portion of the St. Brendan's (2C/13) map area, Newfoundland. Newfoundland Department of Mines and Energy, Mineral Development Division, Report 77-5, 20 pages.

1978: Northeastern Gander Zone. *In* Report of Activities for 1977. *Edited by* R.V. Gibbons. Newfoundland Department of Mines and Energy, Mineral Development Division, Report 78-1, pages 72-79.

1979: Geology of the Gander River ares (2E/2), Newfoundland. *In* Report of Activities for 1978. *Edited by* R.V. Gibbons. Newfoundland Department of Mines and Energy, Mineral Development Division, Report 79-1, pages 38-42.

1980: Geology of the Gander (west) area (2D/15), Newfoundland. *In* Current Research. Newfoundland Department of Mines and Energy, Mineral Development Division, Report 80-1, pages 53-61.

1981: Geology of the West Gander Rivers area, Newfoundland. *In* Current Research. *Edited by* C.F. O'Driscoll and R.V. Gibbons. Newfoundland Department of Mines and Energy, Mineral Development Division, Report 81-10, pages 50-56.

1982: Geology of the Gander Lake (2D/15) and Gander River (2E/2) area. Newfoundland Department of Mines and Energy, Mineral Development Division, Report 82-4, 56 pages.

Blackwood, R.F. and Kennedy, M.J.
1975: The Dover Fault: Western boundary of the Avalon Zone in northeastern Newfoundland. Canadian Journal of Earth Sciences, Volume 12, pages 320-325.

Botsford, J.W.
1987: Depositional history of Middle Cambrian to Lower Ordovician deep water sediments, Bay of Islands, western Newfoundland. Ph.D. Thesis, Department of Earth Sciences, Memorial University, St John's, 509 pages.

Boulter, C.A., Fotios, M.G. and Phillips, G.N.
1987: The Golden Mile, Kalgoorlie: A giant gold deposit localized in ductile shear zones by structurally induced infiltration of an auriferous metamorphic fluid. Economic Geology, Volume 82, pages 1661-1678.

Boyce, W.D.
1987: Cambrian–Ordovician biostratigraphy in central Newfoundland. *In* Current Research, Report 87-1. *Edited by* D. Walsh, R.F. Blackwood and Gibbons, R.V. Newfoundland Department of Mines and Energy, Mineral Development Division, St. John's, pages 335-342.

Boyce, W.D., Ash, J.S., O'Neill, P. and Knight, I.
1988: Ordovician biostratigraphic studies in the Central Mobile Belt and their implications for Newfoundland tectonics. *In* Current Research. *Edited by* R.S. Hyde, D.G. Walsh and R.F. Blackwood, Newfoundland Department of Mines, Mineral Development Division, Report 88-1, pages 177-182.

Bruckner, W.D.
1972: The Gander Lake and Davidsville groups of northeastern Newfoundland: New data and geotectonic implications. Discussion. Canadian Journal of Earth Sciences, Volume 9, pages 1778-1779.

Bruton, D.L. and Harper, D.A.T.
1985: Early Ordovician (Arenig–Llanvirn) faunas from oceanic islands in the Appalachian–Caledonide orogen. *In* The Caledonide Orogen–Scandanavia and related areas. *Edited by* D.G. Gee and B.A. Sturt. John Wiley and Sons Ltd., pages 359-368.

Buisson, G. and LeBlanc, M.
1985: Gold in carbonatized ultramafic rocks from ophiolitic complexes. Economic Geology, Volume 80, pages 2028-2029.

Butler, A.J., Miller, H.G. and Vanderveer, D.G.
1984: Geoscience studies in the Weir's Pond area northeast of Gander, Newfoundland. *In* Current Research. *Edited by* M.J. Murray, J.G. Whelan and R.V. Gibbons. Newfoundland Department of Mines, Mineral Development Division, Report 84-1, pages 271-278.

Butler, D.J.
1988: Report on geological and geochemical surveys on licence number 3291, Third Pond property (NTS 2E/2), Newfoundland. September 1988 for Falconbridge Ltd. [2E/2 (637)]

Cann, J.R.
1970: Rb, Sr, Y, Nb and Zr in some ocean floor basalts. Earth and Planetary Science Letters, Volume 10, pages 7-11.

1971: Major element variations in ocean-floor basalts. Philosophical Transactions of the Royal Society of London, Volume A268, pages 495-505.

Chorlton, L.B.
1984: Geological development of the southern Long Range Mountains, southwest Newfoundland: A regional synthesis. Unpublished PhD thesis, Memorial University of Newfoundland, St John's, 600 pages.

Colman, L.C.
1954a: Lower Gander River area. Nalco unpublished report.

1954b: The Great Bend area, Northwest Gander River. Nalco unpublished report, 4 pages. [2D/11 (27)]

Coleman, R.G.
1977: Ophiolites–Ancient Oceanic Lithosphere? Minerals and Rocks, 12. Springer-Verlag, New York, 229 pages.

Coleman, R.G. and Donato, M.M.
1979: Oceanic plagiogranite revisited. *In* Trondhjemites, Dacites and Related Rocks. *Edited by* F. Barker. Developments in Petrology 6, Elsevier Scientific, Amsterdam, pages 149-168.

Coleman, R.G. and Peterman, Z.E.
1975: Oceanic plagiogranite. Journal of Geophysical Research, Volume 80, pages 1099-1108.

Colman-Sadd, S.P.
1976: Geology of the St. Alban's map area, Newfoundland (1M/B). Newfoundland Department of Mines and Energy, Mineral Development Division, Report 76-6, 19 pages.

1979: Geology of Twillick Brook (2D/4) and part of Burnt Hill (2D/5), Newfoundland. *In* Report of Activities for 1978. Newfoundland Department of Mines and Energy, Mineral Development Division, Report 79-1, pages 30-34.

1980a: Geology of the Twillick Brook map area, Newfoundland (2D/4). Newfoundland Department of Mines and Energy, Mineral Development Division, Report 79-2, 23 pages.

1980b: Geology of south-central Newfoundland and evolution of the eastern margin of Iapetus. American Journal of Science, Volume 280, pages 991-1017.

Colman-Sadd, S.P. and Swinden, H.S.
1984: A tectonic window in central Newfoundland? Geological evidence that the Appalachian Dunnage Zone may be allochthonous. Canadian Journal of Earth Sciences, Volume 21, pages 1349-1367.

Currie, K.L. and Pajari, G.E.
1977: Igneous and metamorphic rocks between Rocky Bay and Ragged Harbour, northeastern Newfoundland. *In* Report of Activities, Part A. Geological Survey of Canada, Paper 77-1A, pages 341-346.

Currie, K.L., Pajari, G.E. and Pickerill, R.K.
1979: Tectono-stratigraphic problems in the Carmanville area, northeastern Newfoundland. *In* Current Research, Part A. Geological Survey of Canada Paper 79-1A, pages 71-76.

1980: Comments on the Boundaries of the Davidsville Group, N.E. Newfoundland: *In* Current Research, Part A. Geological Survey of Canada, Paper 80-1A, p. 115-118.

Currie, K.L., Loveridge, W.D. and Sullivan, R.W.
1982: The Deadmans Bay pluton, northeastern Newfoundland; U/Pb study of zircon reveals a Grenvillian component. *In* Current Research, Part C. Geological Survey of Canada, Paper 82-1C, pages 119-124.

Dallmeyer, R.D. and Rivers, T.
1983: Recognition of extraneous argon components through incremental-release ^{40}Ar/^{39}Ar analysis of biotite and hornblende across the Grenvillian metamorphic gradient in southwestern Labrador. Geochimica et Cosmochimica Acta, Volume 47, Number 3, pages 413-428.

Dallmeyer, R.D., Odom, A.L., O'Driscoll, C.F. and Hussey, E.M.
1981: Geochronology of the Swift Current Granite and host volcanic rocks of the Love Cove Group, southwestern Avalon Zone, Newfoundland: Evidence for a late Proterozoic volcanic-subvolcanic association. Canadian Journal of Earth Sciences, Volume 18, pages 699-707.

Dallmeyer, R.D., Blackwood, R.F. and Odom, A.L.
1981: Age and origin of the Dover Fault: tectonic boundary between the Gander and Avalon Zones of the northeastern Newfoundland Appalachians. Canadian Journal of Earth Sciences, Volume 18, pages 1431-1442.

Dallmeyer, R.D., Hussey, E.M., O'Brien, S.J. and O'Driscoll, C.F.
1983: Chronology of tectonothermal activity in the western Avalon Zone of the Newfoundland Appalachians. Canadian Journal of Earth Sciences, Volume 20, pages 355-363.

Dalrymple, G.B., Alexander, E.C, Lanphere, M.A. and Kraker, G.P.
1981: Irradiation of samples for ^{40}Ar/^{39}Ar dating using the Geological Survey TRIGA Reactor, U.S. Geological Survey, Professional Paper 1176, 55 pages.

Davenport, P.H. and Nolan, L.W.
1988: Gold and associated elements in lake sediment from regional surveys in the Botwood map area (NTS 2E). Newfoundland Department of Mines, Mineral Development Division, Open File Report 2E/563, 28 pages.

Dean, P.L.
1978: The volcanic stratigraphy and metallogeny of Notre Dame Bay, Newfoundland. Geology Report 7, Memorial University of Newfoundland, St. John's, 204 pages.

Dickson, W.L.
1987: Geology of the Mount Sylvester (2D/3) map area, central Newfoundland. *In* Current Research. Newfoundland Department of Mines and Energy, Mineral Development Divisions, Report 87-1, pages 283-296.

Dimmell, P.M. and Jacobs, W.
1989: First year assessment report on the Indian Bay Big Pond property, north central Newfoundland (NTS 2E/1). Corona Corporation. [2E (686)]

Dunlop, W.B.
1955: Evaluation of area between Gander Lake and Sir Charles Hamilton Sound. Nalco unpublished report. [Nfld 109]

Dunning, G.R.
1984: The geology, geochemistry, geochronology and regional setting of the Annieopsquotch Complex and related rocks of southwest Newfoundland. Unpublished Ph.D. thesis, Memorial University of Newfoundland, St. John's, Newfoundland, 403 pages.

Dunning, G.R., Krogh, T.E., O'Brien, S.J., Colman-Sadd, S.P. and O'Neill, P.P.
1988: Geochronologic framework for the Central Mobile Belt in Southern Newfoundland and the importance of Silurian orogeny. Geological Association of Canada–Mineralogical Association of Canada–Canadian Society of Petroleum Geologists, Joint Annual Meeting, St. John's, Newfoundland, Program with Abstracts, Volume 13 page A34.

Durocher, A.C.
1979: Mineral investigations in central Newfoundland. NALCO Lot 2, middle portion, Minorex Limited. Unpublished report, 26 pages. [2D (105)]

England, P.C. and Thompson, A.B.
1984: Pressure–Temperature–Time paths of regional metamorphism I. Heat transfer during the evolution of thickened continental crust. Journal of Petrology, Volume 25, Part 4, pages 894-928.

Fairbairn, H.W. and Berger, A.R.
1969: Preliminary geochronological studies in northeastern Newfoundland. 17th Annual Progress Report, Massachusetts Institute of Technology, AEC, 1381-17, pages 19-20.

Floyd, P.A. and Winchester, J.A.
1975: Magma type and tectonic setting discrimination using immobile elements. Earth and Planetary Science Letters, Volume 27, pages 211-218.

1978: Identification and discrimination of altered and metamorphosed volcanic rocks using immobile elements. Chemical Geology, Volume 21, pages 291-306.

Fryer, B.J., Jenner, G.A., Longstaffe, F.J., Dickson, W.L., Colman-Sadd, S., O'Brien, S.J., Kerr, A., Owen, J.V. and Wilton, D.H.C.
1989: The isotopic and LILE compositions of granitoid rocks as clues to deep crustal structure in Lithoprobe East. Report of transect meeting, October 19-20. *Edited by* Garry Quinlan. Memorial University, St John's, Newfoundland.

Fyffe, L.R.
1977: Comparison of some tectonostratigraphic zones in the Appalachians of Newfoundland and New Brunswick: Discussion. Canadian Journal of Earth Sciences, Volume 14, pages 1468-1469.

1982: Taconian and Acadian structural trends in central and northern New Brunswick. *In* Major structural zones and faults of the northern Appalachians. *Edited by* P. St-Julien and J. Beland. Geological Association of Canada Special Paper 24, pages 117-129.

Gagnon, J.
1981: Report on geological, geochemical and geophysical exploration. Jonathan's Pond claims, Gander area. Westfield Minerals Limited. Unpublished report, 10 pages. [2E/2 (410)]

Goff, S.P.
1984: The magmatic and metamorphic history of the East Arm, Great Slave Lake, N.W.T. Unpublished Ph.D. thesis, University of Alberta, 295 pages.

Grant, D.R.
1974: Prospecting in Newfoundland and the theory of multiple shrinking ice caps. Geological Survey of Canada, Paper 74-1, Part B, pages 215-216.

Hanmer, S.
1981: Tectonic significance of the northeastern Gander Zone, Newfoundland: an Acadian ductile shear zone. Canadian Journal of Earth Sciences, Volume 18, pages 120-135.

Harrison, T.M. and McDougall, I.
1980: Investigations of an intrusive contact, northwest Nelson, New Zealand. Thermal, chronological and isotopic constraints. Geochimica et Cosmochimica Acta, Volume 44, pages 1985-2003.

Haq, B.U. and van Eysinga, W.B. Frans
1987: Geological Time Table. Elsevier Science Publishers, Amsterdam.

Hiscott, R.N.
1978: Provenance of Ordovician deep-water sandstones, Tourelle Formation, Quebec, and implications for initiation of the Taconic Orogeny. Canadian Journal of Earth Sciences, Volume 15, Number 10, pages 1579-1597.

Hoschek, G.
1969: The stability of staurolite and chloritoid and their significance in metamorphism of pelitic rocks. Canadian Mineralogy and Petrology, Volume 22, pages 208-232.

Hubacher, F.A. and Lux, D.R.
1987: Timing of Acadian deformation in northeastern Maine. Geology, Volume 15, pages 80-83.

Hughes, C.J.
1973: Spilites, keratophyres, and the igneous spectrum. Geological Magazine. Volume 109, pages 513-427.

Jayasinghe, N.R.
1976: Geology of the Wesleyville area, Newfoundland, M.Sc. Thesis, Memorial University of Newfoundland, St. John's, 288 pages.

1978: Geology of the Wesleyville map area (2F/4) and the east half of the Musgrave Harbour map area (2F/5), Newfoundland. *In* Report of Activities for 1978. *Edited by* R.V. Gibbons. Newfoundland Department of Mines and Energy, Mineral Development Division, Report 78-1, pages 124-128.

Jenness, S.E.
1954: Geology of the Gander River Ultrabasic Belt, Newfoundland. Unpublished Ph.D. thesis, Yale University, New Haven.

1958: Geology of the Gander River Ultrabasic Belt, Newfoundland. Geological Survey of Newfoundland, Report 11, 58 pages.

1960: Late Pleistocene glaciation of eastern Newfoundland. Bulletin of the Geological Society of America, Volume 71, pages 161-180.

1963: Terra Nova and Bonavista Bay map areas, Newfoundland. Geological Survey of Canada, Memoir 327, 184 pages.

1972: The Gander Lake and Davidsville groups of northeastern Newfoundland: New data and geotectonic implications: Discussion. Canadian Journal of Earth Sciences, Volume 9, pages 1779-1781.

Jewell, W.B.
1939: Geology and mineral deposits of the Baie d'Espoir area. Newfoundland Geological Survey Bulletin, Volume 17, 29 pages.

Kamineni, D.C. and Carrara, A.
1973: Comparison of the composition of porphyroblastic and fabric-forming biotite in two metamorphic rocks. Canadian Journal of Earth Sciences, Volume 10, pages 948-953.

Kay, R.W. and Senechal, R.G.
1976: The rare earth element geochemistry of the Troodos ophiolite complex. Journal of Geophysical Research, Volume 81, pages 964-970.

Kean, B.F. and Evans, D.T.W.
1988: Regional metallogeny of the Victoria Lake Group. *In* Current Research. Newfoundland Department of Mines, Mineral Development Division, Report 88-1, pages 319-330.

Kennedy, M.J.
1975: Repetitive orogeny in the northeastern Appalachians—new plate models based upon Newfoundland examples. Tectonophysics, Volume 28, pages 39-87.

Kennedy, M.J. and McGonigal, M.H.
1972: The Gander Lake and Davidsville Groups of northeastern Newfoundland: new data and geotectonic implications. Canadian Journal of Earth Sciences, Volume 9, pages 452-459.

Kerrick, D.M. and Spear, J.A.
1988: The role of minor element solid solution on the andalusite-sillimanite equilibrium in metapeiites and peraluminous granitoids. American Journal of Science, Volume 288, pages 152-192.

Krogh, T.E. and Keppie, J.D.
1990: Age of detrital zircons and titanites in the Meguma Group, southern Nova Scotia, Canada: Clues to the origin of the Meguma Terrane. Tectonophysics, Volume 177, pages 307-323.

Lenters, M.
1986: Report on geology, prospecting, geochemical and geophysical surveys, trenching and diamond drilling during May to September, 1986, Weir's Pond Claim Group, Newfoundland. Esso Minerals Canada Limited. [2E/1 and 8 (557)]

1988: Report on diamond drilling during October/November, 1987, Weir's Pond Claim Group, April 1988. Esso Mineral Canada Limited. [2E (595)]

Lister, G.S. and Snoke, A.W.
1984: S—C Mylonites. Journal of Structural Geology, Volume 6, Number 6, pages 617-638.

Lobochnikov, V.N.
1936: Ilchirsk and other serpentines: Tsentralnogo Geolego Razvedochnogo Institute, Trudy, Number 38, pages 24-56.

Lux, D.R., DeYoreo, J.J., Guidotti, C.V. and Decker, E.R.
1986: Role of plutonism in low pressure—high temperature metamorphic belt formation. Nature, Volume 323, Number 6091, pages 794-797.

MacKenzie, A.C.
1985: First year assessment report (geological, geophysical and geochemical) licence 2472. Noranda Exploration Company Limited. Unpublished Confidential report, 19 pages. [2E (532)]

Malpas, J.
1979: Two contrasting trondhjemite associations from transported ophiolites in western Newfoundland: Initial report. *In* Trondhjemites, Dacites and Related Rocks. *Edited by* F. Barker. Developments in Petrology 6, Elsevier Scientific, Amsterdam, pages 465-487.

Malpas, J. and Stevens, R.K.
1977: The origin and emplacement of the ophiolite suite with examples from Western Newfoundland. Geotectonics, Volume 11, Number 6, pages 453-466.

Malpas, J. and Strong, D.F.
1975: A comparison of chrome-spinels in ophiolites and mantle diapirs of Newfoundland. Geochimica et Cosmochimica Acta, Volume 39, pages 1045-1060.

McGonigal, M.H.
1973: The Gander and Davidsville Groups: major tectono-stratigraphic units in the Gander Lake area, Newfoundland. Unpublished M.Sc. thesis, Memorial University of Newfoundland, St. John's, 121 pages.

Miller, H.G.
1988: Geophysical interpretation of the geology of the northeast Gander Terrane, Newfoundland. Canadian Journal of Earth Sciences, Volume 25, pages 1161-1174.

Miller, H.G. and Weir, H.C.
1972: The northwest portion of the Gander Zone—a geophysical interpretation. Canadian Journal of Earth Sciences, Volume 19, pages 1371-1381.

Miyashiro, A.
1961: Evolution of Metamorphic Belts. Journal of Petrology, Volume 2, pages 277-311.

1974: Volcanic rock series in island arcs and active continental margins. American Journal of Science, Volume 274, pages 321-355.

Miyashiro, A. and Shido, F.
1975: Tholeitic and calc alkali series in relation to the behaviour of titanium, vanadium, chromium and nickel. American Journal of Science, Volume 275, pages 265-277.

Mottl, M.J.
1983: Hydrothermal process at seafloor spreading centers: application of basalt-seawater experimental results. *In* Hydrothermal Processes at Seafloor Spreading Centers. *Edited by* P.A. Rona, K. Bostrom, L. Laubier and K.L. Smith, Jr. NATO Conference Series IV: Marine Sciences, Volume 12, Plenum Press, New York, pages 199-224.

Murray, A. and Howley, J.P.
1881: Reports of the Geological Survey of Newfoundland for 1866-1880. London Edward Standford, 536 pages.

Neuman, R.B.
1964: Fossils in Ordovician tuffs, northeastern Maine: U.S. Geological Survey Bulletin 1181-E, 38 pages.

1976: Early Ordovician (late Arenig) brachiopods from Virgin Arm, New World Island, Newfoundland: Geological Survey of Canada Bulletin 261, pages 11-61.

1984: Geology and paleobiology of islands in the Ordovician Iapetus Ocean: review and implications. Geological Society of America Bulletin, Volume 95, pages 118-1201.

North American Stratigraphic Code
1983: North American Commision on Stratigraphic Nomenclature. AAPG Bulletin, Volume 67, Number 5, pages 841-875.

Nowlan, G.S.
1981: Some Ordovician conodont faunules from the Miramichi Anticlinorium, New Brunswick, Geological Survey of Canada, Bulletin 345.

O'Brien, S.J., O'Neill, P.P., King, A.F. and Blackwood, R.F.
1988: Eastern margin of the Newfoundland Appalachians—A cross section of the Avalon and Gander zones. Field Trip Guidebook, Geological Association of Canada—Mineralogical Association of Canada—Canadian Society of Petroleum Geologists Joint Annual Meeting, St John's, Newfoundland.

O'Connor, J.T.
1965: A classification for quartz-rich igneous rocks based on feldspar ratios. United States Geological Survey, Professional Paper 525-B, pages B79-B84.

O'Neill, P.P.
1985: An economic, metamorphic, structural and geochemical study of the Isle aux Morts prospect, southwest Newfoundland. MSc Thesis, Memorial University of Newfoundland, St. John's, 263 pages.

1987: Geology of the west half of the Weir's Pond area (2E/1) map area. *In* Current Research. *Edited by* D. Walsh, R.F. Blackwood and R.V. Gibbons. Newfoundland Department of Mines and Energy, Mineral Development Division, Report 87-1, pages 271-281.

1990: Geology of the northeast Gander Lake map area (NTS 2D/15) and the northwest Gambo map area (NTS 2D/16). *In* Current Research. *Edited by* C.P.G. Pereira, D.G. Walsh and R.F. Blackwood. Newfoundland Department of Mines and Energy, Geological Survey Branch, Report 90-1, pages 317-326.

O'Neill, P.P. and Knight, I.
1988: Geology of the east half of the Weir's Pond (2E/1) map area and its regional significance. *In* Current Research. *Edited by* R.S. Hyde, D. Walsh and R.F. Blackwood. Newfoundland Department of Mines, Mineral Development Division, Report 88-1.

O'Neill, P.P. and Lux, D.R.
1989: Tectonothermal history and $^{40}Ar/^{39}Ar$ geochronology of the northeastern Gander Zone, Weir's Pond area (2E/1). *In* Current Research. *Edited by* C.P.G. Pereira, D. Walsh and R.F. Blackwood. Newfoundland Department of Mines, Mineral Development Division, Report 89-1, pages 131-139.

O'Neill, P.P. and Blackwood, R.F.
1989: A proposal for revised stratigraphic nomenclature of the Gander and Davidsville groups and the Gander River ultrabasic belt, of northeastern Newfoundland. *In* Current Research. *Edited by* C.P.G. Pereira, D. Walsh and R.F. Blackwood. Newfoundland Department of Mines, Mineral Development Division, Report 89-1, pages 127-130.

Pajari, G.E. and Currie, K.L.
1978: The Gander Lake and Davidsville Groups of northeastern Newfoundland: a reexamination. Canadian Journal of Earth Sciences, Volume 15, pages 708-714.

Pajari, G.E., Pickerill, R.K. and Currie, K.L.
1979: The nature, origin and significance of the Carmanville Melange, northeast Newfoundland. Canadian Journal of Earth Sciences, Volume 16, pages 1439-1451.

Payne, J.G. and Strong, D.F.
1979: Origin of the Twillingate trondhjemite, north-central Newfoundland: Partial melting in the roots of an island arc. *In* Trondhjemites, Dacites and Related Rocks. *Edited by* F. Barker. Developments in Petrology 6, Elsevier Scientific, Amsterdam, pages 489-516.

Pearce, J.A. and Norry, M.J.
1979: Petrogenetic implication of Ti, Zr, Y and Nb variations in volcanic rocks. Contributions to Mineralogy and Petrology, Volume 69, pages 33-47.

Pederson, R.B. and Malpas, J.
1984: The origin of oceanic plagiogranites from the Karmoy ophiolite, Western Norway. Contributions to Mineralogy and Petrology, Volume 88, pages 36-52.

Perfit, M.R., Gust, D.A., Bence, A.E., Arculus, R.J. and Taylor, S.R.
1980: Chemical characteristics of island-arc basalts: implications for mantle sources. Chemical Geology, pages 227-256.

Pettijohn, F.J., Potter, P.E. and Siever, R.
1973: Sand and sandstone. Springer Verlag, 618 pages.

Piasecki, M.A.J.
1988: A major ductile shear zone in the Bay d'Espoir area, Gander Terrane, southeastern Newfoundland. *In* Current Research. Newfoundland Department of Mines, Mineral Development Division, Report 88-1, pages 135-144.

Pickerill, R.K., Pajari, G.E., Currie, K.L. and Berger, A.R.
1978: Carmanville map area, Newfoundland; the northeastern end of the Appalachians. *In* Current Research, Part A. Geological Survey of Canada, Paper 78-1A, pages 209-216.

Pickerille, R.K., Pajari, G.E. and Currie, K.L.
1979: Evidence of Caradocian glaciation in the Davidsville Group of northeastern Newfoundland. *In* Current Research, Part C. Geological Survey of Canada, Paper 79-1C, pages 67-72.

1981: Resedimented volcaniclastics in the Carmanville area, northeastern Newfoundland—depositional remnants of Early Palaeozoic oceanic islands. Canadian Journal of Earth Sciences, Volume 18, pages 55-70.

Potter, P.E., Maynard, J.B. and Pryor, W.A.
1980: Sedimentology of Shale. Springer Verlag, 306 pages.

Rast, N., Kennedy, M.J. and Blackwood, R.F.
1976: Comparison of some tectono-stratigraphic zones in the Appalachians of Newfoundland and New Brunswick. Canadian Journal of Earth Science, Volume 13, pages 868-875.

Reinson, G.E.
1984: Barrier island and associated strandplain systems. *In* Facies Models, 2nd edition. *Edited by* R.G. Walker. Geoscience Canada, Report Series 1, pages 119-140.

Renard, A.
1878: Sur la structure et la composition mineralogique du coticule. Membre Cour. et Membre des Savants Acadamie Royal de Belgique, 16.

Ruitenberg, A.A., Fyffe, L.R., McCutcheon, S.R., St. Peter, C.J., Irrinki, R.R. and Venugopal, D.V.
1977: Evolution of pre-Carboniferous tectonostratigraphic zones in the New Brunswick Appalachians. Geoscience Canada, Volume 4, pages 171-181.

Seyfried, W.E., Jr. and Bischoff, J.L.
1981: Experimental seawater-basalt interaction at 300°C, 500 bars, chemical exchange, secondary mineral formation and implications for the transport of heavy metals. Geochimica et Cosmochimica Acta, Volume 45, pages 135-147.

Seyfried, W.E., Jr., Mottl, M.J. and Bischoff, J.L.
1978: Seawater/basalt ratio effects on the chemistry and mineralogy of spilites from the ocean floor. Nature, Volume 275, pages 211-213.

Shervais, J.
1982: Ti-V plots and the petrogenesis of modern and ophiolitic lavas. Earth and Planetary Science Letters, Volume 59, pages 101-118.

Shiraki, K.
1978: Chromium. *In* Handbook of Geochemistry, 23K-1-7. *Edited by* K.H. Wedepohl. New York: Springer-Verlag.

Simpson, C. and Schmid, S.M.
1983: An evaluation of criteria to deduce the sense of movement in sheared rocks. Geological Society of America Bulletin, Volume 94, pages 1281-1288.

Sisson, V.G. and Hollister, L.S.
1988: Low-pressure facies series metamorphism in an accretionary sedimentary prism, southern Alaska. Geology, Volume 16, pages 358-361.

Skinner, R.
1974: Geology of the Tetagouche Lakes, Bathurst, and Nepisiguit Falls map-areas, New Brunswick with emphasis on the Tetagouche Group. Geological Survey of Canada, Memoir 371.

Snelgrove, A.K.
1933: Geological report on Shoal Pond chrome area, near Carmanville, Sir Charles Hamilton sound, northeast coast of Newfoundland. Geological Survey of Newfoundland, 20 pages. [2E/8 (26)]

1934: Chromite deposits of Newfoundland. Department of Natural Resources, Newfoundland, Bulletin #1, 26 pages.

Spooner, E.T.C., Beckinsadle, R.D., England, P.C. and Senior A.
1977: Hydration, 180 enrichment and oxidation during ocean floor hydrothermal metamorphism of ophiolitic metabasic rocks from E. Liguria, Italy. Geochemica et Cosmochimica Acta, Volume 41, pages 857-871.

Stanton, R.L.
1972: Ore Petrology. McGraw-Hill, New York, pages 713.

Stephenson, L.
1985: Assessment report on Gander River claims, Gander River area. Duval International Corporation. Unpublished report, 11 pages. [2E/8 (26)]

Stevens, R.D., Delabio, R.N. and Lachance, G.R.
1982: Age determinations and geological studies: K-Ar isotopic ages, Report 15, Geological Survey of Canada, Paper 81-2, 56 pages.

Stevens, R.K., Strong, D.F., and Kean, B.F.
1974: Do some eastern Appalachian ultramafic rocks represent mantle diapirs produced above a subduction zone? Geology, Volume 2, pages 175-178.

Stouge, S.
1979: Conodonts from Davidsville Group of the Botwood Zone, Newfoundland. *In* Report of Activities. *Edited by* R.V. Gibbons. Newfoundland Department of Mines and Energy, Mineral Development Division, Report 79-1, pages 43-44.

1980: Conodonts from the Davidsville Group, northeastern Newfoundland. Canadian Journal of Earth Sciences, Volume 17, pages 268-272.

Streckeisen, A.
1976: To each plutonic rock its name. Earth Science Reviews, Volume 12, pages 1-33.

Strickland, R.
1989: Second year report on geological, geochemical and geophysical investigations conducted in the Gander River area, northeastern Newfoundland, July 1988–July 1989. Stride Consulting and Maritec Limited for Newfoundland Resources and Mining Co. Limited. [2E (670)]

Strickland, R. and Sheppard, D.
1989: First year report on geological and geochemical investigations conducted in the Gander River area, northeastern Newfoundland. June to November, 1989. For Newfoundland Minerals Incorporated (1989).

Strong, D.F., Dickson, W.L., O'Driscoll, C.F. and Kean, B.F
1974: Geochemistry of eastern Newfoundland granitoid rocks. Newfoundland Department of Mines and Energy, Mineral Development Division, Report 74-3, 140 pages.

Strong, D.F., Dickson, W.L., O'Driscoll, C.F., Kean, B.F. and Stevens, R.K.
1974: Geochemical evidence for an east-dipping Appalachian subduction zone in Newfoundland. Nature, Volume 248, pages 37-39.

Sun, S.S.
1980: Lead isotope study of young volcanic rocks from mid ocean ridges, ocean islands and island arcs. Philosophical Transactions of the Royal Society of London, Volume 297, pages 409-445.

Suen, C.J., Frey, F.A. and Malpas, J.
1979: Bay of Island ophiolite suite, Newfoundland: Petrologic and geochemical characteristics with emphasis on rare earth element geochemistry. Earth and Planetary Science Letters, Volume 45, pages 337-348.

Swinden, H.S.
1988: Geology and economic potential of the Pipestone Pond area (12A/1 NE; 12A/8 E), Central Newfoundland. Newfoundland Department of Mines, Mineral Development Division, Report 88-2, 88 pages.

Tallman, P.
1989: First year report on the NORONT Big Pond (4714); Licences 3419,3420, NTS 2E/2. July 9, 1988 to July 8, 1989. Noranda Exploration Company Limited. [2E/2 (679)]

Thompson, A.B.
1976: Mineral reactions in pelitic rocks: I. Prediction of P-T-X (Fe-Mg) phase relations. II. Calculation of some P-T-X (Fe-Mg) phase relations. American Journal of Science, Volume 276, pages 401-454.

Thompson, J.B., Jr. and Norton, S.A.
1968: Palaeozoic regional metamorphism in New England and adjacent area. *In* Studies of Appalachian Geology: Northern and Maritime. *Edited by* E-An Zen, W.S. White, J.B. Hadley and J.B. Thompson, Jr. Interscience Publishers, New York, pages 319-327.

Tunbridge, I.P.
1981: Sandy, high energy flood sedimentation—some criteria for recognition with an example from the Devonian of southwest England. Sedimentary Geology, Volume 28, pages 79-95.

Turner, F.J.
1948: Evolution of metamorphic rocks, Geological Society of America Bulletin, Memoir Number 30.

Twenhofel, W.H.
1947: The Silurian of eastern Newfoundland with some data relating to physiography and Wisconsin glaciation of Newfoundland. American Journal of Science, Volume 245, pages 65-122.

Uzuakpunwa, A.B.
1973: Structural studies of the Gander and Davidsville groups in the Carmanville Ladle Cove areas, Newfoundland. MSc Thesis, Memorial University of Newfoundland, St John's, 140 pages.

Vanderveer, D.G.
1985: Quaternary Mapping; Moran Heights, Labrador and Gander-Gambo area, Newfoundland. *In* Current Research. *Edited by* K. Brewer, D. Walsh and R.V. Gibbons. Newfoundland Department of Mines, Mineral Development Division, Report 85-1, pages 55-58.

Wall, R.M.
1954: Northeast-central Newfoundland. Nalco unpublished report, [2D(28)]

Wanless, R.K., Stevens, R.D., Lachance, G.R. and Rimsaite, R.Y.H.
1965: Age determinations and geological studies: Part 1—isotopic ages, Report 5. Geological Survey of Canada, Paper 64-17, 126 pages.

Wanless, R.K., Stevens, R.D., Lachance, G.R. and Delabio, R.N.
1972: Age determinations and geological studies: K-Ar isotopic ages, Report 10. Geological Survey of Canada, Paper 71-2, 96 pages.

Wickham, S.M. and Oxburgh, E.R.
1985: Continental rifts as a setting for regional metamorphism. Nature, Volume 318, pages 330-333.

Williams, H.
1964: Botwood, Newfoundland. Geological Survey of Canada, Map 60-1963 (geological map and descriptive notes).

1968: Wesleyville, Newfoundland. Geological Survey of Canada, Map 1227A.

1972: Stratigraphy of Botwood map area, northeastern Newfoundland. Geological Survey of Canada, Open File 113, 103 pages.

1978: Tectonic Lithofacies Map of the Appalachian Orogen, Memorial University of Newfoundland, Map No. 1A, scale 1:2,000,000.

Williams, H., Colman-Sadd, S.P. and Swinden, H.S.
1988: Tectonic-stratigraphic subdivisions of central Newfoundland. *In* Current Research, Part A. Geological Survey of Canada, Paper 1A.

Williams, H., Kennedy, M.J. and Neale, E.R.W.
1974: The northeastward termination of the Appalachian Orogen. *In* Ocean Basins and Margins, Volume 2. *Edited by* A.E.M. Nairn and F.G. Stehli. Plenum Press, New York, pages 79-123.

Winchester, J.A. and Floyd, P.A.
1977: Geochemical discrimination of different magma series and their differentiation products using immobile elements. Chemical Geology, Volume 20, pages 325-343.

Winkler, H.G.F.
1979: Petrogenesis of metamorphic rocks. Fifth Edition, Springer-Verlag, New York, 348 pages.

Wonderley, P.R. and Neuman, R.B.
1984: The Indian Bay formation: fossiliferous Early Ordovician volcanogenic rocks in the northern Gander Terrane, Newfoundland, and their regional significance. Canadian Journal of Earth Science, Volume 21, pages 525-532.

Wood, D.A., Tarney, J., Varet, J., Saunders, A.D., Bougault, H., Joron, J.L., Treuil, M. and Cann, J.R.
1979: Geochemistry of basalts drilled in the North Atlantic by' IPOD Leg 49: Implications for mantle heterogeneity. Earth and Planetary Science Letters, Volume 42, pages 77-97.

Zuffa, G.G.
1980: Hybrid arenites: their composition and classification. Journal of Sedimentary Petrology, Volume 50, Number 1, pages 21-29.

Zurowski, N.
1974: Summary report on ground geophysical surveys in the Gander-Ragged Harbour ultramafic belt. International Mogul Mines Limited. Unpublished report, 19 pages. [2E (340)]

1977: Drillhole logs and location plan of holes drilled on the Gander Project during 1976. International Mogul Mines Limited. Unpublished report. [2E (370)]

Note: Geological Survey Branch file numbers are given in square brackets.

APPENDIX 1

ELECTRON MICROPROBE TECHNIQUE AND ANALYSES

Silicate minerals were analyzed using a JEOL JXA-50A electron probe microanalyzer housed at the Department of Earth Sciences, Memorial University of Newfoundland. The analyzer is a wavelength dispersive type with three spectrometers, controlled automatically by the Krisel system, and run at an operating voltage of 15Kv and a beam current of 0.22 mA. Silicate data reduction was performed with the Alpha correction program, using the method of Bence and Albee (1968). The analyses' totals used fall within the range of 100 ± 1.5%. The silicate standard used for calibration was FCPX (pyroxene).

Table 1. Replicate analyses of standard samples of FCPX

	Average of 3 spots		
	$\bar{X}$	SD	HI
SiO_2	49.70	0.65	3.59
Al_2O_3	7.96	0.04	0.59
FeO	5.93	0.13	ND
MgO	15.48	0.16	1.10
CaO	18.41	0.04	0.43
Na_2O	1.29	0.05	0.80
K_2O	ND	ND	10.67
TiO_2	0.76	0.01	1.13
MnO	0.11	0.03	5.69
Cr_2O_3	0.02	0.01	25.60
Total	99.7		
Si	1.818		
Al	0.342		
Fe	0.181		
Mg	0.844		
Ca	0.722		
Na	0.091		
K	0.000		
Ti	0.020		
Mn	0.003		
Cr	ND		
Total	4.023		

X – Mean analysis
SD – Standard Deviation
HI – Homogeneity Index
ND – Not detected

Table 2. Electron microprobe analyses of selected samples from mafic rocks of the Gander River Complex.

Rock	Ultramafic	Gabbro	Diabase		
Sample	117(CPX)	347(CPX)	339(CPX)		339(PREH)
			CORE	RIM	
SiO_2	49.73	51.54	51.70	52.02	43.27
TiO_2	0.38	0.47	0.32	0.11	0.03
Al_2O_3	3.01	3.03	3.59	0.66	23.45
Cr_2O_3	0.37	0.02	0.05	0.00	0.00
FeO	4.70	8.80	7.63	17.57	0.14
MnO	0.12	0.23	0.17	0.62	0.04
MgO	15.90	13.79	16.91	10.17	0.02
CaO	24.06	21.84	18.81	19.74	26.55
Na_2O	0.13	0.35	0.30	0.30	0.03
K_2O	0.00	0.00	0.00	0.00	0.00
TOTAL	98.40	100.83	99.48	101.21	93.53
Si	1.872	1.921	1.909	1.985	0
Ti	0.011	0.013	0.009	0.003	0
Al	0.134	0.133	0.156	0.030	0
Cr	0.011	0.001	0.001	0.000	0
Fe	0.148	0.274	0.236	0.561	0
Mn	0.004	0.007	0.005	0.020	0
Mg	0.892	0.766	0.931	0.578	0
Ca	0.970	0.872	0.744	0.807	0
Na	0.009	0.025	0.021	0.022	0
K	0.000	0.000	0.000	0.001	0
TOTAL	4.050	4.010	4.008	4.068	0

APPENDIX 2

GEOCHEMISTRY METHODS AND ANALYSES

Analyses carried out at the Department of Mines and Energy Laboratory.

Major oxides: 0.1 g of sample were fused with 0.5 g of lithium metaborate at 1000°C. The fused sample was digested in a mixture of HF and HCl for 1.5 hours. boric acid was subsequently added to complex the excess HF. The solution was transferred to a polyethylene flask and made up to 100 ml volume. The oxides SiO_2, Al_2O_3, total iron as Fe_2O_3, MnO, CaO, Na_2O, TiO_2 and MnO were determined by atomic absorption spectroscopy.

Phosphorous was determined spectrophotometrically by reduction with hydrazine sulphate. Ferrous iron was determined by addition of vanadium followed by ferrous ammonium sulphate and titration with standard potassium dichromate using barium phenylamine sulphonate as indictor. LOI was determined by heating the sample to 1000°C. (See Wagenbauer, 1983, for detailed description).

Trace Elements: Cr, Ba, Zr. These elements were determined by following the same fusion and digestion procedure as that for major oxides and solutions analyzed by the Induction Coupled Plasma mass spectrometer (ICP-MS)

Ni, Cu, Pb, Zn, Rb, V, Sr, Y, Nb and Ga. Samples were prepared by digestion in a mixture of HF, HCl and $HClO_4$. The elements Ni, Cu, Pb, Zn and Rb were determined by atomic absorption spectroscopy (AAP), whereas Nb, Ga, Y, Va and Sr were determined by ICP-MS.

Analyses carried out at the Department of Earth Sciences, Memorial University of Newfoundland.

The following samples were analyzed at the Department of Earth Sciences, Memorial University of Newfoundland for trace and rare-earth elements; all samples are from the Gander River complex. Sample numbers are as follows: 86-329, 86-334, 86-335, 86-339, 86-340, 86-341, 86-343, 86-352, 86-354, 86-355, 86-360, 86-361, 86-376, 86-384.

Trace Elements: Rb, Sr, Y, Zr, Nb, Ni, Ba, Sc, Cr and V. These trace elements were analyzed using a Phillips 1450 X-ray fluorescence spectrometer. Samples of approximately 10 g were mixed with 1.5 g of bakelite binder and pressed into pellets. The pellets were baked in an oven at 200°C for 20 minutes.

Trace elements Hf and Th are rare-earth-elements La, Ce, Pr, Nd, Sm, Eu, Gd, Tb, Dy, Ho, Er, Yb and Lu.
These elements were determined by the ICP-MS method at the Department of Earth Sciences, Memorial University of Newfoundland.

0.1 g of sample was digested in a mixture of concentrated HF and HNO_3 and the solution evaporated; this procedure was repeated twice. After the third evaporation, the solution is made up to 100 ml with 0.2 N HNO_3. 20 ml of solution were used for the analysis by ICP-MS.

Table 1. Precision (P) of major element analyses

Oxide	P	S.D.	n
SiO_2	0.19	0.15	6
Al_2O_3	0.43	0.29	6
FeO	0.68	0.6	6
MgO	0.75	0.5	6
CaO	1.6	1.06	6
Na_2O	0.54	0.77	6
K_2O	1.12	0.74	5
TiO_2	10.82	15.28	6
MnO	3.11	4.9	6
P_2O_5	12.27	12.9	6
LOI	3.2	2.9	6

Table 2. Precision (P) of trace element analyses

Element	P	S.D.	n
Ga	7.9	9.6	8
Nb	3.2	4.4	3
Zr	15.5	12.9	8
Y	2.9	4.0	8
Ba	5.7	7.4	6
Cu	12.2	8.04	6
Zn	1.3	1.3	6
Pb	34.2	5.7	2
Sr	10.2	13.6	6
Ni	2.59	3.7	6
Rb	21.1	35.5	6
Cr	14.5	15.5	6
V	13.9	15.9	6

Table 3. Precision (P) of rare-earth element and some trace-element analyses

	ICP-MS	
Element	P	n
La	6.3	1
Ce	5.49	1
Pr	5.64	1
Nd	4.8	1
Sm	4.3	1
Eu	7.5	1
Gd	0.24	1
Th	4.4	1
Dy	5.8	1
Mo	4.2	1
Er	2.78	1
Yb	8.10	1
Lu	4.14	1
Hf	10.3	1
Tb	9.6	1
Nb	8	1
Y	0.8	1
Rb	ND	1
Sr	1.6	1
Zr	1.9	1
Ni	ND	1
Ba	0.9	1
Sc	3.8	1
Cr	ND	1
V	0.185	1

Table 4. Accuracy of major-oxides analyses

STM-1 Oxide	Abbey (1983)	NDM
SiO_2	59.66	59.05
Al_2O_3	18.44	18.33
Fe_2O_3	5.2	5.04
MgO	0.1	0.11
CaO	1.09	1.1
Na_2O	8.95	8.98
K_2O	4.29	4.33
TiO_2	0.13	0.14
MnO	0.22	0.23
P_2O_5	0.16	0.14

RGM-1 Oxide	Abbey (1980)	NDM
SiO_2	73.47	73.4
Al_2O_3	13.8	13.79
Fe_2O_3	1.89	1.73
MgO	0.28	0.29
CaO	1.15	1.18
Na_2O	4.12	4.07
K_2O	4.35	4.37
$Ti0_2$	0.27	0.22
MnO	0.04	0.04
P_2O_5	0.05	0.05

MRG-1 Oxide	Abbey (1983)	NDM
SiO_2	39.32	38.5
Al_2O_3	8.5	8.6
Fe_2O_3	17.8	17.9
MgO	13.49	14.08
CaO	14.77	14.78
Na_2O	0.71	0.72
K_2O	0.18	0.17
TiO_2	3.69	3.85
MnO	0.17	0.18
P_2O_5	0.06	0.06

BCR-1 Oxide	Abbey (1983)	NDM
SiO_2	54.53	54.35
Al_2O_3	13.72	13.65
Fe_2O_3	13.41	13.74
MgO	3.48	3.57
CaO	6.97	6.77
Na_2O	3.3	3.32
K_2O	1.7	1.69
TiO_2	2.26	2.22
MnO	0.18	0.19
P_2O_5	0.36	0.33

Table 5. Accuracy of trace-element analyses by XRF

MRG-1 Element	Abbey (1983)	$\bar{X}$	NDM SD	n
Ba	50	87.4	17.3	5
Sr	260	264.0	7.1	5
Rb	8	14.2	4.3	5
Cr	420	312.4	17.3	5
V	520	544.0	15.5	5
Ga	18	26.5	2.6	4
Nb	20	14.2	1.2	4
Zr	105	128.0	11.6	4
Y	16	12.25	0.4	4

Accuracy of trace elements by atomic absorption

Element	Abbey (1983)	$\bar{X}$	NDM SD	n
Cu	135	107.4	4.9	5
Ni	195	147	8.8	5
Zn	185	215.6	18.7	5

Accuracy of trace-element analyses by XRF

SY-2 Element	Abbey (1983)	$\bar{X}$	NDM SD	n
Ba	460	472.0	20.7	4
Sr	275	276.0	4.1	4
Rb	220	211.0	13.3	4
Cr	10	9.0	2.4	4
Ga	28	24.0	0.7	4
Nb	23	26.0	0.7	4
Zr	280	333.5	7.0	4
Th	380	405.0	8.0	4
Y	130	133.0	6.2	4
V	52	55.75	6.3	4

Accuracy of trace elements by atomic absorption

SY-2 Element	Abbey (1983)	$\bar{X}$	NDM SD	n
Cu	5	5.0	0	4
Ni	10	4.25	1	4
Zn	250	259.0	12	4

Table 6. Accuracy of rare-earth-element analyses

	BCR-1	MUN	SY-2	MUN
La	26.9	26.301	75	70.462
Ce	53.7	54.739	175	163.003
Pr	6.8	6.976	18.8	19.901
Nd	28.8	28.907	73	74.552
Sm	6.59	6.698	16.1	15.965
Eu	1.95	1.942	2.42	2.429
Gd	6.68	6.926	17	14.809
Tb	1.05	1.055	2.5	2.90
Dy	6.34	6.45	18.0	20.45
Ho	1.26	1.314	3.8	4.633
Er	3.63	3.76	12.4	15.461
Yb	3.38	3.318	17.0	17.924
Lu	0.51	0.498	2.7	2.956
Hf	4.95	5.033	7.7	8.662
Tb	1.05	1.055	2.5	2.900
Nb	14	12.995	29	30.168
Y	38	32.237	128	115.028

BRC-1 and SY-2 published values from Gouindaraju (1989). 1989 Compilation of Working Values and sample description for 272 geostandards. K. Gouindaraju: Editor-in-Chief, Geostandards Newsletter, Volume 13, Special Issue, July 1989, pages 1-113.

Table 7. Detection limits (D.L.) for trace elements analyzed by XRF

Element	D.L. (ppm)
Cu	5
Zn	5
Ni	5
Cr	10
Ba	20
V	10
Ga	5
Rb	2
Sr	2
Y	10
Zr	10
Nb	5

Table 8. Detection limits (D.L.) for trace elements analyzed by ICP-MS

Element	D.L. (ppm)
Th	.004
Y	.002
Nb	.009

Table 9. Detection limits (D.L.) for rare earth elements analyzed by ICP-MS

Element	DL (ppm)
La	.002
Ce	.001
Pr	.001
Nd	.014
Sm	.005
Eu	.001
Gd	.009
Tb	.001
Dy	.003
Ho	.001
Er	.005
Yb	.009
Lu	.001

Table 10. Normalizing values used in extended REE plots

La	0.315
Ce	0.813
Pr	0.116
Nd	0.597
Sm	0.192
Eu	0.0722
Gd	0.259
Dy	0.325
Er	0.213
Yb	0.208
Lu	0.0323
Nb	0.35
Th	0.05
Tb	0.047
Ho	0.07

Table 11. Major- and trace-element analyses of clinopyroxenites from the Gander River Complex

	PYROXENITES FRESH					
SAMPLE #	86-36	86-43	86-49B	86-50	86-160	86-260
SiO_2	50.55	48.50	52.30	50.40	50.85	50.90
TiO_2	0.06	0.05	0.05	0.05	0.11	0.05
Al_2O_3	1.44	1.60	1.24	2.14	3.56	3.20
FeO	4.23	5.30	4.76	4.19	4.63	5.44
MnO	0.16	0.20	0.12	0.13	0.14	0.17
MgO	21.03	22.18	22.00	20.76	18.77	18.70
CaO	19.38	16.46	14.82	19.04	18.21	17.82
Na_2O	0.06	0.06	0.06	0.07	0.27	0.07
K_2O	ND	ND	ND	ND	0.03	ND
P_2O_5	0.02	0.02	ND	0.02	ND	ND
LOI	2.85	4.77	3.90	2.89	4.11	2.17
TOTAL	99.79	99.15	99.27	99.7	100.69	98.54
Cr	2540	2000	2840	2860	1720	180
Ni	190	257	249	177	136	241
V	134	124	125	143	170	103
Cu	59		13	21	68	92
Pb	1	1	1	1	1	1
Zn	31	37	23	21	34	38
Rb	1	4	5	1	3	5
Ba	70	117	88	80	39	68
Sr	2	1	4	2	15	41
Ga	1	2	11	2	4	3
Nb	1	1	5	1	1	1
Zr	16	29	13	38	23	21
Y	2	2	2	2	4	2
Th	1	1	3	1	1	1

ND – Not detected

Table 12. Anhydrous, major- and trace-element analyses of altered ultramafic rocks of the Gander River Complex

ALTERED ULTRAMAFIC ROCKS

SAMPLE #	86-38	86-42	86-51	86-53	86-55	86-69	86-128	86-159	86-162	86-167	86-265
SiO_2	45.07	48.83	49.88	16.77	39.65	44.30	32.23	51.33	58.73	55.20	31.26
TiO_2	ND	0.02	0.07	0.06	0.01	ND	ND	0.13	0.46	0.09	ND
Al_2O_3	0.20	0.91	1.81	3.16	0.47	0.35	0.34	5.97	0.09	2.60	0.30
FeO	7.31	8.19	8.87	8.04	9.01	7.44	9.70	5.17	9.70	4.69	10.40
MnO	0.06	0.22	0.16	0.35	0.07	0.04	0.10	0.15	0.16	0.11	0.29
MgO	40.86	32.67	34.70	26.56	49.40	39.80	56.43	18.04	51.70	24.14	59.90
CaO	5.93	8.24	2.70	42.14	0.18	6.30	0.31	18.25	0.07	12.76	ND
Na_2O	0.02	0.03	0.03	0.03	0.02	0.02	0.03	0.07	0.02	0.03	ND
K_2O	ND	ND	ND	ND	0.01	ND	ND	0.25	0.02	0.04	ND
P_2O_5	0.01	0.01	0.01	0.04	0.03	ND	0.03	ND	ND	ND	ND
TOTAL	99.58	99.21	98.58	98.33	99.19	98.69	99.58	99.58	100.47	99.79	101.47
Cr	358.0	2056.0	2677.0	4284.0	1397.0	2527.0	551.0	1700.0	661.0	3051.0	545.0
Ni	2763.0	242.0	346.0	259.0	2205.0	279.0	2232.0	159.0	1011.0	278.0	2265.0
V	5.0	8.0	185.0	163.0	1.0	146.0	7.0	140.0	7.0	170.0	5.0
Cu	7.0	4.0	21.0	2.0	5.0	7.0	4.0	143.0	5.0	110.0	4.0
Pb	1.0	1.0	1.0	1.0	1.0	1.0	1.0	1.0	1.0	1.0	1.0
Zn	45.0	38.0	42.0	28.0	43.0	43.0	23.0	26.0	22.0	31.0	20.0
Rb	3.0	5.0	1.0	1.0	3.0	3.0	4.0	8.0	1.0	2.0	4.0
Ba	50.0	44.0	15.0	106.0	13.0	64.0	16.0	254.0	5.0	56.0	5.0
Sr	29.0	6.0	1.0	158.0	1.0	2.0	4.0	91.0	1.0	157.0	2.0
Ga	1.0	2.0	3.0	2.0	1.0	1.0	1.0	2.0	1.0	1.0	1.0
Nb	1.0	1.0	1.0	1.0	1.0	1.0	1.0	1.0	1.0	1.0	1.0
Zr	21.0	18.0	21.0	24.0	44.0	24.0	23.0	13.0	98.0	32.0	93.0
Y	1.0	1.0	2.0	3.0	1.0	1.0	1.0	4.0	1.0	6.0	1.0
Th	1.0	1.0	1.0	1.0	1.0	1.0	1.0	1.0	1.0	3.0	1.0

ND–Not detected

Table 13a. Major oxide and trace-element analyses of mafic rocks of the Gander River Complex

	GABBROS												
SAMPLE #	86-31	86-46	86-330	86-334	86-340	86-342	86-344	86-345	86-346	86-347	86-356	86-359	86-374
SiO_2	51.35	43.55	52.15	52.75	44.25	42.80	40.70	45.10	46.95	46.65	47.30	47.30	48.90
TiO_2	0.37	0.39	0.25	0.35	1.30	2.47	1.90	1.44	0.35	0.34	0.76	0.32	2.42
Al_2O_3	14.15	15.91	14.57	15.11	14.11	12.88	13.38	15.63	18.23	16.09	14.62	16.13	13.00
FeO	8.71	12.81	8.41	8.42	13.42	15.92	15.74	15.99	8.31	8.75	14.01	7.72	14.24
MnO	0.19	0.22	0.21	0.18	0.22	0.28	0.25	0.28	0.17	0.17	0.24	0.15	0.31
MgO	9.65	11.46	8.76	8.66	8.91	9.11	8.70	8.72	7.13	9.48	7.18	11.15	7.09
CaO	8.12	5.54	4.76	7.15	11.69	10.63	11.50	12.83	13.03	9.79	7.63	9.34	7.96
Na_2O	2.78	2.89	3.59	3.84	1.85	1.89	1.89	1.22	2.02	2.70	3.10	2.63	3.27
K_2O	1.18	0.40	0.34	0.76	0.27	0.12	0.12	0.33	0.75	0.43	0.19	0.55	0.54
P_2O_5	0.03	0.02	0.09	0.02	0.02	0.15	0.09	0.02	0.03	ND	0.03	ND	0.23
LOI	2.68	4.86	5.90	2.26	2.55	2.68	2.65	3.87	4.11	4.34	3.75	3.87	2.11
Total	99.21	98.05	99.03	99.5	98.41	98.63	99.02	99.24	99.23	99.05	98.16	99.17	100.07
Cr	274.0	81.0	769.0	313.0	122.0	37.0	46.0	6.0	34.0	48.0	62.0	243.0	87.0
Ni	44.0	33.0	45.0	32.0	11.0	9.0	17.0	9.0	37.0	31.0	17.0	52.0	27.0
Sc	ND	ND	ND	70.0	90.0	ND	ND	ND	ND	ND	ND	ND	ND
V	256.0	332.0	218.0	284.0	564.0	673.0	640.0	458.0	181.0	168.0	421.0	325.0	408.0
Cu	5.0	54.0	31.0	12.0	6.0	11.0	14.0	9.0	47.0	48.0	53.0	69.0	39.0
Pb	1.0	1.0	1.0	1.0	1.0	1.0	1.0	1.0	1.0	1.0	1.0	1.0	1.0
Zn	70.0	76.0	82.0	68.0	50.0	60.0	61.0	70.0	46.0	53.0	118.0	43.0	141.0
Rb	24.0	9.0	14.0	11.0	6.0	14.0	14.0	13.0	18.0	20.0	12.0	15.0	17.0
Ba	749.0	110.0	364.0	544.0	449.0	193.0	217.0	913.0	964.0	453.0	226.0	437.0	240.0
Sr	134.0	116.0	164.0	142.0	156.0	143.0	191.0	234.0	363.0	224.0	166.0	118.0	83.0
Ga	13.0	19.0	13.0	11.0	17.0	20.0	18.0	20.0	14.0	10.0	16.0	9.0	23.0
Nb	1.0	1.0	1.0	0.7	0.2	1.0	1.0	1.0	1.0	1.0	1.0	1.0	1.0
Hf	ND	ND	ND	1.31	0.62	ND	ND	ND	ND	ND	ND	ND	ND
Zr	75.0	22.0	28.0	58.0	17.0	25.0	55.0	44.0	25.0	22.0	57.0	32.0	53.0
Y	19.0	4.0	28.0	13.5	14.0	15.0	16.0	8.0	8.0	6.0	13.0	3.0	53.0
Th	1.0	7.0	1.0	1.04	0.074	1.0	1.0	1.0	1.0	1.0	1.0	1.0	1.0
U	ND	ND	ND	0.23	0.2	ND	ND	ND	ND	ND	ND	ND	ND
Mg#	0.69	0.64	0.67	0.67	0.57	0.53	0.52	0.53	0.63	0.68	0.50	0.74	0.5

ND – Not detected

Table 13a. (Concluded)

SAMPLE #	GABBROS		BASALTS				DIABASE				
	87-809	86-352	86-384	86-47	86-808	86-64	86-12	86-339	86-441	86-343	86-370
SiO_2	51.20	45.95	46.25	49.25	50.15	50.05	51.40	51.00	49.75	53.95	49.95
TiO_2	0.25	0.74	1.25	0.98	1.46	1.26	0.44	0.86	0.83	1.13	0.23
Al_2O_3	15.27	16.04	15.90	16.27	13.56	12.72	14.14	15.10	15.33	15.70	12.33
FeO	7.39	14.12	13.01	11.89	12.41	7.60	10.16	9.86	10.21	11.28	9.46
MnO	0.19	0.24	0.19	0.20	0.20	0.16	0.20	0.19	0.16	0.11	0.19
MgO	9.52	8.54	7.21	7.43	6.68	8.70	7.38	6.20	6.13	3.27	13.13
CaO	9.34	3.96	7.55	4.17	5.98	9.42	7.82	7.94	6.95	4.03	8.24
Na_2O	2.84	3.33	3.28	4.51	4.76	1.86	4.26	4.67	4.73	6.09	0.95
K_2O	1.15	0.83	0.29	0.21	0.05	3.81	0.13	0.15	0.04	0.04	2.35
P_2O_5	0.02	0.04	0.09	0.10	0.11	0.83	0.06	0.06	0.07	0.14	0.03
LOI	2.71	4.40	3.19	4.06	3.98	2.72	3.17	3.45	4.24	3.41	2.78
Total	98.88	98.19	98.61	99.07	99.34	99.13	99.16	99.48	98.44	99.15	99.64
Cr	264.0	ND	20.0	10.0	109.0	422.0	176.0	21.0	34.0	20.0	682.0
Ni	55.0	ND	12.0	7.0	54.0	101.0	29.0	16.0	13.0	16.0	177.0
Sc	ND	85.0	52.0	ND	ND	ND	ND	43.0	49.0	52.0	ND
V	171.0	513.0	448.0	399.0	398.0	263.0	276.0	335.0	352.0	540.0	220.0
Cu	24.0	47.0	52.0	62.0	72.0	38.0	139.0	56.0	47.0	62.0	14.0
Pb	1.0	1.0	1.0	1.0	1.0	27.0	1.0	1.0	1.0	1.0	1.0
Zn	68.0	113.0	116.0	95.0	101.0	74.0	79.0	85.0	81.0	79.0	77.0
Rb	18.0	10.0	5.0	16.0	13.0	55.0	10.0	2.0	ND	ND	24.0
Ba	853.0	596.0	41.0	68.0	367.0	1940.0	112.0	283.0	111.0	105.0	2445.0
Sr	170.0	74.0	139.0	163.0	296.0	321.0	239.0	157.0	88.0	63.0	23.0
Ga	13.0	15.0	22.0	25.0	23.0	16.0	20.0	16.0	17.0	20.0	14.0
Nb	1.0	0.2	1.0	1.0	1.0	16.0	1.0	1.0	1.2	1.0	1.0
Hf	ND	0.37	1.69	ND	ND	ND	ND	1.16	1.21	1.34	ND
Zr	26.0	10.0	58.0	26.0	72.0	473.0	28.0	43.0	40.0	50.0	5.0
Y	20.0	9.0	25.0	17.0	28.0	22.0	11.0	17.0	17.0	22.0	6.0
Th	ND	0.109	0.54	1.0	1.0	33.0	2.0	0.197	0.312	0.351	1.0
U	ND	0.04	0.41	ND	ND	ND	ND	0.09	0.09	0.11	0.0
Mg#	0.72	0.55	0.53	0.56	0.52	0.69	0.59	0.56	0.55	0.36	0.73

Table 13b. Rare-earth-element analyses of selected mafic rocks from the Gander River Complex

SAMPLE #	GABBROS			BASALTS	DIABASE		
	86-352	86-334	86-340	86-384	86-339	86-341	86-343
La	0.557	2.661	0.596	2.668	1.532	1.459	2.575
Ce	1.548	6.778	2.363	7.898	4.578	4.483	7.057
Pr	0.276	0.955	0.496	1.320	0.769	0.778	1.151
Nd	1.501	4.230	3.230	7.438	4.270	4.437	5.993
Sa	0.704	1.418	1.471	2.704	1.682	1.726	2.243
Eu	0.217	0.381	0.743	1.065	0.680	0.550	0.453
Gd	1.612	2.242	3.016	3.426	2.382	2.267	2.408
Tb	0.220	0.345	0.415	0.706	0.456	0.459	0.59
Dv	1.628	2.485	2.788	4.722	3.211	3.232	4.053
Ho	0.377	0.553	0.569	1.009	0.713	0.693	0.863
Er	1.151	1.765	1.734	3.051	2.159	2.099	2.620
Yb	1.159	1.757	1.487	2.808	2.054	2.024	2.463
Lu	0.178	0.285	0.220	0.411	0.315	0.296	0.362
Hf	0.366	1.308	0.620	1.691	1.156	1.206	1.340
Th	0.109	1.040	0.074	0.540	0.197	0.312	0.351

Table 14a. Major-oxide and trace-element analyses of trondhjemites from the Gander River Complex

SAMPLE #	86-8	86-11	86-14	86-32	86-161	86-329	86-335	86-354	86-355	86-360	86-361	86-375	86-377	86-386
SiO_2	68.40	60.65	68.20	70.70	70.05	70.75	74.00	71.55	62.05	64.10	77.05	68.35	74.45	73.25
TiO_2	0.59	0.67	0.59	0.35	0.30	0.56	0.34	0.39	0.65	0.42	0.18	0.51	0.18	0.12
Al_2O_3	14.19	16.25	13.53	13.31	12.34	14.19	11.24	12.52	15.22	14.95	12.04	13.44	13.46	12.33
FeO	4.57	7.76	5.43	3.88	5.69	2.61	2.63	3.53	8.07	4.79	1.56	6.02	1.38	2.03
MnO	0.07	0.13	0.09	0.08	0.04	0.05	0.05	0.07	0.12	0.12	0.05	0.14	0.03	0.05
MgO	2.33	2.96	2.12	1.87	1.57	1.27	1.04	1.77	3.08	2.41	0.43	1.64	0.74	0.41
CaO	1.07	1.62	2.35	0.18	1.29	1.08	4.25	1.08	2.31	3.09	0.73	2.24	0.70	1.54
Na_2O	3.66	4.67	3.25	5.85	4.24	5.20	2.74	3.96	3.95	4.36	5.74	4.49	6.21	5.95
K_2O	1.62	0.92	0.86	0.46	0.79	1.14	0.32	1.09	0.79	0.91	0.20	0.30	0.55	0.27
P_2O_5	0.17	0.17	0.13	0.06	0.05	0.03	0.06	0.11	0.11	0.08	0.02	0.07	0.03	0.02
LOI	2.73	3.11	2.28	1.83	3.77	1.91	1.46	2.40	2.71	2.27	0.67	1.64	0.96	2.08
Total	99.40	98.91	98.93	98.57	100.13	98.79	98.13	98.47	99.06	97.50	98.67	98.84	98.69	98.05
Cr	4.0	7.0	6.0	8.0	9.0	3.0	7.0	4.0	11.0	419.0	3.0	65.0	4.0	3.0
Ni	1.0	2.0	2.0	5.0	11.0	8.0	2.0	4.0	3.0	84.0	1.0	28.0	3.0	1.0
Sc						30.0	19.0	11.0	42.0	21.0	17.0			
V	75.0	133.0	133.0	50.0	23.0	112.0	12.0	69.0	234.0	113.0	6.0	37.0	12.0	8.0
Cu	106.0	7.0	17.0	5.0	13.0	5.0	4.0	6.0	19.0	48.0	7.0	16.0	9.0	2.0
Pb	1.0	1.0	1.0	1.0	1.0	1.0	1.0	1.0	1.0		1.0	1.0	1.0	1.0
Zn	41.0	72.0	46.0	51.0	37.0	24.0	18.0	47.0	70.0	34.0	46.0	62.0	25.0	38.0
Rb	35.0	17.0	16.0	15.0	17.0	9.5	6.0	14.0	11.0	9.0	2.0	18.0	16.0	12.0
Ba	909.0	629.0	1230.0	134.0	302.0	530.0	272.0	528.0	713.0	1242.0	392.0	200.0	447.0	44.0
Sr	86.0	154.0	176.0	53.0	64.0	88.0	177.0	52.0	141.0	152.0	48.0	100.0	73.0	52.0
Ga	5.0	11.0	6.0	6.0	4.0	4.0	3.0	3.0	14.0	5.0	3.0	6.0	3.0	3.0
Nb	1.0	1.0	1.0	1.0	1.0	4.0	0.6	1.0	0.8	0.2	1.5	1.0	1.0	1.0
Hf	-	-	-	-	-	0.68	0.16	0.3	0.61	0.23	2.16	-	-	-
Zr	25.0	9.0	15.0	100.0	13.0	23.0	10.0	10.0	16.0	7.0	135.0	47.0	109.0	75.0
Y	13.0	9.0	11.0	18.0	4.0	9.5	6.0	7.0	9.0	8.5	45.0	24.0	22.0	-
Th	1.0	7.0	2.0	1.0	1.0	1.568	0.116	0.207	0.328	0.109	1.494	1.0	1.0	23.0
U	-	-	-	-	-	0.34	0.02	0.13	0.14	0.02	0.38	ND	ND	1.0

Table 14b. Rare-earth-element analyses of selected trondhjemite samples from the Gander River Complex

SAMPLE #	86-329	86-335	86-354	86-355	86-360	86-361
La	7.742	1.432	1.309	1.627	1.523	6.769
Ce	16.913	3.177	3.543	3.981	3.749	17.616
Pr	2.041	0.454	0.554	0.580	0.571	2.586
Nd	8.408	2.418	2.837	3.014	3.059	12.715
Sm	2.008	0.724	0.885	0.994	1.058	4.398
Eu	0.532	0.999	0.432	0.530	0.622	0.931
Gd	2.005	1.157	1.208	1.529	2.090	5.384
Tb	0.331	0.174	0.207	0.239	0.247	1.193
Dy	2.071	1.103	1.338	1.708	1.662	8.317
Ho	0.422	0.232	0.289	0.375	0.365	1.873
Er	1.335	0.710	0.901	1.186	1.065	5.755
Yb	1.284	0.609	0.819	1.103	0.968	5.423
Lu	0.193	0.093	0.133	0.176	0.150	0.791
Hf	0.680	0.161	0.298	0.608	0.231	2.155
Th	1.568	0.116	0.207	0.328	0.109	1.494

Table 15: CIPW norms for trondhjemites from the Gander River Complex

Sample #	86-8	86-11	86-14	86-32	86-329	86-335	86-354
Quartz	33.519	18.889	35.362	30.174	31.789	48.264	38.690
Corundum	4.794	4.821	3.208	2.974	2.834	ND	3.253
Orthoclase	9.408	5.207	4.954	2.690	6.944	1.953	6.703
Albite	30.436	37.845	26.804	48.986	45.354	23.945	34.869
Anorthite	4.125	6.633	10.536	0.496	4.647	17.997	4.828
Diopside	ND	ND	ND	ND	ND	2.693	ND
Hypersthene	8.990	13.040	9.215	7.701	6.577	2.137	ND
Olivine	ND	ND	ND	ND	ND	ND	10.365
Magnetite	7.239	11.971	8.537	6.185	0.448	2.201	ND
Ilmenite	1.101	1.219	1.092	0.658	1.096	0.667	0.257
Apatite	0.396	0.386	0.300	0.141	0.317	0.147	0.771
Norm Total	100.010	100.010	100.008	100.004	100.008	100.004	100.007

Sample #	86-355	86-360	86-361	86-375	86-377	86-386
Quartz	23.468	24.632	40.841	31.621	33.935	34.106
Corundum	4.071	1.432	1.124	1.874	1.481	ND
Orthoclase	4.836	5.636	1.205	1.821	3.324	1.662
Albite	34.619	38.665	49.538	39.033	53.736	52.441
Anorthite	11.126	15.518	3.560	10.947	3.351	6.394
Diopside	ND	ND	ND	ND	ND	ND
Hypersthene	17.425	10.368	2.686	11.563	3.071	3.437
Olivine	ND	ND	ND	ND	ND	ND
Magnetite	2.914	2.720	0.651	1.981	0.682	0.453
Ilmenite	1.279	0.836	0.349	0.995	0.350	0.237
Apatite	0.270	0.199	0.048	0.170	0.073	0.049
Norm Total	100.007	100.006	100.002	100.006	100.002	100.002

ND–not detectable

Table 16. Major- and trace-element-analyses of sandstone and siltstone and one limestone (sample # 86-800) from the Weir's Pond Formation, Davidsville Group

Sample #	86-6	86-17	86-18	86-23	86-26	86-149	86-151	86-165	86-185	86-186	86-270
SIO_2	61.15	54.55	56.00	63.65	62.55	60.85	83.95	53.50	65.90	61.90	62.90
TIO_2	0.89	0.78	0.86	0.88	0.80	0.54	0.28	0.36	0.16	0.25	0.75
AL_2O_3	14.21	16.51	13.56	14.12	14.10	16.62	5.44	17.41	16.86	16.61	13.50
FEO	8.05	6.28	8.38	8.85	8.47	5.75	2.39	5.59	2.98	4.41	5.13
MNO	0.29	0.11	0.19	0.17	0.12	0.17	0.11	0.10	0.06	0.15	0.14
MGO	5.76	7.71	10.46	3.85	4.92	4.06	1.80	9.40	2.85	4.34	3.06
CAO	0.39	3.11	0.65	0.19	0.15	1.53	0.70	0.30	0.34	1.44	3.68
NA_2O	2.00	2.29	1.89	1.83	3.08	6.45	1.28	0.86	7.94	6.23	1.78
K_2O	1.45	1.44	1.17	1.51	0.68	0.12	0.89	7.09	0.28	0.84	2.71
P_2O_5	0.11	0.10	0.10	0.09	0.09	0.12	0.02	0.07	0.02	0.05	0.15
LOI	4.68	7.04	6.01	3.91	3.74	2.75	1.56	4.94	1.91	3.55	5.85
TOTAL	98.98	99.92	99.27	99.05	98.70	98.96	98.42	99.62	99.30	99.47	99.65
Cr	951.0	486.0	628.0	146.0	124.0	89.0	65.0	27.0	92.0	150.0	112.0
Ni	173.0	223.0	282.0	71.0	50.0	50.0	18.0	51.0	44.0	43.0	48.0
V	255.0	135.0	227.0	141.0	178.0	108.0	57.0	38.0	42.0	105.0	91.0
Cu	35.0	22.0	42.0	22.0	40.0	42.0	14.0	3.0	17.0	27.0	23.0
Pb	1.0	10.0	1.0	7.0	1.0	12.0	2.0	7.0	8.0	5.0	6.0
Zn	113.0	66.0	94.0	121.0	81.0	74.0	37.0	55.0	68.0	73.0	77.0
Rb	54.0	55.0	28.0	52.0	18.0	12.0	18.0	128.0	15.0	17.0	109.0
Ba	256.0	204.0	276.0	387.0	32.0	51.0	178.0	3670.0	139.0	711.0	421.0
Sr	38.0	184.0	45.0	40.0	40.0	164.0	28.0	207.0	154.0	165.0	164.0
Ga	16.0	20.0	20.0	21.0	19.0	6.0	1.0	17.0	5.0	6.0	16.0
Nb	2.0	4.0	7.0	4.0	1.0	9.0	2.0	14.0	9.0	8.0	10.0
Zr	95.0	118.0	98.0	172.0	193.0	103.0	49.0	111.0	67.0	61.0	161.0
Y	13.0	11.0	26.0	23.0	14.0	28.0	8.0	12.0	8.0	13.0	17.0
Th	1.0	7.0	6.0	70.0	1.0	8.0	1.0	7.0	2.0	3.0	9.0

Table 16. (Concluded)

Sample #	86-301	86-328	86-333	86-364	86-365	87-851	86-800
SIO_2	60.15	64.65	62.60	71.85	48.85	62.86	4.16
TIO_2	0.81	0.93	0.77	0.45	0.70	0.42	0.02
AL_2O_3	17.10	15.21	14.50	6.99	15.05	12.90	0.26
FEO	7.78	6.82	8.20	5.33	5.36	2.52	1.64
MNO	0.21	0.14	0.12	0.14	0.19	0.07	0.18
MGO	3.02	3.05	4.82	8.32	7.48	2.20	2.60
CAO	0.52	0.18	0.13	1.08	6.67	5.45	47.64
NA_2O	1.71	1.73	3.05	0.13	2.10	0.89	0.05
K_2O	2.87	2.45	0.85	0.29	1.78	4.93	0.00
P_2O_5	0.06	0.06	0.07	0.05	0.09	0.08	0.04
LOI	4.21	3.38	3.48	4.73	11.15	6.62	38.00
TOTAL	98.44	98.60	98.19	99.36	99.42	99.23	94.60
Cr	125.0	110.0	125.0	321.0	449.0	735.0	423.0
Ni	63.0	52.0	58.0	373.0	212.0	61.0	360.0
V	136.0	141.0	162.0	79.0	120.0	49.0	1.0
Cu	20.0	20.0	42.0	29.0	26.0	6.0	4.0
Pb	6.0	4.0	1.0	4.0	8.0	11.0	1.0
Zn	119.0	94.0	92.0	67.0	74.0	69.0	15.0
Rb	114.0	79.0	24.0	18.0	58.0	103.0	6.0
Ba	387.0	523.0	424.0	55.0	238.0	ND	70.0
Sr	94.0	46.0	43.0	49.0	304.0	62.0	208.0
Ga	24.0	20.0	18.0	4.0	19.0	17.0	1.0
Nb	9.0	8.0	4.0	5.0	4.0	1.0	1.0
Zr	136.0	141.0	115.0	60.0	121.0	ND	1.0
Y	11.0	20.0	8.0	16.0	12.0	12.0	2.0
Th	23.0	20.0	19.0	15.0	17.0	7.0	1.0

ND – not detectable

Table 17a. Major- and trace-element-analyses of sandstone, pelites (sample #'s 86-293, 87-625 and 87-839), calc-silicate rock (sample # 87-286) and a coticule rock (sample # 86-288) from the Jonathans's Pond Formation

SANDSTONES

SAMPLE #	86-108	86-131	86-133	86-134	86-135	86-163	86-191	86-216	86-217	86-221	86-232	86-233
SiO_2	75.75	76.80	78.90	65.65	86.30	81.55	72.80	75.80	72.60	83.80	83.85	73.15
TiO_2	0.63	0.65	0.60	0.86	0.44	0.54	0.69	0.65	0.65	0.47	0.50	0.82
Al_2O_3	11.59	10.72	9.66	15.74	6.52	8.39	12.15	11.40	11.57	6.63	7.08	12.31
FeO	3.56	2.86	2.53	5.91	1.56	2.44	3.71	3.52	3.88	1.90	2.01	4.28
MnO	0.05	0.07	0.07	0.10	0.02	0.06	0.10	0.04	0.11	0.05	0.05	0.06
MgO	1.16	0.99	0.98	2.08	0.42	0.82	1.73	1.23	1.36	0.60	0.74	1.62
CaO	0.36	0.32	0.43	0.39	0.09	0.36	0.79	0.17	2.11	0.68	0.16	0.44
Na_2O	1.99	2.06	1.74	2.44	1.03	1.62	2.98	1.72	2.33	1.69	2.91	2.75
K_2O	2.47	2.14	2.07	2.93	1.37	1.73	1.79	2.49	1.90	1.10	0.35	1.85
P_2O_5	0.11	0.11	0.10	0.13	0.06	0.10	0.12	0.11	0.09	0.08	0.09	0.14
LOI	2.36	2.11	2.10	3.24	1.35	1.70	1.79	2.20	2.83	1.07	1.08	2.11
TOTAL	100.93	98.83	99.18	99.47	99.16	99.31	98.65	99.33	99.43	98.07	98.82	99.53
Cr	51.0	42.0	34.0	86.0	21.0	32.0	46.0	40.0	52.0	25.0	19.0	42.0
Ni	21.0	15.0	16.0	34.0	8.0	11.0	21.0	18.0	20.0	8.0	8.0	18.0
V	51.0	48.0	41.0	103.0	26.0	40.0	17.0	50.0	70.0	34.0	26.0	67.0
Cu	8.0	8.0	10.0	30.0	7.0	8.0	5.0	10.0	14.0	7.0	4.0	16.0
Pb	15.0	10.0	6.0	3.0	1.0	7.0	8.0	22.0	12.0	4.0	9.0	9.0
Zn	48.0	47.0	41.0	83.0	26.0	41.0	67.0	56.0	53.0	34.0	38.0	77.0
Rb	107.0	86.0	81.0	125.0	52.0	72.0	67.0	91.0	61.0	47.0	11.0	72.0
Ba	454.0	358.0	210.0	449.0	192.0	178.0	305.0	425.0	340.0	197.0	83.0	349.0
Sr	74.0	54.0	44.0	77.0	21.0	49.0	92.0	56.0	151.0	64.0	52.0	75.0
Ga	6.0	5.0	4.0	9.0	1.0	4.0	6.0	5.0	6.0	1.0	1.0	7.0
Nb	10.0	11.0	10.0	10.0	4.0	9.0	12.0	12.0	11.0	10.0	8.0	15.0
Hf	ND	ND	ND	ND	ND	ND	ND	ND	ND	ND	ND	ND
Zr	134.0	154.0	145.0	122.0	135.0	155.0	121.0	160.0	116.0	118.0	140.0	160.0
Ti	ND	ND	ND	ND	ND	ND	ND	ND	ND	ND	ND	ND
Y	24.0	22.0	14.0	12.0	10.0	16.0	16.0	19.0	28.0	24.0	14.0	15.0
Th	4.0	5.0	5.0	3.0	4.0	4.0	4.0	5.0	11.0	4.0	3.0	5.0
U	ND	ND	ND	ND	ND	ND	ND	ND	ND	ND	ND	ND

Table 17a. (Concluded)

Sample #	SANDSTONES							PELITES			CALC-SILICATE	COTICULE
	86-252	86-262	86-279	86-289	87-626	87-627	87-628	86-293	87-625	87-839	86-286	86-288
SiO_2	86.70	86.55	82.50	63.80	78.85	82.90	84.90	63.60	55.45	69.40	75.85	55.55
TiO_2	0.52	0.63	0.64	0.80	0.57	0.44	0.65	0.91	1.02	0.85	0.74	0.40
Al_2O_3	5.68	5.88	7.83	14.99	10.01	8.13	6.00	17.27	20.99	13.72	8.95	13.94
FeO	1.93	1.54	2.10	6.81	2.75	1.96	1.86	6.53	7.04	4.96	3.68	5.77
MnO	0.12	0.02	0.08	1.18	0.04	0.04	0.04	0.15	0.05	0.16	0.26	18.41
MgO	0.61	0.49	0.62	2.29	0.97	0.84	0.61	2.31	2.19	2.01	0.82	0.87
CaO	1.55	0.18	0.30	0.56	0.20	0.16	0.14	0.29	0.08	0.53	7.01	3.11
Na_2O	1.32	1.77	1.41	2.59	2.07	2.33	1.54	1.12	1.11	1.69	0.20	0.48
K_2O	0.34	0.62	1.61	3.08	1.77	0.98	0.85	4.01	5.84	2.78	0.29	0.14
P_2O_5	0.07	0.07	0.12	0.12	0.11	0.10	0.11	0.16	0.17	0.13	0.19	0.15
LOI	1.03	1.05	1.46	2.25	1.90	1.34	1.18	3.28	4.87	2.75	1.44	0.60
TOTAL	99.87	98.80	98.67	98.47	99.24	99.22	97.88	99.63	98.81	99.88	99.43	99.42
Cr	24.0	40.0	23.0	61.0	36.0	22.0	28.0	81.0	106.0	68.0	40.0	45.0
Ni	7.0	8.0	9.0	34.0	18.0	10.0	8.0	35.0	33.0	26.0	13.0	16.0
V	30.0	33.0	36.0	79.0	51.0	37.0	41.0	121.0	148.0	86.0	87.0	80.0
Cu	6.0	5.0	6.0	4.0	7.0	8.0	6.0	12.0	22.0	6.0	20.0	4.0
Pb	20.0	4.0	3.0	8.0	1.0	9.0	6.0	13.0	7.0	8.0	23.0	4.0
Zn	32.0	23.0	35.0	125.0	48.0	37.0	32.0	113.0	84.0	87.0	38.0	37.0
Rb	19.0	22.0	62.0	129.0	71.0	34.0	31.0	170.0	275.0	101.0	11.0	18.0
Ba	42.0	89.0	223.0	594.0	486.0	228.0	303.0	606.0	1334.0	743.0	40.0	23.0
Sr	149.0	7.0	28.0	105.0	35.0	48.0	28.0	50.0	23.0	66.0	342.0	46.0
Ga	1.0	1.0	3.0	19.0	11.0	6.0	5.0	2.0	34.0	17.0	7.0	5.0
Nb	12.0	7.0	10.0	13.0	12.0	7.0	11.0	13.0	19.0	18.0	16.0	11.0
Hf	ND	ND	ND	ND	ND	ND	ND	ND	ND	ND	ND	ND
Zr	95.0	162.0	167.0	120.0	128.0	95.0	185.0	143.0	183.0	61.0	79.0	64.0
Ti	ND	ND	ND	ND	ND	ND	ND	ND	ND	ND	ND	ND
Y	19.0	11.0	11.0	30.0	13.0	8.0	10.0	15.0	20.0	18.0	43.0	25.0
Th	5.0	4.0	7.0	5.0	9.0	6.0	12.0	5.0	14.0	12.0	10.0	3.0
U	ND	ND	ND	ND	ND	ND	ND	ND	ND	ND	ND	ND

Table 17b. Major- and trace-element analyses of intrusive mafic bodies in the Gander Group

SAMPLE	86-82	86-84	86-246	86-249	86-284	86-291	86-298	87-462	87-480	87-837
SiO_2	48.20	43.50	48.35	52.60	54.70	46.60	48.00	47.95	50.20	47.95
TiO_2	2.53	2.37	1.65	1.09	0.93	1.74	3.50	2.18	1.81	1.76
Al_2O_3	14.72	14.73	16.70	13.06	15.41	16.21	13.64	16.29	15.25	16.33
FeO	12.36	10.72	9.46	6.03	7.96	9.81	14.64	11.43	10.23	10.13
MnO	0.44	0.20	0.19	0.18	0.31	0.20	0.39	0.97	0.20	0.18
MgO	5.85	6.11	6.26	8.83	8.43	7.40	4.92	7.25	7.56	7.61
CaO	3.73	8.41	10.83	6.18	3.35	9.10	8.22	6.38	10.28	8.56
Na_2O	3.15	3.07	2.25	2.30	1.59	1.64	1.51	1.98	2.47	1.66
K_2O	0.30	0.08	0.09	2.20	1.87	0.02	1.02	2.54	0.27	0.02
P_2O_5	0.32	0.23	0.15	0.62	0.46	0.15	0.42	0.24	0.16	0.18
LOI	7.27	9.51	3.10	6.54	4.12	6.01	1.25	2.30	0.90	5.62
TOTAL	98.87	98.93	99.03	99.63	99.13	98.88	97.51	99.51	99.33	100.00
Cr	79.0	138.0	168.0	450.0	450.0	220.0	28.0	162.0	219.0	199.0
Ni	27.0	28.0	33.0	196.0	146.0	64.0	10.0	48.0	52.0	68.0
V	328.0	283.0	276.0	148.0	163.0	282.0	438.0	297.0	271.0	269.0
Cu	20.0	68.0	33.0	36.0	4.0	58.0	27.0	30.0	24.0	61.0
Pb	2.0	1.0	16.0	50.0	12.0	1.0	14.0	10.0	7.0	3.0
Zn	152.0	101.0	79.0	70.0	153.0	89.0	136.0	176.0	87.0	84.0
Rb	17.0	13.0	10.0	161.0	98.0	14.0	46.0	138.0	10.0	4.0
Ba	81.0	74.0	36.0	381.0	166.0	49.0	169.0	585.0	11.0	13.0
Sr	127.0	263.0	628.0	392.0	266.0	326.0	410.0	334.0	342.0	315.0
Ga	23.0	18.0	21.0	18.0	23.0	18.0	25.0	28.0	22.0	23.0
Nb	1.0	1.0	1.0	20.0	4.0	1.0	3.0	1.0	2.0	2.0
Zr	61.0	66.0	48.0	529.0	136.0	38.0	29.0	20.0	21.0	31.0
Y	16.0	37.0	33.0	20.0	17.0	28.0	54.0	36.0	33.0	32.0
Th	1.0	1.0	1.0	41.0	19.0	1.0	1.0	ND	ND	ND

Table 17c. Major- and trace-element analyses of intrusive intermediate bodies in the Gander Group

SAMPLE #	86-103	86-196	86-207	86-214	86-250	86-259
SiO_2	55.70	68.55	47.85	59.60	54.65	64.70
TiO_2	0.93	0.73	2.56	1.19	1.08	0.47
Al_2O_3	13.09	13.05	16.06	14.44	15.92	15.83
FeO	5.43	6.28	12.06	6.10	6.14	3.52
MnO	0.15	0.14	0.24	0.18	0.13	0.75
MgO	7.96	2.54	5.30	6.00	7.61	0.72
CaO	4.54	0.23	7.56	2.95	6.58	10.88
Na_2O	3.46	5.04	1.33	2.81	3.21	1.07
K_2O	0.02	0.17	2.45	2.07	1.20	0.76
P_2O_5	0.47	0.11	0.38	0.59	0.23	0.28
LOI	7.13	2.02	2.70	3.45	2.69	1.44
TOTAL	98.88	98.86	98.49	99.38	99.44	100.42
Cr	454.0	65.0	102.0	268.0	323.0	24.0
Ni	188.0	34.0	16.0	70.0	151.0	10.0
V	121.0	97.0	328.0	150.0	141.0	120.0
Cu	33.0	4.0	17.0	10.0	7.0	5.0
Pb	17.0	1.0	16.0	16.0	22.0	28.0
Zn	74.0	112.0	125.0	103.0	68.0	32.0
Rb	10.0	9.0	170.0	91.0	60.0	38.0
Ba	40.0	40.0	134.0	593.0	137.0	71.0
Sr	334.0	103.0	617.0	277.0	440.0	582.0
Ga	20.0	16.0	27.0	17.0	18.0	30.0
Nb	14.0	10.0	4.0	12.0	6.0	10.0
Zr	634.0	148.0	51.0	254.0	160.0	78.0
Y	19.0	17.0	62.0	30.0	18.0	44.0
Th	45.0	5.0	2.0	27.0	11.0	7.0

Table 18. Major- and trace-element analyses of sandstone, pelite (sample #'s 87-653, 87-670, 87-677), mafic volcanic rock (sample # 87-698) and intermediate intrusive rock (sample # 87-678) from the Indian Bay Big Pond Formation

SAMPLE #	87-630	87-641	87-645	87-646	87-672	87-683	87-732	87-687	87-697	87-748
SiO_2	64.30	83.50	78.95	74.60	80.25	81.75	78.50	50.85	62.70	74.05
TiO_2	0.85	0.56	0.55	0.76	0.72	0.36	0.65	0.76	0.65	0.66
Al_2O_3	16.78	9.22	9.27	12.33	8.36	7.04	9.63	13.37	11.25	10.72
FeO	4.57	0.70	3.30	3.36	3.91	1.99	3.49	5.90	4.25	3.93
MnO	0.12	0.00	0.08	0.04	0.10	0.12	0.05	0.18	0.13	0.07
MgO	1.76	0.36	0.31	0.98	1.09	0.44	0.35	4.37	3.28	1.27
CaO	0.82	0.14	0.11	0.16	0.37	0.72	0.06	7.44	6.27	0.85
Na_2O	8.12	1.16	1.96	1.85	1.60	1.51	1.51	1.64	0.77	2.37
K_2O	0.09	2.23	1.88	2.62	1.25	1.39	2.45	2.25	1.79	1.71
P_2O_5	0.17	0.09	0.09	0.14	0.10	0.10	0.08	0.14	0.12	0.10
LOI	2.30	1.69	2.15	2.44	2.13	2.16	2.12	12.71	8.06	2.49
TOTAL	99.78	99.66	98.65	99.28	99.88	97.58	98.89	99.61	99.27	98.22
Cr	61.0	27.0	37.0	58.0	36.0	26.0	44.0	121.0	82.0	114.0
Ni	4.0	27.0	12.0	26.0	16.0	10.0	23.0	58.0	36.0	35.0
V	87.0	50.0	52.0	73.0	53.0	33.0	57.0	102.0	83.0	80.0
Cu	5.0	14.0	13.0	18.0	22.0	14.0	13.0	37.0	18.0	18.0
Pb	15.0	30.0	7.0	1.0	1.0	28.0	2.0	10.0	12.0	4.0
Zn	73.0	45.0	39.0	59.0	49.0	50.0	57.0	82.0	58.0	54.0
Rb	12.0	93.0	75.0	116.0	45.0	60.0	98.0	86.0	77.0	62.0
Ba	35.0	456.0	363.0	454.0	282.0	242.0	216.0	365.0	292.0	302.0
Sr	126.0	23.0	32.0	37.0	53.0	68.0	26.0	157.0	243.0	114.0
Ga	23.0	9.0	10.0	15.0	11.0	6.0	11.0	18.0	12.0	13.0
Nb	16.0	11.0	10.0	15.0	11.0	8.0	9.0	11.0	9.0	10.0
Zr	180.0	126.0	132.0	163.0	159.0	93.0	150.0	120.0	104.0	122.0
Y	19.0	14.0	11.0	14.0	22.0	10.0	11.0	17.0	19.0	12.0
Th	9.0	8.0	7.0	12.0	9.0	8.0	9.0	8.0	5.0	8.0

Table 18. (Concluded)

SAMPLE	87-653	87-670	87-677	87-678	87-698
SiO_2	67.20	59.35	56.65	63.30	39.00
TiO_2	0.93	0.97	0.91	0.48	1.74
Al_2O_3	18.45	19.46	20.77	15.41	14.33
FeO	2.57	8.00	7.94	4.21	6.49
MnO	0.04	0.14	0.45	0.09	0.12
MgO	0.90	2.13	1.90	1.11	5.45
CaO	0.20	0.14	0.13	2.71	14.69
Na_2O	0.13	1.35	0.86	4.73	2.92
K_2O	5.83	5.20	4.13	2.01	0.97
P_2O_5	0.17	0.11	0.12	0.12	0.34
LOI	3.44	3.52	4.65	3.27	13.05
TOTAL	99.86	100.37	98.51	99.44	99.10
Cr	94.0	90.0	106.0	36.0	329.0
Ni	24.0	41.0	53.0	25.0	163.0
V	129.0	117.0	166.0	55.0	221.0
Cu	20.0	4.0	44.0	17.0	50.0
Pb	2.0	18.0	8.0	7.0	1.0
Zn	37.0	105.0	120.0	47.0	66.0
Rb	242.0	217.0	188.0	57.0	32.0
Ba	449.0	788.0	586.0	370.0	1030.0
Sr	16.0	38.0	87.0	241.0	488.0
Ga	27.0	29.0	31.0	17.0	18.0
Nb	18.0	14.0	14.0	8.0	31.0
Zr	174.0	150.0	123.0	113.0	130.0
Y	18.0	10.0	17.0	11.0	20.0
Th	12.0	10.0	9.0	2.0	1.0

Table 19. Major- and trace-element analyses of the Deadman's Bay and Ocean Pond granites and Unit 18 (sample # 86-269)

SAMPLE #	89-930	89-931	89-932	89-933	89-934	89-935	89-936	89-937	89-938	89-939	89-941	89-942	89-943
DEADMAN'S BAY GRANITE													
SiO_2	69.54	68.07	68.07	69.16	71.46	71.72	70.93	73.34	72.91	67.42	74.39	75.43	72.34
TiO_2	0.59	0.98	0.83	0.50	0.56	0.59	0.58	0.57	0.30	0.53	0.47	0.46	0.53
Al_2O_3	14.50	13.64	13.56	15.34	13.92	13.71	13.61	12.82	13.34	16.02	12.63	11.99	13.09
FeO	2.41	4.13	3.45	1.99	2.16	2.37	2.52	2.38	1.20	2.22	1.86	1.75	2.30
Fe_2O_3	0.52	0.75	0.81	0.70	0.88	0.69	0.59	0.63	0.43	1.03	0.44	0.54	0.46
MnO	0.07	0.10	0.15	0.09	0.10	0.09	0.08	0.09	0.05	0.09	0.06	0.07	0.09
MgO	0.79	1.40	1.40	0.78	0.89	0.86	0.82	0.81	0.47	0.78	0.64	0.58	0.67
CaO	1.88	1.88	1.12	1.23	0.73	0.81	1.89	0.84	0.48	0.78	1.34	0.94	1.37
Na_2O	3.02	2.72	2.85	3.75	3.23	2.96	3.00	2.52	2.65	2.72	3.12	2.36	2.69
K_2O	4.59	4.38	4.08	4.15	4.41	5.04	3.77	5.01	6.40	7.02	4.05	4.79	4.60
P_2O_5	0.18	0.30	0.26	0.17	0.19	0.18	0.22	0.17	0.17	0.22	0.17	0.14	0.20
LOI	0.92	0.83	1.80	1.62	1.61	1.52	1.17	1.23	1.14	1.55	0.99	0.99	1.06
TOTAL	99.01	99.18	98.38	99.48	100.14	100.54	99.18	100.41	99.54	100.38	100.16	100.04	99.40
Cr	24.0	35.0	23.0	13.0	16.0	1.0	21.0	11.0	1.0	24.0	1.0	9.0	3.0
Ni	4.0	8.0	5.0	3.0	3.0	3.0	5.0	3.0	2.0	5.0	4.0	3.0	3.0
V	42.0	73.0	66.0	38.0	39.0	42.0	43.0	42.0	21.0	41.0	36.0	28.0	35.0
Cu	16.0	12.0	13.0	8.0	10.0	9.0	12.0	10.0	10.0	10.0	8.0	7.0	11.0
Pb	30.0	21.0	81.0	31.0	21.0	26.0	24.0	26.0	52.0	34.0	20.0	27.0	29.0
Zn	59.0	99.0	90.0	54.0	56.0	61.0	59.0	58.0	36.0	64.0	51.0	42.0	56.0
Rb	190.0	226.0	153.0	169.0	153.0	189.0	174.0	216.0	229.0	290.0	147.0	193.0	196.0
Ba	815.0	584.0	796.0	710.0	583.0	764.0	528.0	732.0	656.0	1059.0	607.0	620.0	538.0
Sr	200.0	172.0	248.0	331.0	216.0	167.0	170.0	217.0	154.0	164.0	149.0	205.0	172.0
Ga	24.0	18.0	31.0	27.0	14.0	21.0	25.0	26.0	18.0	30.0	22.0	13.0	20.0
Nb	14.0	27.0	21.0	14.0	15.0	16.0	19.0	17.0	11.0	17.0	14.0	16.0	16.0
Zr	264.0	526.0	283.0	221.0	283.0	283.0	346.0	250.0	185.0	235.0	233.0	307.0	287.0
Y	21.0	28.0	29.0	19.0	24.0	23.0	24.0	22.0	21.0	23.0	19.0	18.0	23.0
Th	29.0	38.0	34.0	26.0	23.0	43.0	31.0	32.0	14.0	24.0	27.0	29.0	29.0

Table 19. (Concluded)

SAMPLE #	89-944	89-945	89-946	89-947	89-948	89-949	89-950	87-846	87-437	86-446	87-847	86-269
	DEADMAN'S BAY GRANITE								OCEAN POND GRANITE			UNIT 18
SiO_2	75.39	76.61	73.04	72.13	71.45	71.38	69.37	71.10	72.20	75.65	74.45	71.45
TiO_2	0.46	0.41	0.51	0.63	0.47	0.51	0.50	0.17	0.17	0.00	0.08	0.17
Al_2O_3	12.23	11.54	12.78	13.63	14.05	14.36	14.97	14.29	14.91	14.46	13.81	14.75
FeO	1.80	1.47	2.19	2.65	1.83	1.88	2.35	1.69	0.67	0.15	0.37	1.69
Fe_2O_3	0.50	0.39	0.75	0.51	0.63	0.69	0.43	0.80	0.46	0.27	0.36	1.88
MnO	0.08	0.09	0.16	0.08	0.08	0.10	0.07	0.07	0.09	0.21	0.06	0.07
MgO	0.58	0.53	0.82	0.85	0.61	0.65	0.70	0.66	0.40	0.03	0.20	0.37
CaO	1.07	0.58	0.80	1.80	1.58	0.84	1.40	1.43	1.02	0.91	0.45	1.66
Na_2O	2.22	2.37	2.73	2.78	3.25	2.73	2.79	2.94	3.82	4.96	3.68	4.27
K_2O	5.22	4.20	4.53	4.60	4.76	6.34	6.02	5.30	4.35	3.21	4.50	2.27
P_2O_5	0.15	0.13	0.19	0.21	0.18	0.13	0.17	0.15	0.21	0.15	0.28	0.11
LOI	1.00	1.25	1.33	0.68	1.11	1.26	1.31	0.92	1.04	0.87	1.06	2.77
TOTAL	100.70	99.57	99.83	100.55	100.00	100.87	100.08	99.52	99.34	100.88	99.30	101.46
Cr	1.0	10.0	21.0	34.0	26.0	26.0	22.0	7.0	13.0	2.0	3.0	4.0
Ni	2.0	2.0	5.0	5.0	4.0	2.0	4.0	3.0	4.0	1.0	2.0	7.0
V	28.0	25.0	38.0	44.0	33.0	31.0	39.0	28.0	13.0	1.0	1.0	11.0
Cu	11.0	8.0	12.0	11.0	11.0	8.0	12.0	7.0	3.0	3.0	5.0	6.0
Pb	27.0	22.0	30.0	26.0	28.0	35.0	33.0	28.0	21.0	9.0	24.0	14.0
Zn	46.0	44.0	62.0	59.0	52.0	61.0	58.0	48.0	38.0	13.0	20.0	15.0
Rb	195.0	162.0	174.0	190.0	204.0	222.0	238.0	228.0	296.0	329.0	307.0	88.0
Ba	517.0	352.0	551.0	623.0	595.0	941.0	836.0	812.0	161.0	46.0	101.0	403.0
Sr	137.0	160.0	251.0	179.0	200.0	217.0	203.0	191.0	54.0	24.0	29.0	158.0
Ga	19.0	20.0	15.0	23.0	24.0	21.0	27.0	15.0	15.0	11.0	10.0	6.0
Nb	14.0	15.0	16.0	17.0	16.0	16.0	19.0	16.0	18.0	46.0	17.0	5.0
Zr	224.0	203.0	246.0	312.0	247.0	239.0	325.0	178.0	48.0	24.0	52.0	99.0
Y	19.0	18.0	25.0	22.0	19.0	23.0	21.0	18.0	7.0	1.0	5.0	6.0
Th	30.0	24.0	28.0	32.0	26.0	25.0	26.0	18.0	6.0	1.0	2.0	6.0

Table 20. CIPW norms of the Deadman's Bay and Ocean Pond granites and Unit 18

Sample #	89-930	89-931	89-932	89-933	89-934	89-935	89-936	89-937	89-938	89-939	89-941	89-942	89-943
	DEADMAN'S BAY GRANITE												
Zircon	0.05	0.11	0.06	0.05	0.06	0.06	0.07	0.05	0.04	0.05	0.05	0.06	0.06
Apatite	0.43	0.72	0.64	0.41	0.46	0.43	0.53	0.41	0.41	0.53	0.41	0.33	0.48
Ilmenite	1.14	1.89	1.63	0.97	1.08	1.13	1.12	1.09	0.58	1.02	0.90	0.88	1.02
Orthoclase	27.63	26.29	24.94	25.04	26.43	30.06	22.71	29.83	38.42	41.95	24.12	28.56	27.62
Albite	26.03	23.38	24.95	32.40	27.72	25.28	25.88	21.48	22.78	23.27	26.61	20.15	23.13
Anorthite	8.54	7.66	4.24	5.35	2.60	3.08	8.26	3.30	1.48	2.73	5.75	3.97	5.75
Corundum	1.52	1.69	3.06	2.82	2.93	2.29	1.66	2.07	1.55	2.99	1.03	1.49	1.64
Magnetite	0.77	1.10	1.22	1.04	1.29	1.01	0.87	0.92	0.63	1.51	0.64	0.79	0.68
Hypersthene	5.21	9.16	8.34	4.45	4.78	5.16	5.48	5.13	2.66	4.51	4.01	3.61	4.88
Quartz	28.69	28.03	30.96	27.50	32.66	31.54	33.44	35.74	31.50	21.49	36.51	40.17	34.76
Enstatite	2.00	3.54	3.61	1.98	2.25	2.16	2.08	2.03	1.19	1.96	1.61	1.46	1.70
Ferrosilite	3.21	5.62	4.73	2.47	2.53	3.00	3.39	3.10	1.47	2.54	2.41	2.16	3.19
Agind	0.69	0.68	0.67	0.70	0.73	0.75	0.66	0.75	0.85	0.75	0.75	0.76	0.72
Israt	1.08	1.08	1.22	1.19	1.22	1.16	1.09	1.15	1.10	1.19	1.06	1.11	1.10

Sample #	89-944	89-945	89-946	89-947	89-948	89-949	89-950	87-846	87-437	87-446	87-847	86-269
	DEADMAN'S BAY GRANITE								OCEAN POND GRANITE			UNIT 18
Zircon	0.05	0.04	0.05	0.06	0.05	0.05	0.07	0.04	0.01	0.00	0.01	0.02
Apatite	0.36	0.31	0.46	0.50	0.43	0.31	0.41	0.36	0.51	0.36	0.68	0.26
Ilmenite	0.88	0.79	0.98	1.20	0.90	0.97	0.96	0.33	0.33	0.02	0.15	0.33
Orthoclase	30.92	25.23	27.16	27.20	28.43	37.59	35.99	31.75	26.15	18.97	27.06	13.59
Albite	18.83	20.39	23.43	23.54	27.79	23.17	23.88	25.22	32.88	41.96	31.69	36.60
Anorthite	4.49	2.19	2.96	7.75	6.92	3.59	6.14	6.43	3.80	3.55	0.44	7.75
Corundum	1.29	2.35	2.35	1.24	1.05	1.70	1.66	1.41	2.59	1.52	2.78	2.50
Magnetite	0.73	0.57	1.10	0.74	0.92	1.00	0.63	1.18	0.68	0.39	0.53	2.76
Hypersthene	3.74	3.24	4.97	5.67	3.77	3.85	5.06	3.99	1.76	0.50	0.87	2.35
Quartz	38.75	44.90	36.55	32.13	29.76	27.79	25.23	29.34	31.31	32.74	35.80	33.86
Enstatite	1.45	1.34	2.07	2.12	1.54	1.62	1.76	1.67	1.01	0.07	0.51	0.93
Ferrosilite	2.29	1.90	2.90	3.55	2.23	2.23	3.30	2.32	0.75	0.43	0.37	1.42
Agind	0.76	0.73	0.74	0.70	0.75	0.79	0.74	0.74	0.74	0.81	0.79	0.64
Israte	1.09	1.21	1.18	1.06	1.05	1.11	1.09	1.08	1.16	1.09	1.17	1.18

APPENDIX 3

GEOCHRONOLOGY

$^{40}Ar/^{39}Ar$

Method

Samples were crushed and sieved in order to isolate those size fractions, in which the micas or amphibole occurred as individual rather than composite grains. Standard density, magnetic and hand-picking techniques were used to purify mineral separates. In all cases, purity was estimated to be greater than 99.0 percent. The samples were encapsulated in aluminum foil, weighed and loaded into silica glass vials, which were then sealed. Samples were irradiated in the H5 facility of the Phoenix Memorial Laboratory at the University of Michigan. Correction factors for Ca and K-derived isotopes were determined through the analysis of irradiated K and Ca salts and are as follows: $(^{40}Ar/^{39}Ar)K = 0.0347$; $(^{36}Ar/^{37}Ar)Ca = 0.0002572$; $(^{39}Ar/^{37}Ar)Ca = 0.0007494$. The primary flux monitor was MMhb-1 (Alexander *et al.*, 1978).

The irradiated samples were heated in a molybdenum crucible within an ultrahigh vacuum extraction system using RF induction heating. Extraction temperatures are estimated to be accurate to ± 50°C. Standard gettering techniques were used to purify the inert gases. The isotopic composition of Ar was determined using a 15 cm Nier type mass spectrometer. Ages were calculated using the equations of Dalrymple *et al.* (1981).

U/Pb–Zircon

The zircon grains were analyzed during testing of new techniques and although all have acceptable sample to background ratios, some have more common lead than normal. Batch 1 was dissolved on PTFE teflon film and the total common lead observed was 8, 9, 26, 30 and 33 picograms for grains 1 to 5 respectively. Batch 2 was done with conventional bombs and the total common lead observed was lower, or more normal at 3.5, 4, 5.6, 6, 7 and 8 picograms for grains 1 to 6 respectively.

Table 1. The ^{40}Ar/^{39}Ar analytical data on muscovites, biotites and amphibole from the Weir's Pond area, northeastern Gander Zone

Release Temp. °C	$(^{40}Ar/^{39}Ar)^*$	$^{37}Ar/^{39}Ar$	$(^{36}Ar/^{39}Ar)^*$	Moles ^{39}Ar	^{39}Ar % of Total	% ^{40}Ar Radiogenic	K/Ca	Apparent Age(Ma)
				MUSCOVITE				
Sample #86-191; Pelite; Gander Group; J = .006113								
825	51.45	0.4392	0.0531	16.3	7.0	69.5	1.12	356.7 ± 19.6
890	43.32	0.4218	0.0117	29.3	12.6	92.0	1.16	393.5 ± 13.7
950	41.22	0.2877	0.0033	49.4	21.3	97.6	1.70	396.7 ± 4.0
1025	40.53	0.2581	0.0018	43.6	18.8	98.6	1.90	394.5 ± 5.2
1115	40.23	0.2332	0.0020	50.1	21.6	98.5	2.10	391.3 ± 4.3
1170	40.15	0.4186	0.0004	29.3	12.6	99.7	1.17	395.0 ± 4.0
1220	40.43	0.8757	0.0024	10.4	4.5	98.3	0.56	392.6 ± 4.9
Fusion	42.46	1.1932	0.0039	3.3	1.4	97.4	0.41	406.9 ± 16.3
Total				231.4	100.0		Total-Gas Age	391.6 ± 6.8
Sample #86-204; Pelite; Gander Group; J = .005926								
825	34.62	0.0147	0.0120	40.3	2.8	89.7	33.27	304.6 ± 8.1
890	39.10	0.0300	0.0040	91.6	6.5	96.9	16.35	365.3 ± 3.6
950	39.95	0.0204	0.0020	168.4	11.9	98.4	24.07	377.9 ± 4.0
1025	39.98	0.0101	0.0015	296.4	21.0	98.8	48.47	379.5 ± 3.8
1115	39.85	0.0144	0.0015	334.8	23.7	98.8	33.93	378.3 ± 3.8
1170	39.68	0.0204	0.0013	270.4	19.1	98.9	24.03	377.4 ± 3.9
1220	39.22	0.0495	0.0016	148.2	10.5	98.7	9.90	372.6 ± 3.7
Fusion	38.88	0.0630	0.0016	64.4	4.5	98.7	7.77	369.7 ± 4.5
Total				1414.4	100.0		Total-Gas Age	374.4 ± 4.0
Sample #86-253; Pelite; Gander Group; J = .005992								
725	38.690	0.0065	0.0107	44.2	2.5	91.7	75.84	347.86 ± 3.69
825	41.400	0.0019	0.0030	175.5	9.9	97.8	261.33	391.72 ± 4.01
890	40.970	0.0014	0.0015	295.8	16.7	98.8	354.56	391.80 ± 3.96
950	40.850	0.0011	0.0010	284.7	16.0	99.2	428.32	392.23 ± 5.03
1025	40.760	0.0037	0.0013	235.3	13.3	99.0	132.08	390.53 ± 3.98
1115	40.660	0.0039	0.0013	249.6	14.1	99.0	126.61	389.74 ± 3.95
1170	40.670	0.0040	0.0012	295.8	16.7	99.1	110.63	390.16 ± 3.93
Fusion	41.200	0.0015	0.0019	195.0	11.0	98.6	336.31	392.99 ± 3.98
Total				1775.8	100.0		Total-Gas Age	390.17 ± 4.13

Table 1. (Continued)

Release Temp. °C	$(^{40}Ar/^{39}Ar)^*$	$^{37}Ar/^{39}Ar$	$(^{36}Ar/^{39}Ar)^*$	Moles ^{39}Ar	^{39}Ar % of Total	% ^{40}Ar Radiogenic	K/Ca	Apparent Age(Ma)
Sample #87-839; Sillimanite Schist; Gander Group; J = .006172								
825	51.97	0.0115	0.0469	28.0	1.8	73.3	42.57	380.8 ± 11.3
890	42.19	0.0060	0.0069	182.0	11.6	95.1	81.26	399.2 ± 4.3
950	40.76	0.0071	0.0034	392.6	25.1	97.5	69.47	395.6 ± 4.1
1025	40.68	0.0021	0.0032	286.0	18.3	97.6	239.02	395.3 ± 5.3
1120	40.98	0.0036	0.0033	201.5	12.9	97.6	136.68	397.9 ± 4.3
1170	40.68	0.0084	0.0027	244.4	15.6	98.0	58.66	396.8 ± 4.0
1220	40.67	0.0035	0.0024	144.3	9.2	98.2	141.70	397.4 ± 5.2
Fusion	40.83	0.0963	0.0030	83.9	5.4	97.7	5.09	397.2 ± 4.4
Total				1562.6	100.0		Total-Gas Age	396.4 ± 4.6
Sample #86-302; Pegmatite; Ocean Pond Granite; J = .006054								
750	45.04	0.0032	0.0197	28.6	0.8	87.0	152.74	384.0 ± 20.8
825	41.23	0.0085	0.0076	54.6	1.5	94.5	57.49	382.0 ± 8.1
890	41.14	0.0008	0.0033	187.2	5.2	97.5	652.64	392.3 ± 4.9
950	40.81	0.0050	0.0030	400.4	11.1	97.7	98.75	390.2 ± 4.3
1025	40.38	0.0003	0.0020	655.2	18.2	98.4	1938.29	389.1 ± 4.2
1115	40.24	0.0004	0.0017	821.6	22.8	98.7	1366.04	388.7 ± 4.1
1170	40.04	0.0012	0.0019	895.7	24.8	98.5	419.52	386.2 ± 4.1
Fusion	40.80	0.0007	0.0018	561.6	15.6	98.6	703.11	393.2 ± 4.5
Total				3604.9	100.0		Total-Gas Age	389.1 ± 4.4
Samples #87-847; Ocean Pond Granite; J = .006168								
825	45.28	0.0026	0.0180	52.7	3.2	88.2	188.90	397.3 ± 4.2
890	42.92	0.0007	0.0095	138.5	8.4	93.4	716.37	398.5 ± 4.0
950	41.85	0.0018	0.0061	387.4	23.4	95.6	274.36	398.1 ± 5.0
1025	41.53	0.0006	0.0048	83.9	5.1	96.5	866.49	398.6 ± 5.5
1120	41.43	0.0010	0.0049	312.7	18.9	96.4	491.38	397.4 ± 4.6
1170	40.88	0.0027	0.0040	411.5	24.8	97.0	184.07	394.8 ± 4.4
1220	41.26	0.0023	0.0045	204.1	12.3	96.7	214.07	396.9 ± 5.3
Fusion	41.40	0.0057	0.0039	67.0	4.0	97.1	86.16	399.6 ± 4.7
Total				1657.5	100.0		Total-Gas Age	397.1 ± 4.7

Table 1. (Continued)

Release Temp. °C	$(^{40}Ar/^{39}Ar)^*$	$^{37}Ar/^{39}Ar$	$(^{36}Ar/^{39}Ar)^*$	Moles ^{39}Ar	^{39}Ar % of Total	%^{40}Ar Radiogenic	K/Ca	Apparent Age(Ma)
BIOTITE								
Sample #86-191; Pelite; Gander Group; J = .005989								
750	42.87	0.0107	0.0086	102.7	11.1	94.0	45.67	390.1 ± 4.9
890	42.35	0.0054	0.0034	133.3	14.1	97.6	91.04	398.9 ± 4.1
925	41.91	0.0089	0.0027	109.2	11.8	98.0	55.21	396.8 ± 4.2
950	41.96	0.0206	0.0022	87.8	9.5	98.4	23.80	398.5 ± 4.2
1025	42.01	0.0159	0.0022	53.9	5.8	98.4	30.76	398.9 ± 4.0
1130	41.55	0.0131	0.0019	229.5	24.8	98.6	37.52	395.8 ± 4.1
Fusion	41.39	0.0158	0.0011	209.3	22.6	99.1	30.97	396.5 ± 3.9
Total				925.6	100.0		Total-Gas Age	396.3 ± 4.2
Sample #86-204; Pelite; Gander Group; J = .006053								
750	32.17	0.0684	0.0148	61.8	8.2	86.3	7.16	280.2 ± 3.1
825	40.88	0.0216	0.0052	106.6	14.1	96.1	22.70	385.0 ± 3.9
900	42.02	0.0160	0.0038	75.4	10.0	97.3	30.55	398.8 ± 3.9
975	44.35	0.0265	0.0026	72.8	9.6	98.2	18.50	422.0 ± 4.2
1050	45.14	0.0281	0.0020	152.1	20.1	98.6	17.44	430.4 ± 4.3
1130	43.68	0.0312	0.0020	139.1	18.4	98.5	15.71	417.8 ± 5.3
Fusion	41.08	0.0523	0.0023	147.6	19.5	98.3	9.37	394.5 ± 4.1
Total				755.3	100.0		Total-Gas Age	398.4 ± 4.2
Sample #87-846; Deadman's Bay Granite; J = .006196								
750	37.46	0.0466	0.0094	80.0	6.9	92.5	10.51	351.0 ± 3.7
825	40.77	0.0158	0.0023	146.3	12.6	98.2	31.04	399.8 ± 4.4
900	41.36	0.0120	0.0025	175.5	15.1	98.1	40.94	404.8 ± 4.1
975	42.04	0.0279	0.0020	118.3	10.2	98.5	17.58	412.2 ± 4.0
1050	42.56	0.0327	0.0014	188.5	16.2	98.9	15.00	418.3 ± 4.1
1130	41.41	0.0324	0.0014	269.8	23.2	98.9	15.11	408.2 ± 4.1
Fusion	41.36	0.0566	0.0017	184.6	15.9	98.7	8.66	406.9 ± 4.0
Total				1162.9	100.0		Total-Gas Age	404.5 ± 4.1

Table 1. (Continued)

Release Temp. °C	(^{40}Ar/^{39}Ar)*	^{37}Ar/^{39}Ar	(^{36}Ar/^{39}Ar)*	Moles ^{39}Ar	^{39}Ar % of Total	%^{40}Ar Radiogenic	K/Ca	Apparent Age(Ma)
Sample #86-172; Detrital muscovite from sandstone, Davidsville Group.								
825	44.88	4.6390	0.0235	20.2	12.7	85.2	0.11	379.2 ± 9.6
890	44.05	2.1480	0.0126	23.4	14.7	92.0	0.23	406.9 ± 7.6
950	45.53	0.8749	0.0066	22.7	14.3	95.8	0.56	425.5 ± 4.7
1025	46.27	0.3671	0.0026	22.7	14.3	98.3	1.33	441.7 ± 5.4
1115	45.66	0.2193	0.0029	24.7	15.5	98.1	2.23	435.5 ± 4.9
1170	40.88	0.1820	0.0094	13.7	8.6	93.2	2.69	376.7 ±13.9
1220	40.92	0.1787	0.0037	18.2	11.4	97.3	2.74	392.1 ± 7.3
Fusion	42.53	0.2854	0.0101	13.7	8.6	93.0	1.72	389.6 ± 13.1
TOTAL				159.3	100.0			
Sample #86-269; Muscovite from granite (Unit 18)								
825	46.03	0.1504	0.0038	76.1	6.1	97.5	3.26	426.0 ± 4.6
850	45.78	0.0338	0.0039	128.1	10.4	97.5	14.51	423.5 ± 4.4
950	45.95	0.0083	0.0018	162.5	13.2	98.8	59.08	430.3 ± 4.6
1025	45.46	0.0004	0.0022	289.9	23.5	98.5	1370.25	425.1 ± 5.2
1120	45.49	0.0009	0.0016	195.0	15.8	98.9	547.06	427.0 ± 4.7
1170	45.49	0.0010	0.0023	175.5	14.2	98.4	475.73	425.0 ± 5.1
1220	45.77	0.0050	0.0017	165.1	13.4	98.9	98.14	429.1 ± 4.3
Fusion	45.59	0.0030	0.0061	42.6	3.5	96.0	163.66	416.4 ± 13.4
TOTAL				1235.0	100.0			
Sample #87-809; Hornblende from gabbro, Gander River Complex.								
800	326.20	11.610	0.8897	2.6	1.4	19.7	0.042	601.6 ± 200.4
900	99.12	4.664	0.1471	16.9	9.4	56.5	0.105	532.8 ± 13.7
950	75.90	7.990	0.0837	27.3	15.2	68.2	0.061	498.7 ± 8.8
1000	66.95	31.290	0.0726	20.2	11.2	71.5	0.015	472.9 ± 15.2
1070	62.25	53.970	0.0631	11.7	6.5	76.6	0.009	478.7 ± 12.9
1100	64.73	60.500	0.0625	17.5	9.8	78.5	0.008	580.5 ± 16.2
1140	67.39	63.690	0.0633	27.3	15.2	79.4	0.007	532.9 ± 15.2
1200	64.64	66.050	0.0494	22.1	12.3	85.1	0.007	547.0 ± 9.6
Fusion	62.75	64.190	0.0428	33.8	18.8	87.6	0.007	545.7 ± 7.9
TOTAL				179.4	100.0			

APPENDIX 4

RESULTS OF POINT COUNTING REPRESENTATIVE SAMPLES FROM THE GANDER AND DAVIDSVILLE GROUPS

Table 1. Point counts of sedimentary rocks of the Davidsville Group

Quartz (monocrystalline)	.	45.0	X	.	.	91.0	93.0	.	31.7	.	.	.	.	.	.	.	75.7	59.7	.	.	91.0	67.0
Quartz (polycrystalline)	.	13.3	X	.	.	6.7	4.0	.	1.3	.	?	.	-	.	.	.	9.7	6.3	.	.	-	5.3
K-feldspar	.	3.3	X	.	.	-	-	.	2.3	.	-	-	-	-	-	-	1.0	1.7	.	-	8.3	6.3
Plagiclase	.	18.3	X	-	-	1.0	-	.	0.3	.	.	.	.	.	.	4.0	11.3	.	-	-	.?	11.7
Albite	-	-	X	.	.	-	-	.	-	-	-	-	-	.?	-	-	-	-	-	-	-	-
Lithic fragments	^{1,2,3,4,5}	^{1,4}17.3	^{1,2,3,6}	^{1}	^{1,4}	^{1}	2.0	^{2,4,5}	^{1,2}18.3	^{1,4}	^{1}	^{1}	^{2}	$^{1?}$	^{1,2,4,6}	^{1,2}	^{1,4}7.3	^{1}20.3	^{1,4,5}	^{1}	0.7	^{1,5}3.0
ACCESSORY MINERALS																						
Zircon	.	.	X	.	.	.	.	.	tr	.	.	-	.	.	.	.	tr	.	-	.	-	tr
Sphene	.	-	X	.	-	.?	-	-	tr	-	-	-	-	.	-	.	-	-	-	-	-	tr
Garnet	-	-	X	.	.?	-	-	.	tr?	.	-	-	-	-	-	.	-	.	-	-	-	-
Sillimanite	-	-	X	-	-	-	-	-	-	-	-	-	-	-	-	-	-	-	-	.	-	-
Clinozoisite	-	.	X	-	-	-	-	-	-	-	-	.	-	.	-	-	-	-	-	.	-	-
Epidote	-	.	X	.	-	-	-	-	-	-	-	-	-	.	-	-	.?	-	.	.	-	tr
Allanite	-	-	X	-	-	-	-	-	-	-	-	-	-	-	-	-	-	-	-	-	-	-
Tourmaline	-	.	X	.	.	-	-	-	-	-	.	-	-	.	-	-	-	-	-	.	-	-
Muscovite	.	.	X	.	.	.	.	-	46.0	-	.	.	-	-	.	-	tr	.?	-	.	.	1.3
Biotite	.	.	X	-	.	-	-	-	tr	-	-	-	-	-	-	.	tr	.	.	.?	-	1.3
Chlorite	.	.	X	-	-	.?	-	-	-	.	.	-	.	-	-	-	-	-	.	.	.?	1.3
Ore	.	-	X	-	-	.	.	.	-	-	-	.	-	-	.	-	.	-	.	.	.	tr
Ilmenite		-	X	-	.	-	-	.	-	-	.	-	-	-	-	-	-	-	-	.	-	tr
Chromite	.	-	X	-	-	.	-	-	-	-	-	.	-	-	-	-	.	-	.	-	tr	tr
Apatite	-	.	X	-	.	.	-	-	tr	-	-	.	-	.	-	.	-	.	.	-	tr	tr
Matrix (<0.0625m) and cement of the whole rock (%)	.	75.8	X	X	X	75.8	75.0	X	X	87.5	X	X	X	X	X	X	55.5	56.0	X	X	X	71.3
Approximate grain size	CGL	VFG	CGL	MG	FG	FG	FG	CGL	CG	VCG	SLT	FG	MG	VCG	CGL	CGL	FG	CG	CGL	FG		FG
Sample Number: (86-)	16	23	27	44	90	104A	104B	148A	165	170	171	183A	185	187	332	366	368	369	380	87-804		860
Unit	6a	6	6a	10	9	7	7	6a	6	6	9	7	6	6	6a	6a	6	6a	6a	7		5

Table 2. Point counts of sedimentary rocks of the Jonathan's Pond Formation

Quartz (monocrystalline)	.	.	.	.	.	.	.	.	.	.	.	85.5	.	.	79.5	74.3
Quartz (polycrystalline)	.	.	-	.	.	.	.	.	?	.	.	5.0	.	.	6.5	6.0
K-feldspar	.	.		.	-	-	.	.	.	.	.	tr	-	?	-	1.0
Plagioclase (other than albite)	.	.	.	.	.	.	.	.	.	.	.	5.5	.	?	3.5	4.7
Albite	.$^{?}$	.	.	-	-	.	.	.	.	-	.	.	.	-	-	-
Lithic fragments	^{1}	$^{?}$	^{12}	^{1}	^{1}	^{12}	^{1}	?	^{1}	^{1}	^{1}	3.5^{1}	^{1}	^{12}	10.0^{12}	13.0^{1}
ACCESSORY MINERALS																
Zircon	.	.	.	.	.	.	.	.	.	.	.	tr	.	.	tr	tr
Sphene	.	.	.	.	.	-	.	.	.	.	.	tr	.	.	tr	tr
Garnet	.	-	.	.	.$^{?}$	.	-	.	-	.	.$^{?}$	tr	-	-	-	tr$^{?}$
Sillimanite	-		-	-	-	-	-	-	-	-	-	-	-	-	-	-
Andalusite		.	-	-	-	-	-	-	-		-	-	-	-	-	-
Clinozoisite	-	-	-	-	-	-	-	-	-	.	-	-	.	-	-	-
Epidote	.$^{?}$	-	.	.	.$^{?}$	.	.	.	-	.	-	-	.	.	-	tr
Allanite	.	-	.$^{?}$	-	-	-	.	.	-	-	-	-	-	-	-	-
Tourmaline	.	-	.	.	.	-	.	-	.	.	-	-	-	.	-	tr
Muscovite	.	.	.$^{?}$	.	.	.	-	.	.	.	-	tr	.	-	tr	-
Biotite	-	-	-	.	-	-	-	-	.	.	-	tr	.	-	-	-
Chlorite	.	-	-	.	-	.	-	-	.	-	-	tr	-	-	-	-
Ore	.	.	.	.	.	.	.	.	-	-	.	.	.	-	tr	tr
Ilmenite	-	-	-	.	-	-	.	.	-	-	-	-	-	-	-	-
Chromite	-	-	-	.	-	.$^{?}$	-	-	-	-	-	-	-	-	tr$^{?}$	-
Apatite	.	-	.	.	.	-	-	.	-	.	.	.	.	.	tr	tr
Matrix (<0.0625mm) & cement of the whole rock (%)	X	X	X	X	X	X	X	X	X	X	X	32.0	X	X	48.8	57.6
Approximate grain size	FG	VCG	CG	CG	FG	MG	VCG	MG	MG	MG	VCG	VCG	VCG	VCG	MG	VCG
Sample number (86-)	98	100	107	129	144	146	187	194	210	244	275	276	496	667	669A	671

Explanations

^{1} –metamorphic (approximately high to low grade foliated rocks)
^{2} –volcanic
^{3} –chert
^{4} –sedimentary clastic rocks
^{5} –granite
^{6} –trondhjemite
X–not established
. –present
- –absent

tr –trace amount
? –?
* ' –sample of clast
CGL–conglomerate
VCG–very coarse-grained sandstone (ss.)
CG –coarse-grained ss.
MG –medium-grained ss.
FG –fine-grained ss.
VFG–very fine-grained ss.
SLT –siltstone

Table 3. Point counts of sedimentary rocks of the Indian Bay Big Pond Formation. (Key to abbreviations, sub- and superscripts at the end of Table 2, page 143.)

Quartz (monocrystalline)	.	.	.	25.0	19.7	.	72.6	73.3	83.0	88.0	.	.	95.7	.	93.0	78.0	90.3	.	.	.
Quartz (polycrystalline)	.	.	.	10.7	19.3	.	10.8	7.3	5.0	3.3	.	.	3.0	.	3.3	11.0	5.3	.	.	-
K-feldspar	-	.	-	-	-	-	tr	1.7	-	1.0	-	-	$^{?}$	-	tr$^{?}$	-	0.7	-	-	-
Plagioclase (other than albite)	.	.	.	1.3	1.7	.	4.4	5.7	8.6	4.3	.	.	0.7	.	-	5.0	1.7	.	.	.
Albite	-	-	-	-	.	-	-	-	-	.	.$^{?}$		tr	.$^{?}$	-	-	tr	-	-	-
Lithic fragments	1	1	^{1,2,3}	^{1,4}62.0	^{1,4}51.3	^{1}	^{1}2.4	^{1}6.7	^{1}1.3	^{1}1.0	-	^{n}	tr^{n}	^{1}	1.7^{n}	2.7	tr^{1}	^{1}	^{1,2,4}	^{2,4,5}
ACCESSORY MINERALS																				
Zircon	.	.	.	tr	tr	-	tr	tr	tr	tr	.	-	tr	.	.	tr	.	.	.	.
Sphene	-	.	.	tr	tr	.	tr	-	tr	tr	-	.	-	-	-	-	.	-	-	.
Garnet	-	.	.	tr	tr	-	tr	tr	tr	tr$^{?}$	.	-	tr	.$^{?}$	-	tr	-	.	-	-
Sillim..nite	-	-	-	-	-	-	-	-	-	-	.$^{?}$	-	-	-	-	-	-	.$^{?}$	-	-
Clinozosite	-	-	-	-	-	-	-	-	-	tr		-	-	-	-	-	-	-	.	.
Epidote	.	.	.	tr	tr	.	tr	tr	tr	tr	-	.	tr	-	-	-	-	-	.$^{?}$	-
Allanite	.	-	-	-	-	-	-	-	tr	tr$^{?}$	-	-	-	-	-	-	-	-	-	-
Tourmaline	.	.	.	-	tr	.	tr	tr	tr$^{?}$	tr	.	.	tr	.	.	-	tr	.	.	.
Muscovite	.	.	.	tr	tr	-	tr	1.7	1.7	tr	.	.	2.7	.	.	tr	tr	.	.	-
Biotite	.	.	.	tr	-	-	-	-	-	-	-	-	-	-	-	-	tr	-	.	-
Chlorite	?	.	.	tr	tr	-	-	-	-	-	-	-	-	-	-	-	-	-	.	-
Ore	.	.	.	tr	tr	.	tr	tr	tr	tr	.	.	.	.	.	-	-	.	.	.
Chromite	-	-	.	-	tr	-	-	-	-	-	-	-	-	-	-	-	-	-	.	.
Apatite	.	.	.	tr	tr	-	tr	tr	tr	tr	.	.	.	.	.	tr	.	-	.	
Matrix (<0.0625mm) and cement of the whole rock(%)	.	.	.	15.3	33.8	.	75.2	76.8	70.7	70.7	.	.	86.7	.	76.6	78.0	62.6	40	.	.
Approximate grain size	VFG	CG	MG	CGL	CG	C/MG	CG	FG	VCG	VCG	FG	MG	FG	MG	CG	VFG	VCG	FG	CG	CG
Sample number: (87-)	641	684	687	696A	696B	729	731B	733	734	758	759	760	761	762	765	766	771	788$^{?}$	693A*	693B*

APPENDIX 5

TABLE OF SAMPLES MENTIONED IN TEXT AND THEIR GRID REFERENCES

Table 1. Location numbers and military grid references, (MGR), for all samples mentioned in the text, and for which geochemical analyses are listed

GANDER RIVER COMPLEX

Sample #	Grid Ref.	Sample #	Grid Ref.	Sample #	Grid Ref.
86-8	856549	86-117	831497	86-346	842531
86-11	884561	86-159	821507	86-347	842453
86-12	887565	86-160	822506	86-352	881552
86-14	870548	86-162	822506	86-354	875550
86-31	865542	86-167	826517	86-355	875550
86-32	870529	86-260	824490	86-356	875550
86-36	881543	86-265	826465	86-359	892551
86-38	937576	86-329	862546	86-360	888545
86-42	854532	86-330	862546	86-361	888545
86-43	854532	86-334	864543	86-370	877539
86-46	864526	86-335	864543	86-374	889539
86-47	864527	86-339	842531	86-375	889539
86-47B	845530	86-340	842531	86-377	892546
86-50	846530	86-341	842531	86-386	818492
86-51	846530	86-342	842531	87-441	022536
86-53	850528	86-343	842531	87-443	018493
86-55	841525	86-344	842531	87-808	884559
86-64	883543	86-345	842531	87-809	956547
86-69	924570				

DAVIDSVILLE GROUP

Sample #	Grid Ref.	Sample #	Grid Ref.	Sample #	Grid Ref.
86-6	835567	86-151	826507	86-333	864544
86-16	902570	86-165	829513	86-364	900561
86-17	904563	86-170	824519	86-365	904563
86-18	900561	86-183	835528	86-366	914571
86-23	862548	86-185	830513	86-369	914571
86-26	865544	86-186	830513	86-380	905576
86-27	893556	86-187	830513	86-381	905576
86-44	857530	86-270	825561	87-800	905552
86-90	836556	86-301	833542	87-804	905552
86-104	905554	86-328	862549	87-851	858525
86-148	826507	86-332	864544	87-860	857525
86-149	826507				

OCEAN POND GRANITE

Sample #	Grid Ref
86-302	009475
87-437	035544
87-446	016490
87-847	029493

UNIT 18

Sample #	Grid Ref.
86-269	829568

JONATHAN'S POND FORMATION

Sample #	Grid Ref.	Sample #	Grid Ref.	Sample #	Grid Ref.
86-82	980584	86-204	972433	86-279	978341
86-84	986584	86-207	964405	86-284	975457
86-98	956516	86-210	942411	86-288	964468
86-100	967513	86-214	960392	86-289	960474
86-103	956491	86-216	934394	86-291	967479
86-107	904535	86-217	926396	86-293	974477
86-108	946471	86-221	940377	86-298	994456
86-129	904435	86-232	014396	87-462	022449
86-131	913421	86-233	986387	87-480	031480
86-133	889412	86-244	953460	87-496	977520
86-134	892411	86-246	957458	87-625	079388
86-135	860397	86-249	960456	86-626	079388
86-144	867308	86-250	960456	87-627	996345
86-146	841384	86-252	966450	87-628	008331
86-163	858363	86-253	966450	87-667	186382
86-187	830513	86-259	982449	87-669	154382
86-191	967412	86-262	834469	87-671	147380
86-194	917443	86-275	820337	87-837	965481
86-196	928451	86-276	934336	87-839	101571

INDIAN BAY BIG POND FORMATION

Sample #	Grid Ref.	Sample #	Grid Ref.	Sample #	Grid Ref.
87-630	023322	87-687	071350	87-748	121384
87-641	055327	87-693	104380	87-758	121384
87-645	050329	87-696	111383	87-759	121384
87-646	050329	87-697	111383	87-760	121384
87-653	052333	87-698	116385	87-761	121384
87-670	152381	87-729	108371	87-762	121384
87-672	093382	87-731	115375	87-765	121384
87-677	097382	87-732	115375	87-766	121388
87-678	106387	87-733	115375	87-771	148409
87-683	056336	87-734	115375	87-788	161434
87-684	072337				

DEADMAN'S BAY GRANITE

Sample #	Grid Ref.	Sample #	Grid Ref.	Sample #	Grid Ref.
87-846	138510	89-936	138508	89-944	182534
89-930	162554	89-937	140499	89-945	182511
89-931	148549	89-938	140480	89-946	162516
89-932	147540	89-939	146470	89-947	149509
89-933	153530	89-941	160540	89-948	151492
89-934	159532	89-942	170540	89-949	166493
89-935	139491	89-943	172529	89-950	160460

MAPS NOT FILMED

CARTES NON REPRODUITES

micromedia
a division of IHS Canada

20 Victoria Street
Toronto, Ontario M5C 2N8
Tel.: (416) 362-5211
Toll Free: 1-800-387-2689
Fax: (416) 362-6161
Email: info@micromedia.on.ca